



**HAL**  
open science

# Synthesis of Carboxylic Acids from Oxygenated Substrates, CO<sub>2</sub> and H<sub>2</sub>

Matilde Valeria Solmi

► **To cite this version:**

Matilde Valeria Solmi. Synthesis of Carboxylic Acids from Oxygenated Substrates, CO<sub>2</sub> and H<sub>2</sub>. Catalysis. Université de Lyon; Rheinisch-westfälische technische Hochschule (Aix-la-Chapelle, Allemagne), 2018. English. NNT : 2018LYSE1287 . tel-02024554

**HAL Id: tel-02024554**

**<https://theses.hal.science/tel-02024554>**

Submitted on 19 Feb 2019

**HAL** is a multi-disciplinary open access archive for the deposit and dissemination of scientific research documents, whether they are published or not. The documents may come from teaching and research institutions in France or abroad, or from public or private research centers.

L'archive ouverte pluridisciplinaire **HAL**, est destinée au dépôt et à la diffusion de documents scientifiques de niveau recherche, publiés ou non, émanant des établissements d'enseignement et de recherche français ou étrangers, des laboratoires publics ou privés.



N°d'ordre NNT : 2018LYSE1287

## **THESE de DOCTORAT DE L'UNIVERSITE DE LYON**

opérée au sein de  
**l'Université Claude Bernard Lyon 1**

**Ecole Doctorale de Lyon**

N° ED206

**Spécialité de doctorat : Chimie**  
**Discipline : Chimie Industrielle Durable**

Soutenue publiquement le 17/12/2018, par :

**Matilde Valeria Solmi**

---

# **Synthèse d'acides carboxyliques à partir de substrats oxygénés, de CO<sub>2</sub> et de H<sub>2</sub>**

---

Devant le jury composé de :

Prof. Albonetti, Stefania  
Prof. Andrioletti, Bruno  
Prof. Centi, Gabriele  
Prof. Claver, Carmen  
Dr. Di Renzo, Francesco  
Prof. Leitner, Walter  
Prof. Palkovits, Regina  
Dr. Quadrelli, Alessandra

Examinatrice  
Examineur  
Rapporteur  
Rapporteuse  
Examineur  
Directeur de thèse  
Examinatrice  
Directrice de thèse

Università di Bologna  
Université Claude Bernard Lyon 1  
Università degli Studi di Messina  
Universitat Rovira i Virgili  
CNRS-ICG Montpellier  
RWTH Aachen University  
RWTH Aachen University  
CNRS-C2P2 Lyon

# UNIVERSITE CLAUDE BERNARD - LYON 1

## **Président de l'Université**

Président du Conseil Académique  
Vice-président du Conseil d'Administration  
Vice-président du Conseil Formation et Vie  
Universitaire  
Vice-président de la Commission Recherche  
Directrice Générale des Services

## **M. le Professeur Frédéric FLEURY**

M. le Professeur Hamda BEN HADID  
M. le Professeur Didier REVEL  
M. le Professeur Philippe CHEVALIER  
M. Fabrice VALLÉE  
Mme Dominique MARCHAND

## **COMPOSANTES SANTE**

Faculté de Médecine Lyon Est – Claude  
Bernard

Directeur : M. le Professeur G.RODE

Faculté de Médecine et de Maïeutique Lyon Sud  
– Charles Mérieux

Directeur : Mme la Professeure C.  
BURILLON

Faculté d'Odontologie

Directeur : M. le Professeur D. BOURGEOIS

Institut des Sciences Pharmaceutiques et  
Biologiques

Directeur : Mme la Professeure C.  
VINCIGUERRA

Institut des Sciences et Techniques de la  
Réadaptation

Directeur : M. X. PERROT

Département de formation et Centre de  
Recherche en Biologie Humaine

Directeur : Mme la Professeure A-M.  
SCHOTT

## **COMPOSANTES ET DEPARTEMENTS DE SCIENCES ET TECHNOLOGIE**

Faculté des Sciences et Technologies

Directeur : M. F. DE MARCHI

Département Biologie

Directeur : M. le Professeur F.  
THEVENARD

Département Chimie Biochimie

Directeur : Mme C. FELIX

Département GEP

Directeur : M. Hassan HAMMOURI

Département Informatique

Directeur : M. le Professeur S. AKKOUCHE

Département Mathématiques

Directeur : M. le Professeur G. TOMANOV

Département Mécanique

Directeur : M. le Professeur H. BEN HADID

Département Physique

Directeur : M. le Professeur J-C PLENET

UFR Sciences et Techniques des Activités  
Physiques et Sportives

Directeur : M. Y. VANPOULLE

Observatoire des Sciences de l'Univers de Lyon  
Polytech Lyon

Directeur : M. B. GUIDERDONI

Directeur : M. le Professeur E. PERRIN

Ecole Supérieure de Chimie Physique  
Electronique

Directeur : M. G. PIGNAULT

Institut Universitaire de Technologie de Lyon 1

Directeur : M. le Professeur C. VITON

Ecole Supérieure du Professorat et de l'Education

Directeur : M. le Professeur A.  
MOUGNIOTTE

Institut de Science Financière et d'Assurances

Directeur : M. N. LEBOISNE

**Vorlage für das Titelblatt beim Einreichen der Pflichtexemplare  
nach bestandener Doktorprüfung**

***Synthesis of Carboxylic Acids from Oxygenated  
Substrates, CO<sub>2</sub> and H<sub>2</sub>***

Von der Fakultät für Mathematik, Informatik und Naturwissenschaften der RWTH  
Aachen  
University zur Erlangung des akademischen Grades einer  
Doktorin der Naturwissenschaften oder einer Doktorin der Ingenieurwissenschaften  
genehmigte Dissertation

vorgelegt von

*„Solmi, Matilde Valeria, M.Sc.“*

aus

*„Modena, Italia“*

Berichter: *Prof. Dr. Walter Leitner*

*Prof. Carmen Claver*

Tag der mündlichen Prüfung: *17-12-2018*

Diese Dissertation ist auf den Internetseiten der Universitätsbibliothek verfügbar.

The present doctoral thesis was mainly carried out at the Institut für Technische und Makromolekulare Chemie (ITMC) of RWTH Aachen University between October 2015 and September 2018 under the supervision of Prof. Dr. Walter Leitner. Part of the thesis was carried out at the UMR5265 – C2P2 (CNRS, CPE Lyon, Université Claude Bernard Lyon 1) between April 2017 and November 2017 under the supervision of Dr. Alessandra Quadrelli. Part of the work was performed at the CAT Center in Aachen between February 2018 and April 2018 under the supervision of Prof. Dr. Walter Leitner.



## **Acknowledgments**

This PhD could not have been completed without the support and encouragement of many people.

At first, I would like to thank Prof. Walter Leitner for being my supervisor during the past 3 years. In particular, I want to acknowledge him for giving me suggestions and support, helping me developing new skills and knowledge.

I am grateful to Dr. Alessandra Quadrelli, for supporting, understanding and helping me during my period in Lyon. Working in her group, helped me improving my personal and professional skills.

In addition, I am particularly thankful to all my colleagues of RWTH Aachen. In particular, I want to thank Marc for the help he gave me from the very beginning until the end of my PhD. Special thanks go to my lab-mates Ole, Ivo, Stefan for making the laboratory 38B 436 such a nice and friendly place and for helping me in technical and personal matters. Many thanks to Philipp, who helped me with everything including the German translations in this thesis. Again, I am really grateful to Ole and Marc for reading this thesis and giving me their suggestions. This thesis would not have been possible without the support of the GC department, the mechanical and electronical workshops and the NMR department. I would like to thank Andrey, Andreas, Ole, Philipp, Lisa, Giuliana, Hannah, Stefan, Alexis, Celine, Sami, Martin, Suman, Karolin, Gilles, Deven, Cesar and all the others who participated during our great lunch debates. Finally, I am grateful I met all the people in the AK Leitner and Klankermayer who made the ITMC a welcoming place every day.

I am equally grateful to the colleagues of the CPE in Lyon. In particular, I want to thank Tapish, Kristin and Pooja for the support and help they always gave me. Thanks to Matthieu for helping me with the French translation, to Marc for the great time we spent together during the French class, to Gleb for the help with the characterization and to Ravi, Clement, Walid, Vittoria, Iurii, Sebastien and Arianna for the amazing time together in Lyon. I would like to thank Laurent and all the people in CPE who made my work easier with their knowledge. A big thank again for Tapish, who gave me his suggestions regarding this thesis and many other things.

I was incredibly lucky to be part of the SINCEM project. Thanks to Prof. Stefania Albonetti for coordinating this project, to Stefanie Mersmann and Markus Hoelscher for helping with the bureaucratic issues and to all the professors and researchers of the project for making it such an exciting environment. I am incredibly thankful to Giuliana,

for being the first one going through this experience, for helping and suggesting me. I want to thank Danilo, Aisha, Pooja, Kristin, Tapish, Ulisse, Chalechew, Akash, Ravi, Daniel, Ana, Payal, Phouc, Olena, Emilia, Alba, Valeriia, Shiming, Iqra, Sonia, Marcelo and all the others who shared with me this amazing experience.

Overall, I am really happy I had the chance to meet so many great friends in Aachen, Lyon and in the SINCHEM network. All of you contributed to make my PhD unforgettable and amazing.

In the end, I want to thank my Italian friends Stefano, Giovanni, Lorenzo, Charlotte, Lidia, Vasco, Anna, Noemi and the others who supported me from far away. I am particularly grateful to Matteo for the help and the encouragement he has given me. Eventually, I want to thank my parents for the support, the help and the inspiration they have always given me.



## **Abstract**

Aliphatic carboxylic acids are used in many industrial sectors and their importance from an economical point of view is increasing. They are currently produced in large quantities, through processes exploiting the mostly non-renewable CO as C1 synthon. Carbon dioxide is a potential environmentally friendly, renewable and abundant C1 building block. The aim of this work is to provide a catalytic protocol converting CO<sub>2</sub>, H<sub>2</sub> and oxygenated substrates to obtain useful chemicals, like carboxylic acids.

To this end a homogeneous catalytic Rh system, used to produce aliphatic carboxylic acids starting from oxygenated substrates, CO<sub>2</sub> and H<sub>2</sub> was investigated and optimized. The system consists of a Rh precursor, iodide additive and PPh<sub>3</sub> ligand working in a batch reactor under CO<sub>2</sub> and H<sub>2</sub> pressure. The reaction conditions were optimized for each class of investigated substrates: primary alcohols, secondary alcohols, ketones, aldehydes and epoxides. The reaction scope was investigated and 30 different molecules were converted into carboxylic acids, leading to yields of up to 80%. In addition, the system was studied using a Design of Experiment approach, obtaining additional information regarding the studied parameters.

The reaction mechanism and the catalytically active species were studied, by different experiments like competitive reactions, NMR and labelling experiments. This investigation resulted in a deeper knowledge of the reaction pathway, composed of some non-catalytic transformations and two catalytic steps. The reaction proceeds through a reverse Water Gas Shift Reaction (rWGS) transforming CO<sub>2</sub> and H<sub>2</sub> into CO and H<sub>2</sub>O, which are consumed in the following hydrocarboxylation of the in-situ formed alkene to give the final carboxylic acid product. The catalytic system is similar to traditional Rh carbonylation and Water Gas Shift catalysts. The PPh<sub>3</sub> is needed to supply additional ligands allowing the catalyst to work in reaction conditions with a minimal amount of toxic CO ligand.

In addition, a heterogeneous catalytic system was investigated for the same reaction. Single atom catalysts (SACs) are receiving much attention as catalytic solution, since they have both the advantages of homogeneous (selectivity, high activity) and heterogeneous (easy separation and recycling) catalysts. Single Rh atoms dispersed on N-doped graphene were synthesized and characterized, obtaining information regarding the chemical and physical structure of the material. Eventually, they were tested as catalysts for CO<sub>2</sub> activation, carboxylic acid production, hydrogenation and hydrogenolysis reactions.



## Zusammenfassung

Aliphatische Carbonsäuren werden in vielen industriellen Bereichen verwendet und ihre wirtschaftliche Bedeutung nimmt zu. Sie werden derzeit in großen Mengen hergestellt, indem das meistens nicht erneuerbare Kohlenmonoxid als C1-Synthon genutzt wird. Kohlendioxid ist ein potenziell umweltfreundlicher, erneuerbarer und abundanter C1-Baustein. Das Ziel dieser Arbeit ist die Entwicklung eines Protokolls zur katalytischen Umwandlung von CO<sub>2</sub>, H<sub>2</sub> und sauerstoffhaltigen Substraten, um nützliche Chemikalien, wie Carbonsäuren zu erhalten.

Zu diesem Zweck wird ein homogenes Rh-Katalysatorsystems zur Herstellung aliphatischer Carbonsäuren aus sauerstoffhaltigen Substraten, CO<sub>2</sub> und H<sub>2</sub> untersucht und optimiert. Das System besteht aus Rh-Präkursor, Iodid-Additiv und PPh<sub>3</sub> als Ligand, die in einem Batchreaktor unter CO<sub>2</sub> und H<sub>2</sub> eingesetzt werden. Die Reaktionsbedingungen wurden für folgende Substratklassen optimiert: primäre Alkohole, sekundäre Alkohole, Ketone, Aldehyde und Epoxide. Es wurden insgesamt 30 verschiedene Substrate mit Ausbeuten bis zu 80% zu Carbonsäuren umgesetzt. Darüber hinaus wurde das System mit einem „Statistische Versuchsplanung“-Ansatz untersucht, um zusätzliche Informationen zu den untersuchten Parametern zu erhalten.

Mechanismus und katalytisch aktive Spezies wurden durch verschiedene Experimente wie Konkurrenzreaktionen, NMR- und Markierungsexperimenten untersucht. Dies erschloss den Reaktionsweg, der aus mehreren nicht-katalytischen Transformationen und zwei katalytischen Schritten besteht. Die Reaktion verläuft durch eine „reverse Wassergas-Shift-Reaktion“ (rWGSR), die CO<sub>2</sub> und H<sub>2</sub> in CO und H<sub>2</sub>O umwandelt. Diese werden wiederum bei der nachfolgenden Hydrocarboxylierung des *in-situ* gebildeten Alkens unter Bildung der Carbonsäure verbraucht. Das katalytische System ähnelt herkömmlichen Rh-Carbonylierungs- und WGSR-Katalysatoren. PPh<sub>3</sub> fungiert als zusätzlicher Ligand, der es dem Katalysator ermöglicht unter den gleichen Reaktionsbedingungen mit minimaler Menge toxischen CO als Liganden zu arbeiten.

Zusätzlich wurde ein heterogenes katalytisches System für die gleiche Reaktion untersucht. „Single atom catalysts“ (SACs) erhalten große Aufmerksamkeit als neue Katalysatorklasse. Sie kombinieren die Selektivität und hohe Aktivität homogener und die einfache Abtrennung und Recycling heterogener Katalysatoren. Verschiedene Katalysatoren aus auf N-dotiertem Graphen dispergierten Rh-Atomen, wurden synthetisiert und charakterisiert. Dadurch wurden Informationen über die chemische und physikalische Struktur des Materials gewonnen und als Katalysatoren für CO<sub>2</sub>-Aktivierung, Carbonsäuresynthese, Hydrierung und Hydrogenolyse getestet.



## Résumé

Les acides carboxyliques aliphatiques sont utilisés dans de nombreux secteurs industriels et leur importance économique augmente. Ils sont actuellement produits en grande quantité, grâce à des procédés utilisant le CO qui est principalement non-renouvelable. L'anhydride carbonique est une molécule potentiellement écologique, renouvelable et abondante. Cette thèse décrit l'étude et l'optimisation d'un système catalytique homogène de Rh, utilisé pour produire des acides carboxyliques aliphatiques à partir de substrats oxygénés, CO<sub>2</sub> et H<sub>2</sub>.

Le système consiste en un précurseur de Rh, un additif à base d'iodure et un ligand PPh<sub>3</sub>, fonctionnant dans un réacteur discontinu sous une pression de CO<sub>2</sub> et de H<sub>2</sub>. Les conditions de réaction ont été optimisées pour chaque classe de substrats étudiés: alcools primaires et secondaires, cétones, aldéhydes et époxydes. 30 molécules différentes ont été converties en acides carboxyliques, conduisant à des rendements jusqu'à 80%. En plus, le système a été étudié avec une approche de « Design of Experiment », ce qui a permis d'obtenir des informations supplémentaires concernant les paramètres étudiés.

Le mécanisme de réaction et les espèces catalytiques actives ont été étudiés par différentes manipulations comme des réactions compétitives, des expériences de RMN et l'utilisation de molécules marquées. La réaction est composée de transformations non catalytiques et de deux étapes catalytiques. La réaction se déroule à travers une réaction de *reverse* Water Gas Shift (*r*WGS) transformant le CO<sub>2</sub> et l'H<sub>2</sub> en CO et H<sub>2</sub>O, qui sont consommés dans l'hydrocarboxylation suivante de l'alcène formé in situ pour livrer l'acide carboxylique. Le système catalytique est similaire aux catalyseurs traditionnels à base du Rh pour les réactions de carbonylation et de Water Gas Shift. Le PPh<sub>3</sub> est nécessaire pour fournir des ligands supplémentaires, permettant au catalyseur de fonctionner avec une quantité minimale de ligand toxique de CO.

En plus, un système catalytique hétérogène a été étudié pour la même réaction. « Single Atom Catalysts » (SACs) reçoit beaucoup plus d'attention que les solutions catalytiques, car il présente à la fois les avantages des catalyseurs homogènes (sélectivité, haute activité) et des catalyseurs hétérogènes (séparation et recyclage faciles). Des atomes de rhodium simples dispersés sur du graphène dopé avec l'N ont été synthétisés et caractérisés, obtenant des informations concernant la structure chimique et physique du matériau. Finalement, ils ont été testés ainsi que les catalyseurs pour l'activation du CO<sub>2</sub>, la production d'acides carboxyliques, les réactions d'hydrogénation et d'hydrogénolyse.



## Summary

### Introduction

#### ***“Introduction” (Chapter 1) and “Literature overview: production of carboxylic acids using CO<sub>2</sub> as building block” (Chapter 2)***

Carboxylic acids are used in many industrial sectors as fuels, polymers and pharmaceutical productions and agrochemical applications among others.<sup>1</sup> In the past years, their importance from an economical point of view is increasing.<sup>1</sup> In particular, aliphatic carboxylic acids are produced in large quantities through aldehydes oxidation or hydroxycarbonylation process. Considering that the aldehydes are produced from alkenes hydroformylation, all the mentioned protocols are based on the toxic and mostly non-renewable CO as C1 synthon. Carbon dioxide is a potential environmental friendly, renewable and abundant C1 building block.<sup>2-5</sup> To implement the production of carboxylic acids using CO<sub>2</sub> instead of CO new catalytic systems and processes have to be developed. CO<sub>2</sub> coupled with H<sub>2</sub> are used in many procedures for the production of different organic molecules, among which carboxylic acids.<sup>2</sup>

In 2013, remarkably, Leitner *et al.* published about a Rhodium-based system, which produces carboxylic acids from simple alkenes with yields up to 91% using CO<sub>2</sub> and H<sub>2</sub> in a formal hydrocarboxylation. Mechanistic and labelling studies suggest the *in-situ* formation of CO and H<sub>2</sub>O by *reverse* Water Gas Shift (*r*WGSR), which proceeds in a hydroxycarbonylation. The reaction requires acidic conditions, an iodide promoter (likewise the Monsanto process) and PPh<sub>3</sub> as ligand, but no organometallic stoichiometric additives.<sup>6</sup> Leitner and co-workers provided the first example of transformation of alcohols with CO<sub>2</sub> and H<sub>2</sub>, without the need of a stoichiometric organometallic additive, although the yields in carboxylic acids starting from alcohols are little lower (up to 74%) than the yields obtained from alkenes.<sup>6</sup> The *in-situ* production of CO via *r*WGSR is a remarkable way to replace the use of high amount of toxic reagent and to exploit a renewable, non-toxic and waste resource as CO<sub>2</sub>. Already few protocols using this approach were published. In particular, examples of carboxylation-, alkoxy carbonylation- or hydroformylation reactions were presented.<sup>7-11</sup>

Nevertheless, few protocols deal with the production of carboxylic acids from oxygenated substrates and CO<sub>2</sub>. They mainly deal with aromatic or allylic substrates and they require the addition of (over)-stoichiometric organometallic reducing agents.<sup>1</sup>

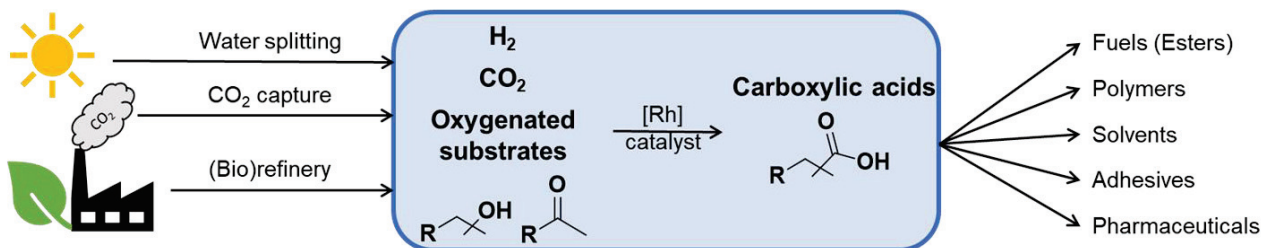


Figure I: Schematic representation of the process reported in this thesis (blue box). Ideally, CO<sub>2</sub> can be obtained from wastes fluxes coming from industrial productions. H<sub>2</sub> can be obtained by H<sub>2</sub>O splitting, using renewable energy. Oxygenated substrates are highly available, both from the traditional petrochemical productions and new bio-refinery processes. As explained in the next session, carboxylic acids can be used in different industrial sector to produce useful goods.

The aim of this work is to provide a catalytic protocol converting CO<sub>2</sub>, H<sub>2</sub> and oxygenated substrates to obtain useful chemicals as carboxylic acids (Figure). Oxygenated substrates (alcohols, ketones, aldehydes and epoxides) are readily available and common molecules which are produced from the petrochemical refinery and the bio-refinery productions. The system was deeply investigated also from a mechanistic point of view. Single atom catalysts were produced and tested for the studied reaction as well as for other interesting transformations.

## Results and discussion

### ***Optimization of the homogeneous catalytic system for the synthesis of carboxylic acids from oxygenated substrates (Chapter 3)***

From the initial study of the system, many different parameters showed an influence on the final yield of carboxylic acids. The solvent and dilution, the temperature and the pressure influence the result. Moreover, the acidic additive (*p*-TsOH•H<sub>2</sub>O), the amount of CHI<sub>3</sub> and PPh<sub>3</sub> and the precursor used can vary the efficiency of the system. The Design of Experiment approach allowed to understand the correlations between the chosen parameters (temperature, volume of acetic acid, amount of CHI<sub>3</sub> and *p*-TsOH•H<sub>2</sub>O) and to prove their importance for the yield in carboxylic acids obtained from oxygenated substrates, CO<sub>2</sub> and H<sub>2</sub>. Moreover, it was verified that the best reaction conditions are found in between the chosen range.

Different substrates require different reaction conditions to achieve good conversion into the desired carboxylic acids, therefore different optimization processes were



performed for each class of substrate. A selection of substrates conversions and the corresponding carboxylic acid yields are reported in Table I.

Butanol (BuOH) was used as model substrate for the optimization of the reaction parameters, being the smaller alcohol having all the possible isomers (1-Butanol, 2-Butanol and *tert*-Butanol). The optimized reaction conditions for 1-BuOH allowed to obtain a yield in VA (valeric acid) and 2-MBA (2-methylbutanoic acid) of 64% (ratio of VA:2-MBA = 2:1), which is more than the double of the one obtained using previously reported conditions.<sup>12</sup> The optimized conditions for 2-BuOH differ from the optimized one for primary alcohols in the amount of solvent used, the presence of *p*-TsOH•H<sub>2</sub>O and the H<sub>2</sub> pressure. The yield reached at the end of the optimization procedure is 77% (ratio of VA:2-MBA = 2:1) which is much higher compared to the one obtained during our preliminary study and the highest reported until now with a similar system. The same developed reaction conditions can be used for the conversion of *tert*-BuOH leading to a yield in isovaleric acid of 44%.

The new conditions developed for ketones lead to a total yield of 83%, which is the best obtained starting directly from ketones, up to now. The optimized reaction conditions differ from those used for the secondary alcohols transformation only in the amount of H<sub>2</sub> used (20 bar instead of 10 bar). The pressure uptake measurement shows that higher pressure of hydrogen is needed in order to first reduce the ketone to the alcohol, which undergoes to the following transformation in carboxylic acid.

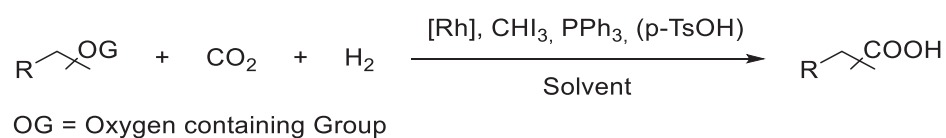
The first example of synthesis of carboxylic acids starting directly from aldehyde, CO<sub>2</sub> and H<sub>2</sub> is reported. Good results are obtained, with a total yield of 45% and no additional reagent is required to perform the transformation. As for ketones, the optimized conditions require more H<sub>2</sub> pressure compared to the primary alcohols one (30 bar are used for converting the aldehyde and 20 bar of H<sub>2</sub> are used for the conversion of primary alcohols). The other reaction parameters are set as for primary alcohols conversion. Also in this case, the first step seems to be the formation of the primary alcohol which is further transformed in the carboxylic acid.

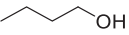
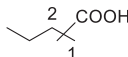
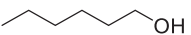
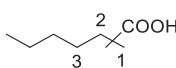
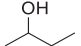
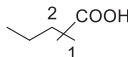
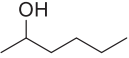
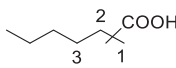
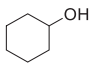
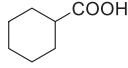
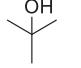
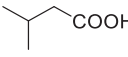
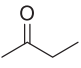
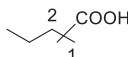
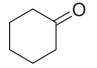
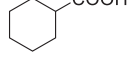
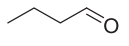
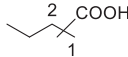
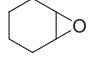
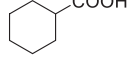
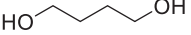
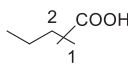
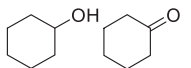
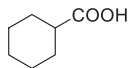
Epoxides are also suitable for the hydrocarboxylation reaction in presence of Rh catalyst. For the first time, the synthesis of carboxylic acid (with a yield of 60%) was achieved. In this case, a change of solvent was necessary. Epoxides polymerize and oligomerize quickly in acidic conditions, therefore toluene was used as substitute of the acetic acid solvent.

Bifunctional substrates (i.e. diols) were converted in the mono carboxylic acids, giving yields up to 42%.

Eventually, mixtures of substrates were converted in the corresponding mixtures of carboxylic acids successfully.

Table I: Examples of hydrocarboxylation of different oxygenated substrates.



Entry	Substrate	Conv. (%)	Products	Yields (%)
1 <sup>[a]</sup>		99		66
2 <sup>[a]</sup>		>99		64
3 <sup>[b]</sup>		>99		77
4 <sup>[b]</sup>		>99		66
5 <sup>[b]</sup>		>99		80
6 <sup>[b]</sup>		>99		44
7 <sup>[c]</sup>		99		54
8 <sup>[c]</sup>		99		83
9 <sup>[d]</sup>		99		45
10 <sup>[e]</sup>		99		66
11 <sup>[a]</sup>		99		42
13 <sup>[c]</sup>		99		79

---

[a] Reaction conditions: 1.88 mmol of substrate, 92  $\mu\text{mol}$  Rh, 1 ml of acetic acid, 2.5 mol/mol<sub>Rh</sub> of  $\text{CHI}_3$ , 5 mol/mol<sub>Rh</sub> of  $\text{PPh}_3$ , 20 bar  $\text{CO}_2$ , 20 bar  $\text{H}_2$ , 160 °C. [b] Reaction conditions: 1.88 mmol of substrate, 92  $\mu\text{mol}$  Rh, 2 ml of acetic, 3.5 mol/mol<sub>Rh</sub>  $p\text{-TsOH}\cdot\text{H}_2\text{O}$ , 2.5 mol/mol<sub>Rh</sub> of  $\text{CHI}_3$ , 5 mol/mol<sub>Rh</sub> of  $\text{PPh}_3$ , 20 bar  $\text{CO}_2$ , 10 bar  $\text{H}_2$ , 160 °C. [c] Reaction conditions: 1.88 mmol of substrate, 92  $\mu\text{mol}$  Rh, 2 ml of acetic acid, 3.5 mol/mol<sub>Rh</sub>  $p\text{-TsOH}\cdot\text{H}_2\text{O}$ , 2.5 mol/mol<sub>Rh</sub> of  $\text{CHI}_3$ , 5 mol/mol<sub>Rh</sub> of  $\text{PPh}_3$ , 20 bar  $\text{CO}_2$ , 20 bar  $\text{H}_2$ , 160 °C. [d] Reaction conditions: 1.88 mmol of substrate, 92  $\mu\text{mol}$  Rh, 1 ml of acetic acid, 2.5 mol/mol<sub>Rh</sub> of  $\text{CHI}_3$ , 5 mol/mol<sub>Rh</sub> of  $\text{PPh}_3$ , 20 bar  $\text{CO}_2$ , 30 bar  $\text{H}_2$ , 160 °C. [e] Reaction conditions: 1.88 mmol Cyclohexane Oxide, 46  $\mu\text{mol}$   $[\text{RhCl}(\text{CO})_2]_2$ , 2.5 eq. of  $\text{CHI}_3$ , 2 ml of toluene, 3.5 mol/mol<sub>Rh</sub> of  $p\text{-TsOH}\cdot\text{H}_2\text{O}$  and 160 °C.

### ***Mechanistic investigation and reaction pathway (Chapter 4)***

The understanding of mechanisms and of the catalytic active species can give new input to the optimization of the overall process. Knowing the deactivation pathway of a catalyst and which the important steps are in a catalytic cycle can help the future research on the topic. Hence, the reaction mechanism and the catalytic active species were studied, by different experiments like competitive reactions, NMR and labelling experiments. This investigation brought to a deeper knowledge of the reaction pathway composed of some non-catalytic transformations and two catalytic steps.

The reaction conditions (acidity, temperature and additives present) lead to transformations which happen even in absence of the catalyst. These transformations involve the alcohol (starting material or intermediate) reacting with the other component of the reaction mixture. Even without the addition of the Rh precursor, alkyl-iodide, acetate and alkene are formed. In addition to these compounds, traces of completely hydrogenated alkane are found as well.

The Rh system catalyzes the conversion of  $\text{CO}_2$  and  $\text{H}_2$  into CO and  $\text{H}_2\text{O}$  (rWGS). The system is able to perform the rWGS giving up to 3% yield of CO. In addition to the Rh, the presence of the iodide additive ( $\text{CHI}_3$ ) results crucial. On the other hand, its amount need to be controlled in order to avoid the deactivation of the system if too much of it is added. On the contrary, the  $\text{PPh}_3$  ligand is not significantly influencing the yield of CO, especially when it is not used. Although the amount of CO produced is not high, the result is still good considering the mild conditions used.

The same Rh system can catalyze the hydroxycarbonylation (using CO and  $\text{H}_2\text{O}$ ) of the alcohols. In particular, the yield and the regio-selectivity of the produced carboxylic acids are the same using the amount of CO and  $\text{H}_2\text{O}$  produced by the system (in absence of  $\text{CO}_2$  and  $\text{H}_2$ ) using  $\text{CO}_2$  and  $\text{H}_2$ . Competitive experiments and labelling experiments confirmed that the second step is an alkenes hydroxycarbonylation.

Therefore, the optimized reaction conditions must be different depending on the class of oxygenated substrates which have to be transformed. They have to allow the formation of enough alkene with a rate capable to overcome secondary reactions. As for the *r*WGS,  $\text{CHI}_3$  has a major influence on the yield of carboxylic acids and its amount has to be carefully balanced. On the contrary,  $\text{PPh}_3$  is not crucial for the reaction and carboxylic acids are produced even in absence of it.

The reaction proceeds through a *reverse* Water Gas Shift Reaction (*r*WGS) transforming  $\text{CO}_2$  and  $\text{H}_2$  into  $\text{CO}$  and  $\text{H}_2\text{O}$ , which are consumed in the following hydrocarboxylation of the *in-situ* formed alkene to give the final carboxylic acid product. The catalytic system is similar to traditional Rh carbonylation and Water Gas Shift catalysts.<sup>13, 14</sup> The two catalytic cycles have already been reported in previous literature work on Rh homogeneous catalysis. Their unification allows the production of the carboxylic acid starting directly from an important green reagent, such as  $\text{CO}_2$ . In this context, the addition of an additional ligand the  $\text{PPh}_3$  is crucial for the success of the transformation. The  $\text{PPh}_3$  is needed to supply additional ligands allowing the catalyst to work in reaction conditions with minimal amount of toxic  $\text{CO}$  as ligand. A full reaction pathway and catalytic cycles are reported in Figure 1-1.

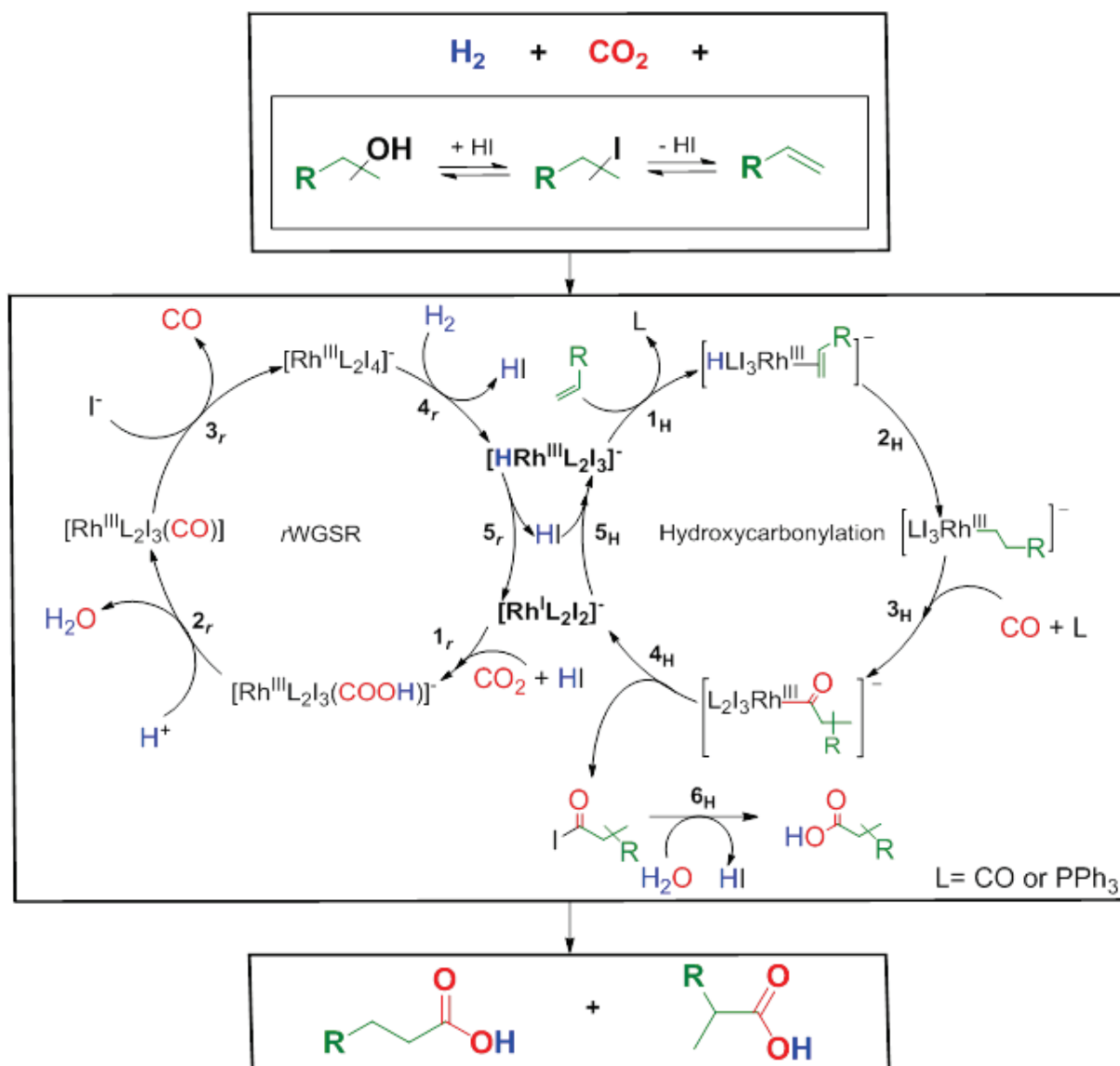


Figure 1-1: Proposed mechanism for the hydrocarboxylation of alcohols.

The proposed **rwgSR** cycle consists of 5 ( $1_r$  -  $5_r$ ) steps:  $1_r$ ) coordination of  $\text{CO}_2$  and  $\text{HI}$  to the  $[\text{RhL}_2\text{I}]^-$  and formation of a metallacarboxylic acid;  $2_r$ ) degradation of  $\text{Rh-COOH}$  releasing  $\text{H}_2\text{O}$  and leaving the  $\text{CO}$  group originating from  $\text{CO}_2$  on the  $\text{Rh}$ ;  $3_r$ ) substitution of the  $\text{CO}$  ligand by a  $\text{I}^-$  leading to the species  $[\text{RhL}_2\text{I}_4]^-$ ;  $4_r$ ) activation of  $\text{H}_2$ , forming the metal hydride species  $[\text{HRhL}_2\text{I}_3]^-$ ;  $5_r$ ) reduction to  $\text{Rh}^{\text{I}}$  after the reductive elimination of  $\text{HI}$ .

The proposed **hydroxycarbonylation** cycle consists of 5 ( $1_H$  -  $5_H$ ) steps and a non-catalytic one ( $6_H$ ):  $1_H$ )  $[\text{HRhL}_2\text{I}_3]^-$  generated via  $\text{H}_2$  activation coordinates the alkene intermediate substituting a ligand;  $2_H$ ) insertion of the alkene in the  $\text{Rh-H}$  bond forming the alkyl- $\text{Rh}$  species;  $3_H$ )  $\text{CO}$  coordination and migratory insertion into the  $\text{Rh-alkyl}$  bond;  $4_H$ ) reductive elimination of the acyl iodide;  $5_H$ ) oxidative addition of  $\text{HI}$  regenerating the  $\text{Rh}^{\text{III}}$  species  $[\text{HRhL}_2\text{I}_3]^-$ ;  $6_H$ ) nucleophilic substitution of the acyl iodide giving the carboxylic acid.

## Single atom catalysts (SACs) (Chapter 5)

Single atoms supported on a solid material are receiving much attention as catalytic solution, since they have both the advantages of homogeneous and heterogeneous catalysts. Ideally, they show high selectivity and activity as homogeneous catalysts, but they are also easy to recover and recycle as heterogeneous catalysts.<sup>15-18</sup> Examples of supported Rh SACs active for the *m*WGS<sup>19</sup> and hydroformylation<sup>18, 20</sup> reaction were reported.

Carbon materials (graphene<sup>21-24</sup>, doped graphene<sup>21, 25-27</sup>, activated carbon<sup>27, 28</sup>, g-C<sub>3</sub>N<sub>4</sub><sup>29</sup>, etc.) are promising supports for single metal atoms. In these supports, the metal is often found in the structure's defects and is stabilized by an electron donation from the support.<sup>16, 17, 30</sup> For this reason, in this study, this type of supports was used, inserting N and/or P atoms in the lattice. Using simple wet chemistry methods, many materials were synthesized.

The used characterization techniques allowed the analysis of the Rh dispersion on the supports, revealing the presence of single atom catalysts (SACs) on samples with Rh loading equal or lower than 0.1% (wt %). The isolated Rh atoms supported on N-doped thermal treated graphene oxide (sample 0.1Rh-GN) are highlighted in the HAADF-STEM image reported in Figure 1-2.

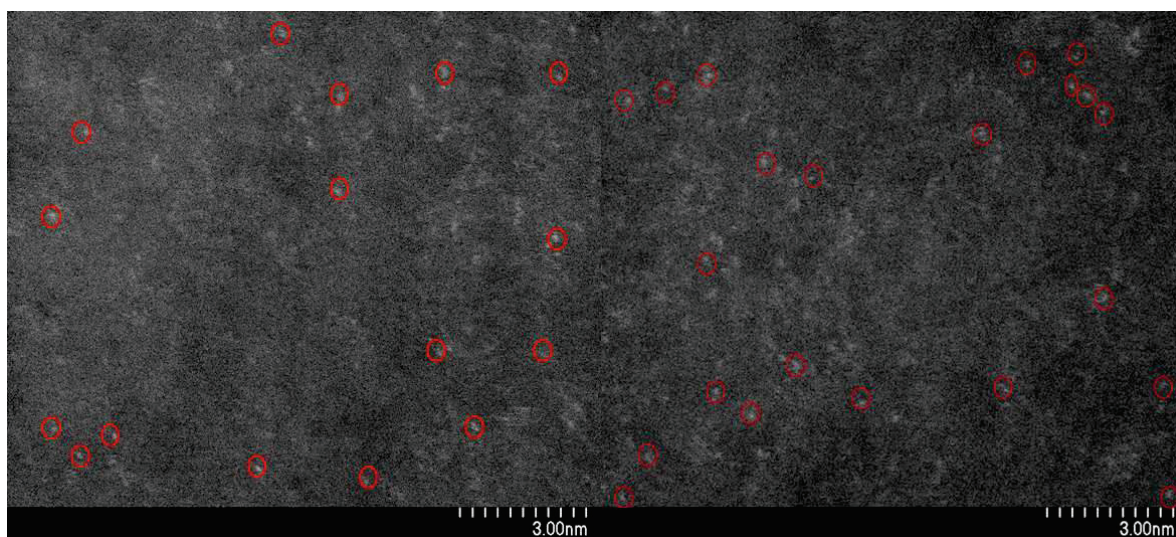


Figure 1-2: HAADF-STEM images of the sample 0.1Rh-GN.

The samples prepared with higher amount of Rh (1%) present nanoparticles well dispersed on the solid surface. The dimension of the nanoparticles depends on the heteroatom-doping. N-doping leads to Rh nanoparticles with an average diameter of

4.2 ( $\pm$  3) nm. P-doping leads to Rh nanoparticles with an average diameter of 3.1 ( $\pm$  2) nm.

The thermal treatments performed on the original GO lead to different materials: thermally processed GO or heteroatom-doped graphene-like materials. The presence of the metal leads to the production of different bonds in the final materials. For instance, the presence of the Rh facilitates the insertion of the N dopant in the carbon lattice.

The materials synthesized contain potentially highly active single Rh atoms dispersed on a tunable support such as doped graphene oxide. Unfortunately, they do not result active for the *r*WGS or for the hydrocarboxylation reaction. Alkenes or aromatic hydrogenation are not catalyzed by these materials. They seem promising catalysts for interesting hydrogenolysis reactions. In particular, they were able to give TON of 22758 converting the cyclohexane oxide into cyclohexanol (yield 25%). Nevertheless, further studies on the catalytic activity should be performed.

## Conclusions and outlook

Overall, a new way to exploit CO<sub>2</sub> as C<sub>1</sub> building block to produce valuable compounds such as carboxylic acids has been designed. The goal of producing carboxylic acids with an innovative and theoretically more sustainable way is achieved using a large variety of oxygenated non-activated organic substrates, which are available both from the traditional petrochemical refinery and bio-refinery. The system described in this thesis can convert the CO<sub>2</sub> using only H<sub>2</sub> as reducing agent and no stoichiometric organometallic reagent. In addition, the use of a highly active Rh molecular catalyst allows performing the transformation in relatively mild conditions.

Besides, the deeper knowledge gained regarding the catalytic cycle and the active species could lead to a more analytical and aware development for further applications. Increasing the TON, the selectivity, the scale and the substrate scope (i.e. including aromatic compounds and methanol) are improvements of the system which can profit this knowledge.

Potentially highly active heterogeneous catalysts were synthesized and characterized. The synthetic protocol and the knowledge gained from the characterization can lead to the development of more and diverse materials. The produced materials can be used in the future for the development of protocols toward selective conversions.

## References

1. M. V. Solmi, M. Schmitz and W. Leitner, in *Horizons in Sustainable Industrial Chemistry and Catalysis*, eds. S. Albonetti, S. Perathoner and E. A. Quadrelli, Elsevier, In press.
2. W. Leitner and J. Klankermayer, *Science*, 2015, **350**, 629-630.
3. J. Klankermayer, S. Wesselbaum, K. Beydoun and W. Leitner, *Angew. Chem. Int. Ed.*, 2016.
4. J. Artz, T. E. Muller, K. Thenert, J. Kleinekorte, R. Meys, A. Sternberg, A. Bardow and W. Leitner, *Chem. Rev.*, 2018, **118**, 434–504.
5. G. Centi, E. A. Quadrelli and S. Perathoner, *Energy Environ. Sci.*, 2013, **6**, 1711.
6. T. G. Ostapowicz, M. Schmitz, M. Krystof, J. Klankermayer and W. Leitner, *Angew. Chem. Int. Ed.*, 2013, **52**, 12119-12123.
7. K. Dong and X. F. Wu, *Angew. Chem. Int. Ed.*, 2017.
8. E. Kirillov, J. F. Carpentier and E. Bunel, *Dalton Trans.*, 2015, **44**, 16212-16223.
9. L. Wu, Q. Liu, R. Jackstell and M. Beller, *Angew. Chem. Int. Ed.*, 2014, **53**, 6310-6320.
10. L. Wu, Q. Liu, I. Fleischer, R. Jackstell and M. Beller, *Nat. Commun.*, 2014, **5**.
11. M. D. Porosoff, B. Yan and J. G. Chen, *Energy Environ. Sci.*, 2016, **9**, 62-73.
12. M. Schmitz, PhD, RWTH Aachen University, 2018.
13. D. Forster, A. Hershman and D. E. Morris, *Catalysis Reviews*, 1981, **23**, 89-105.
14. E. C. Baker, D. E. Hendriksen and R. Eisenberg, *J. Am. Chem. Soc.*, 1980, **102**, 1020-1027.
15. H. Yan, C. Su, J. He and W. Chen, *Journal of Materials Chemistry A*, 2018, **6**, 8793-8814.
16. X.-F. Yang, A. Wang, B. Qiao, J. Li, J. Liu and T. Zhang, *Acc. Chem. Res.*, 2013, **46**, 1740-1748.
17. S. Liang, C. Hao and Y. Shi, *ChemCatChem*, 2015, **7**, 2559-2567.
18. R. Lang, T. Li, D. Matsumura, S. Miao, Y. Ren, Y. T. Cui, Y. Tan, B. Qiao, L. Li, A. Wang, X. Wang and T. Zhang, *Angew. Chem. Int. Ed.*, 2016, **55**, 16054-16058.
19. J. C. Matsubu, V. N. Yang and P. Christopher, *J. Am. Chem. Soc.*, 2015, **137**, 3076-3084.
20. L. Wang, W. Zhang, S. Wang, Z. Gao, Z. Luo, X. Wang, R. Zeng, A. Li, H. Li, M. Wang, X. Zheng, J. Zhu, W. Zhang, C. Ma, R. Si and J. Zeng, *Nat. Commun.*, 2016, **7**, 14036.
21. D. Deng, X. Chen, L. Yu, X. Wu, Q. Liu, Y. Liu, H. Yang, H. Tian, Y. Hu, P. Du, R. Si, J. Wang, X. Cui, H. Li, J. Xiao, T. Xu, J. Deng, F. Yang, P. N. Duchesne, P. Zhang, J. Zhou, L. Sun, J. Li, X. Pan and X. Bao, *Sci. Adv.*, 2015, **1**, e1500462/1500461-e1500462/1500469.
22. H. Yan, H. Cheng, H. Yi, Y. Lin, T. Yao, C. Wang, J. Li, S. Wei and J. Lu, *J. Am. Chem. Soc.*, 2015, **137** 10484–10487.



23. L. Xu, L.-M. Yang and E. Ganz, *Theor. Chem. Acc.*, 2018, **137**.
24. C. Gao, S. Chen, Y. Wang, J. Wang, X. Zheng, J. Zhu, L. Song, W. Zhang and Y. Xiong, *Adv. Mater.*, 2018, **30**, e1704624.
25. C. Zhang, J. Sha, H. Fei, M. Liu, S. Yazdi, J. Zhang, Q. Zhong, X. Zou, N. Zhao, H. Yu, Z. Jiang, E. Ringe, B. I. Yakobson, J. Dong, D. Chen and J. M. Tour, *ACS Nano*, 2017.
26. H. Fei, J. Dong, M. J. Arellano-Jiménez, G. Ye, N. Dong Kim, E. L. G. Samuel, Z. Peng, Z. Zhu, F. Qin, J. Bao, M. J. Yacaman, P. M. Ajayan, D. Chen and J. M. Tour, *Nature Communication*, 2015, **6**, 1-8.
27. W. Liu, Y. Chen, H. Qi, L. Zhang, W. Yan, X. Liu, X. Yang, S. Miao, W. Wang, C. Liu, A. Wang, J. Li and T. Zhang, *Angew. Chem. Int. Ed.*, 2018, **57**, 7071-7075.
28. Y. Chen, S. Ji, Y. Wang, J. Dong, W. Chen, Z. Li, R. Shen, L. Zheng, Z. Zhuang, D. Wang and Y. Li, *Angew. Chem. Int. Ed.*, 2017, **56**, 6937-6941.
29. W. Liu, L. Cao, W. Cheng, Y. Cao, X. Liu, W. Zhang, X. Mou, L. Jin, X. Zheng, W. Che, Q. Liu, T. Yao and S. Wei, *Angew. Chem. Int. Ed.*, 2017.
30. S. Back, J. Lim, N.-Y. Kim, Y.-H. Kim and Y. Jung, *Chem Sci*, 2017, **8**, 1090-1096.

## Résumé substantielle

### Introduction

**«Introduction» (Chapitre 1) et «Aperçu de la littérature: production d'acides carboxyliques en utilisant le CO<sub>2</sub> comme élément constitutif» (Chapitre 2)**

Les acides carboxyliques sont utilisés dans de nombreux secteurs industriels comme les combustibles, les polymères, les produits pharmaceutiques et entre autre pour des applications en agrochimie.<sup>1</sup> Ces dernières années, leur importance économique a augmenté.<sup>1</sup> En particulier, les acides carboxyliques aliphatiques sont produits en grande quantité par oxydation des aldéhydes ou par un procédé d'hydroxycarbonylation. Sachant que les aldéhydes sont produits à partir de l'hydroformylation des alcènes, tous les protocoles mentionnés sont basés sur le CO toxique et principalement non renouvelable sous forme de building block C1. Le dioxyde de carbone est un élément constitutif C1 (keep building block) potentiellement respectueux de l'environnement, renouvelable et abondant.<sup>2-5</sup> Afin de produire des acides carboxyliques en utilisant du CO<sub>2</sub> au lieu du CO, de nouveaux procédés et systèmes catalytiques doivent être développés. Le CO<sub>2</sub> couplé à l'H<sub>2</sub> est utilisé dans de nombreuses procédures pour la production de différentes molécules organiques, parmi lesquelles les acides carboxyliques.<sup>2</sup>

En 2013, Leitner *et al.* ont publié un système à base de rhodium qui produit des acides carboxyliques à partir d'oléfines simples avec des rendements allant jusqu'à 91% en utilisant le CO<sub>2</sub> et l'H<sub>2</sub> dans une hydrocarboxylation formelle. Des études mécanistiques et des études de marquage suggèrent la formation *in-situ* de CO et de H<sub>2</sub>O par un procédé de « *reverse Water Gas Shift Reaction (rWGSR)* » qui se déroule dans une hydroxycarbonylation. La réaction nécessite des conditions acides, un promoteur iodure (comme le procédé Monsanto) et le PPh<sub>3</sub> comme ligand, mais aucun additif stœchiométrique organométallique.<sup>6</sup> Leitner et ses collaborateurs ont fourni le premier exemple de transformation d'alcools avec CO<sub>2</sub> et H<sub>2</sub>, sans nécessiter d'additif stœchiométrique organométallique, bien que les rendements en acides carboxyliques à partir d'alcools soient légèrement inférieurs (jusqu'à 74%) aux rendements obtenus à partir d'oléfines.<sup>6</sup> La production *in-situ* de CO *via* rWGSR est un moyen remarquable de remplacer l'utilisation de grandes quantités de réactif toxique et d'exploiter une ressource renouvelable, non toxique et une ressource de déchet sous forme de CO<sub>2</sub>.

Peu de protocoles utilisant cette approche ont été publiés. En particulier, des exemples de réactions de carboxylation, d'alcoycarbonylation ou d'hydroformylation ont été présentés.<sup>7-11</sup>

Néanmoins, peu de protocoles s'intéressent à la production d'acides carboxyliques à partir de substrats oxygénés et de CO<sub>2</sub>. Ils utilisent principalement des substrats aromatiques ou allyliques et nécessitent l'ajout d'agents réducteurs organométalliques dans des proportions stoechiométriques.<sup>1</sup>

Le but de ce travail est de fournir un protocole catalytique permettant de convertir le CO<sub>2</sub>, l'H<sub>2</sub> et les substrats oxygénés pour obtenir des produits chimiques utiles comme d'acides carboxyliques (Figure). Les substrats oxygénés (alcools, cétones, aldéhydes et époxydes) sont des molécules facilement disponibles et communes qui sont produites par des raffineries pétrochimiques et des productions de bio-raffinerie. Le système a également fait l'objet d'une étude approfondie d'un point de vue mécanistique. Des catalyseurs à un seul atome ont été produits et testés pour la réaction étudiée ainsi que pour d'autres transformations intéressantes.

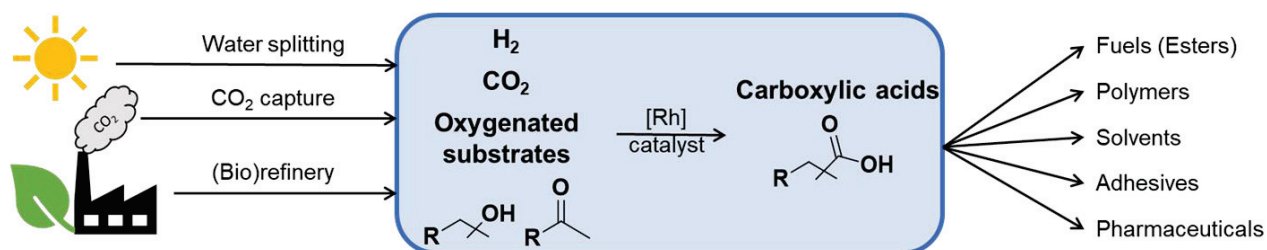


Figure 1: Représentation schématique du processus développé dans cette thèse (encadré bleu). Idéalement, le CO<sub>2</sub> peut être obtenu à partir de flux de déchets provenant de productions industrielles. Le H<sub>2</sub> peut être obtenu par fractionnement de H<sub>2</sub>O en utilisant une énergie renouvelable. Les substrats oxygénés sont abondants, aussi bien dans les productions pétrochimiques traditionnelles que dans les nouveaux procédés de bio-raffinage. Comme expliqué dans la prochaine session, les acides carboxyliques peuvent être utilisés dans différents secteurs industriels pour produire des biens utiles.

## Résultats et discussion

### *Optimisation du système catalytique homogène pour la synthèse d'acides carboxyliques à partir de substrats oxygénés (Chapitre 3)*

A partir de l'étude initiale du système, différents paramètres ont montré une influence sur le rendement final en acides carboxyliques. Le solvant et la dilution, la température et la pression influencent le résultat. De plus, l'additif acide (*p*-TsOH•H<sub>2</sub>O),

la quantité de  $\text{CHI}_3$  et de  $\text{PPh}_3$  et le précurseur utilisé peuvent modifier l'efficacité du système. L'approche « Design of Experiment » a permis de comprendre les corrélations entre les paramètres choisis (température, volume d'acide acétique, quantité de  $\text{CHI}_3$  et  $p\text{-TsOH}\cdot\text{H}_2\text{O}$ ) et de prouver leur importance pour le rendement en acides carboxyliques obtenus à partir de substrats oxygénés,  $\text{CO}_2$  et  $\text{H}_2$ . De plus, il a été vérifié que les meilleures conditions de réaction se situaient entre la plage choisie.

Différents substrats nécessitent des conditions de réaction différentes pour obtenir une bonne conversion en acides carboxyliques souhaités, par conséquent, différents processus d'optimisation ont été effectués pour chaque classe de substrat. Une sélection de conversions de substrats et les rendements en acide carboxylique correspondants sont rapportés dans le tableau I.

Le butanol ( $\text{BuOH}$ ) a été utilisé comme substrat modèle pour l'optimisation des paramètres de réaction, étant le plus petit alcool ayant tous les isomères possibles (1-butanol, 2-butanol et tert-butanol). Les conditions réactionnelles optimisées pour 1-BuOH ont permis d'obtenir un rendement en AP (acide pentanoïque) et en 2-MBA (acide 2-méthylbutanoïque) de 64% (rapport AP: 2-MBA = 2: 1), ce qui est deux fois plus importants en comparaison aux conditions précédemment rapportées.<sup>12</sup> Les conditions optimisées pour 2-BuOH diffèrent de celles optimisées pour les alcools primaires dans la quantité de solvant utilisée, la présence de  $p\text{-TsOH}\cdot\text{H}_2\text{O}$  et la pression de  $\text{H}_2$ . Le rendement atteint à l'issue de la procédure d'optimisation est de 77% (ratio VA:2-MBA = 2:1), ce qui est beaucoup plus élevé que celui obtenu lors de notre étude préliminaire et le plus élevé jusqu'à présent avec un système similaire. Les mêmes conditions de réaction développées peuvent être utilisées pour la conversion du *tert*-BuOH conduisant à un rendement en acide isovalérique de 44%.

Les nouvelles conditions développées pour les cétones conduisent à un rendement total de 83%, ce qui est le meilleur résultat obtenu directement à partir des cétones jusqu'à présent. Les conditions réactionnelles optimisées ne diffèrent de celles utilisées pour la transformation des alcools secondaires que dans la quantité de  $\text{H}_2$  utilisée (20 bars au lieu de 10 bars). La mesure de l'absorption de pression montre qu'une pression d'hydrogène plus élevée est nécessaire pour réduire d'abord la cétone en alcool, lequel subit la transformation suivante en acide carboxylique.

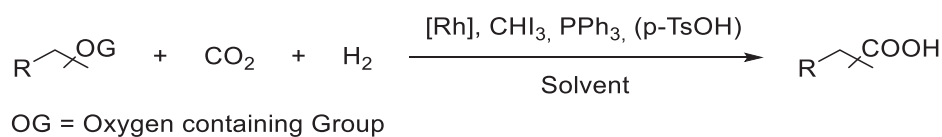
Le premier exemple de synthèse d'acides carboxyliques à partir directement d'aldéhyde,  $\text{CO}_2$  et  $\text{H}_2$  est rapporté. De bons résultats sont obtenus avec un rendement total de 45% et aucun réactif supplémentaire n'est requis pour effectuer la

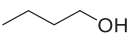
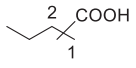
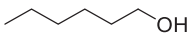
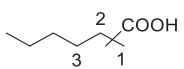
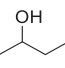
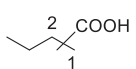
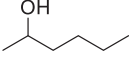
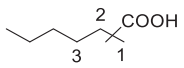
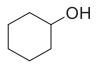
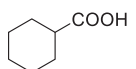
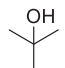
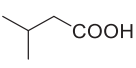
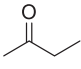
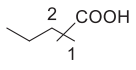
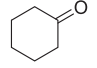
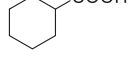
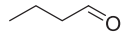
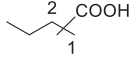
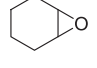
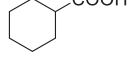
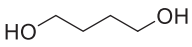
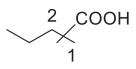
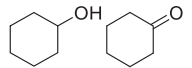
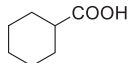
transformation. En ce qui concerne les cétones, les conditions optimisées requièrent une pression de H<sub>2</sub> supérieure à celle des alcools primaires (30 bars sont utilisés pour convertir les aldéhydes et 20 bars de H<sub>2</sub> pour la conversion des alcools primaires). Les autres paramètres de réaction sont définis comme pour la conversion des alcools primaires. Dans ce cas également, la première étape semble être la formation de l'alcool primaire qui est encore transformé dans l'acide carboxylique. Les époxydes conviennent également à la réaction d'hydrocarboxylation en présence d'un catalyseur Rh. Pour la première fois, la synthèse de l'acide carboxylique (avec un rendement de 60%) a été réalisée. Dans ce cas, un changement de solvant était nécessaire. Les époxydes polymérisent et oligomérisent rapidement dans des conditions acides, par conséquent, du toluène est utilisé comme substitut du solvant de l'acide acétique.

Les substrats bifonctionnels (c'est-à-dire les diols) ont été convertis en acide monocarboxylique, donnant des rendements allant jusqu'à 42%.

Finalement, les mélanges de substrats ont été convertis avec succès en des mélanges d'acides carboxyliques.

Tableau I: Exemples d'hydrocarboxylation de différents substrats oxygénés.



Entry	Substrate	Conv. (%)	Products	Yields (%)
1 <sup>[a]</sup>		99		66
2 <sup>[a]</sup>		>99		64
3 <sup>[b]</sup>		>99		77
4 <sup>[b]</sup>		>99		66
5 <sup>[b]</sup>		>99		80
6 <sup>[b]</sup>		>99		44
7 <sup>[c]</sup>		99		54
8 <sup>[c]</sup>		99		83
9 <sup>[d]</sup>		99		45
10 <sup>[e]</sup>		99		66
11 <sup>[a]</sup>		99		42
13 <sup>[c]</sup>		99		79

[a] Conditions de réaction: 1.88 mmol of substrate, 92  $\mu\text{mol}$  Rh, 1 ml of acetic acid, 2.5 mol/mol<sub>Rh</sub> of  $\text{CHI}_3$ , 5 mol/mol<sub>Rh</sub> of  $\text{PPh}_3$ , 20 bar  $\text{CO}_2$ , 20 bar  $\text{H}_2$ , 160 °C. [b] Conditions de réaction: 1.88 mmol of substrate, 92  $\mu\text{mol}$  Rh, 2 ml of acetic, 3.5 mol/mol<sub>Rh</sub>  $p\text{-TsOH}\cdot\text{H}_2\text{O}$ , 2.5 mol/mol<sub>Rh</sub> of  $\text{CHI}_3$ , 5 mol/mol<sub>Rh</sub> of  $\text{PPh}_3$ , 20 bar  $\text{CO}_2$ , 10 bar  $\text{H}_2$ , 160 °C. [c] Conditions de réaction: 1.88 mmol of substrate, 92  $\mu\text{mol}$  Rh, 2 ml of acetic acid, 3.5 mol/mol<sub>Rh</sub>  $p\text{-TsOH}\cdot\text{H}_2\text{O}$ , 2.5 mol/mol<sub>Rh</sub> of  $\text{CHI}_3$ , 5 mol/mol<sub>Rh</sub> of  $\text{PPh}_3$ , 20 bar  $\text{CO}_2$ , 20 bar  $\text{H}_2$ , 160 °C. [d] Conditions de réaction: 1.88 mmol of substrate, 92  $\mu\text{mol}$  Rh, 1 ml of acetic acid, 2.5 mol/mol<sub>Rh</sub> of  $\text{CHI}_3$ , 5 mol/mol<sub>Rh</sub> of  $\text{PPh}_3$ , 20 bar  $\text{CO}_2$ , 30 bar  $\text{H}_2$ , 160 °C. [e] Conditions de réaction: 1.88 mmol Cyclohexane Oxide, 46  $\mu\text{mol}$   $[\text{RhCl}(\text{CO})_2]_2$ , 2.5 eq. of  $\text{CHI}_3$ , 2 ml of toluene, 3.5 mol/mol<sub>Rh</sub> of  $p\text{-TsOH}\cdot\text{H}_2\text{O}$  and 160 °C.

## ***Etude mécanistique et réaction (Chapitre 4)***

La compréhension des mécanismes et des espèces catalytique actives peut contribuer à l'optimisation du processus global. Connaître la voie de désactivation d'un catalyseur et les étapes importantes d'un cycle catalytique peuvent aider les recherches futures sur le sujet. Par conséquent, le mécanisme de réaction et les espèces catalytiques actives ont été étudiés par différentes expériences telles que des réactions compétitives, des expériences de RMN et de marquage. Cette étude a permis d'approfondir la connaissance de la voie de réaction composée de certaines transformations non catalytiques et de deux étapes catalytiques.

Les conditions de réaction (acidité, température et additifs présents) conduisent à des transformations qui se produisent même en absence du catalyseur. Ces transformations impliquent que l'alcool (produit de départ ou intermédiaire) réagit avec l'autre composant du mélange réactionnel. Même sans l'addition du précurseur de Rh, il se forme un iodure d'alkyle, un acétate et un alcène. En plus de ces composés, on trouve également des traces d'alcane complètement hydrogéné.

Le système Rh catalyse la conversion du CO<sub>2</sub> et de H<sub>2</sub> en CO et H<sub>2</sub>O (*r*WGSR). Le système est capable d'effectuer le *r*WGSR jusqu'à 3% de rendement en CO. En plus du Rh, la présence des additifs iodures (CHI<sub>3</sub>) est indispensable. Il faut contrôler sa quantité afin d'éviter la désactivation du système si une quantité trop grande est ajoutée. A contrario, le ligand PPh<sub>3</sub> n'influence pas de manière significative le rendement en CO, surtout lorsqu'il n'est pas utilisé. Bien que la quantité de CO produite ne soit pas élevée, le résultat est toujours bon compte tenu des conditions douces utilisées.

Le même système Rh peut catalyser l'hydroxycarbonylation (en utilisant CO et H<sub>2</sub>O) des alcools. En particulier, le rendement et la régio-sélectivité des acides carboxyliques produits sont les mêmes en utilisant la quantité de CO et d'H<sub>2</sub>O produite par le système (en l'absence de CO<sub>2</sub> et H<sub>2</sub>) en utilisant CO<sub>2</sub> et H<sub>2</sub>. Des expériences compétitives et des expériences de marquage ont confirmé que la deuxième étape est une hydroxycarbonylation des alcènes. Par conséquent, les conditions réactionnelles optimisées doivent être différentes selon la classe de substrats oxygénés à transformer. Ils doivent permettre la formation d'une quantité suffisante d'alcène avec une vitesse capable de surmonter les réactions secondaires. Comme pour le *r*WGSR, CHI<sub>3</sub> a une influence majeure sur le rendement en acides carboxyliques et sa quantité

doit être soigneusement équilibrée. Au contraire, le  $\text{PPh}_3$  n'est pas indispensable pour la réaction et les acides carboxyliques sont produits même en son absence.

La réaction se déroule à travers une  $r\text{WGSR}$  transformant le  $\text{CO}_2$  et l' $\text{H}_2$  en  $\text{CO}$  et  $\text{H}_2\text{O}$ , qui sont consommés dans l'hydrocarboxylation suivante de l'alcène formé *in situ*, pour donner l'acide carboxylique final. Le système catalytique est similaire aux catalyseurs traditionnels à base de Rhodium pour la carbonylation et la Water Gas Shift Reaction (WGSR).<sup>13, 14</sup> Les deux cycles catalytiques aussi ont déjà été rapportés dans des travaux sur la catalyse homogène à base de Rhodium. Leur unification permet la production des acides carboxyliques à partir d'un réactif vert important tel que le  $\text{CO}_2$ . Dans ce contexte, l'ajout d'un ligand supplémentaire, le  $\text{PPh}_3$ , est indispensable pour le succès de la transformation. Le  $\text{PPh}_3$  est nécessaire pour fournir des ligands supplémentaires permettant au catalyseur de fonctionner dans des conditions de réaction avec une quantité minimale de  $\text{CO}$  toxique comme ligand. Une voie de réaction complète et des cycles catalytiques sont rapportés sur la figure II.



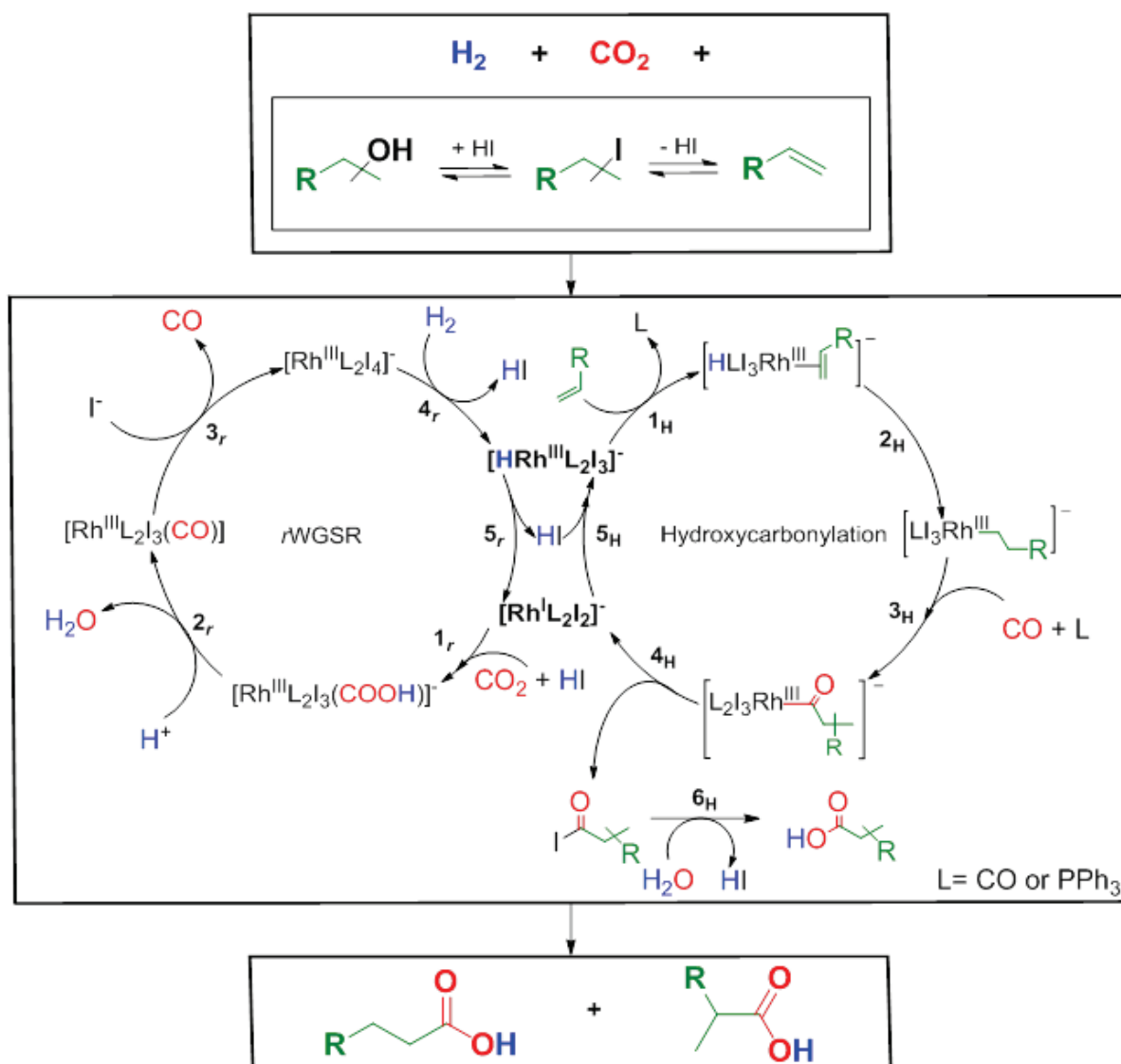


Figure II: Mécanisme proposé pour l'hydrocarboxylation des alcools.

Le cycle de *r*WGSR proposé comprend 5 étapes (**1<sub>r</sub>** - **5<sub>r</sub>**): **1<sub>r</sub>**) coordination du CO<sub>2</sub> et du HI à le [RhL<sub>2</sub>l<sub>2</sub>]<sup>-</sup> et formation d'un acide métallacarboxylique; **2<sub>r</sub>**) dégradation de Rh-COOH libérant H<sub>2</sub>O et laissant le groupe CO provenant du CO<sub>2</sub> sur le Rh; **3<sub>r</sub>**) substitution du ligand CO par un I conduisant à l'espèce [RhL<sub>2</sub>l<sub>4</sub>]<sup>-</sup>; **4<sub>r</sub>**) activation de H<sub>2</sub>, formant les espèces hydruure métallique [HRhL<sub>2</sub>l<sub>3</sub>]<sup>-</sup>; **5<sub>r</sub>**) réduction à Rh<sup>I</sup> après l'élimination réductive de l'HI.

Le cycle d'hydroxycarbonylation proposé comprend 5 étapes catalytique (**1<sub>H</sub>**-**5<sub>H</sub>**) et une étape non catalytique (**6<sub>H</sub>**): **1<sub>H</sub>**) [HRhL<sub>2</sub>l<sub>3</sub>]<sup>-</sup> générée par l'activation de H<sub>2</sub>, coordonne l'intermédiaire oléfinique en substituant un ligand; **2<sub>H</sub>**) insertion de l'alcène dans la lien Rh-H formant les espèces alkyl-Rh; **3<sub>H</sub>**) coordination de CO et insertion migratoire dans la liaison Rh-alkyle; **4<sub>H</sub>**) élimination réductive de l'iodure d'acyle; **5<sub>H</sub>**) addition oxydante de HI régénérant l'espèce de Rh<sup>III</sup> [HRhL<sub>2</sub>l<sub>3</sub>]<sup>-</sup>; **6<sub>H</sub>**) substitution nucléophile de l'iodure d'acyle donnant l'acide carboxylique.

### Single Atom Catalysts (SACs) (Chapitre 5)

Les atomes supportés sur un matériau solide sont beaucoup plus étudiés que les solutions catalytiques car ils présentent à fois les avantages des catalyseurs homogènes et des catalyseurs hétérogènes. Idéalement, ils ont une sélectivité et une activité élevées comme les catalyseurs homogènes, mais ils sont également faciles à récupérer et à recycler comme les catalyseurs hétérogènes.<sup>15-18</sup> Des exemples de SAC de Rh pris en charge pour la réaction rWGS<sup>19</sup> et hydroformylation<sup>18, 20</sup> ont été rapportés.

Les matériaux carbonés (graphène<sup>21-24</sup>, graphène dopé<sup>21, 25-27</sup>, charbon actif<sup>27, 28</sup>, g-C<sub>3</sub>N<sub>4</sub><sup>29</sup>, etc.) sont des supports prometteurs pour des atomes de métal simples. Dans ces supports, le métal se retrouve souvent dans les défauts de la structure et est stabilisé par un don d'électrons du support.<sup>16, 17, 30</sup> Pour cette raison, dans cette étude, ce type de supports a été utilisé, en insérant N ou P dans le réseau. En utilisant des méthodes simples de «wet chemistry», de nombreux matériaux ont été synthétisés.

Les techniques de caractérisation utilisées ont permis d'analyser la dispersion de Rh sur les supports, révélant la présence de SACs sur des échantillons avec une charge de Rh égale ou inférieure à 0,1% (% en poids). Les atomes de Rh isolés supportés sur de l'oxyde de graphène traité thermiquement avec de l'NH3 (échantillon 0,1Rh-GN) sont mis en évidence dans l'image HAADF-STEM indiquée sur la figure III.

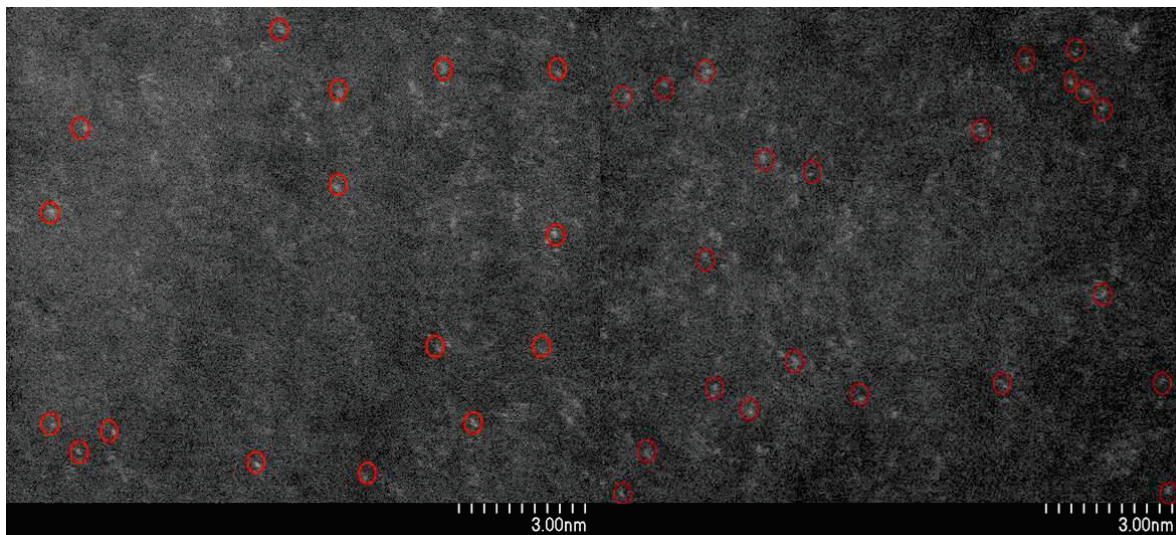


Figure 1-3: Images HAADF-STEM de l'échantillon 0,1Rh-GN.

Les échantillons préparés avec une quantité plus élevée de Rh (1%) présentent des nanoparticules bien dispersées sur la surface du solide. La dimension des

nanoparticules dépend du l'hétéroatome utilisé pour le dopage. Le dopage avec N conduit à des nanoparticules de Rh d'un diamètre moyen de 4,2 ( $\pm$  3) nm. Le dopage avec P conduit à des nanoparticules de Rh de diamètre moyen de 3,1 ( $\pm$  2) nm.

Les traitements thermiques effectués sur le GO d'origine conduisent à des matériaux différents. La présence du métal conduit à la production de différents liens dans les matériaux finaux. Par exemple, la présence du Rh facilite l'insertion de l'N dans le réseau carboné.

Les matériaux synthétisés contiennent des atomes de Rh isolés potentiellement hautement actifs, dispersés sur un support facilement transformable tel que l'oxyde de graphène dopé. Ils ne sont pas actifs pour le *WGS*R ou pour la réaction d'hydrocarboxylation. L'hydrogénation des molécules aromatiques et des alcènes ne sont pas catalysés par ces matériaux. Les catalyseurs sont prometteurs pour des réactions d'hydrogénolyse. En particulier, ils ont donné un TON de 22758 en convertissant l'oxyde de cyclohexane en cyclohexanol (rendement 25%). Cependant, d'autres études sur l'activité catalytique devraient être effectuées.

## **Conclusions et perspectives**

Dans l'ensemble, une nouvelle façon d'exploiter le CO<sub>2</sub> comme composante de base C1 pour produire des composés de valeur tels que les acides carboxyliques a été conçue. L'objectif étant de produire des acides carboxyliques de manière innovante et théoriquement plus durable est obtenu en utilisant une grande variété de substrats organiques oxygénés non activés, disponibles à la fois dans la raffinerie pétrochimique traditionnelle et dans la bio-raffinerie. Le système décrit dans cette thèse peut convertir le CO<sub>2</sub> en utilisant uniquement l'H<sub>2</sub> comme agent réducteur et aucun réactif organométallique stœchiométrique. De plus, l'utilisation d'un catalyseur moléculaire Rh hautement actif permet d'effectuer la transformation dans des conditions relativement douces.

En outre, les connaissances approfondies concernant le cycle catalytique et les espèces actives pourraient mener à un développement plus analytique et plus conscient pour de futures applications. L'augmentation du TON, de la sélectivité, des substrats que peuvent être utilisés (par exemple, des composés aromatiques et du méthanol) sont des améliorations du système qui peuvent bénéficier de ces connaissances.

Des catalyseurs hétérogènes potentiellement hautement actifs ont été synthétisés et caractérisés. Le protocole de synthèse et les connaissances acquises par l'intermédiaire de la caractérisation peuvent conduire à la mise au point de divers matériaux. Les matériaux produits peuvent être utilisés dans le futur pour le développement de protocoles de conversion sélective.

## References

1. M. V. Solmi, M. Schmitz and W. Leitner, in *Horizons in Sustainable Industrial Chemistry and Catalysis*, eds. S. Albonetti, S. Perathoner and E. A. Quadrelli, Elsevier, In press.
2. W. Leitner and J. Klankermayer, *Science*, 2015, **350**, 629-630.
3. J. Klankermayer, S. Wesselbaum, K. Beydoun and W. Leitner, *Angew. Chem. Int. Ed.*, 2016.
4. J. Artz, T. E. Muller, K. Thenert, J. Kleinekorte, R. Meys, A. Sternberg, A. Bardow and W. Leitner, *Chem. Rev.*, 2018, **118**, 434–504.
5. G. Centi, E. A. Quadrelli and S. Perathoner, *Energy Environ. Sci.*, 2013, **6**, 1711.
6. T. G. Ostapowicz, M. Schmitz, M. Krystof, J. Klankermayer and W. Leitner, *Angew. Chem. Int. Ed.*, 2013, **52**, 12119-12123.
7. K. Dong and X. F. Wu, *Angew. Chem. Int. Ed.*, 2017.
8. E. Kirillov, J. F. Carpentier and E. Bunel, *Dalton Trans.*, 2015, **44**, 16212-16223.
9. L. Wu, Q. Liu, R. Jackstell and M. Beller, *Angew. Chem. Int. Ed.*, 2014, **53**, 6310-6320.
10. L. Wu, Q. Liu, I. Fleischer, R. Jackstell and M. Beller, *Nat. Commun.*, 2014, **5**.
11. M. D. Porosoff, B. Yan and J. G. Chen, *Energy Environ. Sci.*, 2016, **9**, 62-73.
12. M. Schmitz, PhD, RWTH Aachen University, 2018.
13. D. Forster, A. Hershman and D. E. Morris, *Catalysis Reviews*, 1981, **23**, 89-105.
14. E. C. Baker, D. E. Hendriksen and R. Eisenberg, *J. Am. Chem. Soc.*, 1980, **102**, 1020-1027.
15. H. Yan, C. Su, J. He and W. Chen, *Journal of Materials Chemistry A*, 2018, **6**, 8793-8814.
16. X.-F. Yang, A. Wang, B. Qiao, J. Li, J. Liu and T. Zhang, *Acc. Chem. Res.*, 2013, **46**, 1740-1748.
17. S. Liang, C. Hao and Y. Shi, *ChemCatChem*, 2015, **7**, 2559-2567.
18. R. Lang, T. Li, D. Matsumura, S. Miao, Y. Ren, Y. T. Cui, Y. Tan, B. Qiao, L. Li, A. Wang, X. Wang and T. Zhang, *Angew. Chem. Int. Ed.*, 2016, **55**, 16054-16058.
19. J. C. Matsubu, V. N. Yang and P. Christopher, *J. Am. Chem. Soc.*, 2015, **137**, 3076-3084.

20. L. Wang, W. Zhang, S. Wang, Z. Gao, Z. Luo, X. Wang, R. Zeng, A. Li, H. Li, M. Wang, X. Zheng, J. Zhu, W. Zhang, C. Ma, R. Si and J. Zeng, *Nat. Commun.*, 2016, **7**, 14036.
21. D. Deng, X. Chen, L. Yu, X. Wu, Q. Liu, Y. Liu, H. Yang, H. Tian, Y. Hu, P. Du, R. Si, J. Wang, X. Cui, H. Li, J. Xiao, T. Xu, J. Deng, F. Yang, P. N. Duchesne, P. Zhang, J. Zhou, L. Sun, J. Li, X. Pan and X. Bao, *Sci. Adv.*, 2015, **1**, e1500462/1500461-e1500462/1500469.
22. H. Yan , H. Cheng , H. Yi , Y. Lin , T. Yao , C. Wang , J. Li , S. Wei and J. Lu, *J. Am. Chem. Soc.*, 2015, **137** 10484–10487.
23. L. Xu, L.-M. Yang and E. Ganz, *Theor. Chem. Acc.*, 2018, **137**.
24. C. Gao, S. Chen, Y. Wang, J. Wang, X. Zheng, J. Zhu, L. Song, W. Zhang and Y. Xiong, *Adv. Mater.*, 2018, **30**, e1704624.
25. C. Zhang, J. Sha, H. Fei, M. Liu, S. Yazdi, J. Zhang, Q. Zhong, X. Zou, N. Zhao, H. Yu, Z. Jiang, E. Ringe, B. I. Yakobson, J. Dong, D. Chen and J. M. Tour, *ACS Nano*, 2017.
26. H. Fei, J. Dong, M. J. Arellano-Jiménez, G. Ye, N. Dong Kim, E. L. G. Samuel, Z. Peng, Z. Zhu, F. Qin, J. Bao, M. J. Yacaman, P. M. Ajayan, D. Chen and J. M. Tour, *Nature Communication*, 2015, **6**, 1-8.
27. W. Liu, Y. Chen, H. Qi, L. Zhang, W. Yan, X. Liu, X. Yang, S. Miao, W. Wang, C. Liu, A. Wang, J. Li and T. Zhang, *Angew. Chem. Int. Ed.*, 2018, **57**, 7071-7075.
28. Y. Chen, S. Ji, Y. Wang, J. Dong, W. Chen, Z. Li, R. Shen, L. Zheng, Z. Zhuang, D. Wang and Y. Li, *Angew. Chem. Int. Ed.*, 2017, **56**, 6937-6941.
29. W. Liu, L. Cao, W. Cheng, Y. Cao, X. Liu, W. Zhang, X. Mou, L. Jin, X. Zheng, W. Che, Q. Liu, T. Yao and S. Wei, *Angew. Chem. Int. Ed.*, 2017.
30. S. Back, J. Lim, N.-Y. Kim, Y.-H. Kim and Y. Jung, *Chem Sci*, 2017, **8**, 1090-1096.









## Contents

1.	Introduction .....	5
1.1	Context and motivation .....	7
1.2	Applications of carboxylic acids .....	7
1.3	Carboxylic acids production .....	9
1.4	CO <sub>2</sub> Chemistry.....	12
1.4.1	General properties and reactivity .....	12
1.4.2	Carboxylic acids from CO <sub>2</sub> .....	15
1.4.3	rWGSR (reverse Water Gas Shift Reaction) .....	16
1.5	Objectives and structure of the thesis .....	17
2.	Literature overview: production of carboxylic acids using CO <sub>2</sub> as building block	19
2.1	General aspects .....	21
2.2	Organometallic substrates .....	22
2.2.1	Grignard reagents.....	23
2.2.2	Organoalane reagents.....	24
2.2.3	Organolithium reagents .....	25
2.3	Organometallic substrates coupled with catalytic systems .....	25
2.3.1	Organozinc reagents .....	27
2.3.2	Alkenylzirconocenes and organostannanes.....	28
2.3.3	Boronic esters .....	28
2.3.4	Organosilanes .....	29
2.4	Non-activated substrates .....	30
2.4.1	C-Halide bonds (organohalides) .....	30
2.4.2	C-O Bonds (oxygenated substrates).....	33
2.4.3	C(sp)-H bonds (alkynes).....	36
2.4.4	C(sp <sup>2</sup> )-H bond (alkenes) .....	37

2.4.5	C(sp <sup>2</sup> )-H bond (aromatics).....	39
2.4.6	C(sp <sup>3</sup> )-H bonds.....	42
2.5	Conclusions and outlook.....	45
3.	Homogeneously Rhodium catalysed synthesis of carboxylic acids from oxygenated substrates.....	47
3.1	State of the art and starting point.....	49
3.2	Design of Experiment (DoE).....	54
3.3	Secondary alcohols and ketones.....	58
3.3.1	2-butanol.....	58
3.3.2	Cyclohexanone.....	65
3.3.3	Scope of the reaction.....	71
3.4	Primary alcohols and aldehydes.....	74
3.4.1	1-butanol.....	74
3.4.2	Butanal.....	80
3.4.3	Scope of the reaction.....	82
3.5	Epoxides.....	84
3.6	Multifunctional substrates and industrial relevant mixtures.....	90
3.7	Conclusions.....	93
3.8	Experimental part.....	95
4.	Mechanistic investigation and reaction pathway.....	97
4.1	State of the art.....	99
4.2	Non-catalytic step.....	105
4.3	Reverse Water Gas shift.....	108
4.4	Hydroxycarbonylation step.....	111
4.5	Overall hydrocarboxylation.....	126
4.6	Conclusions and outlook.....	136
4.7	Experimental part.....	137

4.7.1	General .....	137
4.7.2	Solvents and Chemicals .....	137
4.7.3	Autoclave reactions .....	137
4.7.4	Mass Spectrometry.....	138
4.7.5	Gas chromatography .....	138
4.7.6	Design of Experiment (DoE) .....	139
4.7.7	NMR analysis .....	140
5.	Single atom catalysts (SACs).....	143
5.1	State of the art.....	145
5.2	Synthesis of the catalysts .....	151
5.3	Characterization of the catalysts .....	151
5.3.1	Characterization of the supported Rh .....	153
5.3.2	Characterization of the carbon-based material .....	156
5.4	Catalytic tests .....	165
5.5	Conclusion and outlook .....	171
5.6	Experimental.....	172
5.6.1	Preparation of SACs.....	172
5.6.2	Autoclaves reactions .....	173
5.6.3	Gas chromatography .....	174
5.6.4	Infrared spectroscopy (FTIR) – Attenuated Total Reflection (ATR) ...	174
5.6.5	Elemental Analysis .....	174
5.6.6	Raman spectroscopy.....	175
5.6.7	X-Ray Diffraction (XRD).....	175
5.6.8	Transmission Electron Microscopy (TEM).....	175
6.	Conclusions .....	177
7.	References.....	179



**1. Introduction**



## 1.1 Context and motivation

The carbon and fossil fuels based industry and energy production emit large amounts of CO<sub>2</sub> contributing to the high CO<sub>2</sub> level in the atmosphere (403.3 ppm in October 2017).<sup>31</sup> The capture, followed by the transformation or utilization of CO<sub>2</sub> for common chemicals, fuels and materials would contribute to a close anthropogenic carbon cycle. Although these technologies would not be able to consume the 36 gigatons of CO<sub>2</sub> emitted in the atmosphere,<sup>32</sup> the exploitation of CO<sub>2</sub> as resource would reduce the carbon footprint of these production processes.<sup>4, 33, 34</sup> The shortage of fossil resources and their rising cost are driving forces for intensifying the use of CO<sub>2</sub> as new and sustainable resource, especially being a C1 synthon for the production of basic chemicals.<sup>35, 36</sup>

CO<sub>2</sub> is a renewable, unique, ubiquitous, non-toxic, non-flammable and a highly versatile building block. This makes it a highly interesting material from a “Green Chemistry” point of view.<sup>2, 4, 5, 34, 37</sup> In this context, the abundance of CO<sub>2</sub> and its non-harmful properties compared to conventional C1 building blocks like CO, phosgene, HCN or formaldehyde embodies positive aspects for the industry. It also forms a potentially important feedstock for a future largely renewable energy-chemistry nexus.<sup>1, 5, 37</sup> The growing number of CO<sub>2</sub> utilization contributions and reviews also highlights the interest of both fundamental and applied research in this field.<sup>3, 11, 34, 37-40</sup>

Among many target products, carboxylic acids appear highly attractive, but are at the same time particularly challenging. Their general formula RC(O)OH implies a close relationship to the CO<sub>2</sub> molecule. However, while CO<sub>2</sub> reacts readily with O- and N-nucleophiles to give carbonic and carbamic acids, corresponding reactions to form C-C bonds require typically stoichiometric use of carbanions such as Grignard reagents or other metal alkyl and aryl species. Alternative pathways involving catalytic combination of suitable substrates with CO<sub>2</sub> are of great interest to synthesize carboxylic acids.<sup>1</sup>

## 1.2 Applications of carboxylic acids

In general, carboxylic acids and their derivatives are highly important for their synthetic utilization in the production of polymers, pharmaceuticals, solvents, food additives (commodities), etc.<sup>1</sup> The global market for carboxylic acids is predicted to grow yearly by 5% to 2023, reaching about 20 billion \$, testifying their importance from an economical point of view.<sup>41</sup>

The most important applications of carboxylic acids are in polymer industry, where they are used both as monomers and additives. Many uses are known from fibers to packaging and coating.<sup>1</sup> Polyvinyl acetate (glue) is produced from vinyl acetate monomer, mainly obtained from acetic acid.<sup>42, 43</sup> The extremely important polyamides are generally produced from dicarboxylic acids and amines. For example, adipic acid (annual production in 1999: 2 500 000 t/a) is used for the production of Nylon fibers, which are well known and used to substitute natural polyamides (i.e. wool and silk).<sup>44</sup> Acrylic and methacrylic acids are the precursors of acrylic and methacrylic polymers, which find applications as solid detergents, dishwasher powders, cement additives, super absorbers and further products of daily life.<sup>1</sup> Moreover, polymers with different properties are obtained by mixing these monomers with other acids or derivatives (i.e. maleic anhydride and fumaric acid). Some of them are highly employed in paint formulation.<sup>45</sup> Polyesters are obtained from dicarboxylic acids and diols. Among them, PET (polyethylene terephthalate) is obtained from terephthalic acid (annual production: 12 600 000 t/a) and ethylene glycol and it is the most important polymer in terms of application and commercial value. PET is mainly employed in beverage packaging. The properties of the polymer can be tuned changing the type of starting acid, leading to different applications.<sup>46</sup> Cellulose esters are commonly used as fibers. They are mainly produced from acetic acid and cellulose, but fibers with different properties are obtained when different acids are used instead (up to C<sub>4</sub>). Additional types of polymers can be obtained starting from different carboxylic acids.<sup>47</sup> Polyimides are important heat resistant materials, synthesized from aromatic acids.<sup>48</sup> Alkyd resins are obtained from diacids and alcohols and are applied in coatings. In addition to the reported applications as monomers, carboxylic acids are also employed as additives to modify the properties of the synthesized polymers. Long chain carboxylic acids (> C<sub>9</sub>) are used as additives for alkyd resins films,<sup>49</sup> while trimellitic anhydride is added as a plasticizer.<sup>48</sup>

In addition to their uses in polymers industry, carboxylic acids are applied for treatments of textile and leather. In particular, oxalic acid<sup>50</sup> and formic acid (ca. 800 000 t/a)<sup>51, 52</sup> are used for pickling or dyeing.<sup>53, 54</sup> Oxalic acid is also employed in metal industry for different purpose (i.e. rust removal).<sup>53</sup>

Some aliphatic carboxylic acids and their derivatives find application as solvents: acetic acid and isobutyric acid, C<sub>5</sub> acids esters and other derivatives (i.e. acetamide) are employed as solvents.<sup>55</sup> In particular, acetic acid is used as solvent in the production processes of terephthalic acid and of acetic acid itself.<sup>1</sup>



Carboxylic acids are important in agrochemical industry. For instance, propionic acid (annual production in 2012: > 45000 t/a) and malonate are employed in the production of herbicides. Fungicides and rodenticides are produced from isovaleric acid.<sup>55</sup>

In pharmaceutical industry, carboxylic acids are important synthetic tools as well as medicine. The most important examples of molecules containing a carboxylic acid moiety and used as medicines are acetyl salicylic acid, commercialized as aspirin,<sup>56</sup> 2-(4-isobutylphenyl)propionic acid, commonly known as ibuprofen<sup>41</sup> and (*RS*)-2-(3-benzoylphenyl)-propionic acid, usually sold as ketoprofen.<sup>57</sup>

Furthermore, carboxylic acids are employed in food and feed industry. Acetic acid diluted with water is used in vinegar,<sup>1</sup> while propionic acid, formic acid and salts of isobutyric acid are used to obtain preservatives for food and feed.<sup>58</sup> Moreover, carboxylic acids are aroma and flavors enhancers. Depending on the chain length they can have fruity or cheese aroma. Esters of carboxylic acids have in general a fruity smell, for this reason they are highly employed in perfumes industry.<sup>55</sup>

In addition to the above-mentioned applications, carboxylic acids are used in dyes and pigments.

Recently, carboxylic acids have been studied as energy carrier. Shell reported the use of valeric acid esters as biofuels<sup>59</sup>, while formic acid is becoming an attractive H<sub>2</sub> storage molecule, since its decomposition leads to the production of CO<sub>2</sub> and H<sub>2</sub>.<sup>60, 61</sup>

To sum up, mainly all types of carboxylic acids (aliphatic, aromatic, mono- or bi-carboxylic acids) and their derivatives have a high importance on industrial level by a wide range of different applications: from bulk chemicals (i.e. polymers production) to fine chemicals (i.e. perfume and food industries application).

### **1.3 Carboxylic acids production**

Most carboxylic acids are produced *via* oxidation processes. Aromatic carboxylic acids are usually obtained from the oxidation of alkyl substituted aromatic compounds. These processes are commonly catalyzed by Co or Mn salts. As for aldehydes oxidation processes, O<sub>2</sub> is used as oxidant and both gas and liquid phase processes are feasible.<sup>48, 55</sup> Terephthalic acid is produced through a liquid phase oxidation of *p*-xylene.<sup>62</sup> Adipic acid is produced in large scale from the oxidation of cyclohexanol, cyclohexanone or a mixture of them (KA-Oil) with HNO<sub>3</sub>.<sup>63</sup> KMnO<sub>4</sub> is also used as oxidant in the Reichstein process which converts along a multistep synthesis D-glucose

into ascorbic acid (vitamin C).<sup>64</sup> Oxidation reactions have the drawback of being highly exothermic. Therefore, efficient methods to remove the generated heat during the reactions must be developed, to avoid dangerous side reactions and ultimately the runaway. Besides, some important products are obtained with stoichiometric amounts of oxidants which lead to toxic by-products (i.e. NO<sub>x</sub>).

Aliphatic aldehydes are oxidized to carboxylic acids (C<sub>4</sub>-C<sub>13</sub>). The reactions are carried on both in liquid and gas phase, generally, using metal salts as catalysts and O<sub>2</sub> as oxidizing reagent. Nevertheless, liquid phase processes are generally more implemented. The synthesis of the aldehydes intermediates which usually obtained by the Oxo synthesis (hydroformylation). Hydroformylation is one of the largest homogeneously catalyzed industrial processes, in volume.<sup>65, 66</sup> This reaction involves the addition of CO and H<sub>2</sub> to an alkene molecule to give the final aldehydes. This reaction is catalyzed mainly by Rh complexes with phosphorous-based ligands (mono- and multi-dentate phosphines or P-O ligands), although other metal substitute are studied.<sup>65</sup>

Other aliphatic carboxylic acids are produced by carbonylation of alcohols or alkenes. Tertiary alcohols such as pivalic acid are produced from alkenes with the Koch synthesis. H<sub>3</sub>PO<sub>4</sub>•BF<sub>3</sub> or H<sub>2</sub>SO<sub>4</sub> are catalysts for the hydroxycarbonylation reaction which adds CO and H<sub>2</sub>O to the original alkene giving the final carboxylic acid.<sup>55, 67</sup> The Reppe synthesis (catalyzed by Ni complexes) uses high pressure of CO and H<sub>2</sub>O to hydroxycarbonylate ethylene and obtains propionic acid.<sup>68, 69</sup> The production of formic acid is based on a carbonylation process as well. It is mainly synthesized by BASF with a two-step strategy: first a base-catalyzed carbonylation of methanol to methyl formate, followed by the hydrolysis of the intermediate to formic acid and methanol.<sup>51</sup> The industrial production of acetic acid is performed through methanol carbonylation. A lot of processes using CO as carbonylating agent were developed. The production of acetic acid is with no doubt one of the biggest homogeneously catalyzed process worldwide<sup>70</sup>. In 1960 BASF developed the large-scale production of acetic acid using a Co complex as catalyts. Later, in 1966, Monsanto implemented the process using a [Rh(CO)<sub>2</sub>I<sub>2</sub>]<sup>-</sup> as catalyst.<sup>71-75</sup> Different improvements of the process were developed to reduce the selectivity problems. The Cativa process ([Ir(CO)<sub>2</sub>I<sub>2</sub>]<sup>-</sup> complex as catalyst) was developed leading to further improvement in the selectivity of the process.<sup>76, 77</sup> Recently, heterogenous catalysts and associated processes were derived from these fundamental works. The Acetica process uses an immobilized Rh complex as catalyst.<sup>78</sup> A different approach is the SaaBre process, which uses zeolites

as catalyst for a multistep synthesis of acetic acid<sup>43</sup>. From the 1970s, few studies on the direct carbonylation of higher alcohols (C<sub>2+</sub>) have been reported. In particular, the Monsanto group proved that the carbonylation of higher alcohols is possible with the same system used for the carbonylation of methanol. The rate of the catalysis and the mechanism were diverse for different alcohols (primary, secondary).<sup>79</sup> The carbonylation of higher alcohols was studied by further groups using both homogeneous<sup>67, 80-93</sup> and heterogeneous<sup>94-96</sup> catalysts. The processes still need to be developed to compete with the carbonylation of methanol or alkenes. Therefore, no industrial processes to produce carboxylic acids from higher alcohols and CO are implemented, yet.<sup>97</sup>

Carbonylation and hydroxycarbonylation are widely applied processes for the synthesis of aliphatic carboxylic acids. The only process to produce carboxylic acids from CO<sub>2</sub> implemented to an industrial level is the Kolbe-Schmitt synthesis. This process converts phenol with CO<sub>2</sub> in a basic environment (NaOH) into salicylic acid. This process is limited to aromatic substrate with an adjacent phenyl group.<sup>98</sup> Formic acid production from CO<sub>2</sub> and H<sub>2</sub> has been widely studied recently, as testified by the high number of review papers published in the past years.<sup>4, 60, 61</sup>

Many strategies have been studied to obtain carboxylic acids from CO<sub>2</sub>, in order to overcome the use of CO. CO is a toxic chemical and it is currently produced mainly from fossil fuels (by steam reforming), from natural gas or from coal gasification.<sup>99</sup> Hence, the use of CO<sub>2</sub> would replace a non-renewable chemical with a readily available and renewable one. Nevertheless, very few of the studied processes are fully catalytic approaches and they are commonly not obtained starting from very simple substrates such as organic molecules containing a C-O bond. None of these processes have been implemented on an industrial scale so far. These other strategies starting from different types of substrates have been summarized in Chapter 2 of this thesis and part of the examples were reported in a recent book chapter.<sup>1</sup>

## 1.4 CO<sub>2</sub> Chemistry

### 1.4.1 General properties and reactivity

CO<sub>2</sub> is available from various industrial sources in high quantity and it can be recovered in order to reduce the emissions in the atmosphere by techniques defined as Carbon Capture and Storage. Carbon Capture and Utilization (CCU) or Carbon Capture and Recycling (CCR) offer strategies to use CO<sub>2</sub> produced in energy, steel or cement productions as a feedstock for chemical transformation.<sup>100-102</sup> Usually, aqueous solutions of amine are used to capture CO<sub>2</sub>. Due to the several drawbacks of these agents (such as corrosivity and volatility), recently, solid capture agents have been developed: silicas, activated carbons, polymers and calcium oxide. CO<sub>2</sub> is then transported to geological reservoir and stored.<sup>103, 104</sup>

The exploitation of CO<sub>2</sub> as CO substitute includes challenges. In particular, the very different (re)activity of CO<sub>2</sub> compared to CO requires the development of new well-designed catalytic systems and processes.<sup>1</sup> To do that, it is important to consider the chemical properties of the CO<sub>2</sub> molecule.

The CO<sub>2</sub> molecule itself shows three types of reactivity which provide many opportunities for chemical utilizations: two nucleophilic centers located at the oxygen atoms (blue arrows), an electrophilic carbon atom (red arrow) and a  $\pi$ -system (black arrow) (Figure 1-1).<sup>105</sup> Nevertheless, the absence of an overall dipole moment ( $\mu = 0$ ) goes together with a difficulty in shifting the electron density within the molecule. However, the linear shape of the CO<sub>2</sub> molecule in combination with the regular electron distribution (resonance) of the C=O bonds and the oxygen lone pairs limit its reactivity. Hence, activation and utilization of CO<sub>2</sub> still suffers from its thermodynamic stability and kinetic inertness.

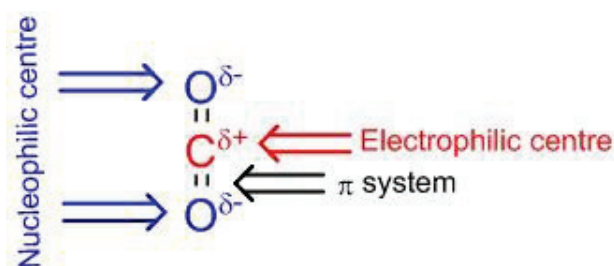


Figure 1-1: Threefold reactivity of carbon dioxide.

The general exploitation of CO<sub>2</sub> as a carbon building block requires an activation of this molecule. In order to cover these requirements catalysis is a crucial tool and therefore counts as key element in this manner.<sup>106</sup> To address the energetic challenge in reactions involving CO<sub>2</sub>, two approaches can be used as shown in Figure 1-2. Organometallic reagents (or other high energetic reagents) can be used to increase the energy level of the starting systems (Grignard reagents, organolithiums, etc.). The energy of the starting system can also be improved by means of additives such as organometallic or metallic reagents or other reducing agents i.e. H<sub>2</sub>. These additives can interact (sometimes by the mean of a catalytic system) with the substrates or the CO<sub>2</sub> molecule. In most cases, a catalytic system is required also to decrease the energetic barrier influencing the energy of the transition state.

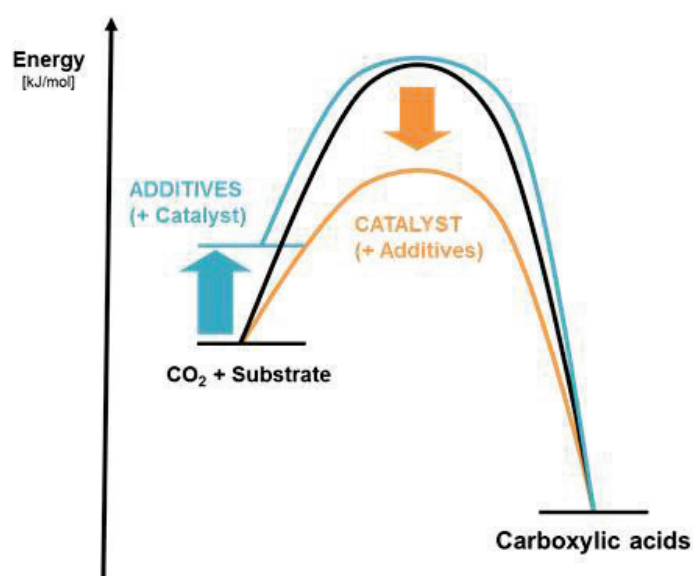


Figure 1-2: The synthesis of carboxylic acids using CO<sub>2</sub> as building block can be reached reducing the energy barrier by different strategies: increasing the energy of the starting system using highly reactive substrates or additives (organometallic reagents, metals, H<sub>2</sub>, etc.) or decreasing the energy barrier acting on the transition state in the presence of a catalyst (homogeneous, heterogeneous or photocatalysts). The two approaches are often combined and both additives and catalysts are present to reduce the energy barrier. Reproduced with permission from “M. V. Solmi, M. Schmitz, W. Leitner; CO<sub>2</sub> as a building block for the catalytic synthesis of carboxylic acids, *Horizons in Sustainable Industrial Chemistry and Catalysis*, eds. S. Albonetti, S. Perathoner and E. A. Quadrelli, Elsevier, 2019”.

Among the catalysts for the transformation of CO<sub>2</sub> in chemicals and fuels, a portfolio of organometallic agents and transition metal complexes can be found.<sup>107</sup> Today, many complexes with coordinating CO<sub>2</sub> are known.<sup>108</sup> Mostly, late transition metals like Ru, Ni, Pd, Pt, Rh or Ir are reported in literature.<sup>109</sup> Figure 1-3 comprises some coordination modes of CO<sub>2</sub> to the metal center, which are determined by the electronic properties of the metal center. CO<sub>2</sub> can coordinate the metal through the electrophilic carbon atom, if the metal is nucleophilic or with Lewis base properties.<sup>108</sup> It can coordinate through the nucleophilic oxygens atoms,<sup>110</sup> if the metal as Lewis acid properties (it is electrophilic), or it can coordinate using the  $\pi$ -system (as in the Aresta's complex).<sup>111</sup>

The catalytic conversion of CO<sub>2</sub> can be summarized into three major areas according to the nature of the chemical transformation and to the reduction level of the carbon atom.<sup>61</sup> Besides the complete incorporation of CO<sub>2</sub> into products without formal reduction<sup>107, 112, 113</sup> and the full reduction of the CO<sub>2</sub> to saturated hydrocarbons, the

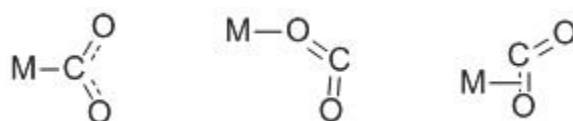


Figure 1-3: Possible coordination modes of CO<sub>2</sub> to a transition-metal complex.

partial reduction of the carbon atom (to +III, + II or +I) by formation of new bonds, opens opportunities for the synthesis of functional molecules.<sup>112</sup> An energetic reactant, such as hydrogen, can enhance CO<sub>2</sub> reactivity leading to a “greener” alternative to conventional reductants, if H<sub>2</sub> is formed e.g. by water splitting provided by renewable energies.<sup>2</sup> By using the combination of CO<sub>2</sub> and H<sub>2</sub>, a broad range of chemicals (i.e. methanol, carboxylic acids, aldehydes etc.) would be produced reducing the carbon footprint and avoiding toxic and wasteful reagents compared to the traditional petrochemical way.<sup>61</sup>

CO<sub>2</sub> can lead to several valuable chemical conversions enabled by different catalytic systems. Further investigations will bring several advantages, since the exploitation of CO<sub>2</sub> will generate value from a common waste and not consume fossil fuels.<sup>114</sup>

### 1.4.2 Carboxylic acids from CO<sub>2</sub>

An interesting reaction involving partial CO<sub>2</sub> reduction is the synthesis of carboxylic acids and their derivatives. CO<sub>2</sub> can be coupled with H<sub>2</sub> to form formic acid, while other carboxylic acids can be obtained by the reaction of CO<sub>2</sub> with an organometallic or organic reagent<sup>113</sup>. Herein, a selection of examples reporting about the production of carboxylic acids starting from oxygenated substrates and CO<sub>2</sub> is reported. This transformation reaction will be discussed in detail in Chapter 2.

The very first synthesis of higher carboxylic acids from CO<sub>2</sub> was developed in the 1860s by Kolbe and Schmitt. This process is still in use for the production of salicylic acid by carboxylation of sodium phenolate.<sup>56, 98</sup> Later on, the conversion of C-O bonds into carboxylic acids *via* carboxylation or hydrocarboxylation reactions have mainly involved the transformation of sulfonates.<sup>115</sup> On the contrary, less reactive C-O bonds have not been widely used in this sense.<sup>1</sup> Few examples of esters and alcohols conversion were reported, while C-O bonds of ketones, aldehydes, epoxides or mixtures of reagents were never transformed directly into carboxylic acids.<sup>1</sup> A brief overview of these processes is reported in Section 2.4.2.

In 2013, Leitner *et al.* published about a Rhodium-based system, which produces carboxylic acids from simple alkenes with yields up to 91% using CO<sub>2</sub> and H<sub>2</sub> in a formal hydrocarboxylation.<sup>6</sup> Mechanistic and labelling studies suggest the *in-situ* formation of CO and H<sub>2</sub>O by *r*WGS, which proceed in a hydroxycarbonylation. The reaction requires acidic conditions, an iodide promoter (likewise the Monsanto process) and PPh<sub>3</sub> as ligand, but no organometallic stoichiometric additives.<sup>6</sup> Leitner and co-workers provided the first example of transformation of alcohols with CO<sub>2</sub> and H<sub>2</sub>, without the need of a stoichiometric organometallic additive, although the yields in carboxylic acids starting from alcohols are little lower (up to 74%) than the yields obtained from alkenes.<sup>6</sup> The *in-situ* production of CO via *r*WGS is a remarkable way to replace the use of high amount of toxic reagent and to exploit a renewable, non-toxic and waste resource as CO<sub>2</sub>. Already few protocols using this approach were published. In particular, examples of carboxylation-, alkoxy-carbonylation- or hydroformylation reactions were presented.<sup>7-11</sup>

It is worth to study more in details the *r*WGS itself and to develop other systems capable of coupling it with other reaction. In this way, many chemicals obtained today from CO could be produced starting from CO<sub>2</sub>.

### 1.4.3 *rWGSR (reverse Water Gas Shift Reaction)*

A fascinating and useful reaction of the combination CO<sub>2</sub> and H<sub>2</sub> is the *reverse* Water Gas Shift Reaction (*rWGSR*):



The CO can be used easily as a C<sub>1</sub> building block in chemical synthesis and existing applications, as discussed in the previous chapter. Hence, the conversion of CO<sub>2</sub> to CO seems an innovative and promising tool for carbon dioxide exploitation. In particular, this transformation can be useful in cases where CO<sub>2</sub> has to be used as CO substitute. However, deoxygenation of CO<sub>2</sub> is highly energy demanding, thus requires the development of well-designed metal catalysts which allow this transformation.

The endothermicity of the *rWGSR* ( $\Delta H = +41 \text{ kJ mol}^{-1}$ )<sup>116</sup> makes the reaction favorite at high temperature. Many heterogenous catalysts have been developed, performing the reaction at high temperature (normally higher than 200 and up to 750 °C) and in continuous flow systems.<sup>11, 116-118</sup> Generally, two mechanisms are proposed. One mechanism would involve the oxidation of the catalyst (i.e. Cu<sup>0</sup> → Cu<sup>+1</sup>) together with CO<sub>2</sub> reduction to CO and a following reduction of the metal (i.e. Cu<sup>+1</sup> → Cu<sup>0</sup>) by H<sub>2</sub> oxidation to H<sub>2</sub>O. The other suggested mechanism involves a first hydrogenation of CO<sub>2</sub> to formate, followed by a bond cleavage giving the final CO product.<sup>11</sup> Many metal nanoparticles supported on metal oxide, to enhance the interfacial area, are known to be active catalysts for this transformation.<sup>11</sup> Iron based catalysts are the most commonly used at high temperature, while copper based nanoparticles are used to catalyze the reaction at lower temperature<sup>116</sup>. A good interaction between the nanoparticles and the support is important to avoid the sintering of the active phase, highly likely at the high temperature used to perform the reaction. Therefore, much effort is put in attempts to increase the stability of the active catalysts developing new preparation methods or using suitable dopants<sup>116, 117</sup>. At the same time, many works focused on the increase of the selectivity (reducing methanation activity) and of the activity of the catalysts.<sup>116, 118</sup>

The development of innovative highly active and selective catalysts able to reach good production of CO is investigated as well. Some highly active system can achieve good yields of CO even at 250 °C.<sup>118</sup> Good activity at even lower temperature (200 °C) was achieved when Single Rh atoms dispersed on TiO<sub>2</sub> were used as catalysts.<sup>19</sup> In addition, in this case, it was proved that the presence of Single Atom



Catalysts (SACs) is catalyzing selectively the *r*WGSR, while nanoparticles are mostly active for the complete reduction of CO<sub>2</sub> to CH<sub>4</sub>.<sup>19</sup> The development of system making CO at temperature low enough could allow the coupling of this step with a subsequent *in-situ* conversion to other product.<sup>6-11</sup>

The performance of the reaction in a batch reactor, in condensed phase can change its thermodynamic properties. As an example, under certain conditions (i.e. high pressures) water can be liquid, shifting the equilibrium. An homogeneously catalyzed *r*WGSR was reported by Tominaga and co-workers. They demonstrate that Ru complexes catalyze the *r*WGSR with a TON of 96 based on a Ru atom. This reaction proceed at mild conditions (180°C, 1 MPa of CO<sub>2</sub>, 3MPa of H<sub>2</sub>), thanks to the efficient catalytic system developed.<sup>119</sup>

Other strategies to achieve the desired CO have been developed. Recently, the increasing attention towards artificial photosynthesis inspired many studies on the photocatalytic conversion of CO<sub>2</sub> in CO<sup>24, 120</sup>. The separation of the process in two following step (oxidation and reduction), is referred to as *r*WGSR- chemical looping (*r*WGSR-CL). An oxygen containing material, such as metal oxides (i.e. Fe<sub>2</sub>O<sub>3</sub>, perovskite oxides) can be used as catalysts, leading to higher efficiency and lower formation of by-products<sup>99, 121</sup>.

In this thesis, a homogeneous Rh catalytic system able to perform the *r*WGSR and a following transformation of the CO and H<sub>2</sub>O produced into carboxylic acids is reported. In addition, an attempt to synthesize heterogeneous catalysts able to perform this reaction at low temperature is shown.

## 1.5 Objectives and structure of the thesis

In this thesis, a report of the research carried on the synthesis of carboxylic acids starting from oxygenated substrates (alcohols, ketones, aldehydes and multifunctional substrates), CO<sub>2</sub> and H<sub>2</sub> is presented. After reviewing the protocols present in literature for the synthesis of carboxylic acids by CO<sub>2</sub> incorporation (Chapter 2), the new protocol is presented. A Rh catalytic system (Figure 1-4) able to convert potentially renewable resources (CO<sub>2</sub> and H<sub>2</sub>) into chemicals (carboxylic acids) which are currently produced using CO was studied in detail. In particular, the study on the reactions parameters for all the investigated substrates is reported in Chapter 3. This study allowed us to obtain optimized reaction conditions tailored for each class of reagents. Moreover, proves in support of the already suggested reaction pathway (*r*WGSR followed by an

hydroxycarbonylation)<sup>6</sup> are reported in Chapter 4. In addition to these, new evidences lead us to propose a detailed mechanism and catalytic active species. Eventually, heterogeneous single atom catalysts (SACs) were developed and their catalytic activity for CO<sub>2</sub> activation and carboxylic acids production was investigated. The preparation, characterization and catalytic investigation are reported in Chapter 5.

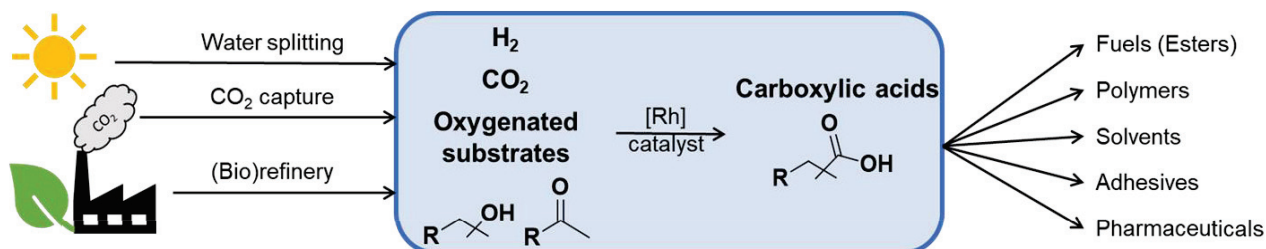


Figure 1-4: Schematic representation of the process reported in this thesis (blue box). Ideally, CO<sub>2</sub> can be obtained from wastes fluxes coming from industrial productions. H<sub>2</sub> can be obtained by H<sub>2</sub>O splitting, using renewable energy. Oxygenated substrates are highly available, both from the traditional petrochemical productions and new biorefinery processes. Carboxylic acids can be used in different industrial sector to produce useful goods.

## 2. Literature overview: production of carboxylic acids using CO<sub>2</sub> as building block

**Parts of this chapter are published:**

M. V. Solmi, M. Schmitz, W. Leitner; CO<sub>2</sub> as a building block for the catalytic synthesis of carboxylic acids, *Horizons in Sustainable Industrial Chemistry and Catalysis*, eds. S. Albonetti, S. Perathoner and E. A. Quadrelli, Elsevier, 2019



## 2.1 General aspects

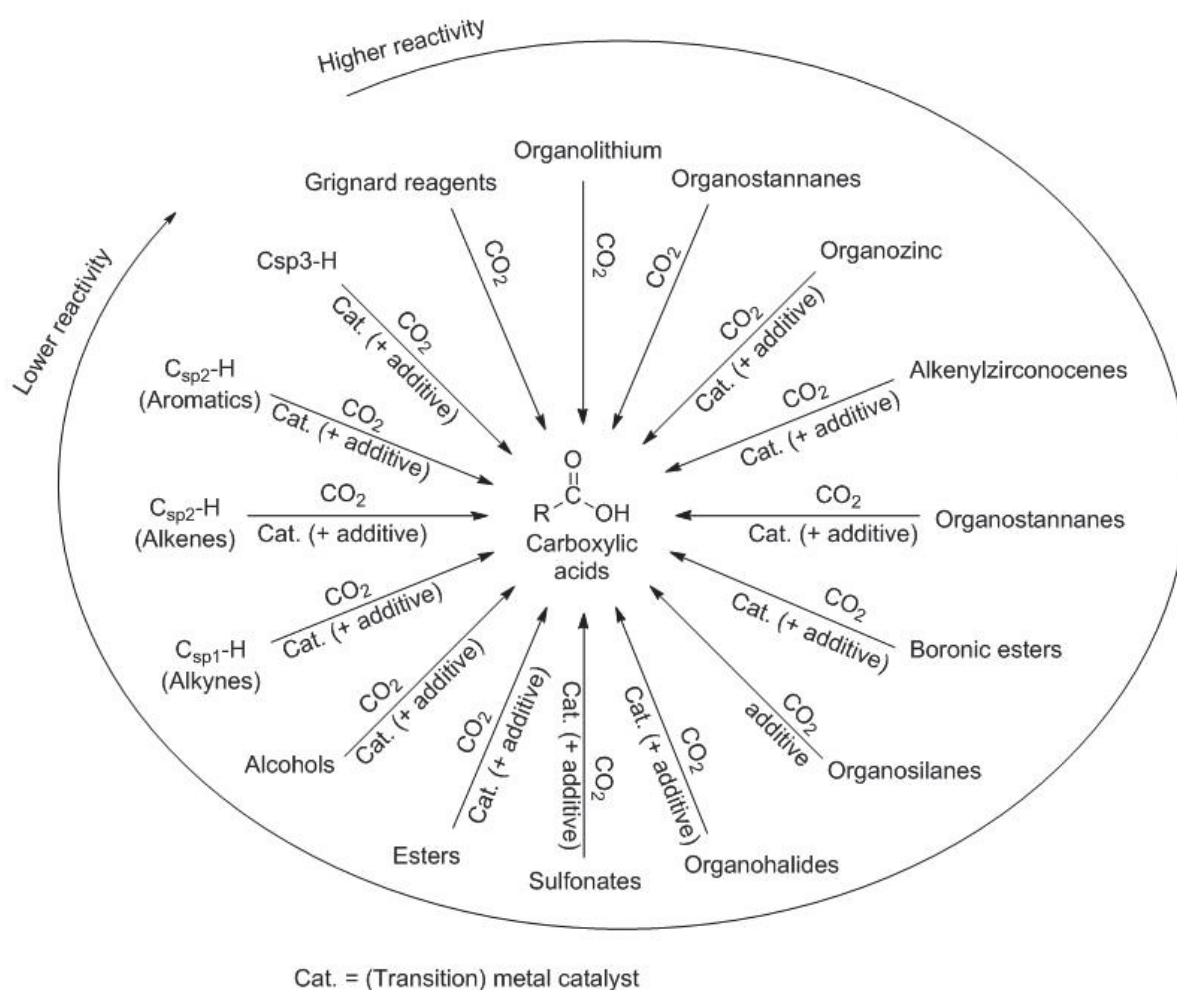


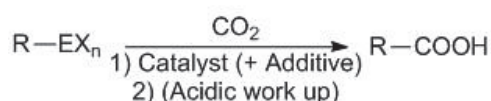
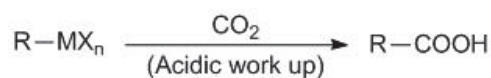
Figure 2-1: Schematic overview of the substrates illustrated in this chapter. The substrates are depicted starting from the more reactive (Grignard reagents) to the less reactive ( $sp^3$  C-H bonds). Reproduced with permission from “M. V. Solmi, M. Schmitz, W. Leitner;  $CO_2$  as a building block for the catalytic synthesis of carboxylic acids, *Horizons in Sustainable Industrial Chemistry and Catalysis*, eds. S. Albonetti, S. Perathoner and E. A. Quadrelli, Elsevier, 2019”.

In the following Chapter a review of the most important processes transforming  $CO_2$  into carboxylic acids is reported. The discussion of the processes is organized based on the organometallic or organic reagent which reacts with  $CO_2$  to give the carboxylic acid. A schematic overview of the considered processes is reported in Figure 2-1. At the beginning, highly polarized C-MX<sub>n</sub> (C-Metal-ligands) bonds of organometallic substrates (Grignard reagents, organolithium and organoalanes) will be described.

Following, less polarized C-EX<sub>n</sub> (C-Element-Ligands) bonds of organozinc, alkenylzirconocenes, organostannanes, alkenylboronic esters and organosilanes will be addressed. To conclude, simple organic compounds conversion will be reported <sup>1</sup>. Apart from the use of highly reactive organometallic reagents, the other approaches require catalysts and/or additives to give the desired products.

## 2.2 Organometallic substrates

In this section, various examples for carboxylations of organometallic substrates are reported. Most of these substrates have a nucleophilic position which reacts with the electrophilic C atom of CO<sub>2</sub> to give carboxylic acids, typically after acidic work-up (general scheme in Figure 2-2).



M = Mg, Al, Li.

E = Zn, Zr, Sn, B, Si.

X = Halogen, C<sub>x</sub>H<sub>y</sub> or O-C<sub>x</sub>H<sub>y</sub>

Figure 2-2: General reaction scheme of organometallic reagents with CO<sub>2</sub>. The organic substrates are transformed into organometallic reagents. Grignard reagents, organoalanes and organolithium do not need catalysts or additive to activate CO<sub>2</sub> (top scheme). Other reagents require a transition metal catalyst to activate CO<sub>2</sub> (bottom scheme). Reproduced with permission from "M. V. Solmi, M. Schmitz, W. Leitner; CO<sub>2</sub> as a building block for the catalytic synthesis of carboxylic acids, *Horizons in Sustainable Industrial Chemistry and Catalysis*, eds. S. Albonetti, S. Perathoner and E. A. Quadrelli, Elsevier, 2019".

Table 2-1: Examples of organometallic reagents carboxylation.

Entry	Substrate	Catalyst	(Organo)metallic additive	Products and Yield (%)
1 <sup>122</sup>		-	-	 <b>&gt;99</b>
2 <sup>123</sup>		[Fe] (1%)	EtMgBr (1.2 eq.)	 <b>93</b>
3 <sup>124, 125</sup>		-	1) R <sup>1</sup> R <sup>2</sup> Al (1 eq.) 2) CH <sub>3</sub> Li (1 eq.)	 <b>78</b>
4 <sup>126</sup>		-	[Al] (1 eq.)	 <b>75</b>
5 <sup>127</sup>		-	EtAlCl <sub>2</sub> (1 eq.)	 <b>99</b>
6 <sup>110</sup>		AlBr <sub>3</sub> (20%)	-	 <b>55</b>
7 <sup>128</sup>		-	BuLi (excess)	 <b>90</b>
8 <sup>129</sup>		-	RLi (1.05 eq.)	 <b>89</b>

### 2.2.1 Grignard reagents

Grignard reagents (RMgX, X = halogen, R = alkyl or aryl) are highly polarized nucleophiles. Already in 1900, Grignard reported about the activation of CO<sub>2</sub> thanks to these reagents.<sup>130</sup> Their high reactivity represents a limit for the use of substrates with electrophilic functional groups which would readily react with the Grignard nucleophile reducing the chemoselectivity in carboxylic acid. Nevertheless, it is possible to transform them in carboxylic acids under mild conditions (1 bar of CO<sub>2</sub> and room temperature). The development of continuous flow processes was reported in 2011 by Ley *et al.* to transform aryl-Grignard into carboxylic acids like 3-phenylpropionic acids

and many others (Entry 1, Table 2-1). They used a tube-in-tube membrane reactor in which CO<sub>2</sub> can pass quickly into the liquid phase to generate the carboxylic acids.

Separation and purification steps were also developed at the outlet from the reactor. A yield of >99 % was achieved, without the need of external organometallic agents or catalysts.<sup>122</sup> In 2012, Thomas *et al.* transformed alkenes into Grignard reagents with a Fe homogeneous catalyst (Entry 2, Table 2-1). The formed nucleophile reacts *in situ* with CO<sub>2</sub> to give the corresponding carboxylic acid, with yields up to 93 %.<sup>123</sup> Due to the fast reaction of Grignard reagents with CO<sub>2</sub> under mild conditions, they have the potential to be used for Carbon Capture and Utilization (CCU) reagents. Dowson reported that the synthesis of acetic acid starting from CH<sub>3</sub>MgX and captured CO<sub>2</sub> is estimated to be economically feasible.<sup>131</sup> However, from a “Green Chemistry” point of view this process does not seem to represent an improvement compared to the traditional acetic acid production. Difficulties in handling the Grignard reagents on a large scale and the high amounts of energy required for the regeneration of it from Mg salts make the application of this strategy challenging.<sup>1</sup>

### 2.2.2 Organoalane reagents

Organoalanes (R- $\text{AlR}'_2$ , R = C<sub>x</sub>H<sub>y</sub> or O-C<sub>x</sub>H<sub>y</sub>, R' = C<sub>x</sub>H<sub>y</sub> or halogen) compounds as well give carboxylic acids in presence of CO<sub>2</sub>. In 1888, Friedel and Crafts reported that PhAl<sub>2</sub>Cl<sub>5</sub> reacts with CO<sub>2</sub> giving the benzoic acid.<sup>132</sup> Vinyl carboxylic acids were obtained in 1967 from Zweifel (Entry 3, Table 2-1)<sup>124</sup> and in 1968 by Eisch.<sup>125</sup> They started from alkynes, which react with Al compound to give the vinylalanes, this is activated in the presence of methyl lithium and reacts with CO<sub>2</sub> in mild conditions to give the carboxylic acids in quite good yields (78%).<sup>124</sup>  $\beta$ -ketocarboxylic acids are produced starting from a ketone, in presence of 1 eq. of Al-porphyrin complex which lead to the production of the organoalane compound which is following reacting with CO<sub>2</sub> in mild conditions in presence of visible light (Entry 4, Table 2-1).<sup>126</sup> In 2016, Hattori suggested a very similar procedure to obtain  $\alpha,\beta$ - and/or  $\beta,\gamma$ -unsaturated carboxylic acids in good yields starting from  $\alpha$ -arylalkanes and EtAlCl<sub>2</sub> (Entry 5, Table 2-1).<sup>127, 133</sup>

AlBr<sub>3</sub> can coordinate to the oxygen atom of the phenol, which is transformed into salicylic acid in presence of supercritical CO<sub>2</sub> (Entry 6, Table 2-1).<sup>110</sup> This procedure exploits the Lewis acidity of aluminum salts which can coordinate one oxygen atom of the CO<sub>2</sub> molecule leading to a higher electrophilic carbon. For this reason, Al



compounds are also used in carboxylation reactions to activate the CO<sub>2</sub> and catalyze its reaction with organic substrates.

### 2.2.3 Organolithium reagents

Organolithiums are strong nucleophiles, which can act as substrates for carboxylations. In 1998, a Merck's patent described the transformation of aryl halides via organolithium compounds to carboxylic acids (Entry 7, Table 2-1).<sup>128</sup> As Grignard reagents, organolithiums easily react with electrophilic functional groups. In order to produce carboxylic acids bearing electrophilic functional groups, Yoshida and co-workers developed a continuous flow process which is able to form *in-situ* the organolithium and consume it fast enough to avoid side reactions between the organolithium moiety and the electrophilic functional group of the molecule (Entry 8, Table 2-1). Interestingly, they were able to obtain yields up to 89 % for aromatic carboxylic acids like benzoic acids and aromatic acids with diverse substituents in different positions of the rings.<sup>129</sup>

## 2.3 Organometallic substrates coupled with catalytic systems

The major drawback of the strong nucleophiles presented before is that generally, they are limited to substrates with few functional groups. Hence, to obtain carboxylic acids with a wider group tolerance, less polarized metal-carbon bonds need to be used.<sup>134</sup> Since they are less reactive than Grignards, organolithiums and organoalanes, suitable catalytic systems ([M]) have to be developed in order to speed up the reaction. Up to now, only examples of homogeneously catalyzed carboxylation have been reported.<sup>1</sup>

Generally, all the following reported examples follow a very similar reaction mechanism. The first stage is a transmetalation step, leading to a [M]-C bond. CO<sub>2</sub> is then inserted into the [M]-C bond to give the [M]-O(O)C-C complex. Usually, [M] is a late transition metal complex. In this way, the break of the [M]-O bond is easier compared to the [M]-C bond of the starting complex, allowing producing the carboxylic acid.<sup>135</sup> Often, the reductive elimination needs an additive or the organometallic reagent helping in regenerating the active species and releasing the carboxylic acid or derivatives. In some cases, the corresponding carboxylate salts are produced, and an acidic work up is required to observe the free carboxylic acids.

Table 2-2: Examples of organometallic substrates carboxylation, mediated by catalysts and/or additives.

Entry	Substrate	Catalyst	(Organo)metallic additive	Products and Yield (%)
1 <sup>136</sup>		[Ni] (5%) or [Pd] (1%)	-	 <b>95</b>
2 <sup>137</sup>	Alkyl-ZnI•LiCl	[Ni] (5%)	-	Alkyl-COOH <b>79</b>
3 <sup>138</sup>		-	LiCl (2.5 eq.)	 n = 0, 1 <b>89</b>
4 <sup>139</sup>	R <sup>1</sup> ≡R <sup>2</sup>	[Ni] (1-3%)	CsF (1 eq.) ZnEt <sub>2</sub> (3 eq.)	 <b>91</b>
5 <sup>140</sup>	R <sup>1</sup> ≡R <sup>2</sup>	[Cu] (10%)	Cp <sub>2</sub> ZrR <sup>3</sup> (1 eq.)	 <b>77</b>
6 <sup>141</sup>		[Pd] (8%)	-	 <b>90</b>
7 <sup>135</sup>		[Pd] (3.5%)	-	 <b>80</b>
8 <sup>142</sup>		[Rh] (3%)	CsF (3 eq.)	 <b>95</b>
9 <sup>143</sup>		[Cu] (1%)	-	R-COOH <b>97</b>
10 <sup>144</sup>		[Ag] (10%)	-	Ar-COOH <b>91</b>
11 <sup>145</sup>		[Cu] (5%)	MgSO <sub>4</sub> (0.5 eq.)	 <b>94</b>
12 <sup>146</sup>		[Cu] (5%)	(9-BNN) <sub>2</sub> (1 eq.) CsF (3 eq.)	 <b>94</b>
13 <sup>146</sup>	R≡	[Cu] (10%)	(9-BNN) <sub>2</sub> (1.2 eq.) CsF (2.2 eq.)	 <b>76</b>

14 <sup>147</sup>		-	AlX <sub>3</sub> (1 eq.)		45
15 <sup>148</sup>		[Ir] (5%) or [Ru] (6%)	H <sub>3</sub> SiEt <sub>3</sub> (5-7 eq.) CsF (3-5 eq.)		90
16 <sup>149</sup>	R <sup>1</sup> -C≡C-SiMe <sub>3</sub>	-	CsF (1.2 eq.)	R <sup>1</sup> -C≡C-COOH	96
17 <sup>150</sup>		-	CsF (3 eq.)		97
18 <sup>151</sup>		[Cu] (10%)	PhMe <sub>2</sub> SiBpin		93
19 <sup>152</sup>		-	[(Ph <sub>3</sub> SiF <sub>2</sub> )(N( <i>n</i> Bu) <sub>4</sub> ) <sup>+</sup> ] (1 eq.)		99

[a] In the table, only organometallic, metallic and salts additives are reported. Organic acids and bases are not listed in the table. [b] A mixture of  $\alpha,\beta$  and  $\beta,\gamma$ -unsaturated carboxylic acids is always obtained.

### 2.3.1 Organozinc reagents

Organozinc compounds are sensitive and highly reactive compounds, but more functional groups are tolerated compared to more nucleophilic organometallic reagents.

In 2008, Dong *et al.* synthesized aryl carboxylic acids starting from arylzinc compounds and CO<sub>2</sub>. Ni( $\eta^2$ -CO<sub>2</sub>)(PCy<sub>3</sub>)<sub>2</sub> (Aresta complex) or Pd analogous are active catalysts for this reaction. The transformation is efficient and up to 95 % yield of the desired acid product is produced at mild conditions (Entry 1, Table 2-2).<sup>136</sup> Ni complexes with phosphorus based ligands were also used as catalysts for the carboxylation of alkyl-ZnI•LiCl compounds into the corresponding carboxylic acids, like shown by Oshima *et al.* (Entry 2, Table 2-2).<sup>137</sup> A similar system was reported in 2009 by Kondo and co-workers (Entry 3, Table 2-2).<sup>138</sup>  $\alpha,\beta$ -unsaturated carboxylic acids were obtained from alkynes, *via* an *in-situ* formed vinylzinc compound. Further in this context, a homogeneous Ni catalyst was used for synthesizing the corresponding carboxylic acid through a organozinc intermediate (Entry 4, Table 2-2).<sup>139</sup>

### 2.3.2 Alkenylzirconocenes and organostannanes

In 2015, the synthesis of  $\alpha,\beta$ -unsaturated tri-substituted carboxylic acids were performed starting from alkynes, after an initially coordination step on a Zr complex (Entry 5, Table 2-2). The obtained alkenylzirconocenes react with CO<sub>2</sub> in presence of a Cu catalyst bearing a NHC ligand (*N*-Heterocyclic Carbene).<sup>140</sup>

$\alpha,\beta$  and  $\beta,\gamma$ -unsaturated carboxylic acids can also be synthesized starting from organostannanes. A Pd complex is used as catalyst. In these reactions, different selectivities in  $\alpha,\beta$  and  $\beta,\gamma$ -unsaturated carboxylic acids were obtained by different groups (Entry 6-7, Table 2-2).<sup>135, 141</sup>

### 2.3.3 Boronic esters

Boronic esters are nucleophiles which, in presence of a transition metal catalyst, react with CO<sub>2</sub> towards carboxylic acids. Boronic esters can be easily synthesized and they tolerate a broad range of functional groups.<sup>142</sup> Due to the lower reactivity of boronic esters compared to other nucleophiles, usually a (over) stoichiometric amount of base is required to obtain the desired carboxylic acids derivatives.<sup>1</sup>

Iwasawa *et al.* reported the transformation of arylboronic esters to carboxylic acids, catalyzed by a Rh complex and CsF in over stoichiometric amounts (Entry 8, Table 2-2).<sup>142</sup> Other systems requiring CsF as additive were further developed as reported in (Entry 12, Table 2-2).<sup>146</sup> In 2008, a wide variety of carboxylic acids were obtained starting from alkenylboronic esters, using a Cu complex (NHC ligand) as catalyst (Entry 9, Table 2-2). Good yields up to 97% were achieved and <sup>t</sup>BuOK was used instead of CsF as stoichiometric basic additive.<sup>143</sup> In 2012, Lu and co-workers reported a similar system to get arylcarboxylic acids (Entry 10, Table 2-2). They used Ag(I) salts in combination with PPh<sub>3</sub> as ligand for their catalytic system and <sup>t</sup>BuOK as stoichiometric base.<sup>144</sup>

Skrydstrup and co-workers developed a system able to obtain even dicarboxylic acids starting from alkynes (yields up to 76 %, Entry 13, Table 2-2).<sup>146</sup> In 2018, Lail and co-workers achieved the double carboxylation of bisboronate arenes to terephthalic acids. A copper complex with NHC ligand with the addition of a base and MgSO<sub>4</sub> is able to perform the reaction and obtain this important monomer using a green reagent, such as CO<sub>2</sub>.<sup>145</sup>

### 2.3.4 Organosilanes

Organosilanes are attractive nucleophiles compared to other organometallic species, because of their lower toxicity, easier preparation and handling. The carboxylation of organosilanes differs from the previously mentioned, since no transition metal catalyst is needed. However, they are not as reactive as Grignard reagents, organolithium or organoalanes. Therefore, an additional activation is required.<sup>152</sup>

The first example of synthesis of carboxylic acids from organosilanes was reported by Vol'pin in 1993. Allyltrimethylsilane reacts with  $AlX_3$  to give  $\beta,\gamma$ -unsaturated carboxylic acids (Entry 14, Table 2-2). In that case, the Lewis acid property of  $AlX_3$  supports the activation of  $CO_2$ . Nevertheless, the silane is needed for the product-forming intramolecular transmetallation step in order to eliminate the carboxylic acid from the Al center.<sup>147</sup>

The C-Si bond features lower polarity compared to other organometallic reagents, therefore additives allowing the reaction with  $CO_2$  are needed. In the following examples, a fluoride source is added to produce a carbanion synthon ( $[R_4FSi]^-$ ) which reacts with  $CO_2$  to form a carboxylic acid.<sup>152</sup> In 2012, the group of Mita and Sato developed a system which generates in situ the organosilane using an Ir or Rh catalyst (Entry 15, Table 2-2). By that, they managed to activate a  $C(sp^3)$ -H bond close to an aromatic ring. The actual carboxylation step happens with the help of over-stoichiometric amounts of CsF yielding up to 90 % of the corresponding carboxylic acid.<sup>148</sup> Alkynylcarboxylic acids (Entry 16, Table 2-2)  $\alpha$ -hydroxy acids derivatives (Entry 17, Table 2-2) and  $\alpha$ -amino acids (Entry 18, Table 2-2) were attained starting respectively from the corresponding alkynylsilanes,  $\alpha$ -siloxy silane and *N*-Sulfonylimines with very good yields by different groups always using stoichiometric amounts of CsF to activate the silane.<sup>149-151</sup> In 2016, the group of Cantat presented a system able to produce heteroaromatic esters starting from the corresponding organosilanes (Entry 19, Table 2-2). A stoichiometric fluoride source (TBAT = tetrabutylammonium difluorotriphenylsilicate) and an organohalide are used as additives to perform the transformation. This example is remarkable for the production of oligomers with eight  $CO_2$  molecules incorporated. This is the first example of polyesters production incorporating  $CO_2$ .<sup>152</sup>

To conclude, all the cited organometallic reagents can be converted into carboxylic acids using relatively mild reaction conditions, such as low pressures of  $CO_2$  (~1 bar)

and room temperature. The main reason is the high reactivity of these substrates, which brings some drawbacks such as difficult preparation and handling of the starting materials. In addition, the use of stoichiometric amounts of (organo)metallic reducing agents, salts or activating (metal) groups results in the production of stoichiometric amount of wastes. Although no Life Cycle Assessment (LCA) has been reported for all the shown systems, these processes appear to not match in total the principles of "Green Chemistry".<sup>1, 153</sup> In particular, the development of purely catalytic processes activating CO<sub>2</sub> and an organic substrate, without the need of previous functionalization of it, is desirable. The removal of stoichiometric reagents would maximize the atom efficiency and minimize the production of side-products.

## 2.4 Non-activated substrates

This section will focus on state-of-the-art protocols dealing with ways to couple CO<sub>2</sub> with organic substrates towards carboxylic acid product. Organohalides, oxygen-containing substrates, alkynes, alkenes, aromatics and C-H bonds carboxylation is considered here. These substrates are obtained from well-established processes, like common petro- (cracking-, reforming- or Fischer-Tropsch-products) or biochemical techniques. Hence, their transformation into carboxylic acids would result more convenient compared to the transformation of highly reactive organometallic substrates. However, the energy barriers involved in these types of process result much higher and more challenging. New processes, catalytic systems and strategies have been implemented in order to transform non-activated substrates into carboxylic acids via (hydro)carboxylation processes.

### 2.4.1 C-Halide bonds (organohalides)

Organohalides are versatile substrates for the carboxylation reaction. The carbonylation of organic halides (using CO as carbonylating agent) is well developed and applied in industrial processes.<sup>154</sup> Processes using CO<sub>2</sub> instead of CO have been developed in the past years.

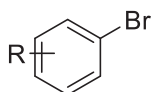
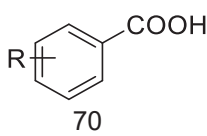
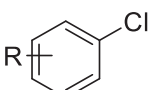
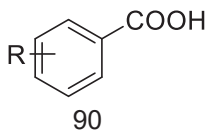
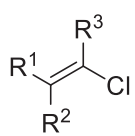
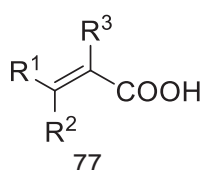
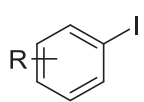
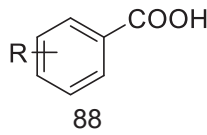
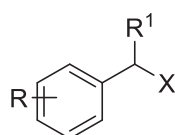
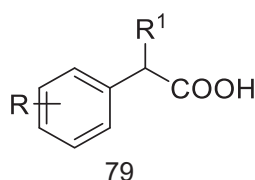
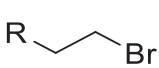
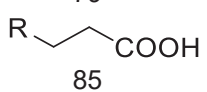
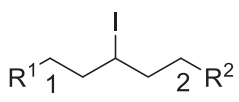
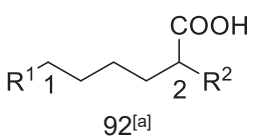
The catalytic cycles of the different processes have some common features. Commonly, the first step is an oxidative addition of the halide substrate to the catalyst. The oxidative addition of aryl, benzyl or methyl halides results faster compare to other classes of halides due to their higher tendency towards nucleophilic substitution. For this reason, these compounds are the main substrates used for these transformations,

as it is for traditional carbonylation processes using CO. Generally, the following step is the insertion of the carbonylating agent (CO<sub>2</sub> or CO) into the metal-carbon bond. At last, the elimination of the product occurs (carboxylic acids or derivatives i.e. salts or esters, are obtained). This last step is normally quite difficult, therefore an additional stoichiometric reducing (organo)metallic reagent (Et<sub>2</sub>Zn, Mn, MgCl<sub>2</sub>/Zn)<sup>155-158</sup> or H<sub>2</sub> is required.<sup>1</sup>

A method for using CO<sub>2</sub> in carboxylation reactions was demonstrated by Fukuoka and Komiya.<sup>159</sup> In their reaction of organic iodides, the corresponding carboxylic acids were obtained in presence of CO<sub>2</sub> and H<sub>2</sub> (yields up to 50%). A synergetic effect of the used bimetallic catalyst, consisting of Ru/Co- or Ni/Co-carbonyls, was essential for the conversion (Entry 1, Table 2-3). Despite the presence of CO in the gas phase from a possible *r*WGSR, Fukuoka *et al.* assumed a direct insertion of the CO<sub>2</sub> into the M-CH<sub>3</sub> bond after oxidative addition of H<sub>3</sub>C-I to the metal center. Aryl carboxylic acids were obtained from aryl halides and CO<sub>2</sub> from different groups using diverse catalytic systems (Pd, Ni and Cu complexes), with yields between 70 and 90 %. These transformations are reported in Entries 2-5, Table 2-3. The highest yields (up to 90 %) were obtained by Tsuji in 2012 (Entry 3, Table 2-3). They used a Ni complex with PPh<sub>3</sub> and Mn as reducing agent. The same system could produce  $\alpha,\beta$ -unsaturated carboxylic acids starting from vinyl chlorides.<sup>156</sup> Simple linear alkyl-halides with  $\beta$ -hydrogen carboxylation was reported in 2014 (Entry 6, Table 2-3). The first step of the catalytic cycle (oxidative addition) results more difficult, when alkyl compounds are used as substrates. Moreover,  $\beta$ -hydrogen elimination is possible. Generating alkenes, side reactions (i.e. dimerization) could occur, reducing the selectivity of the process. Therefore, the yield of carboxylic acids achieved (85%) with this catalytic system (Ni as catalyst, bidentate and bulky N-ligands, Mn as reducing agents) was a significant result.<sup>160</sup> Secondary bromides are even less feasible to undergo an oxidative addition and could not be carboxylated using the catalytic system developed. In 2016, Martin and co-workers presented a remarkable system to convert secondary alkyl halides into carboxylic acids. In particular, exploiting the  $\beta$ -hydrogen elimination reaction, the C-H bonds of the molecules are activated, leading selectively to different carboxylic acids starting from the same substrates (position 1 or 2 in Entry 7, Table 2-3).<sup>41</sup> If one of the two positions is hindered, the other will be preferred, and changing the reaction conditions (i.e. temperature) the regio-selectivity can be tuned.<sup>41</sup>

The transformation of C-X bonds into C-COOH bonds using CO<sub>2</sub> requires harsher conditions compared to the transformation of the previously mentioned reagents (C-MX<sub>n</sub> or C-EX<sub>n</sub>). Nevertheless, the preparation and handling of organohalides is easier compared to the activated substrates,<sup>1</sup> making their transformation highly interesting.<sup>115</sup>

Table 2-3: Examples of organohalides carboxylation with CO<sub>2</sub> to carboxylic acids.

Entry	Substrate	Catalyst	(Organo)metallic additive	Products and Yield (%)
1 <sup>161</sup>	R-I (R = CH <sub>3</sub> , CH <sub>3</sub> CH <sub>2</sub> , Ph)	[Ru] (1%) and [Co] (10%)	-	R-COOH 50
2 <sup>155</sup>		[Pd] (3.5%)	Et <sub>2</sub> Zn (2 eq.)	 70
	 Or			 90
3 <sup>156</sup>		[Ni] (5%)	Mn (3 eq.)	 77
4 <sup>157</sup>		[Cu] (3%)	Et <sub>2</sub> Zn (3 eq.)	 88
5 <sup>158</sup>		[Ni] (10%)	MgCl <sub>2</sub> (2 eq.) Zn (5 eq.)	 79
6 <sup>160</sup>		[Ni] (10%)	Mn (2 eq.)	 85
7 <sup>41</sup>		[Ni] (2.5%)	Mn (2 eq.)	 92 <sup>[a]</sup>

[a] -COOH group is in position 1 or 2.



### 2.4.2 C-O Bonds (oxygenated substrates)

C-O electrophiles are alternative substrates to organic halides for the carboxylation. They can be obtained from alcohols (which are naturally abundant) and no toxic halogenated wastes are produced with their use.<sup>115</sup> Among all the possible O-containing functionalities, very few have been carboxylated with CO<sub>2</sub> to give carboxylic acids. Generally, more reactive C-O bonds, but also less available, (Figure 2-3) are reported to react with CO<sub>2</sub> giving carboxylic acids.<sup>162</sup> Esters or sulfonates are the most common substrates used for these transformations.

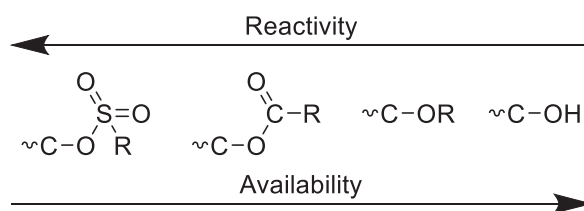
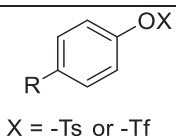
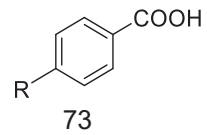
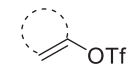
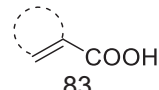
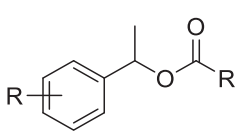
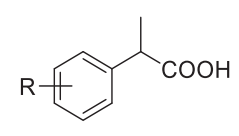
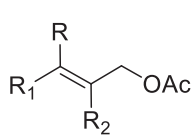
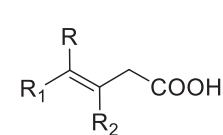
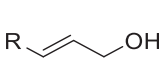
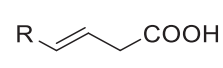
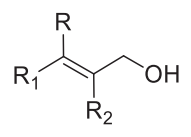
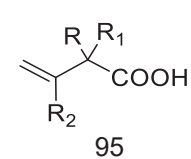
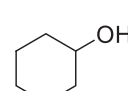
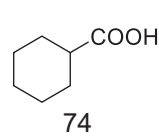
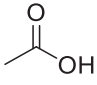
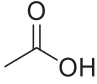


Figure 2-3: C-O bonds which can be transformed in carboxylic groups, ordered based on their reactivity and their availability.

Aryl tosylates and triflates can be transformed into carboxylic acids *via* CO<sub>2</sub> activation using catalytic systems similar to those employed for the conversion of halides.<sup>1</sup> Normally, the catalytic cycle is very similar to that reported for halides carboxylation, the oxidative addition being the first step. The same Ni complex, coupled with Mn and Et<sub>2</sub>Ni, which transform halides and CO<sub>2</sub> into carboxylic acids can catalyze the conversion of sulfonates, just increasing the operating temperature. The system is not as active as for halides, giving yields of 73 % only (Entry 1, Table 2-4).<sup>156</sup> Another Ni complex in similar conditions leads to yields for carboxylic acids up to 61 % starting from a wider variety of aryl tosylates.<sup>163</sup> Later, Tsuji's group reported about the use of a homogeneous cobalt system to convert alkenyl tosylates (as well as sterically hindered aryl tosylates) into the corresponding  $\alpha$ ,  $\beta$ -carboxylic acids (Entry 2, Table 2-4). Yields up to 86 % were feasible with this system.<sup>164</sup> Non-activated mesylates and tosylates are converted with Ni complex and Mn as reducing agent, similarly to alkyl bromides possessing  $\beta$ -hydrogen. This system was able to produce carboxylic acids from sulfonates with yields comparable to those obtained starting from halides (about 76 %) (Entry 3, Table 2-4).<sup>160</sup>

Table 2-4: Examples of C-O bonds carboxylations with CO<sub>2</sub> to carboxylic acids.

Entry	Substrate	Catalyst	(Organo)metallic additive	Products and Yield (%)
1 <sup>156</sup>		[Ni] (10 %)	Mn (3 eq.)	 73
2 <sup>164</sup>		[Co] (5%)	Mn (1.5 eq.)	 83
3 <sup>160</sup>	R-OX (X = -Tf, -Ms, -COCF <sub>3</sub> )	[Ni] (10 %)	Mn (2.4 eq.)	R-COOH 76
4 <sup>165</sup>		[Ni] (10 %)	Mn (2 eq.)	 80
5 <sup>166</sup>		[Ni] (10 %)	Mn (2.4 eq.) and MgCl <sub>2</sub> (2 eq.) or Zn (1.75 eq.) and NaCO <sub>3</sub> (20 %)	 77
6 <sup>162</sup>		[Ni] (10%)	a) Zn (4 eq.) and MgCl <sub>2</sub> (1.2 eq.) b) Zn (1.5 eq.), MgCl <sub>2</sub> (1.2 eq.) and CaCl <sub>2</sub> (4 eq.)	a)  81
7 <sup>167</sup>		[Pd] (10 %)	ZnEt <sub>2</sub> (3.5 eq.)	 95
8 <sup>6</sup>		[Rh] (5%)	-	 74

<b>9</b> <sup>168</sup>	CH <sub>3</sub> OH	[Rh] (0.3 %)	[Ru] (0.3 %)	 70
<b>10</b> <sup>169</sup>	CH <sub>3</sub> OH	[Rh] (0.25 %)	LiCl (4 eq.)	 82

In 2014 by Correa *et al.* reported the reductive carboxylation of aryl (sp<sup>2</sup>) or benzyl (sp<sup>3</sup>) esters with CO<sub>2</sub> using a molecular Ni catalyst together with a stoichiometric amount of Mn as reducing reagent (Entry 4, Table 2-4).<sup>165</sup> They stated out their operational simplicity, the absence of air- or moisture-sensitive reagents, together with the broad scope and chemo-selectivity profile for the utilization of ester derivatives as a suitable alternative to commonly used organic halides. The same year the group of Martin published about the reductive CO<sub>2</sub>-based carboxylation of allyl acetates (Entry 5, Table 2-4).<sup>166</sup> By applying different pyridine-modified ligands, the selectivity of the acid-product could be set up to 99:1 ratio towards the desired linear regio-isomer. However, the catalyst, ligand and reducing reagent loadings limit so far further applications, although the temperature and needed CO<sub>2</sub>-pressure were ambient. Moreover in 2017, a throughout comparable Ni-catalyzed reaction system was feasible to perform the even more challenging regio-divergent synthesis of carboxylic acids based on simple allylic alcohols (Entry 6, Table 2-4).<sup>170</sup>

Carboxylation of alcohols was first reported by Mita, Sato and co-workers in 2015.<sup>167</sup> Allylic acids were achieved starting from allylic alcohol and CO<sub>2</sub>, using Pd complex as catalyst and ZnEt<sub>2</sub> as stoichiometric transmetallation agent (Entry 7, Table 2-4).<sup>167</sup> As explained in the previous Section 1.4.2, the group of Leitner reported the first conversion of aliphatic alcohol with CO<sub>2</sub> and H<sub>2</sub> into carboxylic acids (Entry 8,

Table 2-5).<sup>6</sup> A deeper study of the reaction conditions of this transformation, together with a study of the scope of the reaction and of the mechanism are reported in this thesis.

A remarkable report of the production of acetic acid using methanol and CO<sub>2</sub> was presented in 2016 by the group of Han (Entry 9, Table 2-4).<sup>171</sup> Yields of 70% were achieved using a combination of two molecular catalysts (rhodium and a ruthenium) and H<sub>2</sub> as reducing agent. With imidazole as ligand, the system tends to higher selectivity and almost no formation of CO nor CH<sub>4</sub>. Thus the authors propose a direct CO<sub>2</sub> activation mechanism and the complete incorporation of the building block in the

final product. In 2017, they reported about an improved catalytic system for the CO<sub>2</sub>-based synthesis of acetic acid.<sup>172</sup> Switching to a rhodium-catalyzed system and 4-methylimidazole as most suitable ligand they reached a maximum yield of 84 % of acetic acid at 180 °C (Entry 10, Table 2-4).<sup>172</sup>

Other oxygenated substrates such as ketones, aldehydes or epoxides were never reported to react with CO<sub>2</sub> to give carboxylic acids.<sup>1</sup> The first study of these transformations is reported in the Section 3.3.2, 3.4.2 and 3.5 of this thesis.

### 2.4.3 C(sp)-H bonds (alkynes)

Starting from C-H-acidic sp<sup>1</sup>-bonds, literature protocols comprise generally two routes for reacting an alkyne with CO<sub>2</sub> to carboxylic acids. On one hand, the formation of alkyne carboxylic acids where the initial triple-bond is preserved is described.<sup>173-177</sup> On the other hand, in presence of an additional reducing agent (i.e. Mn, Zn, or silanes)  $\alpha,\beta$ -saturated carboxylic acids can be formed.<sup>178</sup> The second transformation is of high interest due to the formation of acrylic acid and its derivatives, which are important monomers for polymers production.<sup>1</sup> Both pathways generally require basic conditions. Hence, the corresponding carboxylic acids salts are formed and consecutively converted into the desired acid by hydrolysis.

Alkynyl carboxylic acids were obtained using phenylacetylenes as substrates by the group of Kondo. They reported a Cu-phosphine catalytic system, which in presence of over-stoichiometric amounts of base is able to give yields up to 90% of the corresponding ester, which can be transformed into carboxylic acids through acidic work-up (Entry 1, Table 2-5).<sup>175</sup>

Already in 1984, the group of Hoberg described a protocol to incorporate CO<sub>2</sub> into alkynes (acetylene) to obtain carboxylic acids (acrylic acid).<sup>179</sup> This process requires a stoichiometric amount of Ni complex, which reacts with acetylene and CO<sub>2</sub> in an oxidative coupling to an isolable nickelalactone in 60 % yield (Entry 1, Table 2-5). After hydrolysis and work-up in methanol, the methyl ester was formed. In addition to nickel catalyzed processes,<sup>139, 180-182</sup> silver,<sup>176, 183</sup> iron,<sup>184</sup> and copper<sup>173-175, 181, 184, 185</sup> catalysts have been reported.

The transformation of acetylene and CO<sub>2</sub> into acrylic acid is an interesting transformation due to the commercial importance of the product, among those reported in this section. The reported protocols are often performed at mild conditions, but all of them require organometallic (over)stoichiometric reducing agents to obtain the desired

acrylic acid derivatives and an acidic aqueous work-up (e.g.  $\text{HCl}_{\text{aq}}$ ). Another drawback of this process is the difficult handling of acetylene under pressure. For all these reasons, none of the above mentioned processes have been implemented on an industrial level, yet.<sup>1</sup>

Table 2-5: Examples of alkynes and alkenes transformation into carboxylic acids.

Entry	Substrate	Catalyst	(Organo)metallic additive	Products and Yield (%)
1 <sup>175</sup>	$\text{Ph}-\text{C}\equiv\text{C}-\text{H}$	[Cu] (8%)	$\text{Cs}_2\text{CO}_3$	$\text{Ph}-\text{C}\equiv\text{C}-\text{COOH}$ 90
2 <sup>179</sup>	$\text{CH}_2=\text{CH}-\text{C}\equiv\text{C}-\text{H}$	[Ni] <sup>[a]</sup>	DBU	$\text{CH}_2=\text{CH}-\text{COOH}$ 70
3 <sup>186, 187</sup>	$\text{CH}_2=\text{CH}-\text{C}\equiv\text{C}-\text{H}$	[Ni] (2%)	Zn	$\text{CH}_2=\text{CH}-\text{COONa}$ TONs up to 107
4 <sup>188, 189</sup>	$\text{CH}_2=\text{CH}-\text{C}\equiv\text{C}-\text{H}$	[Pd] <sup>[b]</sup>		$\text{CH}_2=\text{CH}-\text{COONa}$ TONs up to 514
5 <sup>190</sup>	$\text{CH}_2=\text{CH}-\text{C}\equiv\text{C}-\text{H}$	[Ni] <sup>[a]</sup>	DBU	$\text{CH}_3-\text{CH}_2-\text{COOH}$ 85
6 <sup>191</sup>	$\text{R}-\text{C}_6\text{H}_4-\text{CH}=\text{CH}_2$ R = H, CH <sub>3</sub> , CF <sub>3</sub> , CO <sub>2</sub> Me, Cl, OMe, ...	[Ni] (10%)	$\text{Cs}_2\text{CO}_3$ Et <sub>2</sub> Zn	$\text{R}-\text{C}_6\text{H}_4-\text{CH}(\text{CH}_3)-\text{COOH}$ R = H, CH <sub>3</sub> , CF <sub>3</sub> , CO <sub>2</sub> Me, Cl, OMe, ... 92
7 <sup>192</sup>	$\text{CH}_2=\text{CH}-\text{C}\equiv\text{C}-\text{H}$	[Rh] <sup>[c]</sup>	$\text{HBr}_{\text{aq}}$	$\text{CH}_3-\text{CH}_2-\text{COOH}$ 38
8 <sup>190</sup>	$\text{C}_6\text{H}_{10}$	[Rh] (5%)	-	$\text{C}_6\text{H}_{11}-\text{COOH}$ 91

[a] Stoichiometric amount. [b] 0.1 mmol of [Pd] and 10 bars of ethylene. [c] 0.02-0.5 g of [Rh] and 700 bars of ethylene/ $\text{CO}_2$  (1/1).

#### 2.4.4 C(sp<sup>2</sup>)-H bond (alkenes)

Alkenes (Csp<sup>2</sup>-H bond) are abundant and can easily be tuned to obtain a wide variety of substrates.<sup>1</sup> The conversion with  $\text{CO}_2$  towards carboxylic acids can be

performed through two pathways, similarly to the alkynes transformations. The double bond can be preserved, and the CO<sub>2</sub> is added giving an  $\alpha$ ,  $\beta$ -carboxylic acid (i.e. acrylic acids). The reaction pathway consist of the formation of an initial metalalactone through coordination of the alkene and CO<sub>2</sub> to the metal center.<sup>1</sup> On the other hand, saturated carboxylic acids can be obtained by addition of CO<sub>2</sub> and hydrogenation of the double bond.<sup>1</sup>

A Ni-catalyzed synthesis of acrylates was shown by Lejkowski *et al.* in 2012.<sup>186, 187</sup> The catalyst promotes the direct carboxylation of simple alkenes, like ethene, styrene and 1,3-dienes with CO<sub>2</sub> to their corresponding linear  $\alpha,\beta$ -unsaturated carboxylic acid salts. Using an electron-rich bisphosphine ligand (BenzP\*) and a suitable base (sodium 2-fluorophenoxide), TONs up to 107 for sodium acrylate were achieved (Entry 3, Table 2-5). In addition to transition metal catalysts such as Ni, Mo and W, especially Pd offers new promising strategies to generate acrylates.<sup>8, 193</sup> Most recently, the group of Schaub developed a system using Pd catalyst, amide as solvent and an alcoholate as base reaching a TON to sodium acrylate of 514 (Entry 4, Table 2-5).<sup>188, 189</sup> In addition, the recycling of the catalysts in the active form was performed and the ethene conversion to acrylate with a total TON from two cycles (TTON<sub>2</sub>) of 235 was achieved.

Rovis and coworkers reported about the first Nickel-catalyzed reductive carboxylation of styrenes and other phenyl substituted alkenes using CO<sub>2</sub> under ambient conditions (23 °C, 1 bar CO<sub>2</sub>). The transformation lead regio-selectively to saturated  $\alpha$ -substituted carboxylic acids (Entry 6, Table 2-5).<sup>191</sup> However, without the addition of the reducing agent (Et<sub>2</sub>Zn), the active complex would not be regenerated.

Complementary to their work on acetylene towards acrylic acid, Hoberg *et al.* published the synthesis of propionic acid catalyzed by the saturated Ni complex (Entry 5, Table 2-5).<sup>190, 194</sup> However, a catalytic carboxylation was not achieved, since the DBU stabilized the Ni-lactone which could not undergo a consecutive  $\beta$ -hydride elimination followed by a reductive elimination to generate an acrylate moiety.<sup>195</sup>

Already in 1978 Lapidus *et al.* reported the synthesis of propionic acid from ethene and CO<sub>2</sub> (Entry 7, Table 2-5).<sup>192</sup> The Wilkinson's complex [RhCl(PPh<sub>3</sub>)<sub>3</sub>] with aqueous HBr can convert ethene and CO<sub>2</sub> under harsh reaction conditions (180 °C, 700 bar) to propionic acid. It is not clear how this reaction happens. The formation of H<sub>2</sub> as reducing agent from HBr or the aqueous media itself seems a good explanation, although the details still remains not clear.<sup>1</sup> The same catalytic system (based on Rh, iodide source and PPh<sub>3</sub> additive) able to transform the alcohols into carboxylic acids

was also studied by Leitner and co-workers for the alkene hydrocarboxylation (Entry 8, Table 2-5).<sup>6</sup> The hydrocarboxylation of alkene was deeply investigated, finding optimized reaction conditions which are milder compared to those previously reported.<sup>12</sup> Besides the milder conditions, this process presents the clear advantages of using H<sub>2</sub> as reducing agent (no organometallic reagents are required) and of producing directly the desired carboxylic acids without the need of additional hydrolysis.<sup>196</sup> This catalytic system is the same used as starting point for this thesis. Further details about the system and the conducted studies are given in the Section 1.4.2 and in the following Sections for comparison with the new work herein presented.

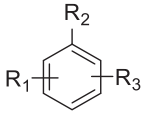
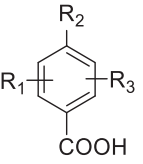
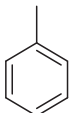
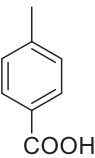
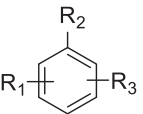
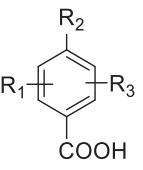
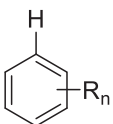
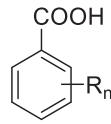
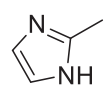
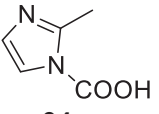
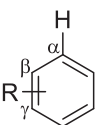
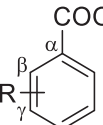
#### 2.4.5 C(sp<sup>2</sup>)-H bond (aromatics)

The directly catalyzed “green” carboxylation of benzene with CO<sub>2</sub> towards benzoic acid would be an extremely interesting reaction, although still presents challenges. These transformations have their roots in the pioneering work of *Kolbe-Schmitt*<sup>197, 198</sup> already mentioned earlier in this thesis. However, this process is suitable for pre-formed sodium phenolate, while other non-activated aromatic rings cannot be converted to the corresponding carboxylic acids. To convert these types of substrates specific catalytic systems have to be developed.<sup>199</sup>

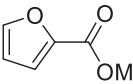
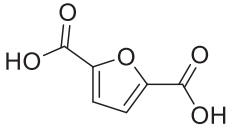
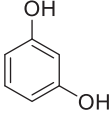
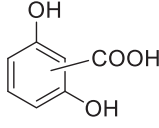
For example, to carboxylate aryl C-H bonds the use of stoichiometric amounts of Al<sub>2</sub>Cl<sub>6</sub>/Al was reported.<sup>199</sup> Later, a similar system was optimized and published in 2002 by the group of Olah. The method, similar to the Friedel-Crafts acylation/alkylation system, can convert benzene into benzoic acid (Entry 1, Table 2-6) after an acidic work-up with HCl<sub>aq</sub>. The role of the additional aluminum is probably to capture the HCl generated to give again the active Lewis acid (AlCl<sub>3</sub>), which is needed to form the dimer Al<sub>2</sub>Cl<sub>6</sub>.<sup>200</sup> Further improvement and studies of the system were reported: modifications of the Lewis acids,<sup>201, 202</sup> systems without the need of Al,<sup>203, 204</sup> a significant improvement of a catalytic system for the carboxylation of toluene towards *p*-methylbenzoic acid was investigated by Munshi (Entry 2, Table 2-6).<sup>203, 205</sup> Here, a combination of a fluorinated solvent and a nitrogen base enabled the catalytic Friedel-Craft-type carboxylation of toluene with CO<sub>2</sub> towards the corresponding carboxylic acid (after aqueous work-up). Al<sub>2</sub>Cl<sub>6</sub> is crucial interacting with CO<sub>2</sub>, making it more reactive for the following carboxylation. In 2015, the group around Zhenmin developed a protocol for the carboxylation of aryl compounds.<sup>204</sup> AlCl<sub>3</sub>/organosilanes derived “Frustrated Lewis Pairs” (FLPs) were used to catalyze this transformation, activating

CO<sub>2</sub> (Entry 3, Table 2-6). 87 % yield of benzoic acid was achieved starting from benzene.

Table 2-6: Examples of transformation of C-H aromatic bonds and CO<sub>2</sub> into carboxylic acids.

Entry	Substrate	Catalyst	(Organo)metallic additive	Products and Yield (%)
1 <sup>199</sup>	 <p>R<sub>1</sub> = H, alkyl R<sub>2</sub>, R<sub>3</sub> = CH<sub>3</sub>, alkyl</p>	Al <sub>2</sub> Cl <sub>6</sub> /Al	-	 <p><b>92</b></p>
2 <sup>203, 205</sup>		Al <sub>2</sub> Cl <sub>6</sub>	-	 <p><b>TONs up to 7.8</b></p>
3 <sup>204</sup>	 <p>R<sub>1</sub> = H, alkyl R<sub>2</sub>, R<sub>3</sub> = H, CH<sub>3</sub>, alkyl</p>	Al <sub>2</sub> Cl <sub>6</sub> /R <sub>3</sub> SiCl R = CH <sub>3</sub> or Ph	-	 <p><b>97</b></p>
4 <sup>206</sup>	 <p>R<sub>n</sub> = F, Cl (n = 2-4)</p>	[Au] (1.5%) or [Cu] (3%)	KOH or CsOH	 <p>R<sub>n</sub> = F, Cl (n = 2-4) <b>96</b></p>
5 <sup>207</sup>		-	<sup>t</sup> BuOK	 <p><b>94</b></p>
6 <sup>208</sup>	 <p>R = H, CH<sub>3</sub>, CF<sub>3</sub>, OMe, ...</p>	[Rh] (0.03%)	AlMe <sub>1.5</sub> (OEt) <sub>1.5</sub>	 <p>R = H, CH<sub>3</sub>, CF<sub>3</sub>, OMe, ... <b>TONs up to 60</b></p>



7 <sup>209</sup>		M <sub>2</sub> CO <sub>3</sub> (75%)	-	
8		2,3-DHBD or SAD (enzymes)	-	

C-H-acidic (hetero)arenes carboxylation was performed as well. In 2010, Boogaerts and Nolan published the C-H (of arenes) and N-H (of N-heterocycles) carboxylation of a broad range of substrates.<sup>210, 211</sup> The transformation required the use of a Au based catalyst with a NHC ligand and a base additive (KOH) (Entry 4, Table 2-6).<sup>206</sup> Excellent 96 % yield were achieved for certain carboxylic acids (after work-up) with this system. Later, Cazin and Nolan reported about the analogue copper catalyst [Cu] in presence of stoichiometric amounts of CsOH as basic additive for this reaction (Entry 4, Table 2-6).<sup>211</sup> They show together with independent reports by Hou and co-workers<sup>181</sup> insights into the scope and mechanism of direct carboxylation reactions using inexpensive copper(I) complexes.<sup>212</sup> A transition metal free carboxylation of oxazol C-H bond was reported in 2016 by Ackermann *et al.* They used <sup>t</sup>BuOK, atmospheric pressure of CO<sub>2</sub> and 100 °C to achieve the desired product (Entry 5, Table 2-6).<sup>207</sup> However, in these examples, the corresponding ester was produced, which had to be cleaved to gain the free acid functionality. In 2014, Iwasawa *et al.* showed a rhodium complex able to catalyze the carboxylation of C-H bonds of simple arenes. In addition to the Rh catalyst, stoichiometric amounts of Al-reagents are needed (Entry 6, Table 2-6).<sup>208</sup> Although the system seems similar to the one reported by Olah and co-workers, Iwasawa ruled out the hypothesis of a similar mechanism and reaction pathway.<sup>199</sup>

Furan-2,5-dicarboxylic acid (FDCA) has receiving large attention as biomass-derived diacids to produce sustainable polymers (polyethylene furandicarboxylate, PEF) as PET substitutes. Recently in 2017, Kanan *et al.*<sup>209</sup> developed a process based on the carboxylation of 2-furoic acid (furan-2-carboxylate), which is obtained by biomass.<sup>213</sup> Alkali carbonates (M<sub>2</sub>CO<sub>3</sub>) promote C–H carboxylation, leading to FDCA from 2-furoic acid and CO<sub>2</sub> (Entry 7, Table 2-6). This product is obtained in high yields and in large laboratory scales (up to 1 mol). The process involves the use of a fixed-bed flow reactor, no solvent is involved, but an acidic work up is needed to obtain 89%

of isolated yield of FDCA. A similar system was later be expanded to the production of other dicarboxylic acids and other compounds.<sup>214</sup>

A recent bio-catalytic approach to the carboxylation of resorcinol was developed. This system uses a *ortho*-benzoic acid decarboxylases (2,3-DHBD) and salicylic acid decarboxylase (SAD) under 30-40 bar of CO<sub>2</sub> to carboxylate the C-H bond of resorcinol, giving up to 68% yield of the desired product (Entry 8, Table 2-6). The atom efficiency calculation provided by the authors confirmed the potentially increased sustainability of this new approach compared to the traditional chemical approach (Kolbe-Schmitt reaction).<sup>215</sup>

#### 2.4.6 C(sp<sup>3</sup>)-H bonds

The carboxylation of C(sp<sup>3</sup>)-H bonds is of high interest due to their high availability, e.g. from petrochemistry, but this transformation remains challenging due to their low reactivity.

Methane transformation into acetic acid by CO<sub>2</sub> insertion has been investigated on heterogeneous materials such as Cu/Co<sup>216</sup> (Entry 1, Table 2-7) or a Ag-doped Rh/SiO<sub>2</sub> material<sup>217</sup> (Entry 2, Table 2-7). These processes are mainly not catalytic due to the challenging thermodynamics of this reaction which leads to very low yields of acetic acid.<sup>218, 219</sup> Nevertheless, some materials as zinc-modified H-ZSM-5 based zeolite<sup>220</sup> showed good selectivity in the desired products.

Pioneering works about the activation of acidic protons were done already in the 1970s. These examples deal with the substitution of the proton in the  $\beta$ -position of ketones with an -COOH group (obtained from CO<sub>2</sub>) leading to  $\beta$ -ketocarboxylic acids. These products are quite unstable, hence they have to be readily converted into more stable compounds such as ester, salt,  $\beta$ -hydroxycarboxylic acids etc.<sup>221</sup> The early reports of this transformation were mainly using over-stoichiometric amounts of reagents like lithium 4-methyl-2,6-di-tert-butylphenoxide (Entry 3, Table 2-7),<sup>222</sup> DBU (Entry 4, Table 2-7),<sup>223</sup> or Magnesium 2-oxoimidazolidine-1,3-diide dibromide (Entry 5, Table 2-7).<sup>224</sup> Good yields were obtained (up to 90 %) but high amounts of reactive reagents were also needed. Later reports tried to avoid the use of over-stoichiometric reagents trying to deal with the transformation using a catalytic approach. Different systems using DBU as promoter, with or without transition metals, were published.<sup>221, 225, 226</sup> An heterogeneous approach was developed in 2013 by Munshi and co-workers. The group immobilized DBU on a methylhydrosiloxane support, obtaining very good

yields for the corresponding  $\beta$ -ketocarboxylic acids (up to 99%) at mild conditions (Entry 6, Table 2-7).<sup>226</sup>

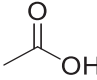
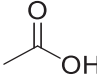
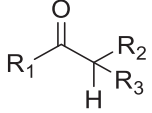
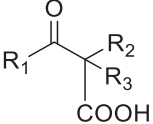
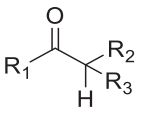
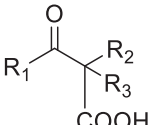
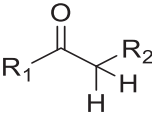
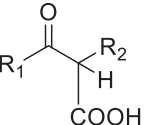
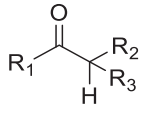
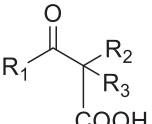
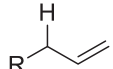
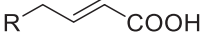
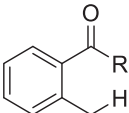
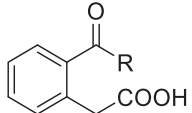
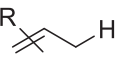
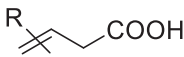
Additionally, allylic C(sp<sup>3</sup>)-H could be transformed in the corresponding  $\beta$ - $\gamma$ -unsaturated carboxylic acids. The allylic bond is needed for the initial coordination of the organic substrate to the metal centre (Cobalt). Catalytic amounts of Co complex are not enough to perform this transformation, therefore AlMe<sub>3</sub> was added in over-stoichiometric amounts to obtain a satisfying yield of carboxylic acids up to 71% (Entry 7, Table 2-7).<sup>227</sup>

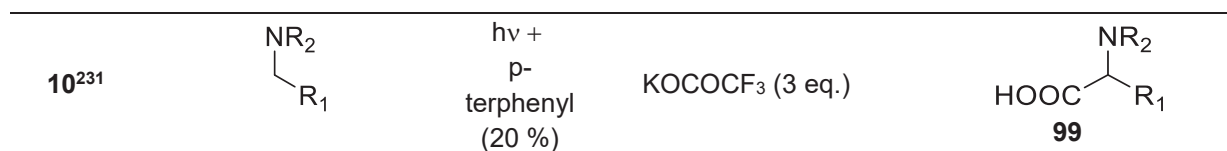
In this context, photocatalytic approaches have been reported as well.<sup>228</sup> In some cases, the transformation of the C(sp<sup>3</sup>)-H bond with CO<sub>2</sub> to form the carboxylic acid does happen without the need of an extra transition metal catalyst. Both UV and sun light were successfully used to obtain the carboxylic acids starting from *o*-alkylphenyl ketones and CO<sub>2</sub> (Entry 8, Table 2-7).<sup>229</sup> In 2016, the combination of photocatalysis (UV light) and homogeneous catalysis (Cu complex) lead to the development of a protocol able to transform allylic C(sp<sup>3</sup>)-H bonds in  $\beta$ - $\gamma$ -unsaturated carboxylic acids, however with low yields, yet (Entry 9, Table 2-7).<sup>230</sup> Recently, Jamison and co-workers reported the first example of a C(sp<sup>3</sup>)-H activation to produce carboxylic acids using a continuous flow system. Their example shows the transformation of *N*-benzylpiperidine into  $\alpha$ -aminoacids. This reaction does not require any transition metal catalysts, just the use of *p*-terphenyl as photoredox catalyst and UV light for activation. During the reaction the system generates an anionic radical (CO<sub>2</sub><sup>-</sup>) which couples with the substrate to give the product. 3 eq. of potassium trifluoroacetate were needed in order to achieve good carboxylic acid yields. Nevertheless, the formation of the active CO<sub>2</sub><sup>-</sup> species is of high interest for future development since it can be applied for the conversion of other starting materials (Entry 10, Table 2-7).<sup>231</sup>

Overall, much progress has been done in the past years regarding the activation of C(sp<sup>3</sup>)-H to give carboxylic acids. Especially, the photocatalytic field revealed many interesting examples in the last years. Anyway, further efforts are needed to develop processes which could be used on an industrial scale.

Table 2-7: Examples of C(sp<sup>3</sup>)-H bond carboxylation with CO<sub>2</sub> to carboxylic acids.

Entry	Substrate	Catalyst	(Organo)metallic additive	Products and Yield (%)
-------	-----------	----------	---------------------------	------------------------

1 <sup>216</sup>	CH <sub>4</sub>	Cu/Co		<b>28 (Selectivity)</b>
2 <sup>217</sup>	H <sub>2</sub>	Ag- Rh/SiO <sub>2</sub>		<b>17 (Selectivity)</b>
3 <sup>222</sup>		-	Lithium 4-methyl-2,6-di-tert-butylphenoxide (4 eq.)	
	Rx = Alkyl, Aryl or H			Rx = Alkyl, Aryl or H <b>89</b>
4 <sup>223</sup>		-	DBU (4 eq.)	
	Rx = Alkyl, Aryl or H			Rx = Alkyl, Aryl or H <b>83</b>
5 <sup>224</sup>		-	Magnesium 2-oxoimidazolidine-1,3-diide dibromide (3 eq.)	
	Rx = Alkyl			Rx = Alkyl <b>75</b>
6 <sup>226</sup>		DBU supported on methylhydrosiloxane	-	
	Rx = Alkyl, Aryl or H			Rx = Alkyl, Aryl or H <b>99</b>
7 <sup>227</sup>		[Co] (10%)	AlMe <sub>3</sub> (1.5 eq.) CsF (1 eq.)	
	R = Alkenyl, alkyl or aryl			R = Alkenyl, alkyl or aryl <b>84</b>
8 <sup>229</sup>		hν	-	
	Rx = Alkyl, Aryl or H			Rx = Alkyl, Aryl or H <b>84</b>
9 <sup>230</sup>		hν + [Cu] (0.5%) and ketone (2.5 %)	-	
	R = alkyl			R = alkyl <b>3</b>



## 2.5 Conclusions and outlook

Many synthetic protocols were developed for the conversion of organometallic or organic substrates and CO<sub>2</sub> to carboxylic acids, testifying the high interest in this topic. The upgrade of these processes to an industrial level would lead to substitute processes based on non-renewable CO with processes more in line with the “Green Chemistry” principles.<sup>153</sup>

However, many of the developed processes suffer from drawbacks which need to be overcome in order to proceed towards their application. The conversion of organometallic substrates, although quite easy, suffers from the drawbacks of handling and preparing such reagents. On the other side, the majority of the processes converting easily obtainable organic substrates suffer from the presence of (over)-stoichiometric organometallic or metallic additives necessary for the success of the reaction. All these processes will lead to the production of high amount of wastes. The activation of low energy substrates requires often the use of harsh conditions such as high temperature and pressure and many protocols still show low TON and TOF. In addition, many of the reported systems are not well understood or studied, making difficult a following optimization or upgrade of them.

The development of processes for the conversion of easily accessible and benign substrates (alkenes, alcohols, aromatics etc.) is highly desired. In addition, the substitution of organometallic reducing agents with H<sub>2</sub> would also be an improvement, giving mostly H<sub>2</sub>O as by-product. To reach these purposes suitable catalytic systems and processes have to be developed. The use of harsh conditions and the production of high quantity of wastes have to be avoided in order to develop processes in line with the “Green Chemistry” principles.



3. **Homogeneously Rhodium catalysed synthesis of carboxylic acids from oxygenated substrates**





### 3.1 State of the art and starting point

Aliphatic carboxylic acids are important chemicals, used in many applications as explained in Section 1.2 of this thesis. Although many protocols for their synthesis through CO<sub>2</sub> incorporation were suggested (see Chapter 2 of this thesis), no protocols starting from aliphatic oxygenated substrates have been reported so far. Alcohols, ketones, aldehydes and epoxides are readily available materials, which can also be obtained easily starting from renewable feedstocks (biomass). Besides, they are easy to handle and mostly non-dangerous, compared to previously reported organometallic substrates.

The Rh homogeneous catalytic system reported in 2013 by Leitner and co-workers was able to convert alkenes and CO<sub>2</sub> into carboxylic acids, using only H<sub>2</sub> as reducing agent.<sup>6</sup> The Rh catalytic system requires the addition of an iodide source (CHI<sub>3</sub>), a phosphine ligand (PPh<sub>3</sub>), an acidic additive (*p*-TsOH·H<sub>2</sub>O) and can be tested in batch reactors (autoclaves). Anyway, no organometallic additive is required.

Herein, the use of this Rh catalytic system for the synthesis of carboxylic acids starting from alcohols, ketones, aldehydes and epoxides is reported (Figure 3-1).

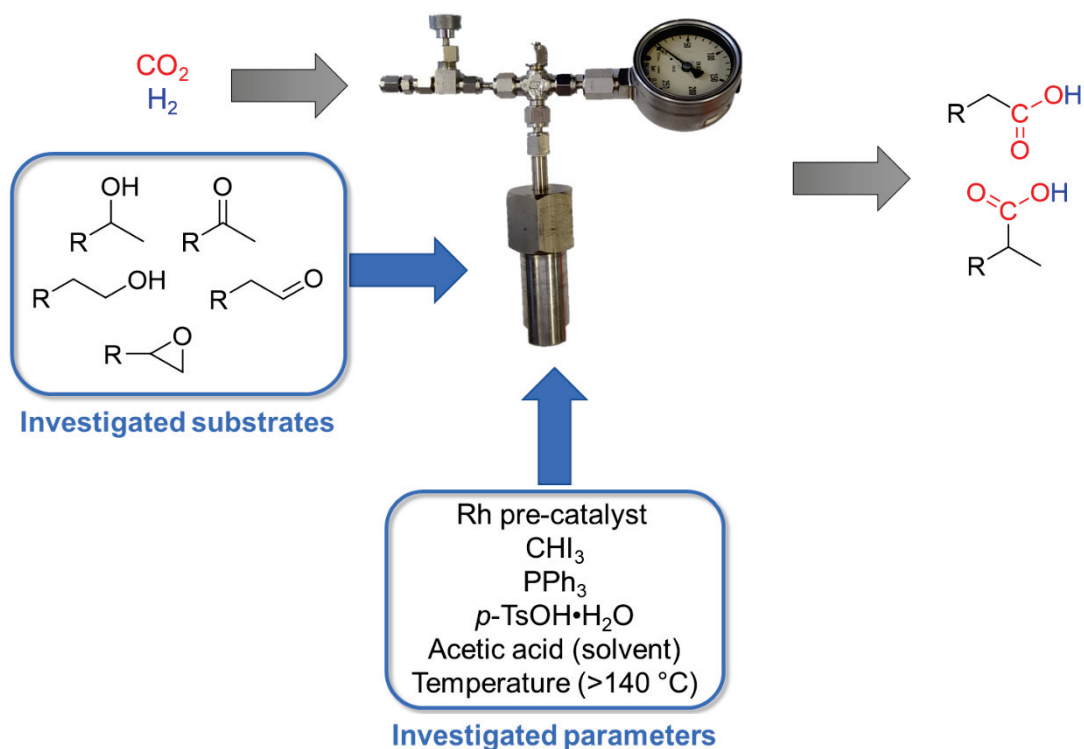


Figure 3-1: Graphic representation of the investigated reactions, process and catalytic system presented in this chapter.

The carboxylation of alcohols to carboxylic acids with CO<sub>2</sub> has been recently developed by different groups,<sup>162, 165, 167</sup> as summarized in the introduction of this thesis and in the recent book chapter.<sup>1</sup> Unfortunately, the majority of the reported studies require the use of an organometallic (over)-stoichiometric reducing agent to perform the transformation.

Few examples of synthesis of carboxylic acids from ketones substrates are reported in literature, since direct oxidation is not possible. In particular, these approaches require a deviation through HCOOH<sup>232</sup> or stoichiometric approaches, which involve the hydrolysis of an intermediate such as cyanide, acetoxyacrylonitriles, phosphoenamines and others.<sup>233, 234</sup> The only reported examples of ketones carboxylation lead to the production of  $\beta$ -ketocarboxylic acids, which are quite unstable and have to be readily transformed into a more stable compound (ester, salt,  $\beta$ -hydroxycarboxylic acids etc.).<sup>221</sup> In all these cases, the acidic proton of the ketone is actually reacting, while the carbonyl group remains intact <sup>1</sup>.

Aldehydes oxidation is the most common industrial process to obtain higher carboxylic acids.<sup>97</sup> Few examples of formaldehyde hydroformylation are reported. In these cases, the resulting aldehyde is further reduced in order to form ethylene glycol.<sup>235, 236</sup> Their carbonylation is challenging, and usually has low efficiency or happens on activated/transformed substrate.<sup>237, 238</sup> Recently, Han and co-workers reported a catalytic system able to catalyze the transformation of paraformaldehyde, CO<sub>2</sub> and H<sub>2</sub> into ethanol. The synthesis includes the hydrogenation of paraformaldehyde to methanol, followed by carbonylation, with CO and H<sub>2</sub>O produced in situ via a RWGS step, and reduction to give ethanol.<sup>239</sup>

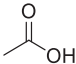
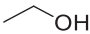

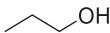
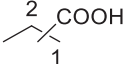
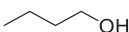
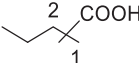
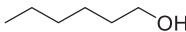
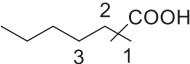
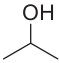
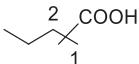
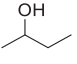
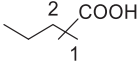
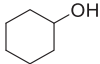
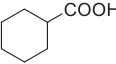
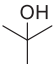
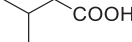
While epoxides coupling with CO<sub>2</sub> to polyethercarbonates polyols,<sup>240</sup> polycarbonates<sup>241</sup> and carbonates<sup>242</sup> is well known and studied, no examples of synthesis of carboxylic acids from epoxides and CO<sub>2</sub> is reported in literature. However, these substrates would be interesting due to their high availability both from traditional petrochemical route<sup>243</sup> and from bio-refinery processes.<sup>241</sup>

A catalytic system for the transformation of C-O bonds (alcohols) into carboxylic acids using CO<sub>2</sub> was reported by Leitner and co-workers.<sup>6</sup> The mentioned system is inspired by the Monsanto homogenous catalysts for the methanol carbonylation,<sup>244</sup> higher alcohols carbonylation<sup>245</sup>, alkene hydroxycarbonylation,<sup>13</sup> and alkene hydroxycarbonylation using formic acid (all included a Rh complex as catalyst, CO as reagent and ligand, iodide additive i.e. CH<sub>3</sub>I and acidic conditions).<sup>246</sup> The system

published in 2013, although focusing on alkenes transformation, was able to obtain carboxylic acids starting from alcohols, CO<sub>2</sub> and H<sub>2</sub> with yields up to 74 %. It was assumed, that the alkenes' reaction pathway was the same followed by the alcohols after a previous dehydration step.<sup>6</sup> Meanwhile, the system was further improved and new optimal milder conditions for the conversion of alkenes were reported.<sup>247</sup> Based on these last results, the system developed by Leitner and co-workers was tested for a range of different alcohols to obtain the corresponding carboxylic acids.

In a typical experiment, 1.88 mmol of substrates were dissolved in 1 ml of acetic acid together with 5 % (mol<sub>Rh</sub>/mol<sub>ROH</sub>) of [RhCl(CO)<sub>2</sub>]<sub>2</sub> precursor. The mixture obtained was then added in the autoclave with 5 eq. (related to Rh) of PPh<sub>3</sub>, 2.5 eq of CHI<sub>3</sub> and 3.5 eq. of *p*-TsOH·H<sub>2</sub>O. The results of these tests are reported in Table 3-1. In all cases, the conversions are around 99%, while yields vary widely.

Table 3-1: Conversions and total yields obtained from preliminary tests on different substrates.

Entry	Substrate	Conv. (%)	Products	Yields (%)
1	<chem>H3C-OH</chem>	>99		13
2		>99		36
3		99		29 <sup>[a]</sup>
4		99		28 <sup>[b]</sup>
5		99		28 <sup>[c]</sup>
6		98		44 <sup>[d]</sup>
7		99		46 <sup>[e]</sup>
8		>99		65
9		99		39

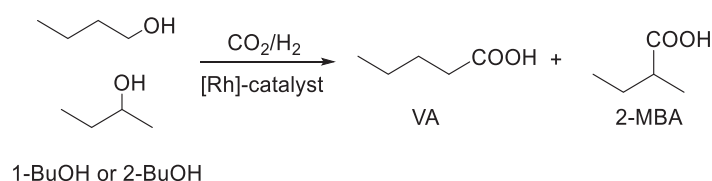
Reaction conditions: 1.88 mmol of substrate, 92  $\mu\text{mol}$  Rh, 1 ml acetic acid, 2.5 mol/mol<sub>Rh</sub> of  $\text{CHI}_3$ , 5 mol/mol<sub>Rh</sub> of  $\text{PPh}_3$ , 20 bar  $\text{CO}_2$ , 10 bar  $\text{H}_2$ , 140 °C. [a] 1: 21, 2: 8; [b] 1: 18, 2: 10; [c] 1: 19, 2: 7, 3: 2; [d] 1: 31, 2: 13; [e] 1: 32, 2: 14.

From the results obtained, it is evident that primary behave differently from secondary and tertiary alcohols. In particular, secondary and tertiary alcohols appear more reactive than the corresponding primary alcohols. Primary alcohols lead to yields around 30% while secondary and tertiary alcohols lead to yields around 40% (on average). For primary and secondary alcohols (with more than two carbon), a mixture of linear and branched isomer is obtained, usually with a linear/branched ratio of 2:1. Tertiary alcohols lead always to the less steric hindered compound, in analogy with the Keulemans rule.<sup>248</sup> Moreover, methanol leads to very low yields under these conditions.

For all the tested compounds, the yields are lower than those obtained with the corresponding alkenes,<sup>247</sup> with the production of side products such as iodoalkanes, acetates and hydrocarbons. This means that an optimization of the reaction conditions is necessary.

The study of the reaction parameters was performed using different techniques. A *Design of Experiment* (DoE) was first used in order to identify the most important parameters. The DoE approach was used to investigate the reaction parameters for the conversion of cyclohexanol into cyclohexylcarboxylic acid (CA) as benchmark substrate.

Following, the optimization procedure was applied for the reaction of 2-butanol (2-BuOH) with  $\text{CO}_2$  and  $\text{H}_2$  to produce valeric acid (VA) and 2-methylbutanoic acid (2-MBA) as shown in Scheme 3-1.



Scheme 3-1: Hydrocarboxylation of 1-butanol and 2-butanol leading to the production of mixtures of valeric acid (VA) and 2-methylbutanoic acid (2-MBA).

Afterwards, ketones have been tested as substrates and deeper investigations of the effects of various reaction parameters are reported.

Primary alcohols transformation into carboxylic acids was investigated. In particular, the optimization of the reaction parameters to maximize the yield was performed using 1-butanol (1-BuOH) as substrate (see Scheme 3-1).

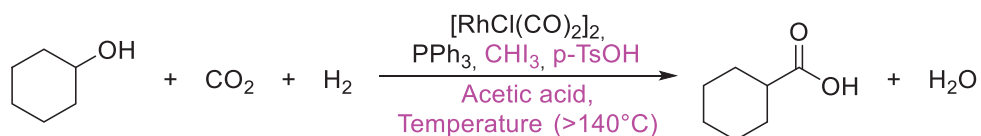
After these studies, to enlarge the scope of the reaction to aldehydes, the hydrocarboxylation of butanal was studied.

Epoxides requires a different optimization of the reaction conditions. Since the DoE applied for secondary alcohols resulted efficient and reliable, it was used also in these cases to find the best parameters in order to obtain the highest yield possible.

### 3.2 Design of Experiment (DoE)

The yield in carboxylic acids is determined by many parameters. The solvent and dilution, as well as the temperature and pressure influence the yield. Moreover, the acidic additive ( $p$ -TsOH $\cdot$ H<sub>2</sub>O), the amount of CHI<sub>3</sub> and PPh<sub>3</sub> and the Rh-precursor used can vary the efficiency of the system. From our preliminary studies reported in the Section 3.1, four parameters seemed to gain most impact on the yield, and they are possibly related to the substrate and between each other. The parameters are: volume of acetic acid, temperature,  $p$ -TsOH $\cdot$ H<sub>2</sub>O and CHI<sub>3</sub> amount. The volume of the solvent,  $p$ -TsOH $\cdot$ H<sub>2</sub>O and the temperature appear to be related to each other. Moreover, the amount of CHI<sub>3</sub> (or I<sup>-</sup>) can be related to the amount of strong acid in solution ( $p$ -TsOH $\cdot$ H<sub>2</sub>O). It is reported that strong acid (i.e. HI) are necessary to keep the Monsanto catalytic active species in solution avoiding the reduction of Rh<sup>I</sup> to metallic Rh<sup>0</sup>.<sup>245</sup> To confirm the importance of the parameters on the yield and their relationship between each other we decided to perform a *Design of Experiment*.

The DoE was used to find the optimal process setting to obtain the highest yield possible for cyclohexanecarboxylic acid (CA) starting from cyclohexanol (Scheme 3-2). A *response surface method* is chosen. This method allows estimating interaction and quadratic effects between different parameters, and therefore giving an idea of the shape of the investigated response surface.<sup>249</sup>



Scheme 3-2: Hydrocarboxylation of cyclohexanol to cyclohexanecarboxylic acid. The parameters studied through the DoE approach are reported in pink in the scheme.

After the previous considerations, the following four factors and their thresholds are chosen for the DoE (Scheme 3-2):

- Temperature: 140-180 °C
- Volume of acetic acid: 1-3 mL
- $p$ -TsOH $\cdot$ H<sub>2</sub>O: 0-0.67 mmol
- CHI<sub>3</sub>: 0.05-0.44 mmol.

The Box-Behnken method is selected subsequently to the choice of the factors. The Box-Behnken design is an independent quadratic design. In this design the treatment combinations are at the midpoints of edges of the process space and at the center. A schematic representation is reported in Figure 3-2. Once all the 29 reactions established by the Design of Experiment program were performed, a positive final response is obtained.

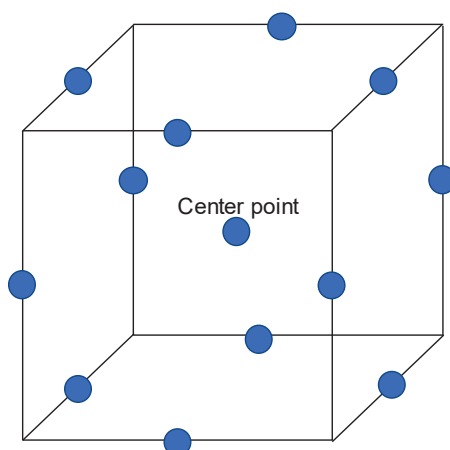


Figure 3-2: Schematic figure of a Box-Behnken design for three factors.

All the chosen parameters are highly important for the yield in carboxylic acid. Graphic visualizations (A-F) and the equation of the yield provided by the DoE calculation of the results (G) are reported in Figure 3-3.  $\text{CHI}_3$  has a positive influence on the total yield as indicated by a positive sign in front of the factor itself. But too much of it has a critical negative effect on the yield as shown by the large negative number which multiply the quadratic factor ( $\text{CHI}_3^2$ ). The same considerations apply on the temperature effect. The simple parameters and the quadratic factors of  $p\text{-TsOH}\cdot\text{H}_2\text{O}$  and volume of acetic acid are multiplied by negative numbers, meaning that their amounts have to be carefully balanced. In addition, their presence in the reaction solution is important due to synergetic effect. The interaction of two parameters can be

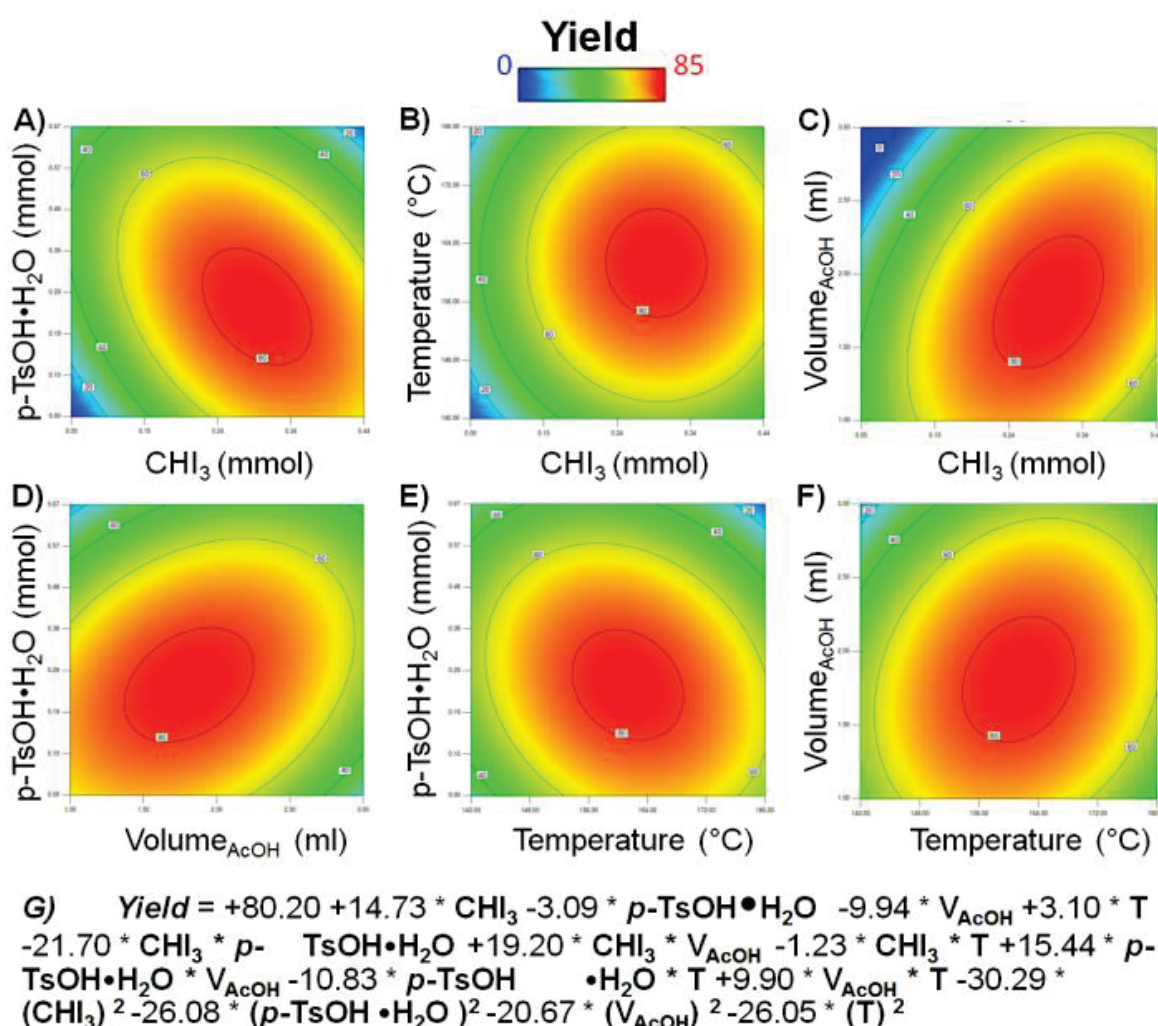


Figure 3-3: Graphic visualization of DoE results and relation between the different parameters (A-F) and equation of the yield calculated from the studied parameters (G).



analyzed on basis of the terms where two parameters are multiplied with each other. Every possible couple is present in the equation, as expected, meaning that all the parameters are correlated with each other. The interaction which has the smallest impact on the yield is the one between  $\text{CHI}_3$  and the temperature (coefficient around 1). The higher the coefficient in front of the couple of parameters, the higher is their coordinated effect on the total yield.  $\text{CHI}_3$  and  $p\text{-TsOH}\cdot\text{H}_2\text{O}$  must be carefully balanced, in order to obtain good yields. Furthermore, the volume of solvent and the amount of  $p\text{-TsOH}\cdot\text{H}_2\text{O}$  are strictly related to the temperature. The balance of all these three parameters is highly important for a good result. The same conclusions can be deduced from the analysis of the graphics elaborated by the DoE program.

The method resulted to be statistically significant (the result of the test is considered correct if there is a mathematical correlation between input and output data) and gave as point with higher yield a set of conditions very close to the center point (Table 3-2). This means that the selected thresholds include the area with maximum yields and no further investigation outside is needed from the selected limits.

Table 3-2: DoE results: both the suggested best conditions and the center point results are reported.

Parameter	DoE solution	Center point
$\text{CHI}_3$	0.9 mmol	0.24 mmol
$p\text{-TsOH}$	0.24 mmol	0.34 mmol
$V$	1.8 ml	2 ml
Temperature	161°C	160°C
<b>Yield predicted from DoE</b>	<b>83 %</b>	<b>80%</b>
<b>Experimental yield</b>	<b>73±5%</b>	<b>80±6%</b>

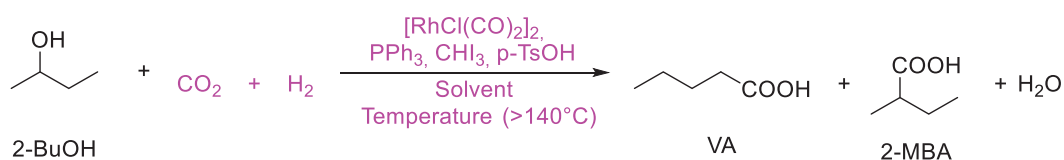
Reaction conditions: 1.88 mmol Cyclohexanol, 46  $\mu\text{mol}$   $[\text{RhCl}(\text{CO})_2]_2$  and 5 eq.  $\text{PPh}_3$ . The errors are given to indicate the limits among which the minimum and maximum yields were obtained (>2 experiments for each point were performed).

Overall, the DoE allowed us to understand the correlations between the chosen parameters (temperature, volume of acetic acid, amount of  $\text{CHI}_3$  and  $p\text{-TsOH}\cdot\text{H}_2\text{O}$ ) and to prove their importance for the yield in carboxylic acids. Moreover, we verified that the best reaction conditions are found within the chosen range.

### 3.3 Secondary alcohols and ketones

#### 3.3.1 2-butanol

The initial yield in VA and 2-MBA obtained from 2-BuOH (Scheme 3-3) applying the optimized conditions for alkenes was 45% (VA: 2-MBA = 2.2: 1), with the conversion over 99% (Entry 1, Table 3-3). After the results obtained from the DoE experiment, a study of the single parameters variation around the center point identified with the DoE was performed. In addition to the parameters analyzed in the previous set of experiments (solvent volume, amount of acidic additive,  $\text{CHI}_3$  amount and temperature), investigations regarding various solvents, and pressures of  $\text{CO}_2$  and  $\text{H}_2$  are reported (Scheme 3-3).



Scheme 3-3: Hydrocarboxylation of 2-butanol (2-BuOH) to 2-methylbutanoic acid (2-MBA) and valeric acid (VA). The parameters studied are reported in pink in the scheme.

Using 2-BuOH in neat leads to the formation of ethers. The influence of solvents and their volume were studied. Acetic acid was studied as solvent, using 1, 2 and 3 ml. 2 ml of acetic acid result to be better than 1 or 3 ml with a yield of 67% (Entries 1-3, Table 3-3), as already shown by the DoE experiment. For toluene, the best volumes are 1 or 2 mL, giving yields of 30% (Entries 4-6, Table 3-3). The use of 3 ml of toluene results in lower yields and lower mass balance. This is probably caused by the production of higher amount of butane, which is hardly quantifiable when produced in high quantity. Based on the obtained results and considering the polarities of the used solvents, 2 mL of polar solvents and 1 mL of apolar solvents were used, for all the following tests. Polar protic (acetic acid, water), polar aprotic (acetonitrile) and apolar solvents (toluene, xylene and dioxane) were tested (Entries 1-11, Table 3-3). Water, dioxane and acetonitrile give low yields in carboxylic acids and low conversions. This result suggests the inactivity or deactivation of the catalyst in the above-mentioned solvents. Toluene and xylene allow obtaining almost the same yields between 37 and 39%. Acetic acid was identified as the best reaction media, with a total yield of 67%.

*p*-TsOH•H<sub>2</sub>O has a big influence on the yield of carboxylic acids and this influence is strictly related to the amount of solvent used. Using acetic acid as solvent the influence of the presence of *p*-TsOH•H<sub>2</sub>O is strictly related to the amount of acetic acid used. When 1 ml of acetic acid was used, *p*-TsOH•H<sub>2</sub>O has no influence on the yield in carboxylic acid (Entries 1 and 12, Table 3-3). On the contrary, it has a great effect of when 2 ml of solvent were used. The best result was obtained using 2 mL of acetic acid and *p*-TsOH•H<sub>2</sub>O as additive (Entry 2, Table 3-3), while the absence of the additive leads to traces of product (Entry 13, Table 3-3). The absence of *p*-TsOH•H<sub>2</sub>O in toluene has no significant effects. This may be due to an effect of the acid on the esterification equilibrium, since the absence causes the formation of *sec*-butyl acetate as main product and no particular influence was noticed using toluene as a solvent (Entry 14, Table 3-3). The influence of *p*-TsOH•H<sub>2</sub>O can be linked to the presence of protic sources in the solution. A solution with protic polar solvents is probably required to keep the likely anionic catalytic active species<sup>13, 14, 79, 244</sup> separate enough from the cationic counterpart, enhancing in this way the catalytic activity.<sup>250</sup> If alkenes are used as substrates and toluene as solvent, *p*-TsOH•H<sub>2</sub>O is required in order to obtain good yields in carboxylic acids<sup>247</sup>. This suggests that *p*-TsOH•H<sub>2</sub>O substitutes the molecules (i.e. alcohols) which could make up for the absence of protic polar molecules in apolar solvents. It is unlikely that the influence of the acidic additive is derived from the formation of the butyl tosylate which has a better leaving group (-OTs) compared to 2-BuOH, because its presence influences the yield negatively in the case of primary alcohols (see Chapter 0).

Further, the influence of the temperature in the range between 140 °C and 180 °C on different settings was tested (Entries 15-18, Table 3-3). The best result was obtained increasing the temperature from 140 °C to 160 °C when 2 mL of acetic acid and the *p*-TsOH•H<sub>2</sub>O were used. The yield in VA and 2-MBA rises to the very good value of 77%, thanks to a reduced production of by-products (Entry 15, Table 3-3). A further increase to 180 °C causes a fall in the carboxylic acids yield, either because of deactivation of the catalyst (as suggested by the observation of black solid during the work-up) and the increased importance of side reactions (such as oligomerization or hydrogenation) as suggested by the lower mass balance obtained for this reaction.

Table 3-3: Hydrocarboxylation of 2-BuOH with CO<sub>2</sub> and H<sub>2</sub>: influence of different reaction parameters.

Entry	Solvent	Volume (ml)	p-TsOH·H <sub>2</sub> O (mol/mol <sub>Rh</sub> )	Temperature (°C)	H <sub>2</sub> pressure (bar)	CO <sub>2</sub> pressure (bar)	Yield (%)
1	Acetic acid	1	3.5	140	10	20	45
2	Acetic Acid	2	3.5	140	10	20	67
3	Acetic Acid	3	3.5	140	10	20	8
4	Toluene	1	3.5	140	10	20	30
5	Toluene	2	3.5	140	10	20	30
6	Toluene	3	3.5	140	10	20	14
7 <sup>[a]</sup>	Water	2	3.5	140	10	20	7
8	Xylene	1	3.5	140	10	20	32
9 <sup>[b]</sup>	Dioxane	1	3.5	140	10	20	2
10 <sup>[c]</sup>	Acetonitrile	2	3.5	140	10	20	2
11 <sup>[d]</sup>	Neat	1	-	140	10	20	1
12	Acetic acid	1	-	140	10	20	46
13	Acetic acid	2	-	140	10	20	2
14	Toluene	1	-	140	10	20	29
15	Acetic acid	2	3.5	160	10	20	77
16	Acetic acid	2	3.5	180	10	20	66
17	Acetic acid	1	-	160	10	20	59
18	Acetic acid	1	-	180	10	20	48
19	Acetic acid	2	3.5	160	5	20	26
20	Acetic acid	2	3.5	160	20	20	26
21	Acetic acid	2	3.5	160	10	10	62
22	Acetic acid	2	3.5	160	10	30	75

If not specified, conversion is over 99%, VA/2-MBA ratio is about 2/1 and MB around or above 80%. Reaction conditions: 1.88 mmol 2-BuOH, 46 μmol [RhCl(CO)<sub>2</sub>]<sub>2</sub>, 2.5 mol/mol<sub>Rh</sub> of CHI<sub>3</sub> and 5 mol/mol<sub>Rh</sub> of PPh<sub>3</sub>. [a] Conversion = 95%. Solid and unknown products formed. [b] Conversion = 90%. [c] Conversion = 34%. [d] MB = 17%. High amount of not quantified secondary products were identified with GC-MS as ethers. Reaction time = 66h.

The pressures used in preliminary studies are 20 bar of CO<sub>2</sub> and 10 bar of H<sub>2</sub>. Reducing the H<sub>2</sub> pressure to 5 bar (Entry 19, Table 3-3) and increasing it to 20 bar (Entry 20, Table 3-3) cause a reduction of the carboxylic acids yields. The increase to 20 bar leads to a reduction of the yields and more inconsistencies, probably due to hydrogenation as side reaction. With the H<sub>2</sub> pressure sets at 10 bar, the screening of different CO<sub>2</sub> pressure was done. CO<sub>2</sub> pressure has a small influence on the yield. In fact, lowering the pressure to 10 bar slightly decrease the yield (62%), while increasing it to 30 bar leads to no significant change (Entries 21 and 22, Table 3-3). 20 bar of CO<sub>2</sub> was chosen for further studies, because no real improvement was reported using higher pressure.

Table 3-4: Hydrocarboxylation of 2-BuOH with CO<sub>2</sub> and H<sub>2</sub>: influence of CHI<sub>3</sub> and PPh<sub>3</sub> and Rh precursor.

Entry	Rh precursor	CHI <sub>3</sub> (mol/mol <sub>Rh</sub> )	PPh <sub>3</sub> (mol/mol <sub>Rh</sub> )	Conv. (%)	Yield (%) (n: iso ratio)
1	[Rh(CO) <sub>2</sub> Cl] <sub>2</sub>	2.5	5	>99	<b>77</b> (1.8)
2	[Rh(COD)Cl] <sub>2</sub>	2.5	5	>99	<b>33</b> (3.1)
3	RhCl(PPh <sub>3</sub> ) <sub>3</sub>	2.5	2	>99	<b>58</b> (2.4)
4	[HRh(CO)(PPh <sub>3</sub> ) <sub>3</sub> ]	2.5	2	>99	<b>1</b> (-)
5	Rh <sub>2</sub> (OAc) <sub>4</sub>	2.5	5	>99	<b>52</b> (2)
6	RhI <sub>3</sub>	2.5	5	>99	<b>4</b> (1)
7	[Rh(CO) <sub>2</sub> Cl] <sub>2</sub>	0	5	>99	<b>0</b> (-)
8	[Rh(CO) <sub>2</sub> Cl] <sub>2</sub>	9.3	5	>99	<b>7</b> (1)
9	[Rh(CO) <sub>2</sub> Cl] <sub>2</sub>	2.5	0	>99	<b>2</b> (1)
10	[Rh(CO) <sub>2</sub> Cl] <sub>2</sub>	2.5	10	>99	<b>48</b> (1.5)

Standard reaction conditions: 1.88 mmol of substrate, 92 μmol Rh, 2 ml of acetic acid, 3.5 mol/mol<sub>Rh</sub> *p*-TsOH•H<sub>2</sub>O, 20 bar CO<sub>2</sub>, 10 bar H<sub>2</sub>, 160 °C.

Once the illustrated reaction parameters were set, experiments on the  $\text{CHI}_3$ ,  $\text{PPh}_3$  amounts and Rh precursor were performed. To investigate the influence of the Rh precursor, different metal complexes were used, with Rh in different oxidation states and different ligand spheres (Table 3-4, Entries 1-6). The species with Rh<sup>I</sup> appear to have a very different reactivity depending on the ligand.  $[\text{HRh}(\text{CO})(\text{PPh}_3)_3]$  resulted to be highly inactive with the main formation of *sec*-butyl acetate (Entries 2, 4, Table 3-4). Probably, this is caused by decomposition of the species at 160 °C.  $[\text{Rh}(\text{COD})\text{Cl}]_2$  lead mainly to the production of *sec*-butyl acetate and butane.  $[\text{Rh}(\text{CO})_2\text{Cl}]_2$  and  $\text{RhCl}(\text{PPh}_3)_3$  resulted to be more active with the maximum yield of 77% for  $[\text{Rh}(\text{CO})_2\text{Cl}]_2$  (Entries 1 and 3, Table 3-4). The Rh<sup>II</sup> species  $\text{Rh}_2(\text{OAc})_4$  leads to a yield of 52% in carboxylic acids (Entry 5, Table 3-4), similarly to  $\text{RhCl}(\text{PPh}_3)_3$ . The Rh<sup>III</sup> species ( $\text{RhI}_3$ ) is not selective for the production of carboxylic acids leading to a mixture of by-products such as butane, butene, *sec*-butyl acetate and iodobutane (Entry 6, Table 3-4). It appears that two main factors have an influence on the total yield: on one hand, the higher oxidation state of the Rh decreases the yield in carboxylic acids, on the other hand, the ligands are important, influencing the formation of the active species and thus the following reactivity.<sup>251</sup>

The amount of iodide additive influences dramatically the total yield in carboxylic acids. The iodide additive may have multiple function: it can form the species which reacts with the catalyst (1-iodobutane as in the Monsanto process<sup>252</sup>), it can stabilize the active species,<sup>245</sup> and it can be a ligand for the catalytic active species ( $\text{L}_x\text{Rh-I}_y$ ).<sup>245</sup> The results obtained with 0.0, 2.5 and 9.3 mol/mol<sub>Rh</sub> of  $\text{CHI}_3$  in solution (corresponding to 0, 7.6 and 28 eq. of  $\text{I}^-$  compared to Rh mol) are reported in Entries 1, 7-8 in Table 3-4. The absence of iodide additive gives 0% yield of carboxylic acids, but at the same time, too much iodide causes a decrease in the yield to 7%. This behavior could be explained with the possible iodide functions. On one hand, too much iodide forms other species which are not active. On the other hand, no iodide causes the absence either of the catalytic active species or of a reactive substrate (iodobutane).<sup>245</sup> In fact, no products are detected except for *sec*-butyl acetate and butane. Moreover, when 9.3 eq. of  $\text{CHI}_3$  are used, the final solution is very dark and high amount of solid materials is present, making the analysis and the collection of the all reaction solution more difficult leading to lower mass balance. The negative effect of high amounts of iodide in the reactor is probably the cause of the low activity observed also when iodobutane is used as substrate directly. In these cases, the total amount of  $\text{I}^-$  present in the solution is

1.88 + 7.6 mmol (derived from the  $\text{CHI}_3$ ) corresponding to 28 eq. (or 9.3 eq. of  $\text{CHI}_3$ ). Using these conditions, the yield in carboxylic acids is 37% from 2-iodobutane.

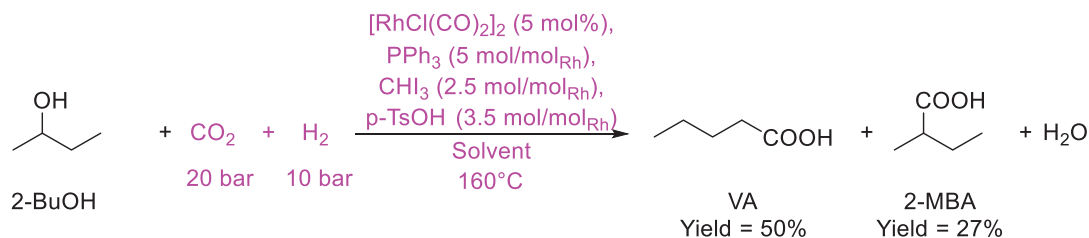
The phosphine additive is generally known to be part of the catalyst for both alcohol carbonylation<sup>254</sup> and alkenes hydroformylation reactions.<sup>255</sup>  $\text{PPh}_3$  instead of CO ligand increases the nucleophile character of the Rh center and, hence, speeds up the oxidative addition of iodocompounds, the rate-determining step in the carbonylation of alcohols with Rh.<sup>254</sup> The phosphine can be involved in the CO insertion in metal-alkyl and metal-phenyl bonds to create the acyl ligand.<sup>256</sup> Besides,  $\text{PPh}_3$  impact the selectivity towards linear/branched aldehydes in the hydroformylation reaction.<sup>255</sup>  $\text{PPh}_3$  is indeed influencing the yield in carboxylic acid. Without  $\text{PPh}_3$ , the yield in carboxylic acids drops to 2%, while with 10 eq. of  $\text{PPh}_3$  the yield decreases to 48% (Entries 9-10, Table 3-4), although no significant change in the n/iso ratio is observed. These observations lead to conclude that phosphine is actually an important part of the catalytic system. Its absence causes secondary reactions such as hydrogenation and a reduced production of carboxylic acids. Once this CO is consumed the catalyst is still able to catalyze hydrogenation, but many other by-products (i.e. butene, iodobutane and *sec*-butyl acetate) are detected as the catalyst deactivates and no further conversion towards final products occur. With excess of  $\text{PPh}_3$ , the slightly higher amount of butane detected and the lower mass balance (probably due to high boiling point products) may testify that the high amount of  $\text{PPh}_3$  results in the occupation of the catalytic active sites and/or in higher activity towards secondary reactions.

A detailed product distribution is shown in Table 3-5. The main by-product is butane. In addition, the corresponding *sec*-butyl acetate, 2-iodobutane and butene are detected. The difference in yield between 14 and 16 hours is minimal (Table 3-5). Therefore, no time extension was considered.

Table 3-5: Products distribution, conversion and mass balance obtained as a result of the transformations of 2-BuOH. Conditions used are the one optimized reported in Entry 15, Table 3-3.

Compounds	Yields after 14 h (%)	Yields after 16 h (%)
2- Methylbutanoic acid (2-MBA)	24	27
Valeric Acid (VA)	48	50
Acids (Sum)	72	77
1-Iodobutane	0	0
2-Iodobutane	1	1
Iodobutane (Sum)	1	1
Butyl acetate	2	2
Butane	7	7
Butene (Sum of 1-butene, 2-butene)	3	4
<b>Conversion</b>	>99	>99
<b>Mass Balance</b>	84	93

At the end of the study on many reaction parameters, the optimized conditions for secondary alcohols results to be those reported in Entry 15, Table 3-3: 0.046 mmol of  $[\text{RhCl}(\text{CO})_2]_2$ , 2.5 mol/mol<sub>Rh</sub> of  $\text{CHI}_3$ , 3.5 mol/mol<sub>Rh</sub> of  $p\text{-TsOH}\cdot\text{H}_2\text{O}$ , 5 mol/mol<sub>Rh</sub> of  $\text{PPh}_3$ , 2 mL of acetic acid, 1.88 mmol of 2-BuOH, 20 bar of  $\text{CO}_2$ , 10 bar of  $\text{H}_2$ , 160 °C and 16h. The yield reached at the end of the optimization procedure is 77% (TON = 16 mol<sub>products</sub>/mol<sub>Rh</sub>) which is much higher compared to the one obtained during the preliminary study (45%) and the highest reported until now with a similar system.<sup>6</sup> A detailed distribution of the obtained products, conversion and mass balance for Entry 15, Table 3-3 is reported in Table 3-5.

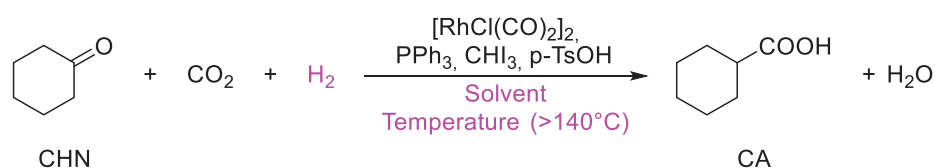


Scheme 3-4: Hydrocarboxylation of 2-BuOH: optimized reaction conditions (pink) and yields of 2-MBA and VA.



### 3.3.2 Cyclohexanone

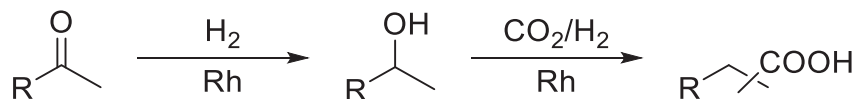
Cyclohexanone (CHN) is used as substrate (Scheme 3-5) for the optimization process due to its simplicity, in fact just one carboxylic acid product is possible (cyclohexanecarboxylic acid, CA). Best conditions for secondary alcohols were used as starting point for the optimization because of the parallel between the two classes of substrates. In these conditions, 68% of CA is formed with a conversion >99% (Entry 1, Table 3-6).



Scheme 3-5: Hydrocarboxylation of cyclohexanone (CHN) to cyclohexanecarboxylic acid (CA). The parameters varied and reported in this chapter are reported in pink.

In the attempt to improve the yield further different parameters are studied: H<sub>2</sub> pressure, volume of acetic acid, temperature (Scheme 3-5).

Based on the hypothesis that ketones reacted in the same way as alcohols, after a pre-hydrogenation step (Scheme 3-6), the effect of H<sub>2</sub> pressure was studied.



Scheme 3-6: Proposed reaction pathway for ketones: hydrogenation to alcohols followed by the hydrocarboxylation step.

The yield obtained for different H<sub>2</sub> pressures (10, 20, 30 bar) are reported in Entries 1-3, Table 3-6. The increase of H<sub>2</sub> pressure to 20 bar rises the yield in carboxylic acid to 83%. A further increase up to 30 bar does not lead to improvement and additional pressure would lead to enhance the hydrogenation (side reaction), without any further improvement of the carboxylic acid yield. The data support the need of H<sub>2</sub> for the initial conversion of ketones to the corresponding alcohols, which undergo to the reaction for producing carboxylic acid. Although Rh is known to be selective toward C=C bond hydrogenation,<sup>257</sup> some examples of C=O bond hydrogenation are also reported.<sup>258-260</sup>

In particular, it is reported that Rh/phosphine systems are active in the reduction of ketones to alcohols in presence of H<sub>2</sub>O, which acts as a promoter.<sup>261, 262</sup>

Table 3-6: Hydrocarboxylation of cyclohexanone with CO<sub>2</sub> and H<sub>2</sub>: influence of different reaction parameters.

Entry	Solvent	Volume (ml)	Temperature (°C)	H <sub>2</sub> pressure (bar)	Yield (%)
1	Acetic acid	2	160	10	68
2	Acetic Acid	2	160	20	83
3	Acetic Acid	2	160	30	82
4	Acetic acid	1	140	20	54
5	Acetic acid	3	180	20	53
6	Acetic acid	2	140	20	66
7	Acetic acid	2	180	20	76
8	Toluene	2	160	20	43

If not specified, conversion is over 99% and MB around or above 80%. Reaction conditions: 1.88 mmol CHN, 46 μmol [RhCl(CO)<sub>2</sub>]<sub>2</sub>, 2.5 eq. of CHI<sub>3</sub> and 5 eq. PPh<sub>3</sub>.

To investigate the possible initial reduction step of the ketone to the alcohol, the pressure drop was measured for 2-butanone and the corresponding alcohol (2-BuOH). The pressure decreases fast in the first 4 h for both substrates (Figure 3-4). In the first part of the reaction, the rate of the pressure drop is higher for the ketone than for the alcohol. This trend continues in the range between 4 h and 15 h, where the decrease of pressure is almost linear. After 15 h the change in the pressure seems to stop. In a microscopic view of a hydrocarboxylation reaction, two molecules in the gas phase, CO<sub>2</sub> and H<sub>2</sub>, and one molecule of substrate react to produce one molecule of carboxylic acid. Hence, in total two molecules (CO<sub>2</sub> and H<sub>2</sub>) are removed from the gas phase, because they are incorporated, together with the liquid substrate, in the liquid main product. This produces a decrease of the pressure ( $\Delta p_{HC}$ ) which can be approximated with the ideal gas law according to the formula reported in Scheme 3-7. Compared to the alcohol, the ketone has to be hydrogenated, before the formal hydrocarboxylation. Considering the conversion of the ketone, one equivalent H<sub>2</sub> is additionally removed from the gas phase and incorporated in the obtained liquid alcohol, which results in a larger decrease of the pressure.

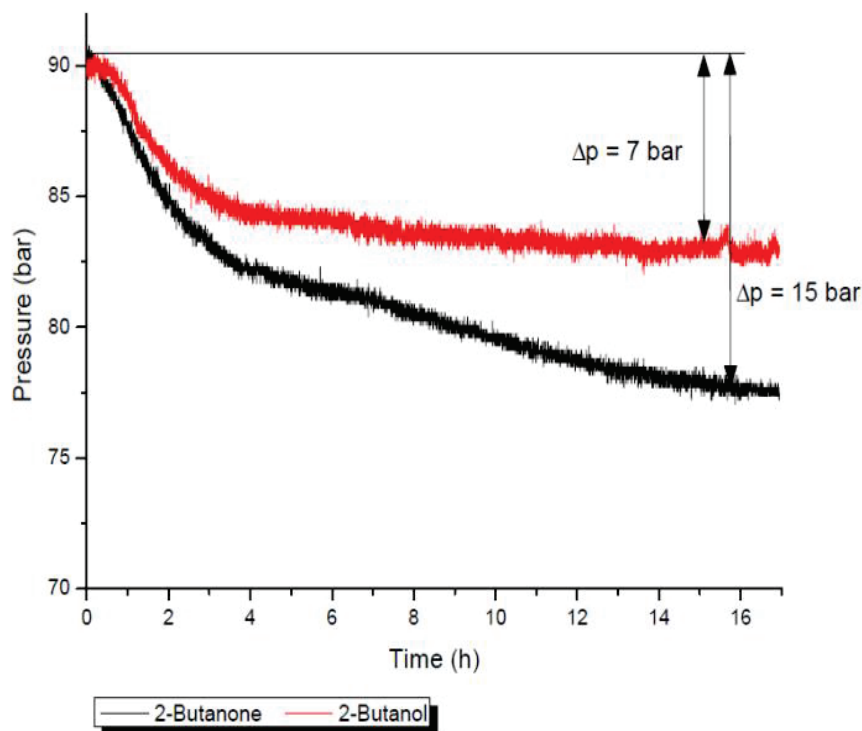
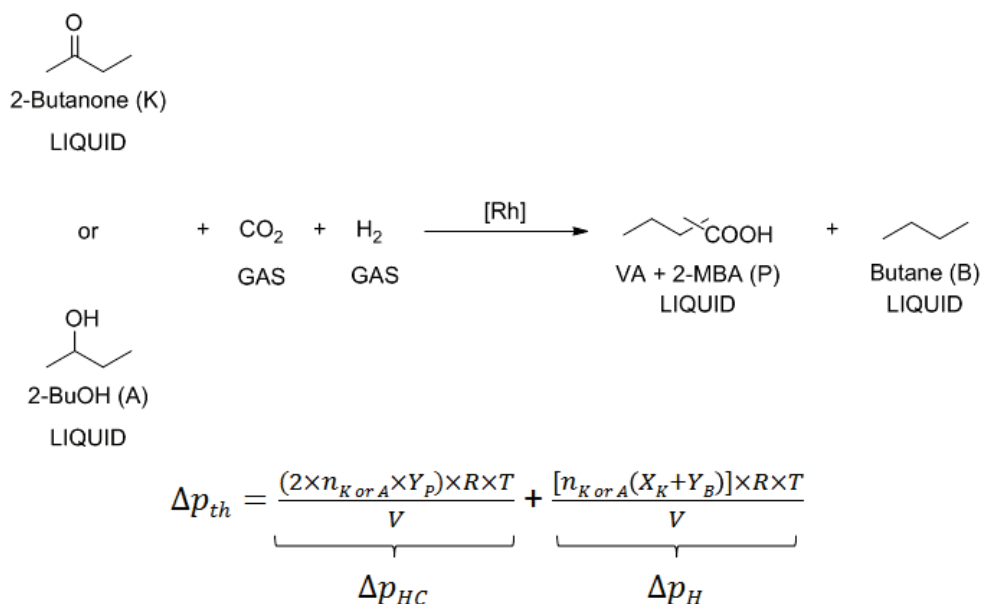


Figure 3-4: Pressure uptake registered for 2-Butanone and 2-Butanol. The values shown are elaborated and are the results of the total pressure uptake normalized removing the experimental pressure drop due to the system without catalyst (blank value) and the pressure drop due to  $\alpha$ WGS activity (presence of the catalyst but no substrate used). Reaction conditions: 1.88 mmol substrate, 92  $\mu$ mol Rh, 3.5 eq. *p*-TsOH $\cdot$ H<sub>2</sub>O, 2.5 eq. CHI<sub>3</sub>, 5 eq. PPh<sub>3</sub>, 2 ml acetic acid, 20 bar CO<sub>2</sub>, 20 bar H<sub>2</sub>, 160 °C

This pressure drop ( $\Delta p_H$ ) can be predicted according to the formula reported in Scheme 3-7. The ideal gas law, the model described in Scheme 3-7, the experimental conversion and yields allowed the calculation of a theoretical pressure drop ( $\Delta p_{th}$ ) for the ketones and alcohols hydrocarboxylation. The results of the calculations and the experimental data are reported in Table 3-7. The experimental  $\Delta(\Delta p)$  (intended as the difference between the measured  $\Delta p$  for ketone and the  $\Delta p$  for alcohol) is 8 bar (experimental error  $\pm 1$  bar), which is in good agreement with the theoretical value of 7 bar based on the ideal gas law and considering for each mol of ketone transformed in alcohol one mol of H<sub>2</sub> to be consumed.

This observation suggests the pathway reported in the Scheme 3-6: ketones are first hydrogenated to alcohols, which react with CO<sub>2</sub> and H<sub>2</sub> to give carboxylic acids. This is further supported by the analysis of the reaction solution at different reaction times (Figure 3-5), where 2-BuOH is detected together with all the other compounds present

in the reaction mixture using 2-BuOH as substrate (*sec*-butyl acetate, 2-iodobutane and 1-iodobutane, butene and butane). Moreover, the blank test (reaction performed in the absence of the Rh precursor) shows that the metal catalyst is crucial for the hydrogenation and the reaction. Indeed, no transformations of the ketones are obtained if [Rh] is not added to the solution.



$\Delta p_{HC}$  = Pressure drop due to hydrocarboxylation (formation of P)

$\Delta p_H$  = Pressure drop due to hydrogenation (formation of B and of A in the case of Ketones)

$\Delta p_{th}$  = Pressure drop due to hydrocarboxylation and hydrogenation

$n_i$  = mol of reagent A or K

$Y_i$  = yield of product P or by-product B

$X_K$  = conversion of reagent K

$R$  = universal gas constant ( $8.314 \text{ kg m}^2 \text{ s}^{-2} \text{ mol}^{-1} \text{ K}^{-1}$ )

$T$  = temperature (433 K)

$V$  = volume of the reactor occupied by gases ( $9.5 \cdot 10^{-6} \text{ m}^3$ )

Scheme 3-7: Reaction scheme and equation used for calculating the theoretical pressure drop in the transformation of 2-BuOH and 2-Butanone into carboxylic acids. Reaction conditions: 1.88 mmol substrate, 92  $\mu\text{mol}$  Rh, 3.5 eq. p-TsOH $\cdot$ H<sub>2</sub>O, 2.5 eq. CHI<sub>3</sub>, 5 eq. PPh<sub>3</sub>, 2 ml acetic acid, 20 bar

Starting from the already satisfying result (yield: 83%), further studies of reaction parameters were performed. For this reason, the effect of different amounts of solvent and of temperature was investigated. The best temperature and solvent for ketones are

again the same as for the secondary alcohols (160 °C and 2 mL of acetic acid), showing further similarities between the two classes of substrates. (Entries 2, 4-5, 8, Table 3-6)

Table 3-7: Results of the experimental and theoretical pressure drop calculations for the hydrocarboxylation of alcohols and ketones

Substrate	Mol of substrate	Conversion (%)	Carboxylic acids (%)	Butane (%)	$\Delta p_{th}$	$\Delta p$
<b>2-Butanone (K)</b>	1.94	91	42	1	13	15
<b>2-BuOH (A)</b>	1.94	99	38	2	5.7	7

Reaction conditions: 1.88 mmol substrate, 92  $\mu$ mol Rh, 3.5 eq. *p*-TsOH $\cdot$ H<sub>2</sub>O, 2.5 eq. CHI<sub>3</sub>, 5 eq. PPh<sub>3</sub>, 2 ml acetic acid, 20 bar

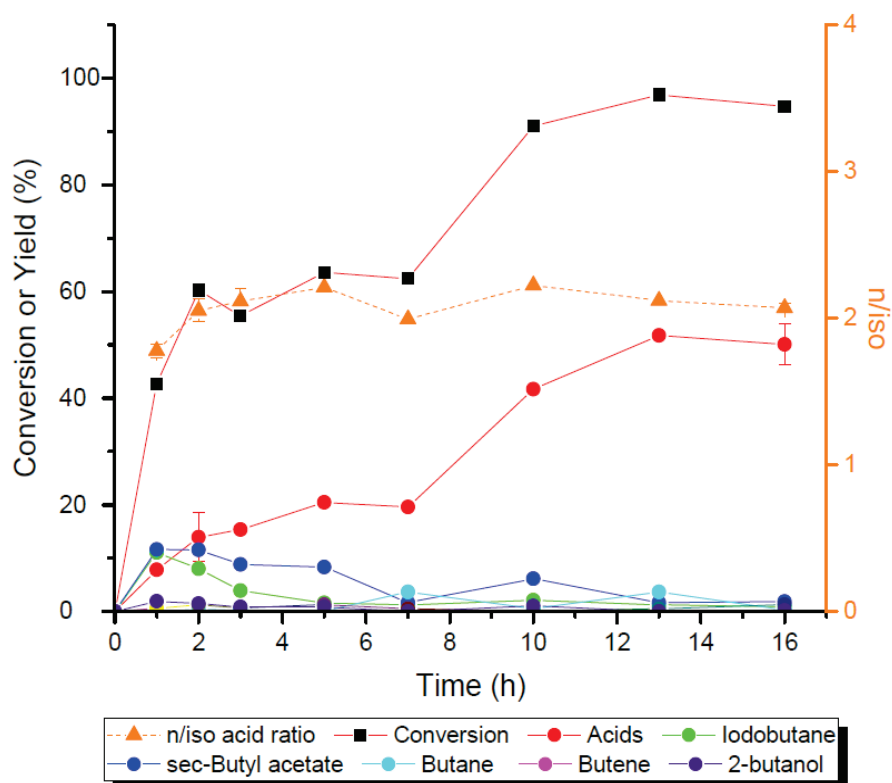
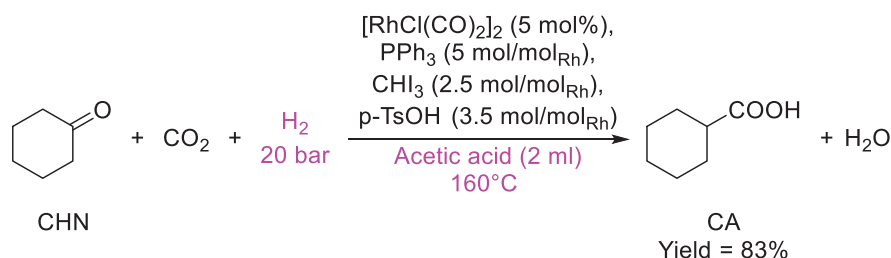


Figure 3-5: Time profile of the reaction of 2-butanone to VA and 2-MBA. Standard reaction conditions: 1.88 mmol of 2-Butanone, 92  $\mu$ mol Rh, 2 ml of acetic acid, 2.5 mol/mol<sub>Rh</sub> of CHI<sub>3</sub>, 5 mol/mol<sub>Rh</sub> of PPh<sub>3</sub>, 3.5 mol/mol<sub>Rh</sub> *p*-TsOH $\cdot$ H<sub>2</sub>O, 20 bar CO<sub>2</sub>, 20 bar H<sub>2</sub>, 160 °C. The points were collected performing separate reactions at different reaction times.

Eventually, after the optimization process, new conditions are adopted and a total yield of 83% is achieved (detailed product distribution for cyclohexanone and butanone are reported in Table 3-8), improving the initial yield of 63%.<sup>12</sup> This is the only process reported to convert ketones in simple carboxylic acids, leading the C=O bond reacting with CO<sub>2</sub> and H<sub>2</sub>. The conditions reported in Entry 2, Table 3-6 are identified as the best: 2 mL of acetic acid, *p*-TsOH·H<sub>2</sub>O, 160°C, 20 bar of H<sub>2</sub> and 20 bar of CO<sub>2</sub>, 2.5 eq. CHI<sub>3</sub>, 5 eq. of PPh<sub>3</sub>.



Scheme 3-8: Hydrocarboxylation of CHN: optimized reaction conditions (pink) and yields of CA.

Table 3-8: Products distribution, conversion and mass balance obtained as a result of the transformations of 2-Butanone (left) and Cyclohexanone (right). Conditions used are the one optimized reported in Entry 2, Table 3-6.

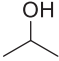
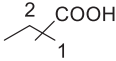
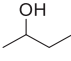
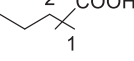
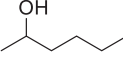
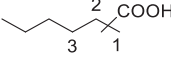
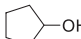
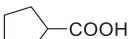
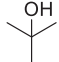
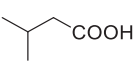
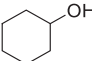
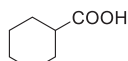
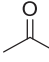
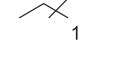
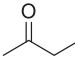
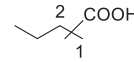
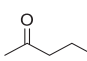
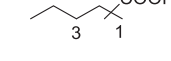
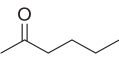
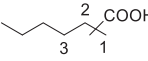
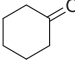
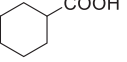
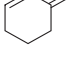
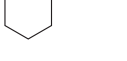
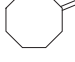
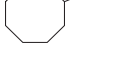

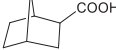
Yields from 2-Butanone (%)		Yields from Cyclohexanone (%)	
2-methylbutanoic acid (2-MBA)	17	Cyclohexylcarboxylic Acid (CA)	83
Valeric Acid (VA)	37	Iodocyclohexane	0.4
ACIDS (Sum)	54	Cyclohexyl acetate	1
1-Iodobutane	0	Cyclohexene	1
2-Iodobutane	1	Cyclohexane	6
Iodobutane (Sum)	1		
Sec-butyl acetate	0.4		
Butane	0.7		
Butene	2		
<b>Conversion</b>	98	<b>Conversion</b>	> 99
<b>Mass Balance</b>	60	<b>Mass Balance</b>	92

### 3.3.3 Scope of the reaction

Having optimized the reaction conditions for secondary alcohols and ketones, the scope of the reaction was expanded. First, simple alkyl alcohols (Entries 1-6, Table 3-9) were tested using the optimized reaction conditions described before. The obtained set of parameters is indeed good for the synthesis of many alkyl carboxylic acids. It is possible to reach yields from 30 to 80 %. Conversions are always over 99 %, due to the formation of by-products and or intermediates in the reaction conditions. The by-products obtained are the same, regardless of the used substrates. They are: corresponding acetate, iodide, alkene and alkane. The main by-product detected in all case is the corresponding alkane. Iodide and alkenes are instead detected in very small quantity, suggesting an intermediate role. Moreover, different isomers are obtained starting from C<sub>3+</sub> alcohols. Interesting, the *n*- isomer is always the more abundant with a ratio 2:1, compared to the *iso*-isomers. In conventional acid catalyzed systems for the synthesis of carboxylic acid via CO (Koch-Haaf), the more substitute carbon is preferentially carbonylated, due to higher stability of the corresponding carbocation intermediate.<sup>263</sup> In the case of the herein reported system, the *n*- isomer product is preferentially formed. *Tert*-butanol was tested in the same optimized conditions as secondary alcohols. In the case of tertiary alcohols, only one isomer is formed and no tertiary carboxylic acid is detected according to the Keulemans rule.<sup>248</sup>

Ketones react well with CO<sub>2</sub> and H<sub>2</sub> giving carboxylic acids in good yields, after an initial hydrogenation step (Entries 7-14, Table 3-9). Increasing the chain length (from C<sub>3</sub> to C<sub>6</sub> ketones) the yields increase from 35% to 75%. Since this trend is not observed for alcohols, the cause must be related to the nature of the ketones. Probably, the formation of a more stable enol form is required in order to have the selective reaction towards carboxylic acids. In general, the enol form is less stable and therefore less favorite compared to the ketone and a sort of stabilization is required (i.e. conjugation of the double bond).<sup>264</sup> In the case of longer chain ketones (C<sub>4+</sub>) the stabilization can originate from the formation of a more stable internal C=C bond. Regarding cyclic ketones, the formation of the enol may be favored by entropic effects. In these cases, the compound is already less flexible compared to a linear one. Therefore, the increase in rigidity due to the double bond is going to be less negative compared to a linear enol form.<sup>265, 266</sup> Nevertheless, yields up to 80% are obtained also starting from this class of substrates. The bifunctional substrate 2-cyclohexen-1-one is producing the monocarboxylic acid with the same yield as cyclohexanone itself (79%).

Table 3-9: Scope of the reaction: different secondary alcohols and ketones were tested.

Entry	Substrate	Conv. (%)	Products	Yields (%)
1		99		30 <sup>[b]</sup>
2		>99		77 <sup>[c]</sup>
3		>99		66 <sup>[d]</sup>
4		>99		72
5 <sup>[a]</sup>		>99		44
6		>99		80
7		99		35 <sup>[e]</sup>
8		99		54 <sup>[f]</sup>
9		99		64 <sup>[g]</sup>
10		99		75 <sup>[h]</sup>
11		99		83
13		99		79
13		99		48
14		99		38 <sup>[i]</sup>

Standard reaction conditions: 1.88 mmol of substrate, 92  $\mu\text{mol}$  Rh, 2 ml of acetic, 3.5 mol/mol<sub>Rh</sub> *p*-TsOH $\cdot$ H<sub>2</sub>O, 2.5 mol/mol<sub>Rh</sub> of CHI<sub>3</sub>, 5 mol/mol<sub>Rh</sub> of PPh<sub>3</sub>, 20 bar CO<sub>2</sub>, 20 bar H<sub>2</sub> (ketones) or 10 bar H<sub>2</sub> (secondary alcohols), 160 °C. [a] Optimized reaction conditions for secondary alcohols were used. [b] 1: 21, 2: 9; [c] 1: 50, 2: 27; [d] 1: 43, 2: 18, 3: 5; [e] 1: 24, 2: 11; [f] 1: 37, 2: 17; [g] 1: 43, 2: 19, 3: 4; [h] 1: 43, 2: 26, 3: 6; [i] Endo: 1, Exo: 37, detected by NMR.



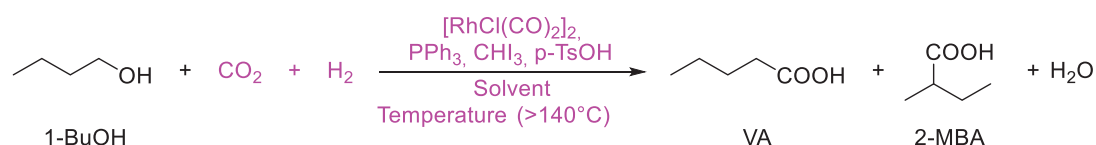
The developed system is capable of catalyzing the reaction of different alkyl secondary alcohols and ketones together with CO<sub>2</sub> and H<sub>2</sub> to a wide variety of carboxylic acids. The system is proved to be versatile and to provide good yields in the desired products starting from renewable resources (CO<sub>2</sub>, H<sub>2</sub>, alcohols and ketones).

Future research targets could be to control of the regio-selectivity and to reduce the amount of catalyst required.

## 3.4 Primary alcohols and aldehydes

### 3.4.1 1-butanol

The initial yield of VA and 2-MBA obtained from 1-BuOH (Scheme 3-9) was 30% (VA: 2-MBA = 2.2: 1), with the conversion over 99% (Entry 1, Table 3-10). As for secondary alcohols, the different parameters were varied to obtain optimized conditions and higher yields. In the following paragraphs, the results obtained for 1-BuOH are commented, highlighting the differences between the primary and secondary isomers.



Scheme 3-9: Hydrocarboxylation of 1-butanol (1-BuOH) to valeric acid (VA) e 2-methylbutanoic acid (2-MBA). The parameters varied and reported in this chapter are reported in pink.

Acetic acid and toluene are employed to investigate which is the best amount of solvent to optimize the yield to carboxylic acids. The results (Entry 1-6, Table 3-10) are different for acetic acid and toluene. For acetic acid, the best volume is 2 ml with a yield of 35%. For toluene, the best volume is 1 ml, giving yields of 39%. Probably, higher volumes of toluene lead to higher production of butane, partially butene, as well as to the formation of high boiling compounds that are difficult to quantify, resulting in lower mass balances. Based on the obtained results and considering the polarities of the used solvents, 2 ml of polar (both protic or aprotic) solvents and 1 ml of apolar solvents were used, for all the following tests. The solvent screening gave similar results to the one obtained when 2-BuOH was used as substrate (Entries 2, 4, 7-11, Table 3-10). The only difference is the slight increase in yield observed using 2 ml of acetic acid (35%, Entry 2, Table 3-10) instead of 1 ml of acetic acid (30%, Entry 1, Table 3-10). Moreover, toluene and xylene (Entries 4, 8 Table 3-10) resulted to be good solvents for the reaction as acetic acid. For this reason, some of the following test were carried out using both acetic acid (1 and 2 ml) and toluene as solvents.

Table 3-10: Hydrocarboxylation of 1-BuOH with CO<sub>2</sub> and H<sub>2</sub>: influence of different reaction parameters.

Entry	Solvent	Volume (ml)	Acidic additive (mol/mol <sub>Rh</sub> )	Temperature (°C)	H <sub>2</sub> pressure (bar)	CO <sub>2</sub> pressure (bar)	Yield (%)
1	Acetic acid	1	3.5	140	10	20	30
2	Acetic Acid	2	3.5	140	10	20	35
3	Acetic Acid	3	3.5	140	10	20	3
4	Toluene	1	3.5	140	10	20	39
5	Toluene	2	3.5	140	10	20	28
6	Toluene	3	3.5	140	10	20	19
7 <sup>[a]</sup>	Water	2	3.5	140	10	20	6
8	Xylene	1	3.5	140	10	20	37
9 <sup>[b]</sup>	Dioxane	1	3.5	140	10	20	3
10 <sup>[c]</sup>	Acetonitrile	2	3.5	140	10	20	2
11 <sup>[d]</sup>	Neet	1	-	140	10	20	1,5
12	Acetic acid	1	-	140	10	20	44
13	Acetic acid	2	-	140	10	20	2
14	Toluene	1	-	140	10	20	33
15	Acetic acid	2	3.5	160	10	20	26
16	Toluene	1	3.5	160	10	20	31
17	Acetic acid	1	-	160	10	20	59
18	Acetic acid	1	-	180	10	20	47
19	Acetic acid	1	-	160	5	20	44
20	Acetic acid	1	-	160	20	20	64
21	Acetic acid	1	-	160	30	20	56
22	Acetic acid	1	-	160	20	10	60
23	Acetic acid	1	-	160	20	30	48

If not specified, conversion is over 99%, VA/2-MBA ratio is about 2/1 and MB around or above 80%. Standard reaction conditions: 1.88 mmol 2-BuOH, 46 μmol [RhCl(CO)<sub>2</sub>]<sub>2</sub>, 2.5 mol/mol<sub>Rh</sub> of CHI<sub>3</sub> and 5 mol/mol<sub>Rh</sub> of PPh<sub>3</sub>. [a] Conversion = 57%. [b] Conversion = 85%; solid and unknown products formed. [c] Conversion = 43%. [d] High amount of not quantified secondary products were identified with GC-MS as ethers. Reaction time = 66h.

The *p*-TsOH•H<sub>2</sub>O has a big influence on the yield of carboxylic acids, depending on the amount of acetic acid used. The best conditions are 1 mL of acetic acid without *p*-

TsOH•H<sub>2</sub>O (yield 44% Entry 12, Table 3-10), whereas the best conditions found for the 2-BuOH were 2 mL of acetic acid without *p*-TsOH•H<sub>2</sub>O. The absence of *p*-TsOH•H<sub>2</sub>O in toluene has no significant effects (Entry 14, Table 3-10). The influence of the temperature in the range between 140 °C and 180 °C was studied on the following settings: 2 mL of acetic acid with *p*-TsOH•H<sub>2</sub>O, 1 mL of acetic acid without *p*-TsOH•H<sub>2</sub>O (Entries 2, 12, 17-18, Table 3-10), and 1 mL of toluene with *p*-TsOH•H<sub>2</sub>O (Entries 4, 16, Table 3-10). The increase of the temperature from 140 °C to 160 °C has two opposite effects: it decreases the yield in carboxylic acids if *p*-TsOH•H<sub>2</sub>O is present, while it increases the yield if *p*-TsOH•H<sub>2</sub>O is absent. A higher temperature in presence of *p*-TsOH•H<sub>2</sub>O increases the formation of by-products such as *n*-butyl ester and iodobutane. On the contrary, the yield in carboxylic acids rises to 59% on average, at 160 °C using 1 mL of acetic acid as solvent and no *p*-TsOH•H<sub>2</sub>O, reducing especially the yield of *n*-butyl acetate. Probably, the formation of the 1-BuOTs species leads to higher rates of nucleophilic substitution reactions (i.e. esterification) at higher temperature. These reactions may compete with the desired one, giving more by-products and reducing the amount of carboxylic acid obtained.

A further increase to 180 °C causes again a drop in the carboxylic acids yield, either for the deactivation of the catalyst or the increased importance of secondary reactions.

These observations are consistent with the analysis of the DoE result. The DoE shows an important correlation between the *p*-TsOH•H<sub>2</sub>O, the volume of the solvent and the temperature. The different effects of temperature, volume of solvent and *p*-TsOH•H<sub>2</sub>O on primary and secondary alcohols isomers are probably caused by their different behavior toward reactions such as esterification, etherification, nucleophilic substitution and elimination. Indeed, the acid may have an influence on the esterification equilibrium, since the absence causes the formation of butyl acetate as main product and no particular influence was noticed using toluene as a solvent. Increasing the temperature may not just increase the rate of the desired reaction, but also of side reactions. Therefore, also the effect of temperature will be related to the nature of the isomer chosen. The pressures used in the preliminary study are 20 bar of CO<sub>2</sub> and 10 bar of H<sub>2</sub>. Herein, first, H<sub>2</sub> pressure is varied. It was found that reducing the H<sub>2</sub> pressure to 5 bar (Entry 19, Table 3-10) causes a reduction of the carboxylic acids yields. Probably, this is due to a reduced production of CO (obtained from CO<sub>2</sub> reduction *via* rWGSR). On the contrary, the increase to 20 bar (Entry 20, Table 3-10) leads to a small increase of the yield up to 64%. A further increase in H<sub>2</sub> pressure

produces a higher hydrogenation rate (9% yield of butane is detected) which results in a lower yield in the desired carboxylic acids (Entry 21, Table 3-10).

With the H<sub>2</sub> pressure sets at 20 bar, the screening of different CO<sub>2</sub> pressure was done. Lowering the pressure to 10 bar slightly decreases the yield (60%), while increasing it to 30 bar gives a decrease to 48% (Entries 22, 23, Table 3-10).

Table 3-11: Hydrocarboxylation of 1-BuOH with CO<sub>2</sub> and H<sub>2</sub>: influence of CHI<sub>3</sub> and PPh<sub>3</sub> and Rh precursor.

Entry	Rh precursor	CHI <sub>3</sub> (mol/mol <sub>Rh</sub> )	PPh <sub>3</sub> (mol/mol <sub>Rh</sub> )	Conv. (%)	Yield (%) (n: iso ratio)
1	[Rh(CO) <sub>2</sub> Cl] <sub>2</sub>	2.5	5	>99	<b>65</b> (2.1)
2	[Rh(COD)Cl] <sub>2</sub>	2.5	5	99	<b>19</b> (3.8)
3	RhCl(PPh <sub>3</sub> ) <sub>3</sub>	2.5	2	99	<b>41</b> (2.4)
4	[HRh(CO)(PPh <sub>3</sub> ) <sub>3</sub> ]	2.5	2	99	<b>1</b> (-)
5	Rh <sub>2</sub> (OAc) <sub>4</sub>	2.5	5	99	<b>39</b> (2.5)
6	RhI <sub>3</sub>	2.5	5	98	<b>22</b> (1)
7	[Rh(CO) <sub>2</sub> Cl] <sub>2</sub>	0	5	98	<b>0</b> (-)
8	[Rh(CO) <sub>2</sub> Cl] <sub>2</sub>	9.3	5	99	<b>20</b> (1.2)
9	[Rh(CO) <sub>2</sub> Cl] <sub>2</sub>	2.5	0	>99	<b>2</b> (-)
10	[Rh(CO) <sub>2</sub> Cl] <sub>2</sub>	2.5	10	99	<b>44</b> (1.8)

Standard reaction conditions: 1.88 mmol 1-BuOH, 92 μmol Rh, 1 ml acetic acid, 20 bar CO<sub>2</sub>, 20 bar H<sub>2</sub>, 160 °C.

As it was done for secondary alcohols optimization, experiments on the CHI<sub>3</sub>, PPh<sub>3</sub> amounts and Rh precursor were performed. The species with Rh<sup>I</sup> appear to have a very different reactivity depending on the ligand. [Rh(COD)Cl]<sub>2</sub> and [HRh(CO)(PPh<sub>3</sub>)<sub>3</sub>] resulted to be inactive with the main formation of *n*-butyl acetate (Entries 2, 4, Table 3-11). [Rh(CO)<sub>2</sub>Cl]<sub>2</sub> and RhCl(PPh<sub>3</sub>)<sub>3</sub> resulted to be more active with the maximum yield of 65% registered for [Rh(CO)<sub>2</sub>Cl]<sub>2</sub> (Entries 1 and 3, Table 3-11). The Rh<sup>II</sup> species Rh<sub>2</sub>(OAc)<sub>4</sub> leads to a yield of 39% in carboxylic acids (Entry 5, Table 3-11), similarly to the RhCl(PPh<sub>3</sub>)<sub>3</sub>. The Rh<sup>III</sup> species (RhI<sub>3</sub>) is not selective for the production of

carboxylic acids leading to a mixture of by-products such as butane, butene, *n*-butyl acetate and iodobutane (Entry 6, Table 3-11). The same conclusion obtained from the experiment performed on 2-BuOH can be drawn (Section 3.3.1).

As explained in section 3.3.1, the iodide additive may have multiple functions. The results obtained with 0.0, 2.5 and 9.3 mol/mol<sub>Rh</sub> of CHI<sub>3</sub> in solution (corresponding to 0, 7.6 and 28 eq. of I<sup>-</sup> compared to Rh mol) are reported in Entries 1, 7-8 in Table 3-11. The amount of iodide influences dramatically the total yield in carboxylic acids. The absence of iodide additive gives 0% yield of carboxylic acids, but at the same time, 9.3 mol/mol<sub>Rh</sub> of iodoform causes a decrease in the yield to 20%. This behavior could be explained with the cited possible iodide functions. On one hand, too much iodide forms other species which are not active (i.e. [Rh(CO)<sub>2</sub>I<sub>4</sub>]<sup>-</sup> or similar Rh<sup>III</sup> stable species which is known to be an inactive species for the Monsanto carbonylation)<sup>253</sup>, hence a smaller activity is noticed. Moreover, when 9.3 eq. of CHI<sub>3</sub> are used, the final solution is very dark and high amount of solid materials is present, making the analysis and the collection of the all reaction solution more difficult leading to lower mass balance. On the other hand, no iodide causes the absence either of the catalytic active species or of a reactive substrate (iodobutane).<sup>245</sup> In fact, no products or by-products are detected except for *n*-butyl acetate, which is present in solution also in the absence of the catalytic active species. The negative effect of high amounts of iodide in the reactor is probably the cause of the low activity observed when iodobutane is used as substrates. In these cases, the total amount of I<sup>-</sup> present in the solution is 1.88 + 7.6 mmol (derived from the CHI<sub>3</sub>) corresponding to 28 eq. (or 9.3 eq. of CHI<sub>3</sub>). In these conditions, the yield in carboxylic acids is 25% from 1-iodobutane, similarly to the one obtained from 1-BuOH if 9.3 eq. of CHI<sub>3</sub> are added to the solution (Entry 8, Table 3-11).

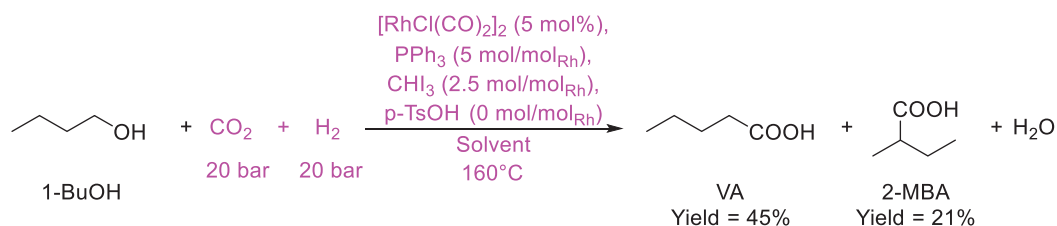
PPh<sub>3</sub> is influencing the yield in carboxylic acid starting from 1-BuOH in the same way as starting from 2-BuOH. Without PPh<sub>3</sub>, the yield in carboxylic acids drops to 2%, while with 10 eq. of PPh<sub>3</sub> the yield decreases to a 44% (Entries 9-10, Table 3-11), although no significant change in the *n*/*iso* ratio is observed. These observations lead to conclude that phosphine is actually an important part of the catalyst. Further explanations of the effect of PPh<sub>3</sub> can be found in the Section 4.

A detailed product distribution is shown in Table 3-12. The main by-products are *n*-butyl acetate and butane, derived from the 2-BuOH hydrogenation. In addition, the corresponding 1-iodobutane and butene are detected. The difference in yield between 14 and 16 hours is minimal (Table 3-12).

Table 3-12: Products distribution, conversion and mass balance obtained as a result of the transformations of 1-BuOH after 14 and 16 hours of reaction. Conditions used are the one optimized reported in Entry 20, Table 3-10.

Compounds	Yields after 14 h (%)	Yields after 16 h (%)
2- Methylbutanoic acid (2-MBA)	18	21
Valeric Acid (VA)	44	45
Acids (Sum)	62	66
1-Iodobutane	1	2
2-Iodobutane	0	1
Iodobutane (Sum)	1	3
Acetate	8	6
Butane	2	8
Butene	1	1
(Sum of 1-butene, 2-butene)	1	1
<b>Conversion</b>	>99	>99
<b>Mass Balance</b>	74	84

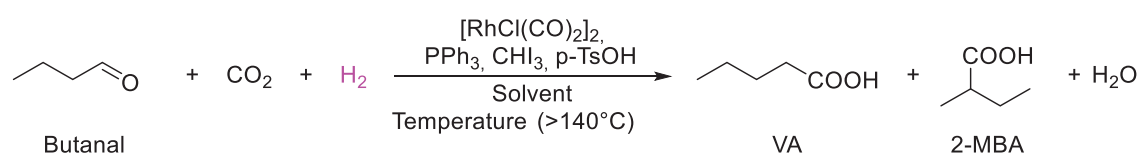
Summing up, the investigation of the effect of many parameters leads to find the optimal value for all of them. The optimized reaction conditions for 1-BuOH are: 0.046 mmol of  $[\text{RhCl}(\text{CO})_2]_2$ , 2.5 mol/mol<sub>Rh</sub> of  $\text{CHI}_3$ , 5 mol/mol<sub>Rh</sub> of  $\text{PPh}_3$ , 1 mL of acetic acid, 1.88 mmol of 1-BuOH, 20 bar of  $\text{CO}_2$ , 20 bar of  $\text{H}_2$ , 160 °C and 16 hours. These conditions differ from the optimized one for secondary alcohols in the amount of solvent used (1 mL of acetic acid for primary and 2 mL for secondary alcohols), the absence of  $p\text{-TsOH}\cdot\text{H}_2\text{O}$  (3.5 eq. of it are used in the reaction of 2-BuOH) and the  $\text{H}_2$  pressure (20 and 10 bar respectively for primary and secondary alcohols). These conditions reported in Entry 20, Table 3-10 allowed us to obtain a yield in VA and 2-MBA of 64%.



Scheme 3-10: Hydrocarboxylation of 2-BuOH: optimized reaction conditions (pink) and yields of 2-MBA and VA.

### 3.4.2 Butanal

Following the example of ketones, the reaction conditions for aldehydes were studied. In particular, due to their similarities with primary alcohols, the chosen starting point were the optimized conditions for primary alcohols and we tested the effect of higher H<sub>2</sub> pressure. Aldehydes, as ketones, may be reduced to the corresponding alcohol in the presence of Rh system and further carbonylated to carboxylic acids.<sup>260</sup> In particular, Rh complexes in presence of CO and H<sub>2</sub>O catalyze the transformation of aldehydes in primary alcohols.<sup>267</sup> Moreover, a very similar system (Monsanto catalytic system) is able to reduce acetaldehyde to ethanol and further carbonylates it to propionic acid.<sup>268</sup>



Scheme 3-11 Hydrocarboxylation of butanal to valeric acid (VA) e 2-methylbutanoic acid (2-MBA). The parameters varied and reported in this chapter are reported in pink.

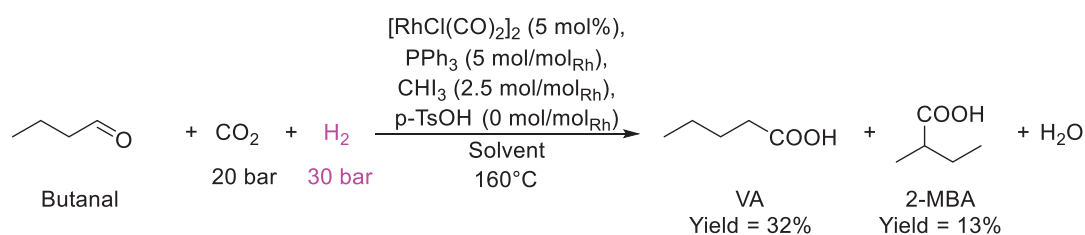
Using the same conditions used for primary alcohols it is possible to obtain a yield of VA and 2-MBA starting from butanal of 37% (n/iso = 2.3). Increasing the H<sub>2</sub> pressure to 30 bar allows to increase the yield up to 45% (n/iso = 2.4). Mass balances for these reactions are lower than those obtained from alcohols or ketones. This is probably due to the formation of longer chain products from aldehydes condensation which were not quantified. GC-MS identified some of them as different C<sub>9</sub> carboxylic acids. They are probably the products of the hydrocarboxylation of the *in situ* formed C<sub>8</sub> ketones. In any case, the detected product distributions obtained from the reaction is very similar to the one obtained from 1-BuOH and traces of it are also detected (Table 3-13). In the optimized conditions for aldehydes, a similar yield in VA and 2-MBA was obtained from butanal and from 2-butanone. Yields are lower than those obtained from the corresponding 1-BuOH (65% is obtained from the alcohol and only 43% is obtained from the aldehyde).



Table 3-13: Products distribution, conversion and mass balance obtained as a result of the transformations of Butanal.

Compounds	Yield after 16 h (%)
2-Methylbutanoic acid (2-MBA)	13
Valeric Acid (VA)	32
Acids (Sum)	<b>45</b>
1-Iodobutane	1
2-Iodobutane	
Iodobutane (Sum)	<b>1</b>
<i>n</i> -butyl acetate	<b>2</b>
Butane	<b>8</b>
Butene (Sum of 1-butene, 2-butene)	<b>2</b>
<b>Conversion</b>	<b>&gt;99</b>
<b>Mass Balance</b>	<b>58</b>

Nevertheless, this is the first reported example of synthesis of carboxylic acids starting directly from aldehyde, CO<sub>2</sub> and H<sub>2</sub>. Fair yields are obtained, with a total yield of 45% and no additional step or addition of stoichiometric organometallic reagents are required.



Scheme 3-12: Hydrocarboxylation of butanal: optimized reaction conditions (pink) and yields of 2-MBA and VA.

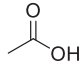
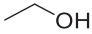

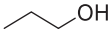

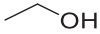
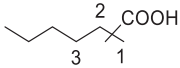
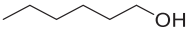
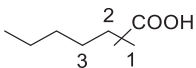
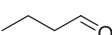
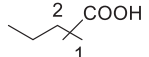
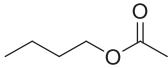
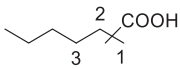
### 3.4.3 Scope of the reaction

Having optimized the reaction conditions for primary alcohols and aldehydes, the scope of the reaction was expanded. The optimized conditions work well for the synthesis of many alkyl carboxylic acids (Table 3-14). It is possible to reach yields up to 80 %. Conversions are always over 99 %, due to the formation of by-products and/or intermediates in the reaction conditions. The by-products obtained are the same, regardless of the substrate used. They are: corresponding acetate, iodide, alkene and alkane. The main by-products detected in all cases are the corresponding alkane and *n*-acetate. Iodide and alkenes are instead detected in very small quantity, suggesting an intermediate role. Moreover, different isomers are obtained starting from C<sub>3+</sub> alcohols, as for secondary alcohols and ketones. Methanol resulted to give the lowest yield among simple alkyl alcohols. For this substrate, only 19% of the desired acetic acid is formed, but higher amount of methane was observed compared to other substrates. Probably, the explanation for this can be in the mechanism of the reaction, as explained in the Section 3.8.

The corresponding acetate ester of the alcohols could be used as substrates as well (Entry 7, Table 3-14). *n*-Butyl acetate leads to the same products as 1-BuOH, but in lower yields. As expected, the system appears to be able to transform the esters (which can be in equilibrium with the corresponding alcohol in acidic conditions) in the same by-products obtained from the corresponding alcohols (iodobutane, butane, butene).

The developed system can catalyze the reaction of various primary alkyl alcohols, aldehydes and esters together with CO<sub>2</sub> and H<sub>2</sub> to a wide variety of carboxylic acids. Although some improvement in the regio-selectivity is still desirable, the system is proved to be versatile and to provide good yields in the desired products starting from renewable resources.

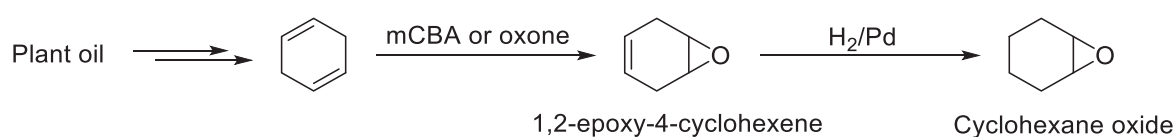
Table 3-14: Scope of the reaction: different primary alcohols, aldehyde and ester were tested.

Entry	Substrate	Conv. (%)	Products	Yields (%)
1	$\text{H}_3\text{C}-\text{OH}$	>99		19
2		>99		80
3		>99		45 <sup>[a]</sup>
4		>99		65 <sup>[b]</sup>
5		>99		64 <sup>[c]</sup>
6		>99		45 <sup>[d]</sup>
7		70		42 <sup>[e]</sup>

Standard reaction conditions: 1.88 mmol of substrate, 92  $\mu\text{mol}$  Rh, 1 mL of acetic acid or propionic acid (only for methanol), 2.5 mol/mol<sub>Rh</sub> of  $\text{CHI}_3$ , 5 mol/mol<sub>Rh</sub> of  $\text{PPh}_3$ , 20 bar  $\text{CO}_2$ , 20 or 30 (only for aldehyde) bar  $\text{H}_2$ , 160 °C. [a] 1: 33, 2: 12; [b] 1: 44, 2: 21; [c] 1: 42, 2: 17, 3: 5; [d] 1: 43, 2: 18, 3: 5; [e] 1: 29, 2: 13.

### 3.5 Epoxides

The production of epoxides is an essential reaction for the oxyfunctionalization of alkenes. Epoxides (or oxiranes) are industrially produced starting from the catalytic oxidation of alkenes.<sup>243</sup> In addition, many epoxides can be obtained from biomass. For instance, cyclohexane oxide can be obtained from the hydrogenation of 1,2-epoxy-4-cyclohexene. This compound is the product of the oxidation of 1,4-cyclohexadiene (Scheme 3-13), which is a waste product in the self-metathesis of some polyunsaturated fatty acids obtained from renewable plant oils (i.e. linoleic acid).<sup>241</sup>



Scheme 3-13: Synthesis of cyclohexane oxide starting from plant oil.

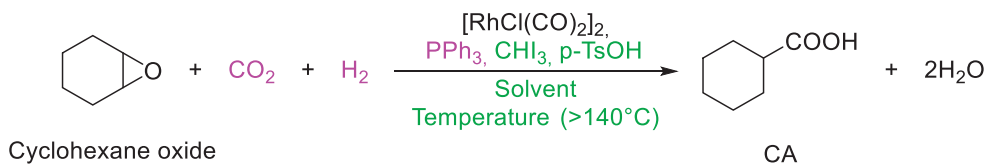
Epoxides are used in many reaction with  $\text{CO}_2$  to obtain polycarbonates,<sup>241</sup> polyethercarbonates polyols<sup>240</sup> and carbonates.<sup>242</sup> However, the coupling of epoxides and  $\text{CO}_2$  to give carboxylic acids has not been reported so far.

Attempts to transform cyclohexane oxide into carboxylic acid using the system optimized for alcohols were initiated. However, every attempt to perform their selective transformation to carboxylic acids in acetic acid as solvent resulted in non-reproducible results ( $8 \pm 7\%$ ) using the optimized conditions for primary alcohols or no yield of the desired product using the optimized conditions for secondary alcohols. The irreproducibility is probably due to a non-controlled polymerization of the epoxide. It is known that epoxides polymerize in presence of acidic catalysts.<sup>269, 270</sup>

To overcome this problem, toluene was selected as solvent, because it was also a good solvent for the transformation of alcohols to carboxylic acids, but provides a non-acidic medium.

Cyclohexane oxide was used as substrates (Scheme 3-14) because only one acid product can be formed (cyclohexancarboxylic acid (CA)). The initial used conditions were: 0.046 mmol of  $[\text{RhCl}(\text{CO})_2]_2$ , 2.5 mol/mol<sub>Rh</sub> of  $\text{CHI}_3$ , 3.5 mol/mol<sub>Rh</sub> of  $p\text{-TsOH}\cdot\text{H}_2\text{O}$ , 5 mol/mol<sub>Rh</sub> of  $\text{PPh}_3$ , 2 ml of toluene, 1.88 mmol of cyclohexane oxide, 20 bar of  $\text{CO}_2$ , 10 bar of  $\text{H}_2$ , 160 °C and 16h. The  $\text{H}_2$  and  $\text{CO}_2$  pressures and the amount

of phosphine were first investigated separately (Scheme 3-14). Subsequently, the Design of Experiment was used for the optimization of the other parameters:  $\text{CHI}_3$ ,  $p\text{-TsOH}\cdot\text{H}_2\text{O}$  amount, toluene volume and temperature (Scheme 3-14).



Scheme 3-14: Hydrocarboxylation of cyclohexane oxide to cyclohexanecarboxylic acid (CA). The parameters varied and reported in this chapter are reported in pink. The parameters reported in green were studied with a DoE approach as reported in this chapter.

Table 3-15 shows the yields of CA obtained varying the  $\text{H}_2$  pressure, the  $\text{CO}_2$  pressure and the amount of  $\text{PPh}_3$ . The mass balance of the reaction never reaches 100 % and it is generally lower than the mass balance observed for the conversion of alcohols. The GC-MS of the reaction mixture identified the fragment  $\text{C}_6\text{H}_{11}\text{O}$  at higher retention time in relation to alcohol, epoxide and carboxylic acid. This signal can be ascribed to oligomers formed directly from the epoxides, which are not quantified leading to a low mass balance.

At first, the  $\text{H}_2$  pressure was increased up to 50 bar (Entries 1-5, Table 3-15). Using higher pressures of  $\text{H}_2$  not only increases the yield in carboxylic acid but also the mass balance, reducing the amount of by-products with high molecular weight. The maximum is obtained applying an  $\text{H}_2$  pressure of 40 bar (Entry 4, Table 3-15). Using 10 bar of  $\text{CO}_2$  reduces the yield in carboxylic acid to 37% (Entry 6, Table 3-15), while increasing  $\text{CO}_2$  pressure up to 30 bar does not give any significant change (Entry 7, Table 3-15). Removing and increasing the amount of  $\text{PPh}_3$  lead to a reduction in carboxylic acid yields, especially when no  $\text{PPh}_3$  is present (Entries 8-9, Table 3-15).

The chosen conditions to continue the investigation of the reaction parameters were those reported in Entry 4, Table 3-15, leading to 51% yield in CA: 40 bar of  $\text{H}_2$ , 20 bar of  $\text{CO}_2$  and 5 mol/mol<sub>Rh</sub> of  $\text{PPh}_3$ .

Table 3-15: Hydrocarboxylation of cyclohexane oxide with CO<sub>2</sub> and H<sub>2</sub>: influence of different reaction parameters.

Entry	H <sub>2</sub> pressure (bar)	CO <sub>2</sub> pressure (bar)	PPh <sub>3</sub> (mmol)	Mass Balance (%)	Yield (%)
1	10	20	5	47	18
2	20	20	5	56	41
3	30	20	5	64	46
4	40	20	5	68	51
5	50	20	5	66	43
6	40	10	5	69	37
7	40	30	5	75	53
8	40	20	0	51	4
9	40	20	10	70	45

Conversion consistently over 99%. Standard reaction conditions: 1.88 mmol Cyclohexane Oxide, 46 μmol [RhCl(CO)<sub>2</sub>]<sub>2</sub>, 2.5 eq. of CHI<sub>3</sub>, 2 ml of toluene, 3.5 mol/mol<sub>Rh</sub> of *p*-TsOH•H<sub>2</sub>O and 160 °C.

Once H<sub>2</sub> and CO<sub>2</sub> pressures and the amount of PPh<sub>3</sub> were defined, the effects of the other parameters were investigated using the program DesignExpert8 to perform the Design of Experiment. The amount of CHI<sub>3</sub>, *p*-TsOH•H<sub>2</sub>O, the temperature and the volume of solvents can be interdependent. For this reason, their optimization was investigated using a Design of Experiment approach. The *response surface method* and the Box-Behnken model were selected in order to use the same method already set for the optimization of reaction parameters in Section 3.2.

The following four factors and their thresholds are chosen for the DoE:

- Temperature: 140-180 °C
- Volume of acetic acid: 1-3 mL
- *p*-TsOH•H<sub>2</sub>O: 0-0.67 mmol
- CHI<sub>3</sub>: 0.05-0.44 mmol.

These values were chosen based on previous test and based on technical limitation (i.e. corrosion of the autoclaves metal).

Once all the 29 reactions established by the Design of Experiment program were performed, a final response is obtained. The method resulted to be statistically significant, but it does not fit properly (mathematically indicated by the fact that the predicted  $R^2$  is different from the adjusted  $R^2$ ). This means that some of the predicted yields does not correspond to the experimental parameters. From the graphs reported in Figure 3-6, it can be concluded that there are large surface areas with a similar predicted yield, where the influence of the variation of the parameters.

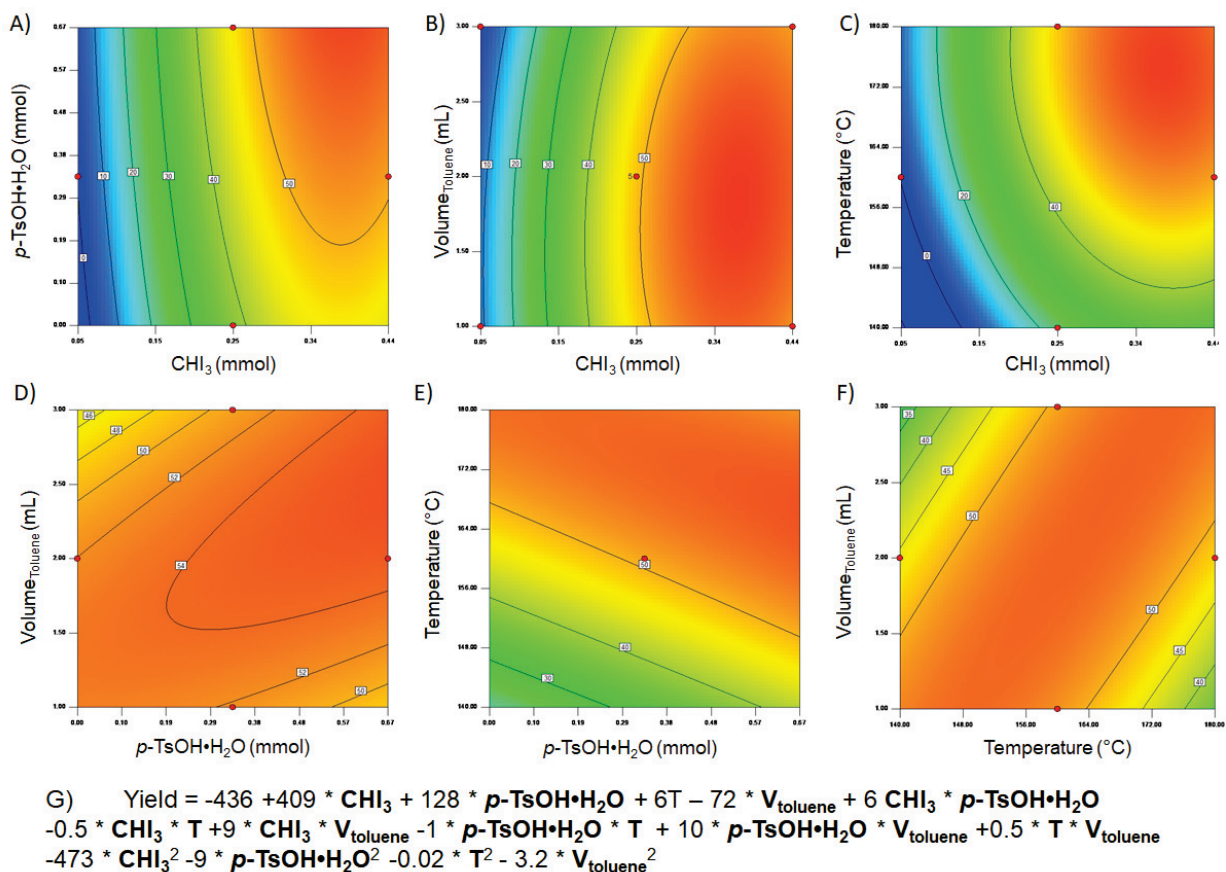


Figure 3-6: Graphic visualization of DoE results and relation between the different parameters (A-F) and equation of the yield calculated from the studied parameters (G).

Graphic visualizations (A-F) and the equation (G) of the yield provided by the DoE calculation of the results are reported in Figure 3-6. Every possible couple is present in the equation, as expected, indicating that all the parameters are correlated with each other.  $\text{CHI}_3$  appears to be the most important parameter. It has a positive influence alone and its combination with the other parameters is also important.  $p\text{-TsOH}\cdot\text{H}_2\text{O}$  has also an important positive effect, while the volume of toluene and the temperature

have a smaller effect, negative and positive respectively. The interaction which has the smallest impact on the yield are those involving the temperature (coefficient around 1), which does not seem to play a crucial role if kept between 140 and 180 °C. The same conclusions can be deduced from the analysis of the plots elaborated by the DoE program.

Table 3-16: DoE results: both the suggested and the experimental best conditions are reported.

Parameter	DoE solution	Run 24
<i>CHI<sub>3</sub></i>	0.38 mmol	0.44 mmol
<i>p-TsOH</i>	0.67 mmol	0.33 mmol
<i>V</i>	1.6 ml	3 ml
<i>Temperature</i>	150°C	160°C
<b>Yield predicted from DoE</b>	<b>57%</b>	<b>51%</b>
<b>Experimental yield</b>	<b>42%</b>	<b>60%</b>

Standard reaction conditions: 1.88 mmol Cyclohexane Oxide, 46 μmol [RhCl(CO)<sub>2</sub>]<sub>2</sub> and 5 eq. PPh<sub>3</sub>, 20 bar of CO<sub>2</sub> and 40 bar of H<sub>2</sub>

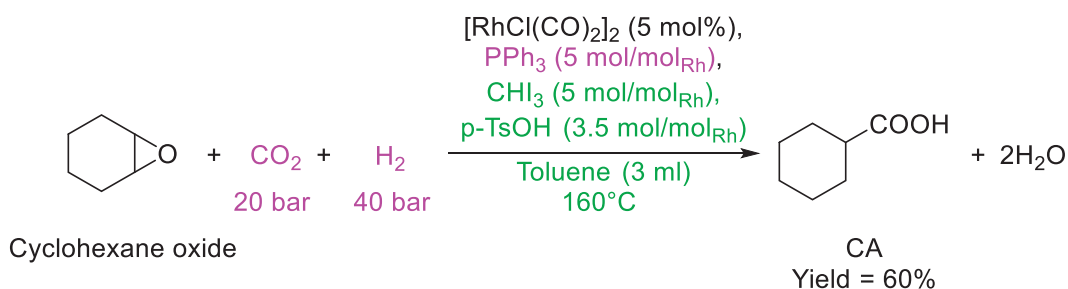
Due to the lack of fit and the broad range of conditions leading to similar yields, the final DoE response did not correspond to the highest yield upon experimental verification (Table 3-16). The reaction 24 of those suggested by the DoE program resulted in a higher yield as predicted (60%). This set of parameters giving the highest yield are found in the surface areas giving high yields according to the model (red parts in the graphs of Figure 3-6).

Table 3-17: Products distribution, conversion and mass balance obtained as a result of the transformations of Cyclohexane Oxide. Conditions used are the one optimized reported in Table 3-16, right.

Yields from Cyclohexane Oxide (%)	
Cyclohexylcarboxylic Acid (CA)	60
Iodocyclohexane	18
Cyclohexene	1
Cyclohexane	4
<b>Conversion</b>	<b>&gt;99</b>
<b>Mass Balance</b>	<b>83</b>

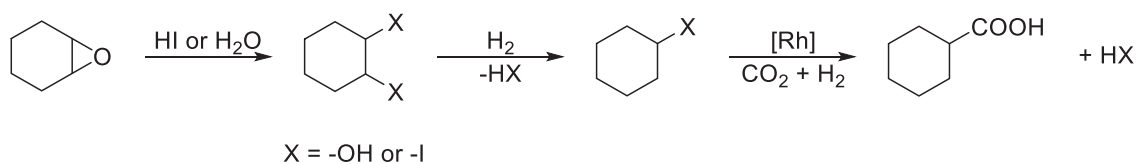


The final optimized reaction conditions allow to obtain a total yield in CA starting from cyclohexane oxide of 60% (Scheme 3-15). The best conditions found are: 0.046 mmol of  $[\text{RhCl}(\text{CO})_2]_2$ , 5 mol/mol<sub>Rh</sub> of  $\text{CHI}_3$ , 3.5 mol/mol<sub>Rh</sub> of  $p\text{-TsOH}\cdot\text{H}_2\text{O}$ , 5 mol/mol<sub>Rh</sub> of  $\text{PPh}_3$ , 3 ml of toluene, 1.88 mmol of Cyclohexane Oxide, 20 bar of  $\text{CO}_2$ , 40 bar of  $\text{H}_2$ , 160 °C and 16h (Scheme 3-15).



Scheme 3-15: Hydrocarboxylation of cyclohexane oxide and yield of cyclohexanecarboxylic acid (CA). The parameters optimized via single parameter variation are reported in pink, the parameters reported in green were studied with a DoE approach.

Using these reaction conditions, the observed by-product and intermediates are identical to those obtained when using cyclohexanol as substrate. (Table 3-17). This suggests a reaction pathway which consists of an intermediate step transforming the epoxide to the mono alcohol or in presence of iodide of the mono-iodide as reported in Scheme 3-16.



Scheme 3-16: Reaction pathway of the transformation of the cyclohexane oxide in CA. X is an hydroxy group or a iodide.

In conclusion, epoxides demonstrated for the first time to be suitable substrates for the formal hydrocarboxylation. Cyclohexane Oxide was converted into cyclohexanecarboxylic acid (CA) with a yield of 60 %.

### 3.6 Multifunctional substrates and industrial relevant mixtures

In order to expand the range of possible applications, some multifunctional and industrial relevant mixtures of oxygenated compounds as substrates were tested.

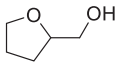
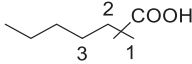
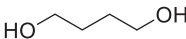
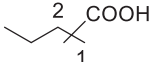
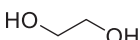
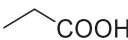
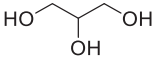
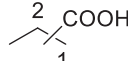
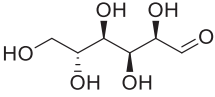
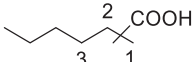
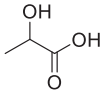
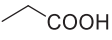
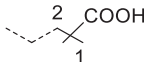
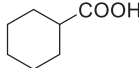
No di-carboxylic acid was formed starting from diols as bifunctional substrates. Starting from dienes had the same effect leading to the production of the mono-carboxylic acid.<sup>12</sup> Although lower yields (maximum 42%) are obtained for diols as compared to the corresponding mono-alcohol (up to 80%), these results clearly show that the synthesis of carboxylic acids may be possible also from diols. Primary vicinal diols (ethylene glycol and glycerol) lead to the lowest yields (maximum 31%). Probably, this could be explained by the formation of cyclic ethers<sup>271, 272</sup> or oligomerization reactions<sup>273</sup> These reactions are known to be facilitated in acidic media and may lead to not quantified products. Interestingly, a heterocyclic compound such as tetrahydrofurfuryl alcohol does not allow producing cyclic carboxylic acids (Entry 1, Table 3-18). The heterocycle opens probably forming pentandiol<sup>274</sup> which reacts to give C<sub>6</sub> carboxylic acids.

An attempt to obtain bifunctional carboxylic acids was carried out starting from lactic acid. No trace of the desired product was detected with GC and by <sup>13</sup>C-NMR techniques. Nevertheless, propionic acid was detected, suggesting that the hydrogenation reaction occurred instead of the carbonylation (Entry 6, Table 3-18).

A highly functionalized substrate such as glucose cannot produce any desirable products. Moreover, the carbon mass balance is very low, bringing to the conclusion that oligomerization reactions may occur, as well as humins formation (Entry 5, Table 3-18).<sup>276, 277</sup>

The presence of hydride sources is reported to be a limiting factor in the synthesis of diacids using CO<sub>2</sub>.<sup>275</sup> The reason is probably the presence of H<sub>2</sub> in the reactor leading to rapid de-functionalization after the first carboxyl group is formed, as confirmed by the lactic acid conversion. Another reason can be the rapid de-functionalization of the diol substrate in presence of H<sub>2</sub> and Rh-catalyst, similarly to the cyclohexane oxide (Scheme 3-16).

Table 3-18: Scope of the reaction: diols and mixture of substrates were tested.

Entry	Substrate	Conv. (%)	Products	Yields (%)
1		>99		34 <sup>[a]</sup>
2		>99		42 <sup>[b]</sup>
3		>99		31
4		>99		15 <sup>[c]</sup>
5		>99		0
6 <sup>[d]</sup>		99		27
7 <sup>[e]</sup>	ABE mixture (Acetone-Butanol-Ethanol)	C <sub>3</sub> : >99 C <sub>4</sub> : >99 C <sub>2</sub> : >99		C <sub>4</sub> : 28 <sup>[f]</sup> C <sub>5</sub> : 43 <sup>[g]</sup> C <sub>3</sub> : 99
8 <sup>[h]</sup>	KA Oil (Ketone Alcohol Oil)	99		79

Standard reaction conditions: 1.88 mmol of substrate, 92  $\mu\text{mol}$  Rh, 1 ml of acetic acid, 2.5 mol/mol<sub>Rh</sub> of  $\text{CHI}_3$ , 5 mol/mol<sub>Rh</sub> of  $\text{PPh}_3$ , 20 bar  $\text{CO}_2$ , 20 bar  $\text{H}_2$ , 160 °C. [a] 1: 25, 2: 8, 3: 1; [b] 1: 31, 2: 11; [c] 1: 11, 2: 4; [d] Standard reaction conditions: 1.88 mmol of substrate, 92  $\mu\text{mol}$  Rh, 2 ml of acetic acid, 3.5 mol/mol<sub>Rh</sub> *p*-TsOH $\cdot$ H<sub>2</sub>O, 2.5 mol/mol<sub>Rh</sub> of  $\text{CHI}_3$ , 5 mol/mol<sub>Rh</sub> of  $\text{PPh}_3$ , 20 bar  $\text{CO}_2$ , 10 bar  $\text{H}_2$ , 160 °C. [e] Acetone:Butanol:Ethanol = 3:6:1, [f] 1: 20, 2: 8; [g] 1: 30, 2: 13; [h] Standard reaction conditions: 1.88 mmol of substrate, 92  $\mu\text{mol}$  Rh, 2 ml of acetic acid, 3.5 mol/mol<sub>Rh</sub> *p*-TsOH $\cdot$ H<sub>2</sub>O, 2.5 mol/mol<sub>Rh</sub> of  $\text{CHI}_3$ , 5 mol/mol<sub>Rh</sub> of  $\text{PPh}_3$ , 20 bar  $\text{CO}_2$ , 20 bar  $\text{H}_2$ , 160 °C.

Interestingly, industrially relevant mixture of substrates, such as the ABE mixture (acetone: butanol: ethanol = 3: 6: 1) from fermentation process, can be successfully transformed in the mixture of the corresponding carboxylic acids (Entry 7, Table 3-18). No previous separation step is needed. In this case, the optimized conditions for primary alcohols were used and even acetone is converted into the desired C<sub>3</sub>

carboxylic acids. Similarly, the KA Oil (cyclohexanone: cyclohexanol = 1: 1) mixture gives very good results. In this case only cyclohexylcarboxylic acid is obtained with a yield of 79% (Entry 8, Table 3-18), applying the optimized conditions for ketones.

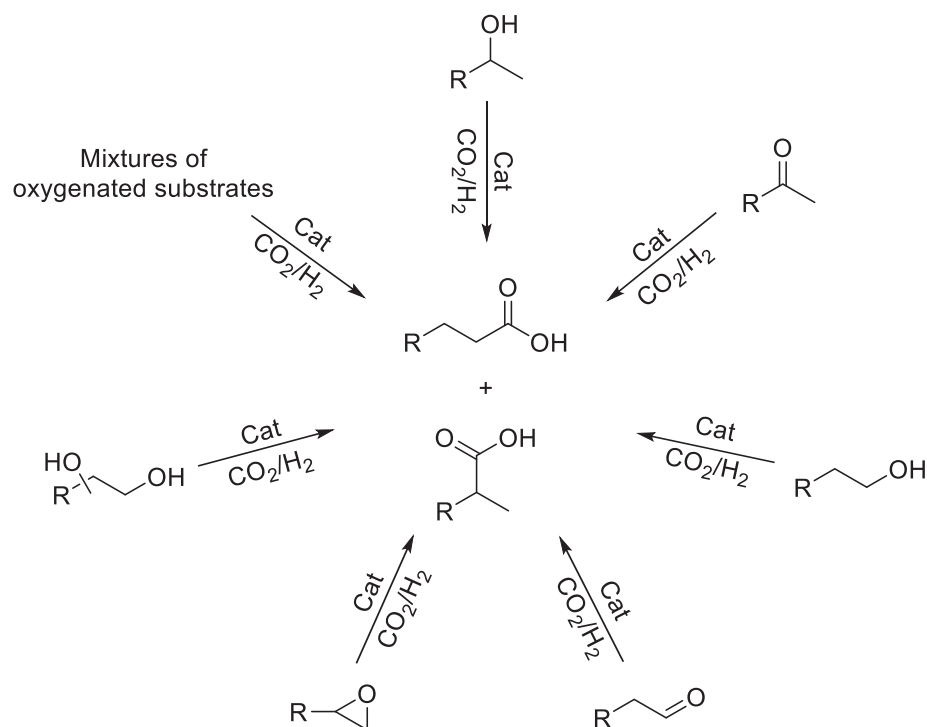
### 3.7 Conclusions

The Rh catalytic system was proven active for the synthesis of carboxylic acids from oxygenated substrates.

Overall, the DoE allowed to understand the correlations between the chosen parameters (temperature, volume of acetic acid, amount of  $\text{CHI}_3$  and  $\text{p-TsOH}\cdot\text{H}_2\text{O}$ ) and to prove their importance for the yield in carboxylic acids obtained from oxygenated substrates,  $\text{CO}_2$  and  $\text{H}_2$ . Moreover, it was verified that the best reaction conditions are found within the chosen range.

Following the DoE results, the effect of many parameters on the yields of the different classes of oxygenated substrates was studied, finding the optimal value for all of them. The optimized reaction conditions for 1-BuOH allowed to obtain a yield in VA and 2-MBA of 64%, which is more than twice as high as under previously reported conditions.<sup>12</sup> The optimized conditions for 2-BuOH differ from those for primary alcohols in the amount of solvent used, the presence of  $\text{p-TsOH}\cdot\text{H}_2\text{O}$  and the  $\text{H}_2$  pressure. The yield reached at the end of the optimization procedure is 77% which is much higher compared to the one obtained during preliminary study. The new conditions developed for ketones lead to a total yield of 83%, which is the best obtained starting directly from ketones, up to now. The first example of synthesis of carboxylic acids starting directly from aldehyde,  $\text{CO}_2$  and  $\text{H}_2$  is reported. Good results are obtained, with a total yield of 45% for this transformation. Epoxides are also suitable for the hydrocarboxylation reaction in presence of Rh catalyst. For the first time, the synthesis of carboxylic acid was achieved with a yield of 60%.

Many different classes of substrates can be transformed in the desired carboxylic acids using  $\text{CO}_2$  and  $\text{H}_2$  with our Rh catalytic system. All the three possible alcohol isomers, ketones, aldehydes, epoxides and diols can be transformed (also when they are used in a mixture or if different functionalities are on the same organic molecule) into mono-carboxylic acids with yields up to 83%. Among these, industrial relevant mixture such as KA Oil and ABE mixture are successfully transformed without any previous separation.



Scheme 3-17: Summary of the oxygenated substrates for the hydrocarboxylation reaction using the Rh catalytic system reported in this chapter.

## **3.8 Experimental part**

See Section 4.7 Experimental part.





**4. Mechanistic investigation and reaction pathway**



## 4.1 State of the art

The catalyst reported in this thesis was already studied for the transformation of alkenes into carboxylic acids. In the previous work, labelling experiments revealed a mechanism consisting of two catalytic cycles: 1) reverse Water Gas-Shift Reaction (*r*WGSR) followed by an 2) hydroxycarbonylation cycle. The proposed catalytic cycle is shown in Figure 4-1.<sup>6</sup>

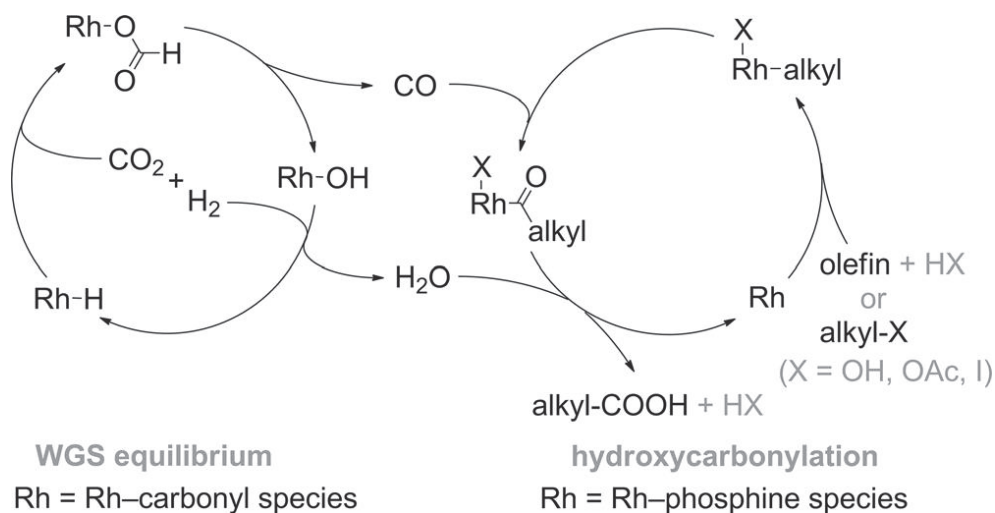
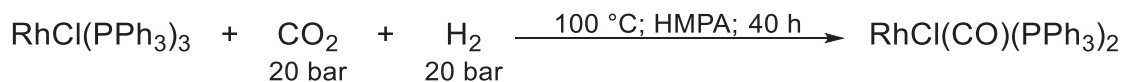


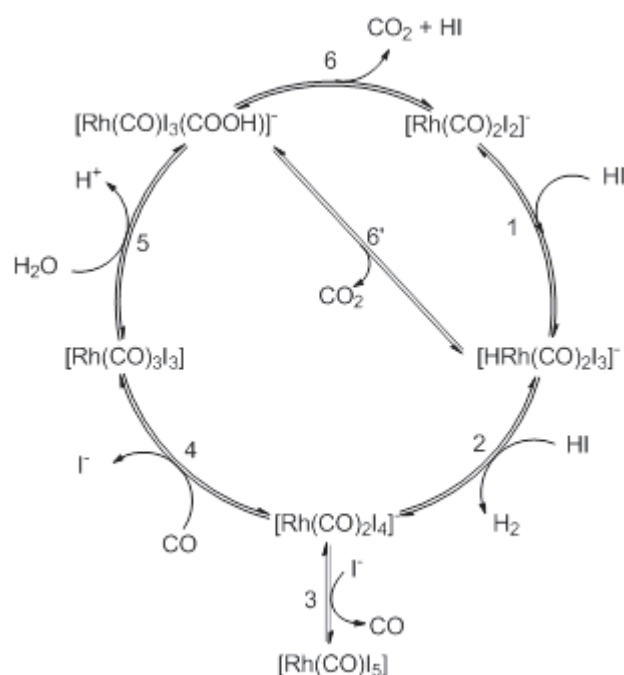
Figure 4-1: Mechanism of the overall hydrocarboxylation composed of catalytic cycles of the *r*WGSR equilibrium and hydroxycarbonylation.<sup>6</sup>

In this chapter, details about the catalytic cycles and the catalytic species for the corresponding hydrocarboxylation of alcohols will be reported.

[Rh] complexes with iodide additives and in acidic conditions are known to perform the reverse Water-Gas Shift Reaction (*r*WGSR),<sup>278</sup> to catalyze the Water-Gas Shift Reaction (WGSR),<sup>14</sup> the carbonylation of alcohols<sup>89, 244, 245</sup> and the hydroxycarbonylation of alkenes.<sup>13, 89, 246</sup> These systems inspired the development of the Rhodium homogeneous catalytic system reported in this thesis. For this reason, a small overview about them and the studied catalytic cycles are reported here.

Scheme 4-1: Scheme of the reaction of  $\text{RhCl}(\text{PPh}_3)_3$ ,  $\text{CO}_2$  and  $\text{H}_2$  reported by Hirai *et al.*

In 1975, Hirai and co-workers synthesized for the first time a Rh-carbonyl complex in presence of  $\text{CO}_2$  and  $\text{H}_2$ . Besides, they detected CO in the reaction mixture. Although the reaction is stoichiometric they demonstrated that Rh is able to activate  $\text{CO}_2$  and to produce CO from it (Scheme 4-1).<sup>278</sup>

Figure 4-2 Catalytic cycle of the WGSR reported by Baker *et al.*

In 1980, Baker, Hendriksen and Eisenberg reported about a Rh homogenous catalytic system which is able to transform  $\text{CO}$  and  $\text{H}_2\text{O}$  into  $\text{CO}_2$  and  $\text{H}_2$  (WGSR). The system requires acidic conditions and iodide as ligand for the (molecular) catalytic species. A detailed study of the influence of different parameters on the reaction is reported, as well as a proposed catalytic cycle (Figure 4-2). The catalytic cycle is composed of 6 steps: 1) oxidative addition of HI to the  $[\text{Rh}]$ ; 2) second addition of HI to  $[\text{Rh}]$  and production of  $\text{H}_2$ ; 3 or 4) depending on the amount of CO in the system there is an equilibrium between the  $\text{I}^-$  and the CO ligand which can leads to the step 3 or 4;

5) addition of  $\text{H}_2\text{O}$  and formation of the metallocarboxylic acid species; 6)  $\text{CO}_2$  and HI elimination regenerate the initial  $\text{Rh}^{\text{I}}$  species to start the cycle again; 6') only  $\text{CO}_2$  is eliminated and the cycle starts again from a  $\text{Rh}^{\text{III}}$  species. Their findings were also confirmed by the research carried on by the Monsanto group in the same period.<sup>253</sup> The reported studies identified different rate-limiting steps depending on the conditions. On one hand, at high temperature, high acid and iodide concentrations the elimination of  $\text{CO}_2$  and HI leading to the formation of the  $\text{Rh}^{\text{I}}$  species seems the rate-limiting step. On the other hand, at low temperature, low acid and iodide concentration the formation of  $\text{H}_2$  and the oxidation of  $\text{Rh}^{\text{I}}$  to  $\text{Rh}^{\text{III}}$  appears to be the slower step of the cycle.

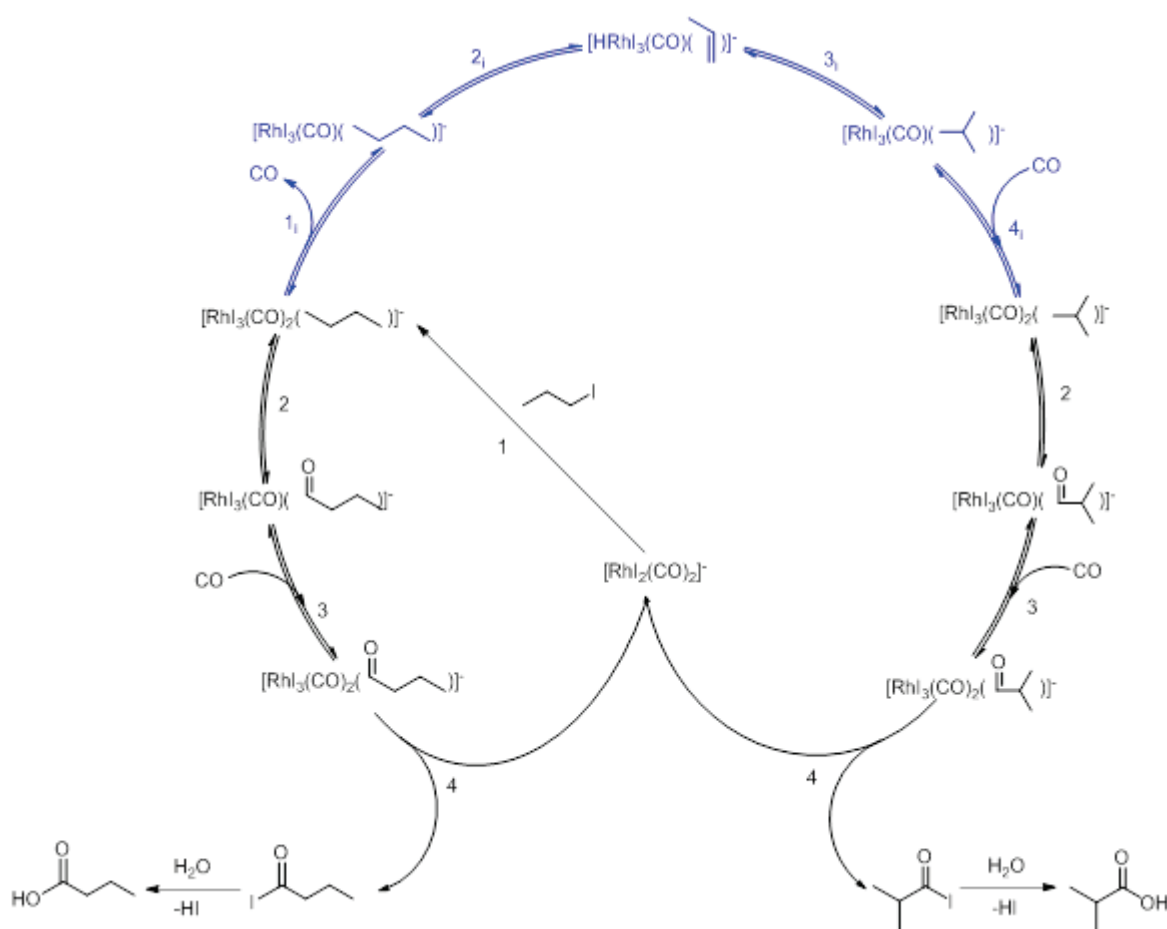


Figure 4-3: Catalytic cycle proposed by the Monsanto group for the carbonylation of primary alcohol in presence of  $[\text{Rh}]$  complex

The Monsanto catalytic system ( $[\text{Rh}]$ , Iodide, in acidic conditions) is known to catalyze the primary alcohol carbonylation in presence of  $\text{CO}$  and  $\text{H}_2\text{O}$ . The same group performed some studies on the catalytic cycle and on the factors, which

influence the system. They found that the rate of the reaction is dependent on both the concentration of [Rh] and R-I species, as for a  $S_N2$  reaction. They suggest that the first step is an oxidative addition of the R-I species to the complex  $[RhI_2(CO)_2]^-$ , as for the  $CH_3OH$  carbonylation. This explains the lower reaction rate observed for higher alcohols. Actually, the  $S_N2$  rate is decreasing with the increasing of the chain length, as well as the rate of the carbonylation. The full catalytic cycle is reported in Figure 4-3 and consists of 1) oxidative insertion of the primary iodide; 2) migratory insertion of CO; 3) coordination of a CO ligand to reform the hexa-coordinated complex; 4) reductive elimination of the acyl iodide; 5) nucleophilic substitution to give carboxylic acid. The isomerization can occur (blue part of the cycle): 1<sub>i</sub>) de-coordination of a CO ligand; 2<sub>i</sub>)  $\beta$ -hydride elimination to stabilize the complex; 3<sub>i</sub>) re-addition of the -H in a different position; 4<sub>i</sub>) coordination of a CO ligand to the complex to give a hexa-coordinated complex; steps 2-4 follow to give the iso-carboxylic acid. The mechanism explains also the influence of CO pressure on the selectivity in n- or iso- carboxylic acids. The lower the CO pressure, the higher is the possibility of de-coordination of one of the ligand leading to  $\beta$ -hydride elimination in order to stabilize the complex. In the case of higher alcohol carbonylation, linear and branched acids can be formed.

In 1994, the DuPont group reported a similar catalytic system (Rh complex and an alkyl iodide additive) which is active for both the carbonylation of alcohols (ethanol) and the hydroxycarbonylation of alkenes. They collected evidences regarding the mechanism and they suggested that the main pathway for the formation of the Rh-alkyl bond is the coordination of the alkene (step 2, Figure 4-4).<sup>89</sup> The mechanism they suggested is very similar to the one suggested from the Monsanto group for the hydroxycarbonylation of alkenes reported in Figure 4-4.

The carbonylation cycle for the carbonylation of secondary alcohols is suggested to differ from the one proposed for the carbonylation of primary alcohols. The kinetic is not comparable with the one of nucleophilic substitution: secondary alcohols react faster than they would if the kinetic would be the same.<sup>245</sup> Secondary alcohols were suggested to go through two different pathways.<sup>279</sup> The first suggested pathway is the dehydration of the alcohol in the reaction mixture and the coordination of the resulting alkene to the Rh center (Figure 4-4): 1) the  $[HRhL_2I_3]^-$  coordinate the alkene; 2) the complex is transformed into an alkyl-Rh species *via* migratory insertion of the alkene in the Rh-H bond; 3) CO coordination and migratory insertion into the Rh-alkyl bond; 4) reductive elimination of the acyl iodide; 5) regeneration of the  $Rh^{III}$  active species by

oxidative addition of the HI to the  $[\text{Rh}^{\text{I}}(\text{CO})_2\text{I}_2]^-$  complex; 6) the carboxylic acid is formed through a non-catalytic nucleophilic substitution of  $\text{H}_2\text{O}$  to the acyl iodide.

In the conditions reported by Dekleva and Forster, the control experiment using propene instead of 2-propanol lead to a different selectivity. Starting from propene, the reaction leads mainly to the *n*-butyric acid (as from 1-propanol), while using 2-propanol as substrate mainly iso-butyric acid was produced. For this reason, they suggested a pathway where an *in-situ* formed secondary-halide is generating a radical species which is coordinating to the Rh center. This second mechanism was never confirmed, but only suggested based on the discrepancy found with all the other possible pathways.<sup>279</sup>

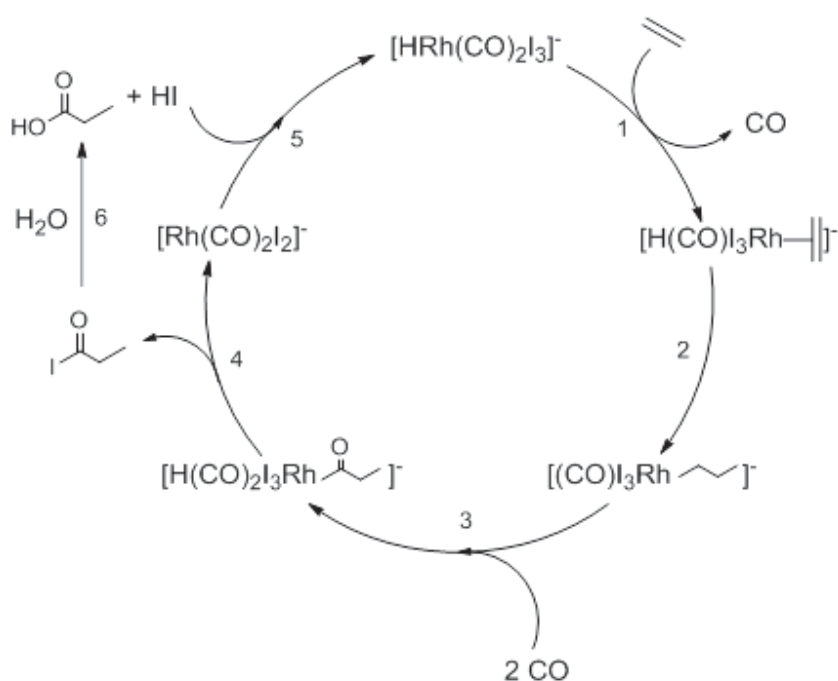


Figure 4-4: Catalytic cycle proposed by Forster and co-workers for the hydroxycarbonylation of alkenes.

The reaction of alkenes to carboxylic acids in presence of  $\text{CO}$  and  $\text{H}_2\text{O}$  was also studied by the Monsanto group.<sup>13</sup> The catalytic system again composed of a Rh precursor and an alkyl iodide as additive. They performed labelling and control experiments to conclude that the main pathway changes over time. At the beginning, the coordination of the *in-situ* formed alkyl iodide to the Rh center is the main pathway which leads to the carboxylic acids. These initial cycles form HI and when the concentration of it is high enough the mechanism changes. Over time, the prevalent

mechanism is the coordination of the alkene/HI to the Rh species. The suggested mechanism and catalytic active species are very similar to the one reported by the DuPont researchers and it is shown in Figure 4-4. Recently, a similar system was investigated by Choi and co-workers.<sup>280</sup> Starting from formic acid, they performed the hydroxycarbonylation of cyclohexene with a catalytic system composed of a Rh precursor, CH<sub>3</sub>I and PPh<sub>3</sub>. Formic acid is known to decompose to CO and H<sub>2</sub>O. They proposed a mechanistic cycle based on computational studies and supported by experimental evidences. They also suggest that at the beginning the main pathway is the coordination of the alkyl iodide. Once HI is formed *in situ*, the coordination of the alkene becomes the main reaction pathway.<sup>280</sup>

Herein, the study of the mechanism was performed dividing it into three steps: a non-catalytic step and two catalytic steps. The non-catalytic part includes organic reactions which are important for the composition of the reaction mixture and therefore the following catalysis. The catalytic parts are a first RWGS cycle and the following hydroxycarbonylation. Linear C<sub>4</sub> alcohols were used for these further studies to obtain important information on the regio-selectivity. After collecting information regarding these steps separately, they were connected in order to draw a complete mechanism. During these studies, information regarding the catalytic active species were collected.



## 4.2 Non-catalytic step

The study of the organic species formed in the reaction conditions is necessary to the understanding of the reaction pathway and mechanism. Knowing which species are present in the reactor gives hints regarding the catalytic system used (Section 4.4).

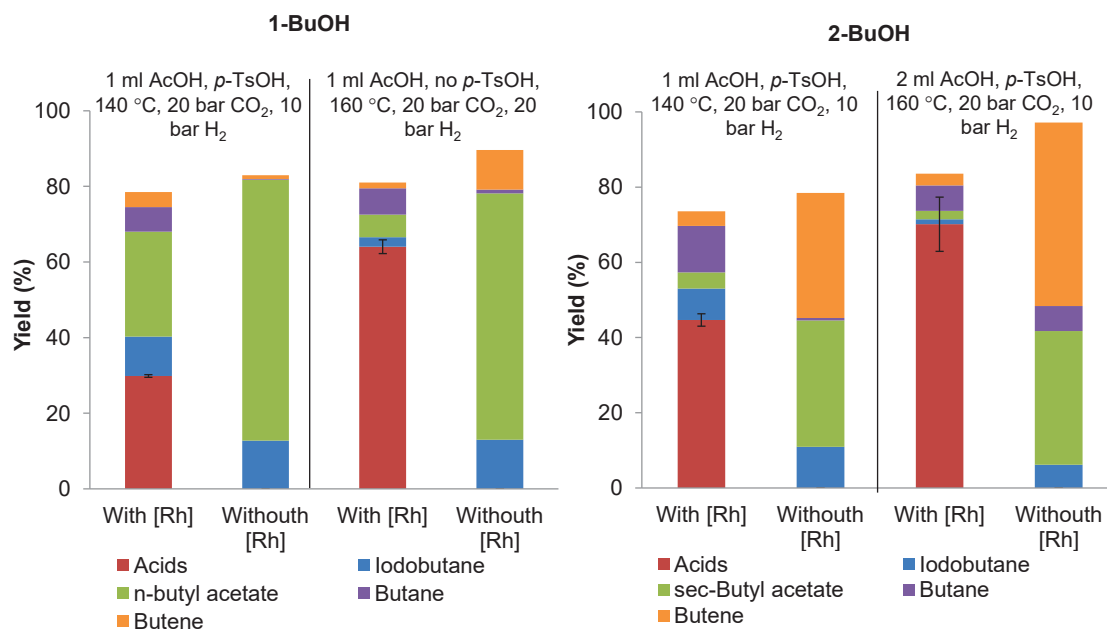


Figure 4-5: Comparison between the composition of the reaction mixture from the blank test and the results obtained with the catalyst for the preliminary conditions (left parts of the graphs) and the optimized conditions for primary alcohols (right parts of the graphs). The test was performed for both 1-BuOH (left graph) and 2-BuOH (right graph).

To study the organic reactions which happen in the reactor and which are not determined by the presence of the catalyst two set of conditions were used. The reaction conditions leading to the highest yield (reported in Chapter 3) are reported on the right side of the two graphs reported in Figure 4-5. The conditions used are: 0.235 mol of CHI<sub>3</sub>, 0.47 mol of PPh<sub>3</sub>, 1 mL of acetic acid (for 1-BuOH) and 2 mL of acetic acid (for 2-BuOH), 1.88 mmol of BuOH, 20 bar of CO<sub>2</sub>, 20 bar of H<sub>2</sub> (for 1-BuOH) and 10 bar of H<sub>2</sub> (for 2-BuOH), 160 °C and 16 hours. The reaction conditions used for the preliminary study (Chapter 3.1) are reported on the left side of the two graphs reported in Figure 4-5. The conditions used are: 0.235 mol of CHI<sub>3</sub>, 0.47 mol of PPh<sub>3</sub>, 1 mL of acetic acid, 1.88 mmol of BuOH, 20 bar of CO<sub>2</sub>, 10 bar of H<sub>2</sub>, 140 °C and 16 hours. The analysis of the reaction mixture in the absence of the catalyst (blank test, Figure 4-5) shows clearly that iodide, acetate, butene and small amounts of butane are formed

outside the catalytic cycle. Indeed, they are present whether or not the Rh catalyst is present. The traces of butane present in the reaction could be caused by the decomposition of the iodobutane.

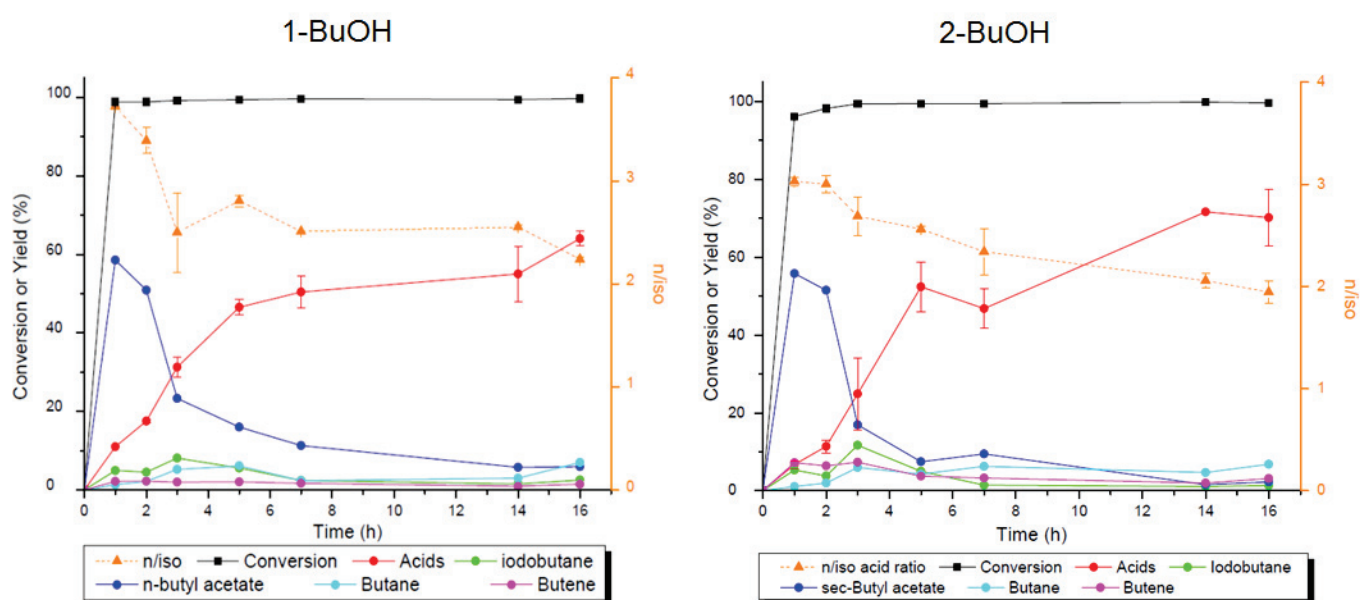
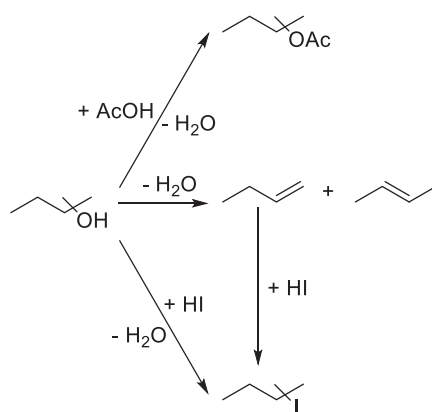


Figure 4-6: Time profile of the reaction of 1- BuOH (left) and 2-BuOH (right) to VA and 2-MBA. Standard reaction conditions: 1.88 mmol of BuOH, 92  $\mu\text{m}$  Rh, 1 mL (for 1-BuOH) or 2 mL (for 2-BuOH) of acetic acid, 2.5 mol/mol<sub>Rh</sub> of  $\text{CHI}_3$ , 5 mol/mol<sub>Rh</sub> of  $\text{PPh}_3$ , 3.5 mol/mol<sub>Rh</sub>  $p\text{-TsOH}\cdot\text{H}_2\text{O}$  (only for 2-BuOH), 20 bar  $\text{CO}_2$ , 10 (for 2-BuOH) or 20 (for 1-BuOH) bar  $\text{H}_2$ , 160  $^\circ\text{C}$ .

Interestingly, the alcohol is fully converted into these products even in the absence of the catalyst (Figure 4-5). These compounds are present also in the reaction mixture when the [Rh] is present (Figure 4-6 shows the time related yields obtained from 1-BuOH and for 2-BuOH). From this information, a brief summary of the reactions which do not need the [Rh] to happen is reported in Scheme 4-2.



Scheme 4-2: Scheme of the transformations observed even without the catalyst. From the top to the bottom: esterification (top), dehydration (middle) and nucleophilic substitution of –OH with –I (bottom).

### 4.3 Reverse Water Gas shift

The first catalytic step of the reaction is the transformation of CO<sub>2</sub> and H<sub>2</sub> into CO and H<sub>2</sub>O. Herein, a quantitative analysis of the rWGSR is reported. This allowed the investigation of the influence of the CHI<sub>3</sub> and PPh<sub>3</sub> additives and the influence of the precursor oxidation state on this step.

The rWGSR was tested using the optimized conditions for either primary or secondary alcohols. The resulting gas phase was collected quantitatively in a gas bag and analyzed by GC. The same experiments were carried out in the absence of the catalyst and in the absence of CO<sub>2</sub>. These tests confirmed that the CO is obtained from the Rh catalyzed CO<sub>2</sub> reduction (Table 4-1).

Table 4-1: rWGSR activity in different reaction conditions.

$\text{CO}_2 + \text{H}_2 \xrightleftharpoons{[\text{Rh}]} \text{CO} + \text{H}_2\text{O}$			
Conditions	Yield of CO with [Rh] (%)	Yield of CO without [Rh] (%)	Yield of CO without CO <sub>2</sub> (%)
Primary alcohols <sup>[a]</sup>	3.1 <sup>[c]</sup>	0.8	0.2
Secondary alcohols <sup>[b]</sup>	2.6 <sup>[d]</sup>	0.1	0.3

[a] Reaction conditions: 92 μmol Rh, 1 ml of acetic acid, 2.5 mol/mol<sub>Rh</sub> of CHI<sub>3</sub>, 5 mol/mol<sub>Rh</sub> of PPh<sub>3</sub>, 20 bar CO<sub>2</sub>, 20 bar H<sub>2</sub>, 160 °C, 16 h. [b] Standard reaction conditions: 92 μmol Rh, 2 ml of acetic acid, 3.5 mol/mol<sub>Rh</sub> *p*-TsOH·H<sub>2</sub>O, 2.5 mol/mol<sub>Rh</sub> of CHI<sub>3</sub>, 5 mol/mol<sub>Rh</sub> of PPh<sub>3</sub>, 20 bar CO<sub>2</sub>, 10 bar H<sub>2</sub>, 160 °C, 16 h. [c] Corresponding amount of CO: 0.7 mmol. [d] Corresponding amount of CO 0.6 mmol. Every result was reproduced at least twice. The maximum error obtained was of ±0.51%. Yields were calculated on the total amount of CO<sub>2</sub> pressurized in the reactor (22.7 mmol).

The Rh system catalyzes the rWGSR, with good yields (up to 3.1%) considering the mild temperature and pressure used (160 °C, 20 bar of CO<sub>2</sub> and 10 or 20 bar of H<sub>2</sub>). This amount of CO corresponds to almost 2 bar, according to the ideal gas law:

$$p = \frac{nRT}{V} = \frac{0.7 \cdot 10^{-3} \text{ mol} \cdot 0.0834 \text{ l bar mol}^{-1} \text{ K}^{-1} \cdot 298 \text{ K}}{0.01 \text{ l}} = 1.75 \text{ bar}$$

Unfortunately, thermodynamic parameters on similar systems are not reported in literature. Hence, it is not possible to compare the results with a thermodynamic limit.

Afterwards, the effect of different amounts of  $\text{CHI}_3$  on the *r*WGSR was investigated (Figure 4-7). The effect of the  $\text{CHI}_3$  seems to be the same, regardless the reaction conditions applied. The iodide additive is required in order to have the desired activity which allows producing CO. At the same time, high amount of  $\text{CHI}_3$  causes a deactivation of the catalyst. These observations are reported in literature about the use of a very similar catalytic system (Rh in acidic media with  $\text{I}^-$  additive) to promote the Water-Gas Shift reaction (WGSR).<sup>14</sup> We can draw a parallel with it thanks to the principle of microscopic reversibility.<sup>104</sup> The inactivity observed in the absence of  $\text{I}^-$  is probably due to the importance of this ligand for the catalytic active species. On the other side, the reduced activity observed at high  $\text{I}^-$  concentration can be linked to the formation of inactive Rh species.

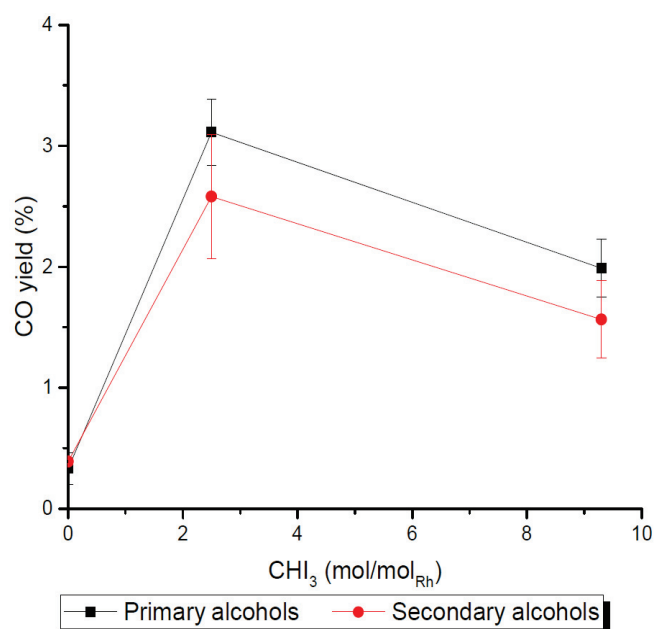


Figure 4-7: Influence of different amount of  $\text{CHI}_3$  on the CO yield using the optimized conditions for primary alcohols and secondary alcohols.

$\text{PPh}_3$  has a small effect on the *r*WGSR (Figure 4-8). The lack of phosphine only slightly influences the rate at which CO is produced. No significant decreases of yield are observed when  $\text{PPh}_3$  is not used. On the other side, an excess of  $\text{PPh}_3$  has a negative influence on the amount of CO produced in the cases of primary and secondary alcohols conditions. Indeed, an excess of ligand may result in a deactivation of the catalyst by saturation of the active species. A similar behavior was observed by

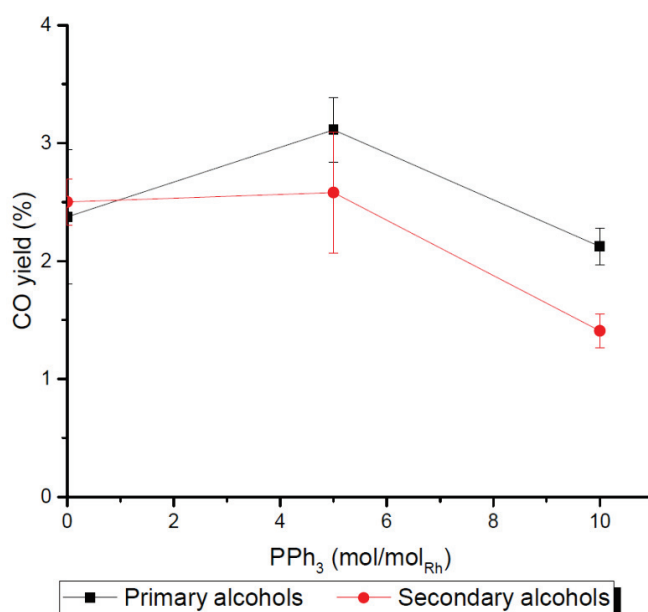


Figure 4-8: Influence of different amount of PPh<sub>3</sub> on the CO yield using the optimized conditions for primary alcohols and secondary alcohols.

Baker *et al.* in the Rh system catalyzing the WGSR: in that case the excess of CO in some conditions resulted in a lower activity.<sup>14</sup>

The other parameter which clearly has an influence on the catalytic system is the Rh precursor. As reported in Chapter 3.3.1 and 0, Rh<sup>III</sup>I<sub>3</sub> is not a good precursor for the reaction, while [RhCl(CO)<sub>2</sub>]<sub>2</sub> allows to obtain good yields. In particular, the use of the Rh<sup>III</sup> precursor has a particularly negative effect on the *r*WGSR step (Table 4-2)

Table 4-2: Influence of the Rh precursor oxidation state on the *r*WGSR.

Catalyst	Alcohol	CO yield (%) <sup>[a]</sup>
[RhCl(CO) <sub>2</sub> ] <sub>2</sub>	1-BuOH	3.1
	2-BuOH	2.6
RhI <sub>3</sub>	1-BuOH	0.9
	2-BuOH	0.5

Reaction conditions: 92 μmol Rh, 1 ml of acetic acid (1-BuOH) or 2 ml acetic acid (2-BuOH), 2.5 mol/mol<sub>Rh</sub> of CHI<sub>3</sub>, 5 mol/mol<sub>Rh</sub> of PPh<sub>3</sub>, 3.5 mol/mol<sub>Rh</sub> of *p*-TsOH·H<sub>2</sub>O (2-BuOH), 20 bar of H<sub>2</sub> (1-BuOH) or 10 bar of H<sub>2</sub> (2-BuOH), 20 bar of CO<sub>2</sub>, 160 °C, 16 h.

## 4.4 Hydroxycarbonylation step

The production of carboxylic acids is obtained *via* a second catalytic step, in which CO and H<sub>2</sub>O are added to the organic substrate. In the case of alcohols, this transformation is usually named carbonylation, since only CO is formally inserted in the product. Because we need CO and H<sub>2</sub>O to perform this transformation, we refer to it as hydroxycarbonylation.

Labeled <sup>13</sup>C<sup>18</sup>O was used to prove that CO is incorporated in the product faster than the CO<sub>2</sub>, if both gases are present in the autoclaves. The competitive experiment was performed using cyclohexanol, 1-BuOH and 2-BuOH as substrates in their corresponding optimized conditions. The gas mixture was formed by CO<sub>2</sub>, H<sub>2</sub> and <sup>13</sup>C<sup>18</sup>O (2 bar). In addition, H<sub>2</sub>O was added in the autoclave in an amount corresponding to the amount of <sup>13</sup>C<sup>18</sup>O used (12 μl).

The same reaction mixture was analyzed by quantitative <sup>13</sup>C-NMR and GC-MS. The reaction was analyzed after 2h and after 16h. The amount of CO is not enough to reach the yield usually obtained in carboxylic acids (65-80 % depending on the substrate), therefore both CO<sub>2</sub> and CO must be converted in order to obtain the final amount of carboxylic acids (after 16h). The GC-MS shows that both <sup>12</sup>C and <sup>13</sup>C are present in the product already after 2 h of reaction. The <sup>13</sup>C-NMR obtained starting from cyclohexanol are reported in Figure 4-9 and the ratio between integrals is reported in Table 4-3. It is interesting to notice that the ratio between the integrals of the newly formed carbonyl group and another carbon of the chain does not change from 2 h to 16 h of reaction. This means that the <sup>13</sup>C<sup>18</sup>O is consumed already during the first hours of reaction even if it is present in very small amounts compared to the CO<sub>2</sub> (CO<sub>2</sub>: 20 bar, <sup>13</sup>C<sup>18</sup>O: 2 bar, <sup>13</sup>C<sup>18</sup>O:CO<sub>2</sub> ≈ 3:100) and confirms that the reaction is formed by two catalytic cycles. The second one is an hydroxycarbonylation which leads to carboxylic acids through CO incorporation. CO<sub>2</sub> is probably incorporated only after its conversion to CO, explaining why <sup>13</sup>C<sup>18</sup>O is incorporated already after 2 h of reaction, even if CO<sub>2</sub> is present in large excess.

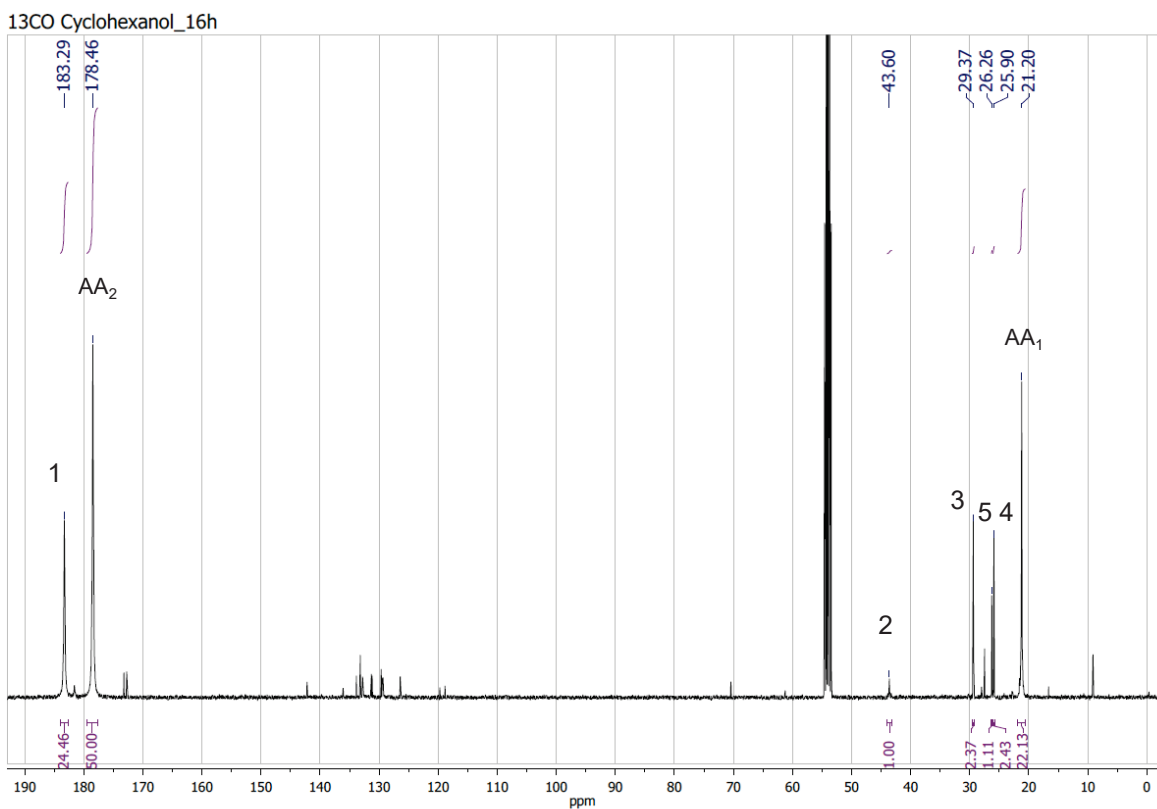
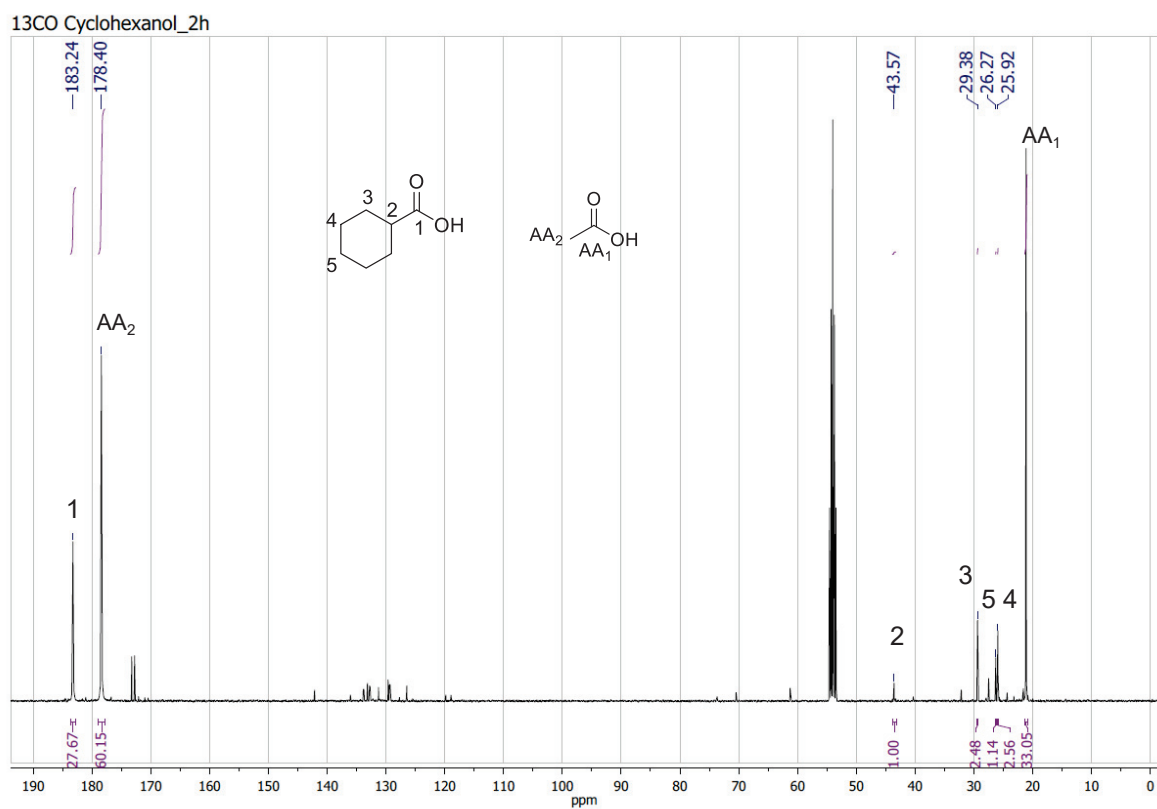


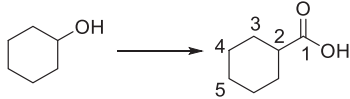
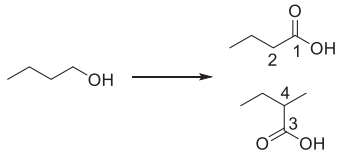
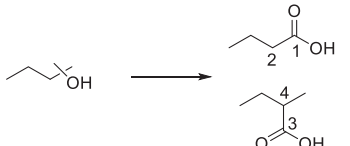
Figure 4-9: <sup>13</sup>C-NMR of the reaction mixture obtained from cyclohexanol, <sup>13</sup>CO (2 bar), H<sub>2</sub>O (12 μl), CO<sub>2</sub> (20 bar) and H<sub>2</sub> (10 bar) after 2h (top) and 16 h (bottom). The other reaction conditions were the optimized one for secondary alcohols: 1.88 mmol of substrate, 46 μmol [RhCl(CO)<sub>2</sub>]<sub>2</sub>, 2 ml of acetic acid, 2.5 mol/mol<sub>Rh</sub> of CHI<sub>3</sub>, 5 mol/mol<sub>Rh</sub> of PPh<sub>3</sub>, 3.5 mol/mol<sub>Rh</sub>, *p*-TsOH·H<sub>2</sub>O



The same experiment was conducted using linear alcohols (1-BuOH and 2-BuOH). In this case, due to isomerization processes, the  $^{13}\text{C}$ -NMR is more difficult to interpret. Nevertheless, through HMBC and HSQC the reference peaks of the products were assigned. Some of the assigned peaks result to be very small (low signal to noise ratio) and partially overlapped with other signals. For these reasons, the calculation of the integrals of these signals results not precise. The results are reported in Table 4-3 and the  $^{13}\text{C}$ -NMR of the reaction mixture obtained from the reaction of 2-BuOH is shown in Figure 4-10. A very similar spectra is obtained from the reaction of 1-BuOH. However, from the analysis of the NMR spectra the same conclusions obtained for cyclohexanol can be drawn. The  $^{13}\text{CO}$  is incorporated in the product already after 2 h of reaction time even if the amount is very low compared to  $\text{CO}_2$ , so it is preferentially used compared to  $\text{CO}_2$ . (Table 4-3) The reaction pathway proceeds preferentially through the hydroxycarbonylation rather than a direct hydrocarboxylation of the organic substrates.

In all cases, it is also interesting to notice that the acetic acid  $-\text{C}_{\text{AA}1}\text{OOH}$  group integral is higher compared to the integral of the methyl  $-\text{C}_{\text{AA}2}\text{H}_3$  group (as shown in Figure 4-7, Figure 4-8 and Table 4-3). In addition to that, it is clear that the incorporation of  $^{13}\text{CO}$  is happening during the first 2 h since the ratio is not changing over time ( $\text{AA}_1/\text{AA}_2 = 2$ ). The lower ratio observed for this acid compared to the other carboxylic acids shows that in this case the amount of  $^{13}\text{CO}$  incorporated is less relevant. This is probably because acetic acid is present in big quantities in the reaction mixture and the  $\text{CH}_3\text{-}^{13}\text{COOH}$  is most likely formed in small quantities. The  $\text{CH}_3\text{-}^{13}\text{COOH}$  can be formed by hydroxycarbonylation of  $\text{CHI}_3$ , which can be hydrogenated to  $\text{CH}_3\text{I}$  in presence of  $\text{H}_2$  and the Rh-catalyst. A test in propionic acid as solvent and without any substrate demonstrated the production of acetic acid. A second pathway which would lead to this product could be the de-carboxylation of the acetic acid to methanol which is further carbonylated to  $\text{CH}_3\text{-}^{13}\text{COOH}$ .

Table 4-3: Ratio between the integrals of the signals obtained in the  $^{13}\text{C}$ -NMR of the reaction mixtures obtained from the hydrocarboxylation ( $\text{CO}_2$  and  $\text{H}_2$ ) and hydroxycarbonylation ( $^{13}\text{CO}$  and  $\text{H}_2\text{O}$ ) of cyclohexanol, 1-BuOH and 2-BuOH. The ratio is obtained using the areas of the carboxyl carbons and the alkyl carbons as indicated in the table. The reaction conditions applied are the one reported in the Chapter 3 with the addition of  $^{13}\text{CO}$  (2 bar) and  $\text{H}_2\text{O}$  (12  $\mu\text{L}$ ). [a]  $\text{C}(\text{AA}_2)\text{H}_3 - \text{C}(\text{AA}_1)\text{OOH}$ :  $\text{AA}_1$  and  $\text{AA}_2$  refer to the carbon atoms of acetic acid.

Reaction	Reaction time	Area <sub>1</sub> /Area <sub>2</sub>	Area <sub>3</sub> /Area <sub>4</sub>	Area <sub>AA1</sub> /Area <sub>AA2</sub> <sup>[a]</sup>
	2h	27	-	2
	16h	24	-	2
	2h	78	168	2
	16h	90	102	4
	2h	38	41	2
	16h	25	34	2

Reaction conditions: 1.88 mmol of substrate, 46  $\mu\text{mol}$   $[\text{RhCl}(\text{CO})_2]_2$ , 2 ml of acetic acid, 2.5 mol/mol<sub>Rh</sub> of  $\text{CHI}_3$ , 5 mol/mol<sub>Rh</sub> of  $\text{PPh}_3$ , 3.5 mol/mol<sub>Rh</sub>, *p*-TsOH $\cdot$ H $_2\text{O}$  160  $^\circ\text{C}$ ,  $^{13}\text{CO}$  (2 bar),  $\text{H}_2\text{O}$  (12  $\mu\text{l}$ ),  $\text{CO}_2$  (20 bar) and  $\text{H}_2$  (10 bar for cyclohexanol and 2-BuOH and 20 bar for 1-BuOH).

The hydroxycarbonylation activity of the system was tested using the exact amount of CO detected in the previous *r*WGSR activity tests. The amount of  $\text{H}_2\text{O}$  was decided considering the ratio  $\text{CO}:\text{H}_2\text{O} = 1:1$ . A catalyst without CO as ligand ( $\text{Rh}_2(\text{OAc})_4$ ) was chosen in order to avoid any influence from external sources (reference value are reported in Section 3). The amount of substrate was consequently diminished to have the opportunity to reach full conversion. All the other reaction parameters were kept as in the optimized conditions for the total reactions. The results are reported in Table 4-4.

CHAPTER 4: MECHANISTIC INVESTIGATION AND REACTION PATHWAY

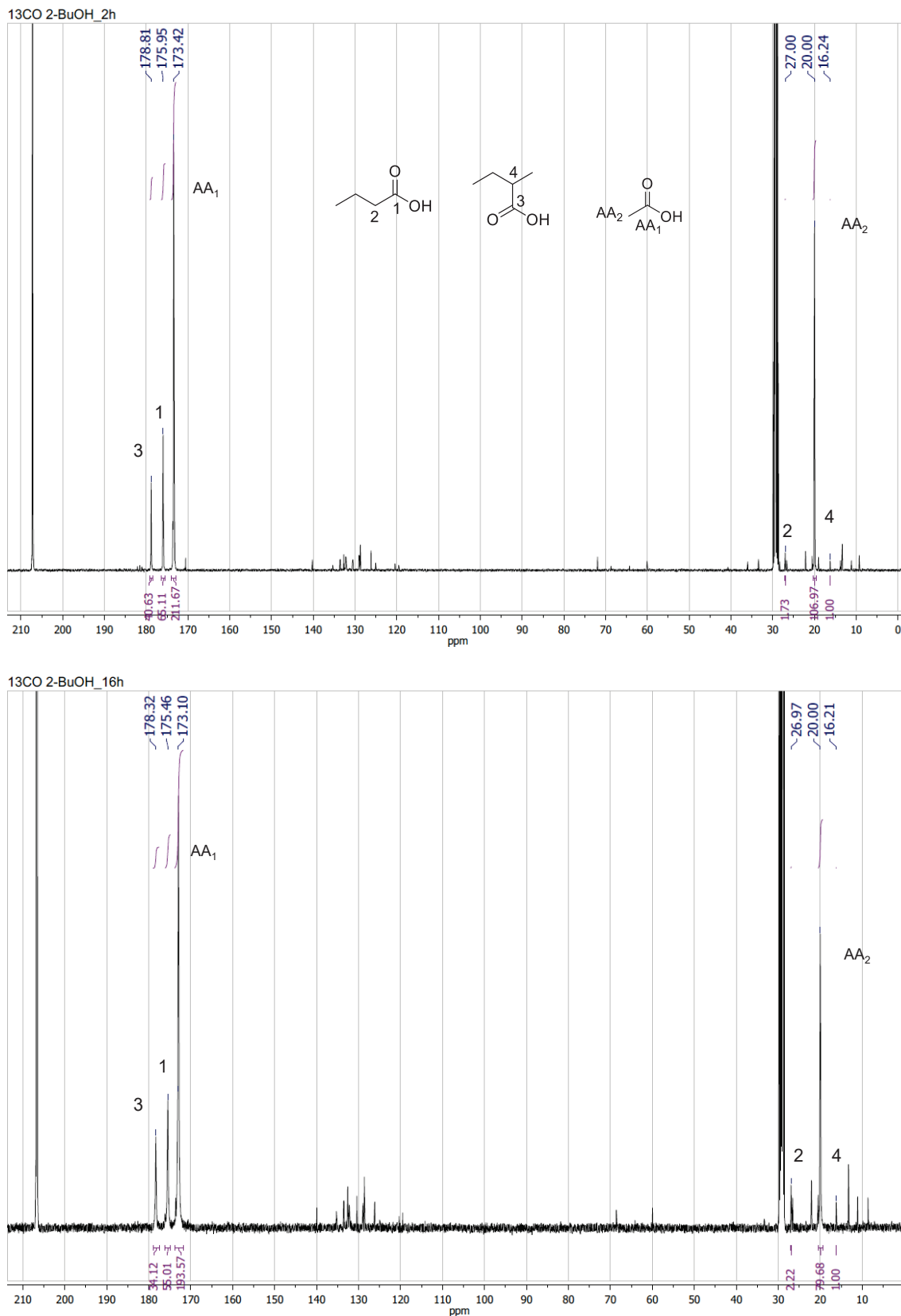
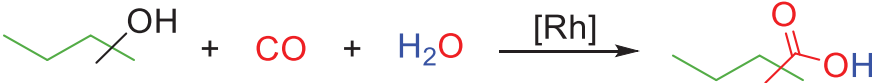


Figure 4-10:  $^{13}\text{C}$ -NMR of the reaction mixture obtained from 2-BuOH,  $^{13}\text{CO}$  (2 bar),  $\text{H}_2\text{O}$  (12  $\mu\text{l}$ ),  $\text{CO}_2$  (20 bar) and  $\text{H}_2$  (10 bar) after 2h (top) and 16 h (bottom). The other reaction conditions were the optimized one for secondary alcohols: 1.88 mmol of substrate, 46  $\mu\text{mol}$   $[\text{RhCl}(\text{CO})_2]_2$ , 2 ml of acetic acid, 2.5 mol/mol<sub>Rh</sub> of  $\text{CHI}_3$ , 5 mol/mol<sub>Rh</sub> of  $\text{PPh}_3$ , 3.5 mol/mol<sub>Rh</sub>,  $p\text{-TsOH}\cdot\text{H}_2\text{O}$  160

Table 4-4: Results of the controlling experiment carried out with CO and H<sub>2</sub>O compared to the standard reactions pressurized with CO<sub>2</sub> and H<sub>2</sub>.



Substrate	Hydroxycarbonylation experiment (CO + H <sub>2</sub> O)		Hydrocarboxylation experiment (CO <sub>2</sub> + H <sub>2</sub> )	
	Amount of CO and H <sub>2</sub> O <sup>[c]</sup> (mmol)	Yield in carboxylic acids (%)	Pressure of CO <sub>2</sub> and H <sub>2</sub> (bar)	Yield in carboxylic acids (%)
1-BuOH <sup>[a]</sup>	0.7	26	CO <sub>2</sub> : 20 H <sub>2</sub> : 20	29
2-BuOH <sup>[b]</sup>	0.6	49	CO <sub>2</sub> : 20 H <sub>2</sub> : 10	59

[a] Standard reaction conditions: 0.5 mmol of substrate, 46  $\mu$ mol Rh<sub>2</sub>(OAc)<sub>4</sub>, 1 ml of acetic acid, 2.5 mol/mol<sub>Rh</sub> of CHI<sub>3</sub>, 5 mol/mol<sub>Rh</sub> of PPh<sub>3</sub>, 160 °C, 16 h. [b] Standard reaction conditions: 0.5 mmol of substrate, 46  $\mu$ mol Rh<sub>2</sub>(OAc)<sub>4</sub>, 2 ml of acetic acid, 3.5 mol/mol<sub>Rh</sub> *p*-TsOH•H<sub>2</sub>O, 2.5 mol/mol<sub>Rh</sub> of CHI<sub>3</sub>, 5 mol/mol<sub>Rh</sub> of PPh<sub>3</sub>, 160 °C, 16 h. [c] The total pressure was adjusted with Ar in order to reach the same pressure normally obtained using CO<sub>2</sub> and H<sub>2</sub> (30 and 40 bar respectively for primary and secondary alcohols). Every result was reproduced at least twice. The maximum error obtained was of  $\pm$ 9%.

The system is active for the hydroxycarbonylation of alcohols even if CO and H<sub>2</sub>O are highly diluted (0.7 mmol, corresponding to 2 bar of CO). The use of higher amounts of CO and H<sub>2</sub>O leads to changes in the activity of the system. 8.2 bar of CO have an inhibiting effect (10% yield in carboxylic acids was obtained from 1-BuOH and 13% from 2-BuOH). In addition to that, the study of the regio-selectivity of the reaction (Table 4-5) further confirms that the conditions used for investigating this cycle are very similar to those obtained starting from CO<sub>2</sub> and H<sub>2</sub>. The reached activities using CO and H<sub>2</sub>O intermediates are very similar to that obtained starting from CO<sub>2</sub> and H<sub>2</sub>. As shown in Table 4-5 when 2 bar of CO are used, the selectivity is similar to the one obtained with CO<sub>2</sub> and H<sub>2</sub>. On the contrary, when 8.2 bar of CO are used to carry out the carbonylation step, selectivity is completely different and highly dependent on the starting alcohol isomer. When CO pressure is over 8 bar the preferred product is the one with the same regio-selectivity as the starting alcohol (Table 4-5).

Varying the amount of iodide additive on the hydroxycarbonylation step shows the comparable results already observed for the *r*WGS (Figure 4-12). This fact indicates

that the two catalytic systems are very similar to each other. Rh precursors with iodide additives in acetic media not only catalyze the WGSR but also the alcohol carbonylation and the alkene hydrocarboxylation. In all cases, iodide is a crucial ligand for the catalytic active species, but at the same time high quantity of HI in solution reacts with the active compound and forms an undesired species.<sup>13</sup>

Table 4-5: n/iso ratio obtained from 1-BuOH and 2-BuOH using different gases and pressure.

	CO <sub>2</sub> /H <sub>2</sub> (n/iso)	CO: 2 bar <sup>[c]</sup> (n/iso)	CO: 8.2 bar <sup>[c]</sup> (n/iso)
<b>1-BuOH<sup>[a]</sup></b>	2.1	1.9	4.5
<b>2-BuOH<sup>[b]</sup></b>	1.8	1.5	0.6

[a] Standard reaction conditions: 1.88 mmol of substrate, 46  $\mu$ m [RhCl(CO)<sub>2</sub>]<sub>2</sub>, 1 ml of acetic acid, 2.5 mol/mol<sub>Rh</sub> of CHI<sub>3</sub>, 5 mol/mol<sub>Rh</sub> of PPh<sub>3</sub>, 160 °C, 16 h. Total yield: CO<sub>2</sub>/H<sub>2</sub> = 29%, CO 2 bar: 26%, CO 8 bar: 10% [b] Standard reaction conditions: 1.88 mmol of substrate, 46  $\mu$ m [RhCl(CO)<sub>2</sub>]<sub>2</sub>, 2 ml of acetic acid, 3.5 mol/mol<sub>Rh</sub> *p*-TsOH•H<sub>2</sub>O, 2.5 mol/mol<sub>Rh</sub> of CHI<sub>3</sub>, 5 mol/mol<sub>Rh</sub> of PPh<sub>3</sub>, 160 °C, 16 h. Total yield: CO<sub>2</sub>/H<sub>2</sub> = 59%, CO 2 bar: 49%, CO 8 bar: 13% [c] The total pressure was adjusted with Ar in order to reach the same pressure normally obtained using CO<sub>2</sub> and H<sub>2</sub> (30 and 40 bar respectively for primary and secondary alcohols).

The same experiments can be performed varying the amount of PPh<sub>3</sub>. The variation of the amount of PPh<sub>3</sub> is reported in Figure 4-11. No significant difference in carboxylic acid yield is observed when using 0 or 5 mol/mol<sub>Rh</sub> of PPh<sub>3</sub>. The additional ligand is not required to obtain the desired product, as for the *r*WGSR. On the other hand, the maximum activity observed is obtained if 10 eq. of PPh<sub>3</sub> are added. Increasing the amount of phosphine to 20 eq. results in a decrease of activity, probably because it occupies the active site of the catalyst.

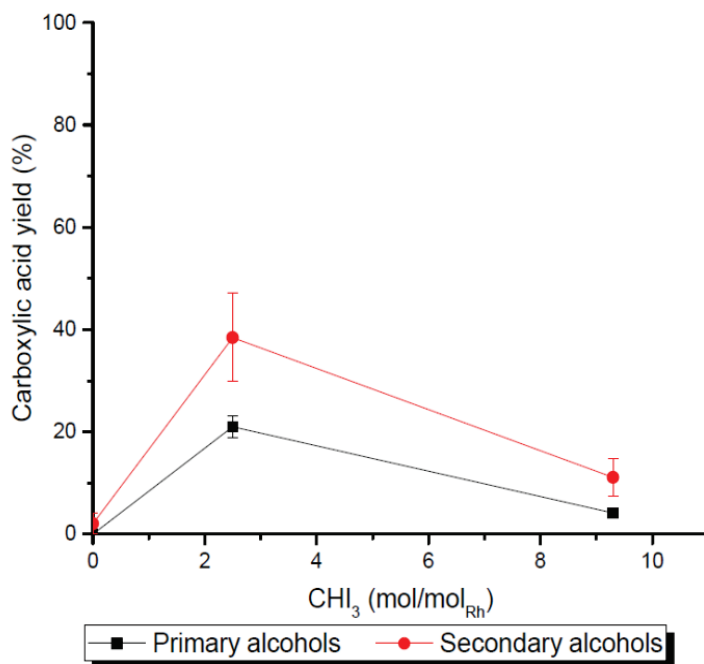


Figure 4-12: Influence of different amount of  $\text{CHI}_3$  on the carboxylic acids yield using the optimized conditions for primary alcohols and secondary alcohols. CO and  $\text{H}_2\text{O}$  were used instead of  $\text{CO}_2$  and  $\text{H}_2$  as explained above.

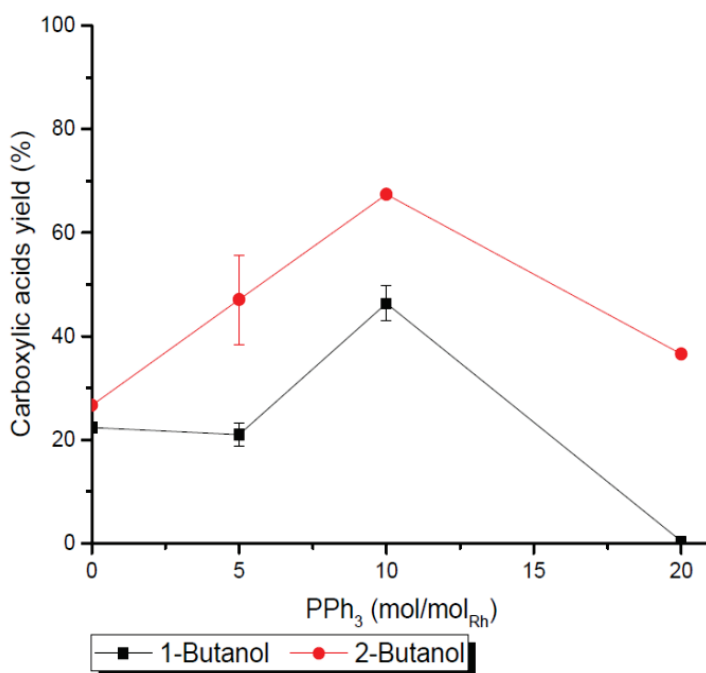


Figure 4-11: Influence of different amount of  $\text{PPh}_3$  on the carboxylic acids yield using the optimized conditions for primary alcohols, secondary alcohols. CO and  $\text{H}_2\text{O}$  were used instead of  $\text{CO}_2$  and  $\text{H}_2$  and the yields were calculated on a total amount of alcohol of 0.5 as explained above.

Table 4-6: Influence of the Rh precursor oxidation state on the hydroxycarbonylation.

Catalyst	Alcohol	Hydroxycarbonylation - VA and 2-MBA yield (%)
[RhCl(CO) <sub>2</sub> ] <sub>2</sub>	1-BuOH	21
	2-BuOH	38
RhI <sub>3</sub>	1-BuOH	15
	2-BuOH	53

Standard reaction conditions: 0.5 mmol of butanol, 92  $\mu$ mol Rh, 1 ml of acetic acid (1-BuOH) or 2 ml acetic acid (2-BuOH), 2.5 mol/mol<sub>Rh</sub> of CHI<sub>3</sub>, 5 mol/mol<sub>Rh</sub> of PPh<sub>3</sub>, 3.5 mol/mol<sub>Rh</sub> of *p*-TsOH·H<sub>2</sub>O (2-BuOH), 2 bar of CO, 160 °C, 16 h. The total pressure was adjusted with Ar in order to reach the same pressure normally obtained using CO<sub>2</sub> and H<sub>2</sub> (30 and 40 bar respectively for primary and secondary alcohols).

As reported in Chapter 3.3.1 and 3.4.1, Rh<sup>III</sup>I<sub>3</sub> is not a good precursor for the reaction, while [Rh<sup>I</sup>Cl(CO)<sub>2</sub>]<sub>2</sub> allows to obtain good yields. On the contrary, the hydroxycarbonylation activity is equally observed if Rh<sup>III</sup> precursor is used as a precursor (Table 4-6).

The synthesis of carboxylic acids starting from alcohols with a similar Rh catalytic system has been reported previously, especially by the Monsanto group. Two main pathways have been suggested/considered in the previous literature: one going through the oxidative addition of R-I to the Rh center<sup>253</sup> and the second one going through the coordination of the alkene and HI.<sup>279</sup> Starting from these findings and considering the similarities between the above mentioned systems and the one herein reported, more studies were performed with the aim to find evidences supporting one reaction pathway or the other.

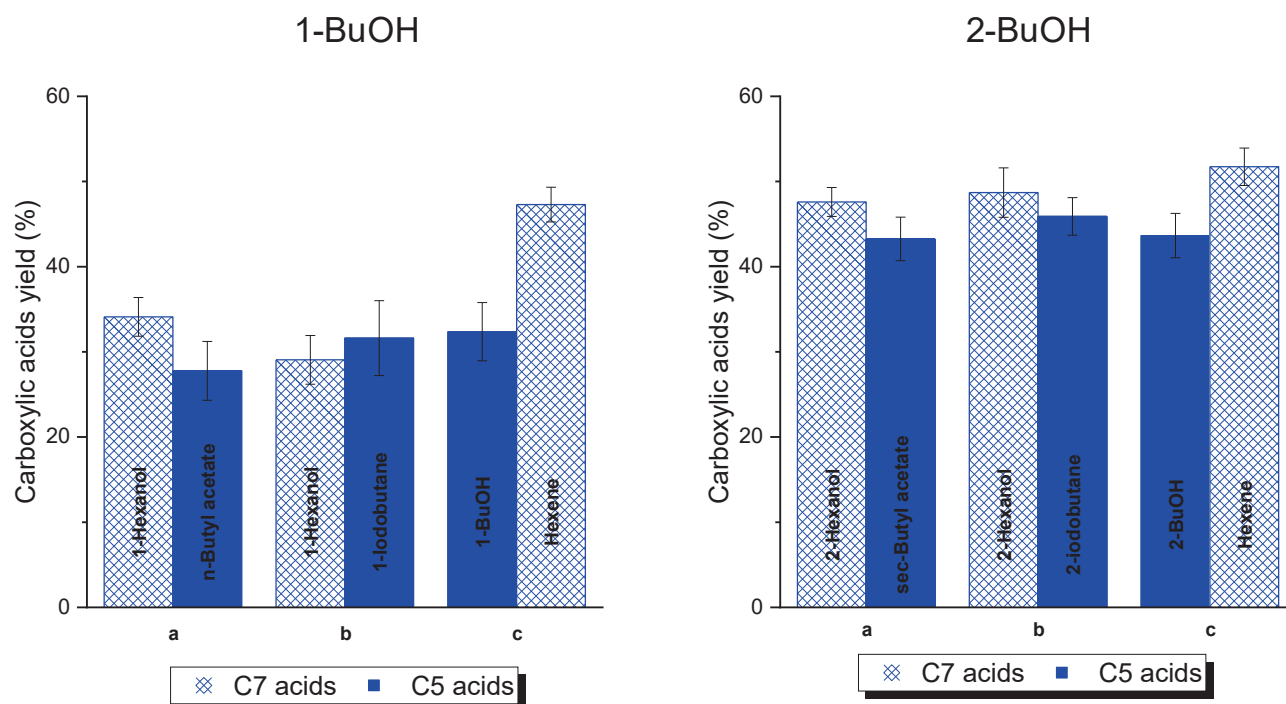


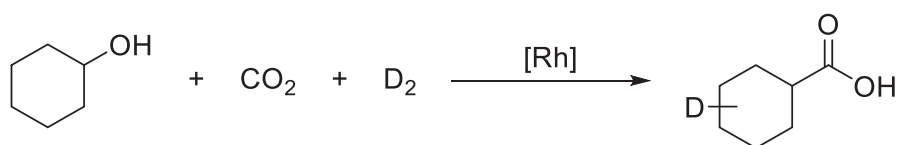
Figure 4-13: Left: Results obtained from the competitive reactions between primary alcohols and intermediates (primary acetate, primary iodide and alkene). Standard reaction conditions: 0.95 mmol of substrate C<sub>4</sub> and 0.95 mmol of substrate C<sub>6</sub>, 92  $\mu$ mol Rh, 1 ml of acetic acid, 2.5 mol/mol<sub>Rh</sub> of CHI<sub>3</sub> (if no other sources of iodide were used), 5 mol/mol<sub>Rh</sub> of PPh<sub>3</sub>, 20 bar CO<sub>2</sub>, 20 bar H<sub>2</sub>, 160 °C, 3h. Right: Results obtained from the competitive reactions between secondary alcohols and intermediates (secondary acetate, secondary iodide and alkene). Standard reaction conditions: 0.95 mmol of substrate C<sub>4</sub> and 0.95 mmol of substrate C<sub>6</sub>, 92  $\mu$ mol Rh, 2 ml of acetic acid, 2.5 mol/mol<sub>Rh</sub> of CHI<sub>3</sub> (if no other sources of iodide were used), 5 mol/mol<sub>Rh</sub> of PPh<sub>3</sub>, 3.5 mol/mol<sub>Rh</sub> *p*-TsOH·H<sub>2</sub>O, 20 bar CO<sub>2</sub>, 10 bar H<sub>2</sub>, 160 °C, 3h.

From the analysis of the reaction mixture at different reaction time some considerations helping the understanding of the hydroxycarbonylation mechanism can be made. The conversion of the alcohol is almost complete after 1 hour. Butene, iodobutane and butyl acetate are increasing at the beginning and then decreasing. This behavior could mean they are intermediates or reservoirs for the reaction. (Figure 4-6 shows the time related yields obtained from 1-BuOH, while Figure 4-6 shows the same for 2-BuOH). For this reason, competitive reactions were performed. Two substrates with different chain length were used to perform the reactions (Figure 4-13 left for 1-BuOH and Figure 4-13 right for 2-BuOH). The alcohol reactivity was compared with the



reactivity of acetate, iodide and alkene. The acetate does not appear to be an intermediate for the reaction, since it does not react faster than the alcohol. On the contrary, the potential intermediates, the iodide and the alkene react faster than the alcohol. For this reason, a deeper investigation on the role of alkene and iodide in the reaction was performed. To do so, the reactivity of these two compounds during the first 5 hours of reaction was studied (Figure 4-14). The results show how 1-iodobutane and 1-hexene have the same reactivity after 1 h, but the 1-hexene reacts faster already after 3 h. Moreover, the *n*/*iso* selectivity obtained from alkene is comparable to the one obtained from alcohol (around 2), while the one obtained from the 1-iodobutane is similar to the *n*/*iso* ratio observed during the first 2 h of reaction (Figure 4-6). These observations suggest that the transformation pathway changes over time: during the first hours the alkyl-iodide oxidative addition to the metal center is favored over the alkene-HI coordination. The initial cycles produce HI, and when the concentration is high enough, the coordination of alkene becomes the fastest and preferred reaction pathway.

To confirm the theory that the key intermediate coordinating with the Rh catalyst is the alkene, labelling experiment with D<sub>2</sub> (according to the Scheme 4-3) were performed and compared with the results obtained starting from alkenes. The deuterium is incorporated in the product with a pattern similar to the one reported by our group for the same product obtained from the corresponding alkene<sup>6</sup> (<sup>2</sup>H-NMR is reported in Figure 4-15). The nature of this finding is obvious considering that alkene can undergo a β-hydride elimination – reinsertion process.



Scheme 4-3: Reaction scheme of the hydrocarboxylation reaction of cyclohexanol performed using D<sub>2</sub> instead of H<sub>2</sub>. Reaction conditions: 1.88 mmol of substrate, 46 μmol [RhCl(CO)<sub>2</sub>]<sub>2</sub>, 2 ml of acetic acid, 2.5 mol/mol<sub>Rh</sub> of CHI<sub>3</sub>, 5 mol/mol<sub>Rh</sub> of PPh<sub>3</sub>, 3.5 mol/mol<sub>Rh</sub>, *p*-TsOH•H<sub>2</sub>O 160 °C, CO<sub>2</sub> (20 bar) and D<sub>2</sub> (10 bar).

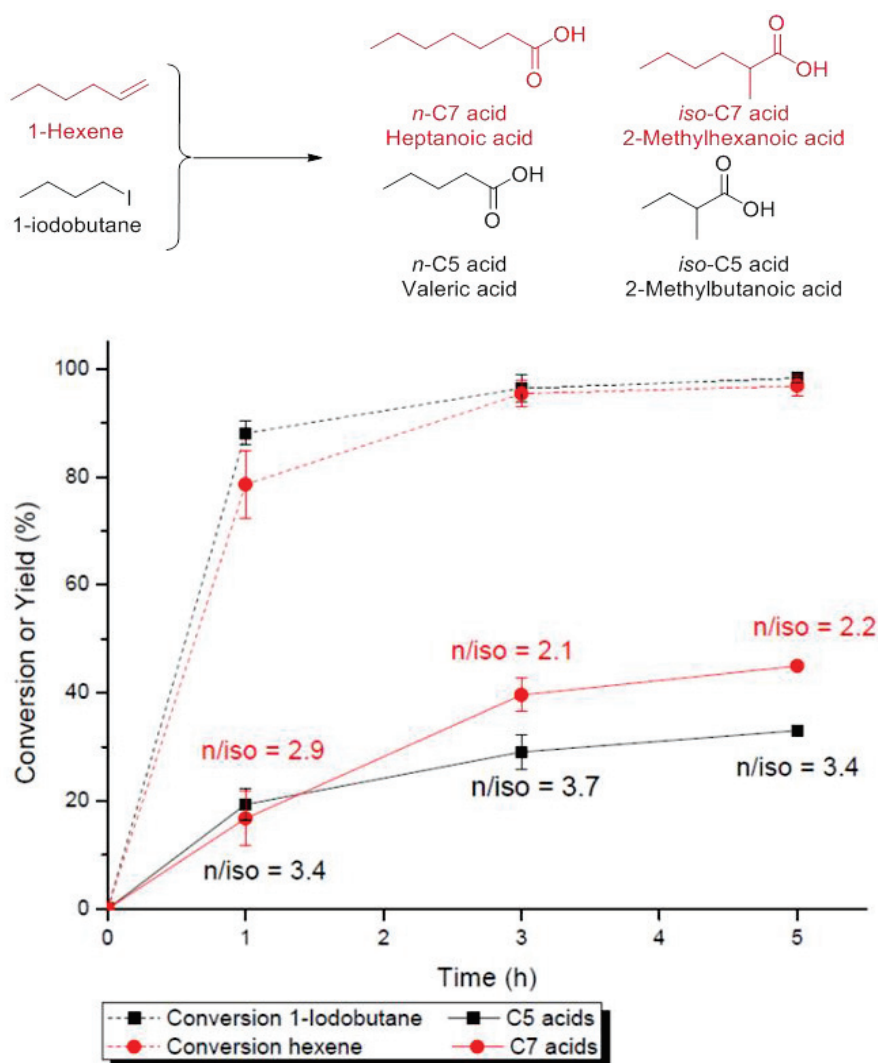


Figure 4-14: Competitive reactions between 1-hexene and 1-iodobutane over the first 5h of reaction. Standard reaction conditions: 0.95 mmol of 1-iodobutane and 0.95 mmol of 1-hexene, 92  $\mu\text{mol}$  Rh, 1 ml of acetic acid, 5 mol/mol<sub>Rh</sub> of PPh<sub>3</sub>, 20 bar CO<sub>2</sub>, 20 bar H<sub>2</sub>, 160 °C. In the reported graph, only the yield in carboxylic acids and the conversions are reported. Nevertheless, acetates, alkene, iodide and alkane are detected as by-products.

The comparison with the secondary alcohol provides further hints which support this mechanism (competitive experiments are reported in Figure 4-16). In that case, 2-iodobutane was used as source of iodide. No reaction is observed until it eliminates HI, producing 1-iodobutane and alkene (after 3h) as shown in the Figure 4-16.

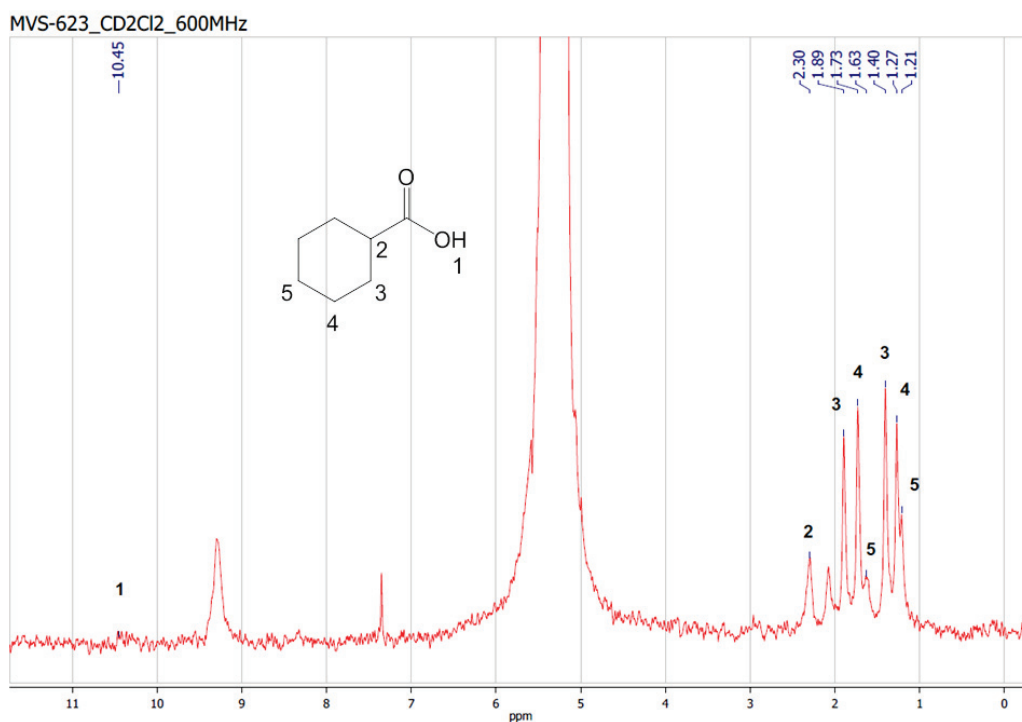


Figure 4-15:  $^2\text{H}$  NMR spectrum of the reaction mixture after the catalysis with signals for the cyclohexanoic acid product (CA). Measured in  $\text{CD}_2\text{Cl}_2$  at ambient temperature with a resonance frequency of 600 Mhz. Reaction conditions: 1.88 mmol of substrate, 46  $\mu\text{mol}$   $[\text{RhCl}(\text{CO})_2]_2$ , 2 ml of acetic acid, 2.5 mol/mol<sub>Rh</sub> of  $\text{CHI}_3$ , 5 mol/mol<sub>Rh</sub> of  $\text{PPh}_3$ , 3.5 mol/mol<sub>Rh</sub>,  $p\text{-TsOH}\cdot\text{H}_2\text{O}$  160 °C,  $\text{CO}_2$  (20 bar) and  $\text{D}_2$  (10 bar).

This can easily be explained thinking about oxidative addition as a nucleophilic substitution, where the rate is dependent on the type of iodide: secondary iodides react slower compared to the corresponding primary. Moreover, the longer the carbon chain the slower the attack, explaining why the use of  $\text{CHI}_3$  or  $\text{CH}_3\text{I}$  is preferred to the use of more hindered alkyl-iodide compounds or other iodide additives.<sup>6, 79</sup>

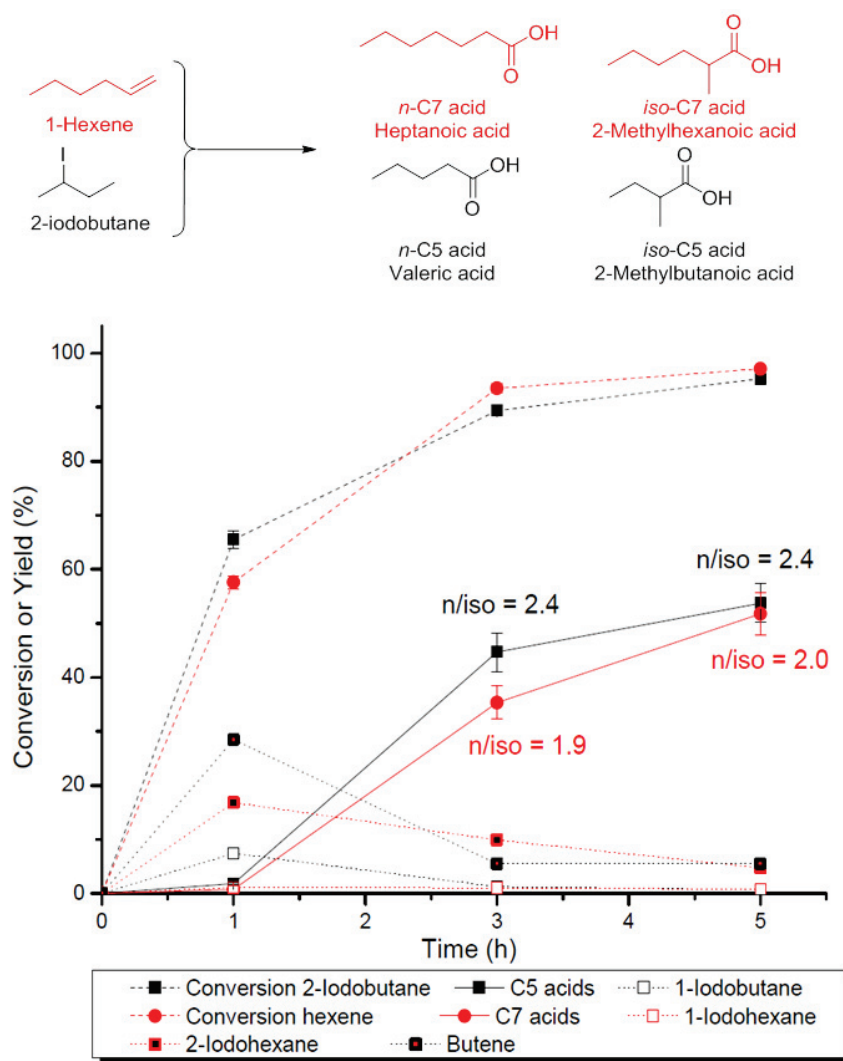
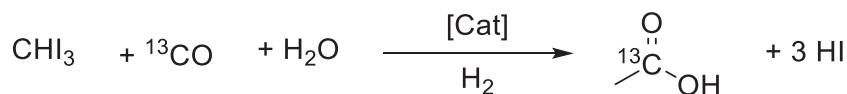


Figure 4-16: Competitive reactions between 1-hexene and 2-iodobutane over the first 5h of reaction. Standard reaction conditions: 0.95 mmol of 2-iodobutane and 0.95 mmol of 1-hexene, 92  $\mu\text{mol}$  Rh, 1 ml of acetic acid, 5 mol/mol<sub>Rh</sub> of PPh<sub>3</sub>, 20 bar CO<sub>2</sub>, 20 bar H<sub>2</sub>, 160 °C.

These results are also consistent with the production rate of carboxylic acids observed during the first 5 h. A lower initial activity is observed when 2-BuOH is used as substrate. At the beginning, CHI<sub>3</sub> reacts much faster than 2-iodobutane, therefore no desired product is detected until enough HI is produced to allow the coordination of the alkene to the Rh center. Starting from 1-BuOH, during the first 5 hours the rate of the production of carboxylic acids is constant, showing no induction period (Figure 4-6). After this initial time, the activity of the catalyst is decreasing leading to a slower production rate of carboxylic acids. This hypothesis can also explain the incorporation of <sup>13</sup>C in the carboxyl group of acetic acid (Figure 4-9, Figure 4-10 and Table 4-3).

$\text{CHI}_3$  is involved in the hydroxycarbonylation step at the beginning as the other iodide giving the corresponding carboxylic acid (Scheme 4-4).



Scheme 4-4: Reaction of  $\text{CHI}_3$  with  $\text{CO}$  and  $\text{H}_2\text{O}$  leading to acetic acid, in presence of Rh catalytic system and  $\text{H}_2$ . Reaction conditions: 1.88 mmol of substrate, 46  $\mu\text{mol}$   $[\text{RhCl}(\text{CO})_2]_2$ , 2 ml of acetic acid, 2.5 mol/mol<sub>Rh</sub> of  $\text{CHI}_3$ , 5 mol/mol<sub>Rh</sub> of  $\text{PPh}_3$ , 3.5 mol/mol<sub>Rh</sub>, *p*-TsOH· $\text{H}_2\text{O}$  160 °C,  ${}^{13}\text{CO}$  (2 bar),  $\text{H}_2\text{O}$  (12  $\mu\text{l}$ ),  $\text{CO}_2$  (20 bar) and  $\text{H}_2$  (10 bar for cyclohexanol and 2-BuOH and 20 bar for 1-BuOH).

To further support this mechanism, the blank test obtained in the non-optimized reaction conditions (0.235 mol of  $\text{CHI}_3$ , 0.47 mol of  $\text{PPh}_3$ , 1 mL of acetic acid, 1.88 mmol of BuOH, 20 bar of  $\text{CO}_2$ , 10 bar of  $\text{H}_2$ , 140 °C and 16 hours) was compared with the one obtained with the respective optimized reaction conditions. As the Figure 4-5 shows, when higher amounts of desired carboxylic acids are obtained, higher amounts of alkenes are produced. Starting from 2-BuOH, alkenes are produced from acetate, alcohol and iodide. Starting from 1-BuOH, the iodide is required to observe alkenes. In all cases, the substitution of the  $-\text{OH}$  group of the alcohols with a better leaving group ( $-\text{I}$ ) favors the production of alkenes.

All the reported observations regarding the influence of the additives and the competitive reactions fit with the mechanism observed by Forster *et al.* (1981) reported in Figure 4-4 with a similar system which catalyzes the alkene hydrocarboxylation.<sup>13</sup> This mechanism involves the alkene coordination to the Rh center as first step. A mechanism of this type would explain why methanol does not react as well as all the other simple alcohols. Since the formation of the corresponding alkene is not possible, a lower selectivity toward acetic acid is observed, while the major product is  $\text{CH}_4$  (>45%). Besides, this mechanism explains why primary and secondary alcohols require different reaction conditions. Indeed, the formation of alkenes from alcohols is highly dependent on the isomers, being easier for secondary and tertiary than for primary.

## 4.5 Overall hydrocarboxylation

Now that information regarding the two steps of the reactions are collected; the whole process has to be investigated and the two cycles have to be unified. Moreover, changes can happen when the two steps are performed in the same reactor. Herein, the complete reaction system is investigated and explained based on the previously reported results for the two separate steps.

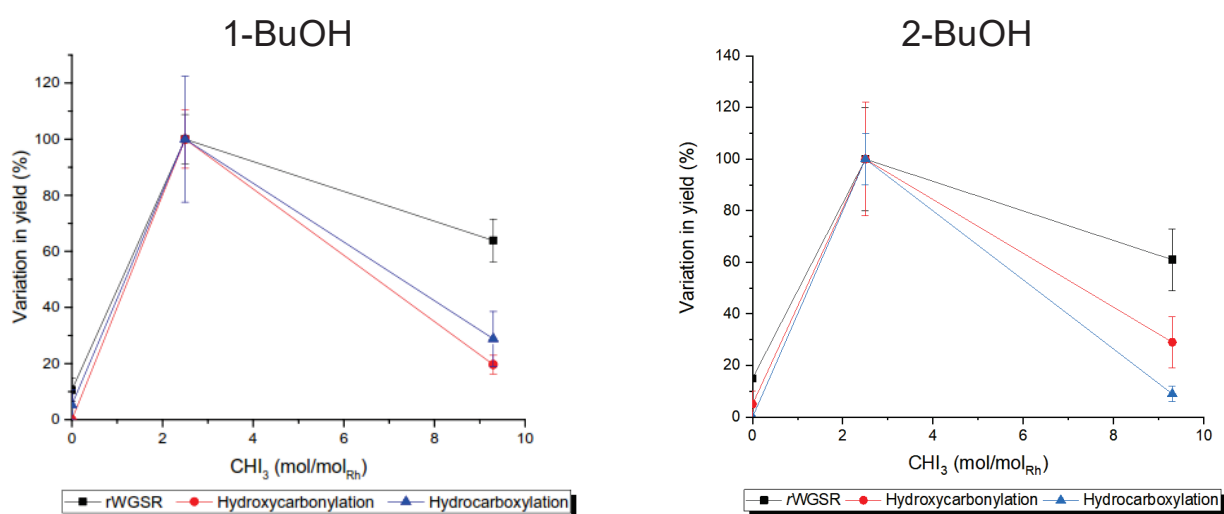


Figure 4-17: Variation of yields of carboxylic acids or CO in percentage, referring to the yields obtained in the optimal conditions (as reported in Chapter 3) as 100%: effect of the variation of  $\text{CHI}_3$  amount on the individual reaction steps (rWGSR and hydroxycarbonylation) and on the overall reaction (hydrocarboxylation). The experiment performed using 1-BuOH or primary alcohols optimized conditions is reported in the left graph and using 2-BuOH or secondary alcohols optimized conditions is reported in the right graph.

The amount of  $\text{I}^-$  in the solution affects the yield of CO as well as the yield of VA and 2-MBA. The results obtained with 0.0, 2.5 and 9.3 mol/mol<sub>Rh</sub> of  $\text{CHI}_3$  in solution for the overall hydrocarboxylation (corresponding to 0, 7.6 and 28 eq. of  $\text{I}^-$  compared to Rh mol) are reported in Entries 1, 7-8 in Table 3-11 for primary alcohol and in the Table 3-4 for 2-BuOH. The results obtained for the two single steps follow the same trend. The absence of iodide additive gives 0% yield of carboxylic acids, but at the same time, too much iodide causes a decrease in the yield to 20% starting from 1-BuOH and to 7% starting from 2-BuOH (Comparison in Figure 4-17, left for 1-BuOH and Figure 4-17, right for 2-BuOH). This behavior could be explained with the cited possible iodide

functions. On one hand, too much iodide forms other catalytic species which are not active, hence a lower activity is noticed. Moreover, when 9.3 eq. of  $\text{CHI}_3$  are used, the final solution is very dark and high amount of solid material is present, making the analysis and the collection of the all reaction solution more difficult leading to lower mass balance. The negative effect of high amounts of iodide in the reactor is probably the cause of the low activity observed when iodobutane is used as substrates. In these cases, the total amount of  $\text{I}^-$  present in the solution is  $1.88 + 7.6$  mmol (derived from the  $\text{CHI}_3$ ) corresponding to 28 eq. (or 9.3 eq. of  $\text{CHI}_3$ ). In these conditions, the yield in carboxylic acids is 25% from 1-iodobutane and 37% from 2-iodobutane, similarly to the one obtained from 1-BuOH and 2-BuOH if 9.3 eq. of  $\text{CHI}_3$  are added to the solution (Entry 8, Table 3-11 for primary alcohol and in Table 3-4 for secondary alcohols).

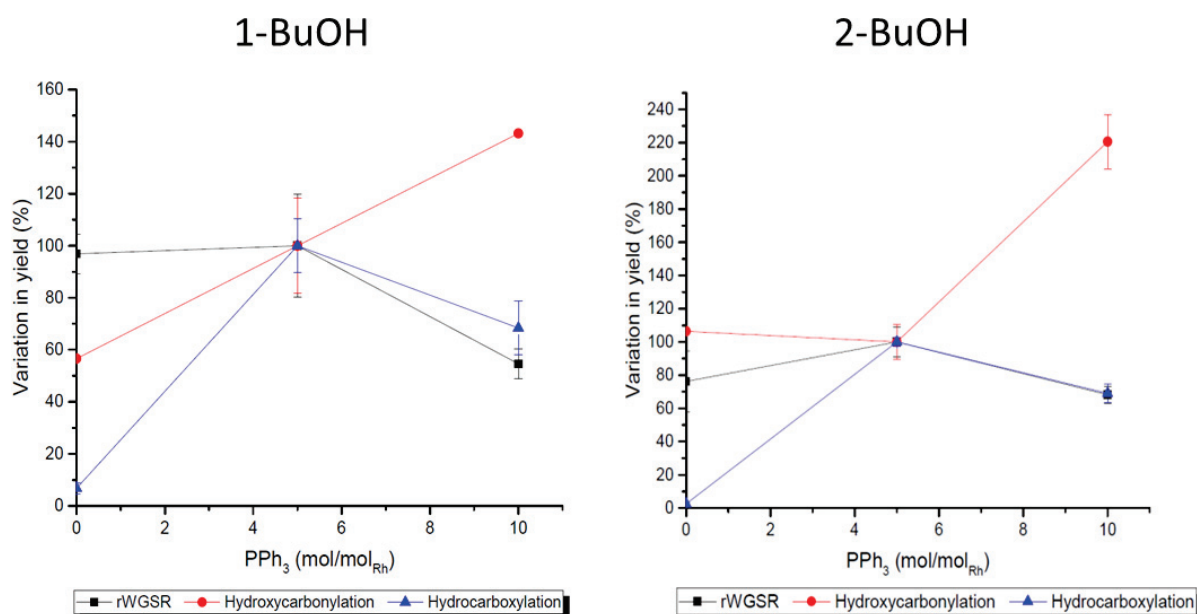


Figure 4-18: Variation of yields of carboxylic acids or CO in percentage, referring to the yields obtained in the optimal conditions (as reported in Chapter 3) as 100%: effect of the variation of  $\text{CHI}_3$  amount on the individual reaction steps (rWGSR and hydroxycarbonylation) and on the overall reaction (hydrocarboxylation). The experiment performed using 1-BuOH or primary alcohols optimized conditions is reported in the left graph and using 2-BuOH or secondary alcohols optimized conditions is reported in the right graph.

Without  $\text{PPh}_3$ , the yield in carboxylic acids obtained from the overall hydrocarboxylation drops to 2% for 1-BuOH and to 5% for 2-BuOH, while with 10 eq. of  $\text{PPh}_3$  the yield decreases to a 44% for 1-BuOH and to 48% for 2-BuOH (Entries 9-10, Table 3-11 for primary alcohol and in Table 3-4 for secondary alcohols), although no significant change in the *n*/*iso* ratio is observed. These observations lead us to conclude that phosphine is an important part of the catalyst. Its absence causes secondary reactions such as hydrogenation and a minimal formation of carboxylic acids which could be obtained from the amount of CO introduced in the system with the Rh precursor. This result is surprising due to the fact that  $\text{PPh}_3$  is not crucial for any of the two reaction steps (namely *r*WGSR and hydroxycarbonylation). The comparison is represented in the Figure 4-18, left for 1-BuOH and Figure 4-18, right for 2-BuOH.

The  $^{31}\text{P}$ -NMR of the reaction mixture after 1h, when the catalyst is highly active, for the reaction of 2-BuOH is reported in Figure 4-19, bottom (2-BuOH\_1h\_Argon). The same experiment was done on the reaction of 1-BuOH obtaining similar results (Figure 4-19, top), although more TPPO ( $\text{Ph}_3\text{PO}$ ) is formed. In the spectra, multiple peaks are observed with the characteristic coupling constant  $J_{\text{Rh-P}}$  above 100 Hz. Few of them could be assigned based on literature data: **B** (Figure 4-19, bottom) is the complex *trans*- $[\text{Rh}(\text{PPh}_3)_2(\text{CO})]^{281}$  and **I** (Figure 4-19, bottom) is  $[\text{RhI}_4(\text{CO})(\text{PPh}_3)][\text{CH}_3\text{-PPh}_3]^{282}$ . **F** and **H** (Figure 4-19, bottom) are probably species such as  $[\text{CH}_3\text{-}i\text{-PPh}_3]^+$ . Species **I** was previously characterized via X-Ray analysis and resulted to be inactive in catalysis.<sup>6</sup> Moreover, the **I** signal increases over time and it is the only one left after the sample was exposed to air (Figure 4-20). It is known, that  $\text{PPh}_3$  could easily substitute CO as ligand in carbonylation catalysts, without leading to any significant change in the performance of the catalytic system.<sup>254</sup> Indeed, the difference in reaction conditions, between the two steps performed separately and the overall reaction, is the quantity of CO inside the reactor. In the first two cases, CO is either produced and not consumed (*r*WGSR) or introduced in the reactor as reagent (hydroxycarbonylation). On the contrary, in the complete reaction, the CO is produced and fast consumed by the second step, as proved by the measurement of the amount of CO during the reaction (about 0.2-0.7% yield, 0.5-1.7 mol/mol<sub>Rh</sub>). Consequently, it seems that  $\text{PPh}_3$  is needed only in the latter case to avoid the deactivation of the catalyst which happens in the absence of ligands such as CO/ $\text{PPh}_3$ .



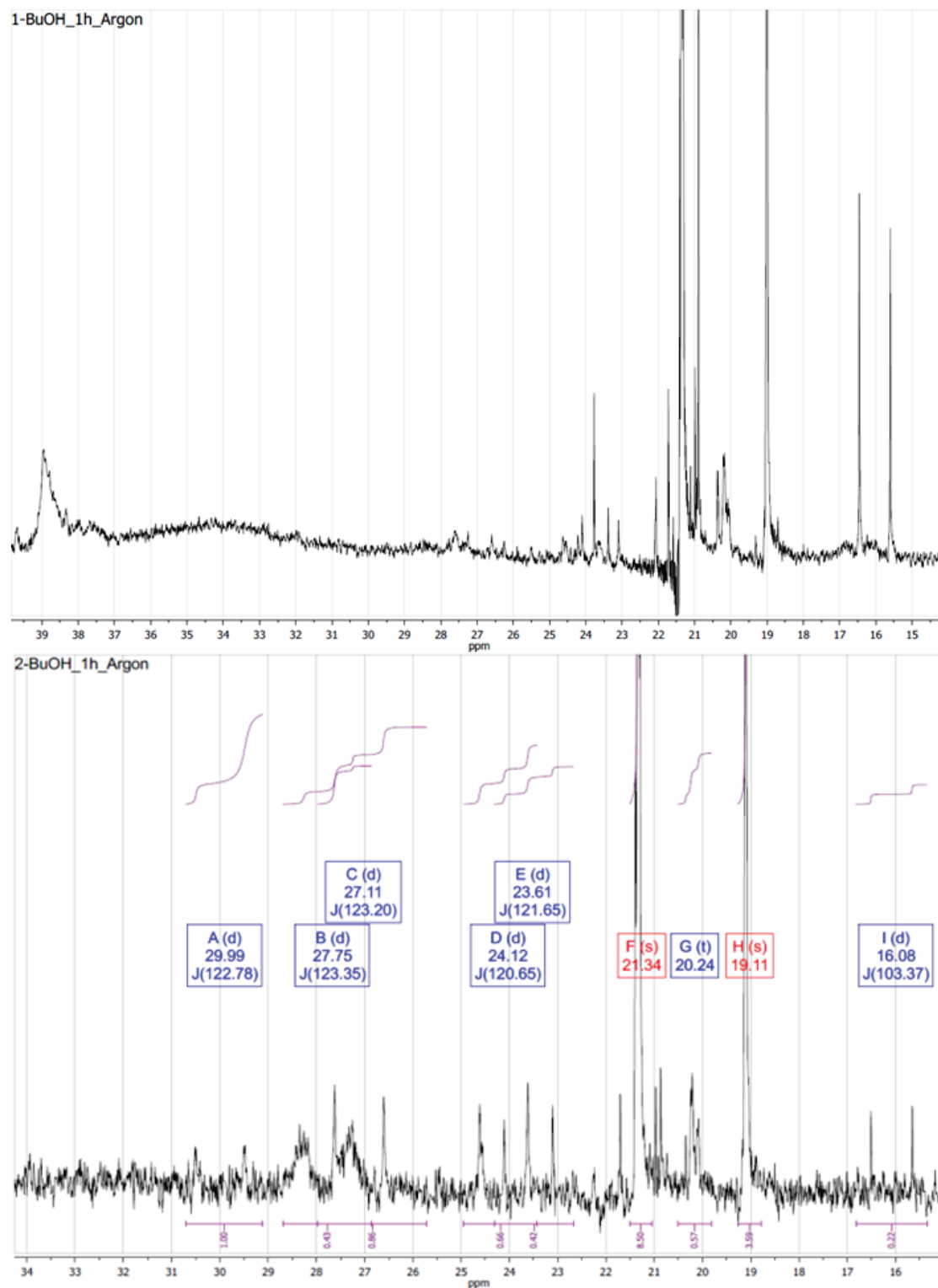


Figure 4-19:  $^{31}\text{P}$ -NMR of the reaction solution for the retransformation of 1-BuOH (top) and 2-BuOH (bottom) to VA and 2-MBA after 1 h.

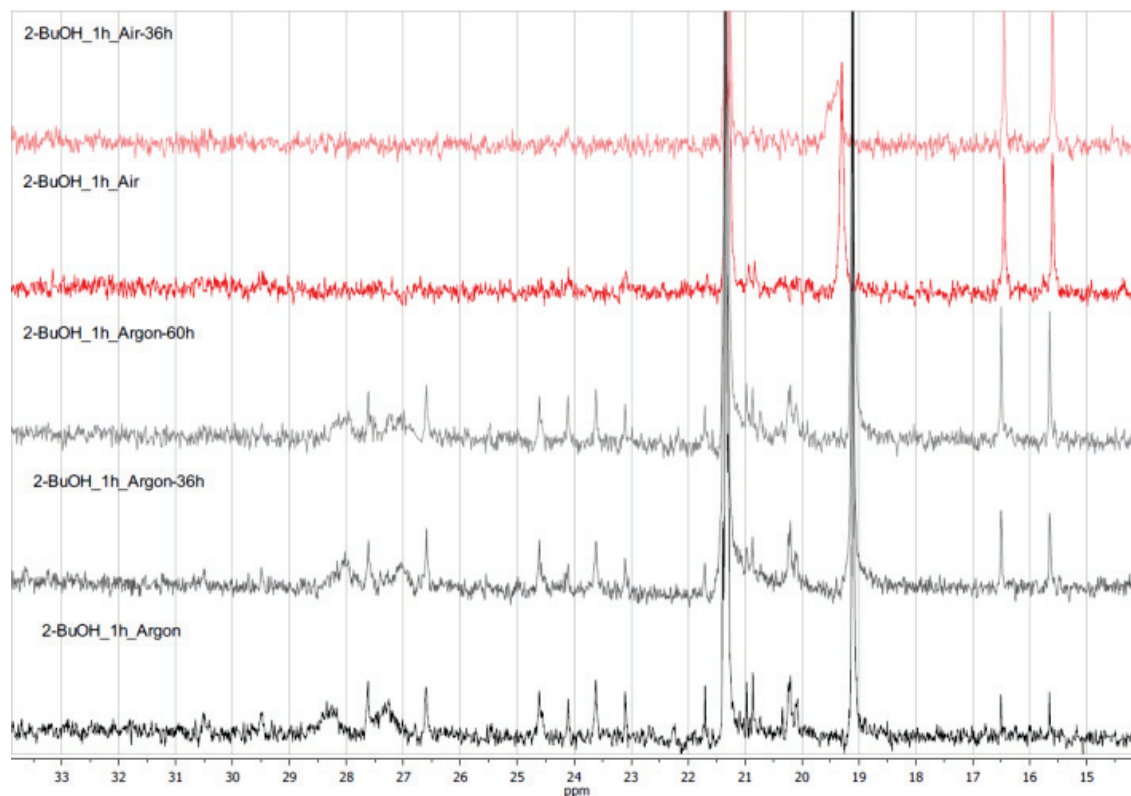


Figure 4-20:  $^{31}\text{P}$ -NMR of the reaction solution for the transformation of 2-BuOH to VA and 2-MBA after 1 h. The same solution has been monitored over time and once in air.

The slightly higher amount of butane detected and the lower mass balance (probably due to high boiling point products) may testify that high amount of  $\text{PPh}_3$  (10 eq.) results in the occupation of the catalytic active sites and/or in higher activity towards secondary reactions. The comparison is represented in the Figure 4-18, left for 1-BuOH and Figure 4-18, right for 2-BuOH. High amount of  $\text{PPh}_3$  (10 eq.) negatively affects the  $r_{\text{WGSR}}$  rate. This is probably one of the reasons why the yield in carboxylic acid obtained from the overall reaction is lower if this quantity of phosphine is used.

Nevertheless, a discrepancy between the total reaction and the hydroxycarbonylation is detected. The same yield in carboxylic acid is obtained with 10 mol/mol $_{\text{Rh}}$  of  $\text{PPh}_3$  if the hydroxycarbonylation is performed separately, while it is obtained with 5 mol/mol $_{\text{Rh}}$  of  $\text{PPh}_3$  if the hydrocarboxylation is performed. with the same functions. Probably, different amount of phosphine ligands are needed to compensate for the different amount of CO.

As a further proof of this theory, a comparison with previously reported similar Rh system can be made. The most interesting comparison is obtained with the system reported by Forster *et al.* (1981) for the hydrocarboxylation of alkenes,<sup>13</sup> very similar to the one reported by the same group for the carbonylation of methanol<sup>244</sup> and other alcohols<sup>245</sup> as well as the one reported by Eisenberg *et al.* (1982) for the WGSR.<sup>14</sup> The catalyst reported in these systems is deactivated by high amount of HI in solution leading to the inactive species  $[\text{Rh}(\text{CO})_2\text{I}_4]^-$ . In our case, if  $\text{PPh}_3$  is substituting CO as ligand a similar pathway could be considered and the formation of the species **I** detected in the NMR and characterized *via* X-Ray can be justified (Figure 4-21).

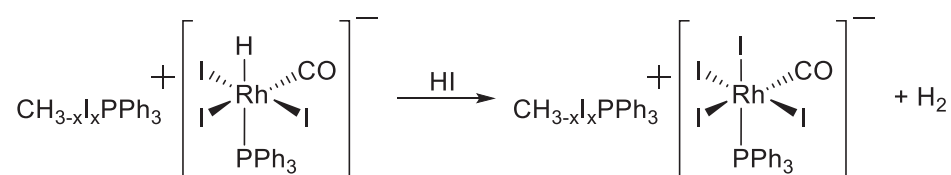


Figure 4-21: Deactivation of the catalyst due to high amount of HI.

Based on the reported observations the mechanism reported in Figure 4-22 is suggested. The *r*WGSR cycle is inspired by the one suggested by Eisenberg for the WGSR,<sup>14</sup> while the hydroxycarbonylation one is inspired by the one reported by Forster.<sup>13</sup> In both cases, the catalytic active species have a ligand (L) which could be either CO or  $\text{PPh}_3$  depending on the amount of CO in the reactor. The same Rh system is responsible for both the *r*WGSR and the hydroxycarbonylation activity, showing a good balance between the two cycles. Unifying the two catalytic cycles allowed to perform the synthesis of carboxylic acids starting from organic substrates,  $\text{CO}_2$  and  $\text{H}_2$ . The substitution of the traditionally used CO and  $\text{H}_2\text{O}$  has advantages, although thermodynamically more challenging. It avoids the utilization of toxic gas (CO) and substitutes it with a renewable and green carbon source,  $\text{CO}_2$ .

The proposed  $\mu$ WGSR cycle consists of 5 ( $1_r$  -  $5_r$ ) steps. The first step ( $1_r$ ) is the coordination of  $\text{CO}_2$  and  $\text{HI}$  to the  $[\text{RhL}_2\text{I}_2]^-$  leading to the formation of a metallacarboxylic acid. In this step, the Rh center is oxidized from a formal oxidation state +I to +III. In presence of  $\text{H}^+$ , the  $\text{Rh-COOH}$  release  $\text{H}_2\text{O}$  and leave the  $\text{CO}$  group originating from  $\text{CO}_2$  coordinated to the Rh ( $2_r$ ). The  $\text{CO}$  ligand is then substituted by a  $\text{I}^-$  leading to the species  $[\text{RhL}_2\text{I}_3]^-$  ( $3_r$ ). The initial  $[\text{RhL}_2\text{I}_2]^-$  is regenerated through two subsequent steps. Step  $4_r$  involves the activation of  $\text{H}_2$ , forming the metal hydride species  $[\text{HRhL}_2\text{I}_3]^-$ . This species is reduced to  $\text{Rh}^{\text{I}}$  after the reductive elimination of  $\text{HI}$  ( $5_r$ ) and the coordination of  $\text{CO}_2$  can start again.

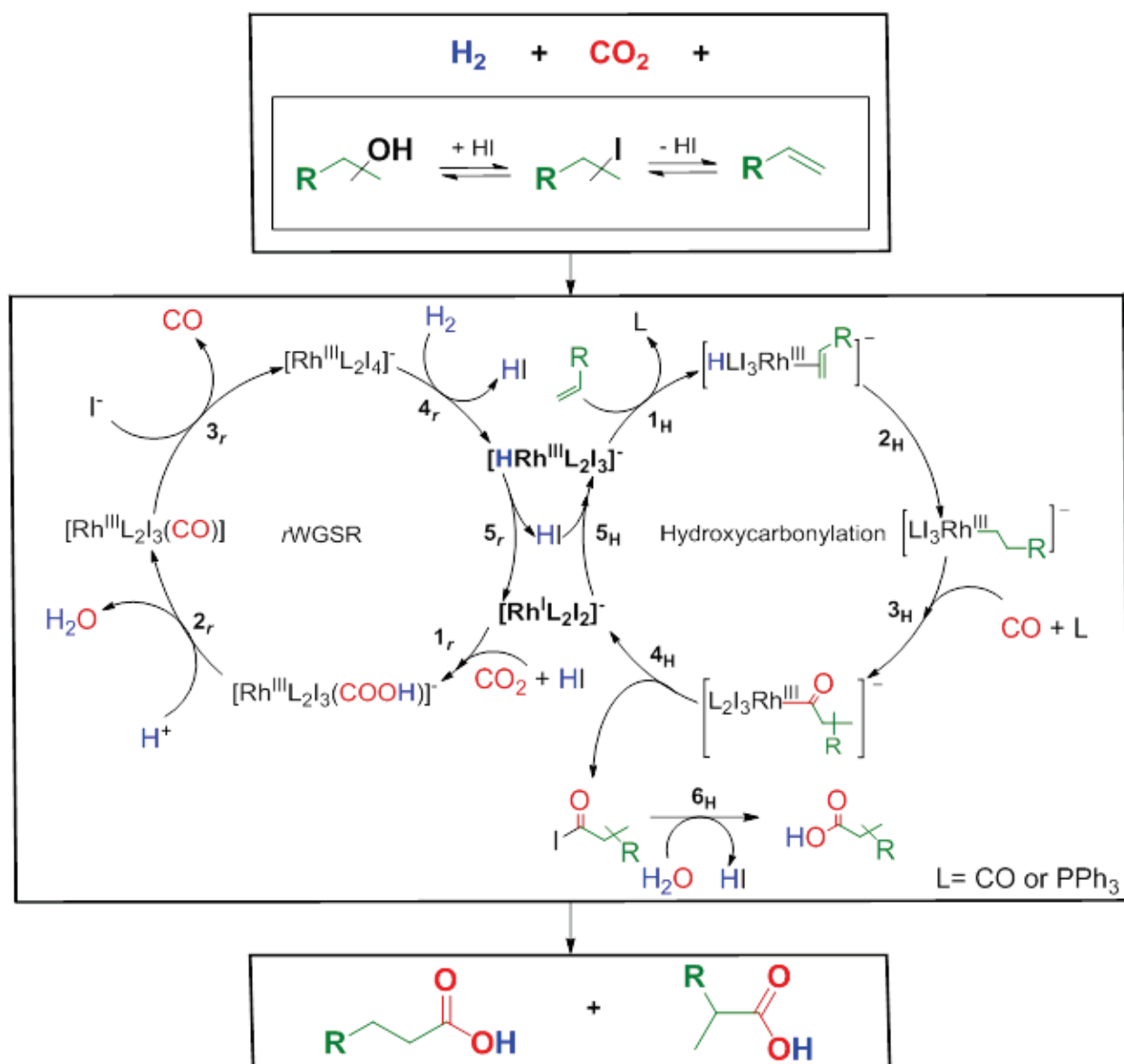


Figure 4-22: Proposed mechanism for the hydrocarboxylation of alcohols.

The metal hydride species  $[\text{HRhL}_2\text{I}_3]^-$  generated via  $\text{H}_2$  activation is able to coordinate the alkene intermediate substituting a ligand (**1<sub>H</sub>**). The alkene is formed *via* non-catalytic substitution and elimination steps. The  $[\text{HRhL}_2\text{I}_3]^-$  complex is transformed into an alkyl-Rh species *via* insertion of the alkene in the Rh-H bond (**2<sub>H</sub>**). These first two steps can explain the obtained *n/iso*-selectivity. The less hindered position of the alkene will probably coordinate to the metal center, leading mainly to the *n*-carboxylic acid. The  $\beta$ -hydride elimination is still possible and isomerization can occur, leading to a mixture of *n*- and *iso*-carboxylic acids. The following step is the CO coordination and migratory insertion into the Rh-alkyl bond (**3<sub>H</sub>**). The **4<sub>H</sub>** step is the reductive elimination of the acyl iodide which is further transformed in the carboxylic acid, through a non-catalytic nucleophilic substitution (**6<sub>H</sub>**). The reductive elimination generates the Rh<sup>I</sup> species  $[\text{RhL}_2\text{I}_2]^-$ . The oxidative addition of HI regenerates the Rh<sup>III</sup> species  $[\text{HRhL}_2\text{I}_3]^-$  to start the cycle again (**5<sub>H</sub>**). This suggested mechanism is similar to the one recently reported for the hydroxycarbonylation of alkenes in presence of formic acid.<sup>280</sup>

Now, from the analysis of the catalytic cycles and the catalytic species, more considerations can be made.

$\text{Rh}^{\text{III}}\text{I}_3$  is not a good precursor for the reaction, while  $[\text{Rh}^{\text{I}}\text{Cl}(\text{CO})_2]_2$  allows to obtain good yields. The Rh<sup>III</sup> precursor has a particularly negative effect on the *r*WGSR step, while it does not inhibit the reaction if used as a precursor for the hydroxycarbonylation step (Table 4-7). Probably, in the *r*WGSR cycle, the slower step is the coordination of  $\text{CO}_2$  to the Rh<sup>I</sup> species. In this case, starting from a Rh<sup>III</sup> precursor would slow down this step even more, because it will produce less Rh<sup>I</sup> active species in the solution compared to a Rh<sup>I</sup> precursor. It is known that the electron density of the Rh center, which is determined also from the oxidation state of the metal, is determining the  $\text{CO}_2$  coordination to the Rh.<sup>283</sup> The rate limitation on this step would slow down the reaction even more, reducing drastically the amount of CO available for the hydroxycarbonylation step and, therefore, affecting negatively the all reaction.

Almost every Rh species is an anion. For this reason, the ionic strength of the solution has to be kept high enough to allow a good freedom of the active anionic species from the corresponding counter cation.<sup>250</sup> This may explain the superiority of a protic and polar solvent such as acetic acid.

Table 4-7: Effect of different Rh precursors on the yields of the different reaction steps and on the yield in carboxylic acids obtained from the total reaction.

Catalyst	Alcohol	<i>r</i> WGSR - CO yield (%) <sup>[a]</sup>	Hydroxycarbonylation - VA and 2-MBA yield (%) <sup>[b]</sup>	Hydrocarboxylation - VA and 2-MBA yield (%) <sup>[c]</sup>
<b>[RhCl(CO)<sub>2</sub>]<sub>2</sub></b>	1-BuOH	3,1	21	64
	2-BuOH	2,6	38	77
<b>RhI<sub>3</sub></b>	1-BuOH	0,9	15	22
	2-BuOH	0,5	53	3

<sup>[a]</sup> Standard reaction conditions: 92  $\mu$ mol Rh, 1 ml of acetic acid (1-BuOH) or 2 ml acetic acid (2-BuOH), 2.5 mol/mol<sub>Rh</sub> of CHI<sub>3</sub>, 5 mol/mol<sub>Rh</sub> of PPh<sub>3</sub>, 3.5 mol/mol<sub>Rh</sub> of *p*-TsOH•H<sub>2</sub>O (2-BuOH), 20 bar of H<sub>2</sub> (1-BuOH) or 10 bar of H<sub>2</sub> (2-BuOH), 20 bar of CO<sub>2</sub>, 160 °C, 16 h. <sup>[b]</sup> Standard reaction conditions: 0.5 mmol of butanol, 92  $\mu$ mol Rh, 1 ml of acetic acid (1-BuOH) or 2 ml acetic acid (2-BuOH), 2.5 mol/mol<sub>Rh</sub> of CHI<sub>3</sub>, 5 mol/mol<sub>Rh</sub> of PPh<sub>3</sub>, 3.5 mol/mol<sub>Rh</sub> of *p*-TsOH•H<sub>2</sub>O (2-BuOH), 2 bar of CO, 160 °C, 16 h. The total pressure was adjusted with Ar in order to reach the same pressure normally obtained using CO<sub>2</sub> and H<sub>2</sub> (30 and 40 bar respectively for primary and secondary alcohols). <sup>[c]</sup> Standard reaction conditions: 1.88 mmol of butanol, 92  $\mu$ mol Rh, 1 ml of acetic acid (1-BuOH) or 2 ml acetic acid (2-BuOH), 2.5 mol/mol<sub>Rh</sub> of CHI<sub>3</sub>, 5 mol/mol<sub>Rh</sub> of PPh<sub>3</sub>, 3.5 mol/mol<sub>Rh</sub> of *p*-TsOH•H<sub>2</sub>O (2-BuOH), 20 bar of H<sub>2</sub> (1-BuOH) or 10 bar of H<sub>2</sub> (2-BuOH), 20 bar of CO<sub>2</sub>, 160 °C, 16 h.

The inhibiting effect of CO and its effect on the selectivity are consistent with the proposed catalytic cycle. The low selectivity towards one of the carboxylic acids isomers is probably due to the low CO pressure observed during the reaction. In these conditions, one of the CO ligands can easily detach from a Rh-alkyl complex leaving an empty coordination site.<sup>253</sup> The  $\beta$ -hydride elimination can occur to stabilize the complex. The following re-insertion of the hydrogen can take place on a different carbon compared to the first one. This is also testified by the deuterium incorporation which leads to place the deuterium in all the positions of the obtained carboxylic acid (Figure 4-15). This results in a similar selectivity starting from different alcohols isomers. At the same time, the increasing CO pressure influences the selectivity. This is probably related to the fact that the CO is hardly lost by the catalytic species due to the high concentration of the ligand, therefore, no rearrangement is observed.

Nevertheless, using CO<sub>2</sub> and H<sub>2</sub> instead of CO and H<sub>2</sub>O could be seen as an advantage. The CO<sub>2</sub> and the H<sub>2</sub> behave as a reserve of the CO reagent, which is provided in the required amount. It is enough to allow a good conversion of the organic

substrate to carboxylic acids, but it does not poison the catalytic active species, occupying the site where alkenes should coordinate. If too much CO is present, the de-coordination of the ligand may be slower.

However, unifying the two steps, shows also irregularities. The amount of CO produced (from 0.23 to 0.77 mmol) is not enough to form all the produced carboxylic acids (1.5 mmol in the best case). Probably, the CO and H<sub>2</sub>O, once they are consumed during the reaction, are regenerated by the *r*WGSR because the equilibrium has been shifted towards these products, according to Le Chatelier principle.

## 4.6 Conclusions and outlook

To conclude, all the obtained results are consistent with a mechanism which involves two consequential steps: the first is a *r*WGSR which creates the reagents for the second step, that is the “hydroxycarbonylation” of the alkene. This balance results in good yield of the desired carboxylic acids. The optimized reaction conditions must be different depending on the class of oxygenated substrates which have to be transformed. They have to allow the formation of enough alkene with a rate capable to overcome secondary reactions.

The same Rh-based catalytic system catalyzes both the *r*WGSR and the hydroxycarbonylation. The activity of the entire system is related to the parameters which influence only one of the two steps or both. In particular, CHI<sub>3</sub> and PPh<sub>3</sub> are highly important. CHI<sub>3</sub> is independently important for *r*WGSR and hydroxycarbonylation. On the contrary, PPh<sub>3</sub> is required only if CO is in low amount, to provide a suitable substitute for it. The obtained results show that the main pathway for the second catalytic cycle involves the alkene coordination to the Rh center. Moreover, this mechanism is consistent with all the information collected while investigating the reaction conditions and the substrate scope. As the mechanism, the suggested catalytic active species explain the effect of many reaction parameters.

Besides, the deeper knowledge of the catalytic cycles presented can inspire a further optimization of the reaction system as well as the development of new catalysts, both homogeneous and heterogeneous (SACs), possibly allowing obtaining higher TON as well as good yields starting from new and valuable substrates.



## 4.7 Experimental part

### 4.7.1 General

All air-sensitive compounds were handled under inert atmosphere (Argon 4.6 Messer, Germany) using Schlenk techniques or in a glovebox (*MBraun LabMaster SP*).

### 4.7.2 Solvents and Chemicals

Acetic acid and further used solvents were pre-dried over molecular sieves (4 Å), then degassed by bubbling argon with a frit for at least 1 h and stored over molecular sieves (4 Å) under argon. All substrates were degassed by three freeze-pump-thaw cycles and stored over molecular sieves (4 Å and 3 Å for methanol) under argon. cyclohexane oxide was treated in the same way, but it was stored over molecular sieves (4 Å) for maximum one day to avoid polymerization. Deionized water was taken from a reverse-osmotic purification system (*Werner EasyPure II*) and degassed by bubbling argon with a frit for at least 1 h. Water contents of all organic solvents and substrates were monitored by Karl-Fischer titration (*Metrohm 756 F Coulometer*) and typically kept under 100 ppm. All reagents were commercially supplied and used as received, unless stated otherwise.

### 4.7.3 Autoclave reactions

The catalytic runs were performed in 10 mL stainless steel finger autoclaves. The autoclaves were equipped with glass inlets to avoid blind activity. Iodoform (CHI<sub>3</sub>), triphenylphosphine (PPh<sub>3</sub>) and *para*-toluensulfonic acid monohydrate (*p*-TsOH·H<sub>2</sub>O) were weighted in the glass inlet and then placed in the autoclaves. Following, the autoclave was evacuated at high vacuum for at least one hour and then charged with an argon atmosphere. The catalyst was weighted in a Schlenk tube (previously evacuated and filled with Ar) inside a glovebox. Afterwards, the solvent and the substrate(s) were added in the Schlenk tube containing the catalyst. The mixture was transferred in the autoclave with a syringe. The autoclave was pressurized with CO<sub>2</sub> and H<sub>2</sub> and heated for the all reaction time. The obtained reaction mixture was analyzed via gaschromatography (GC) and unknown compounds were identified with mass spectroscopy (GC-MS).

Catalytic tests were repeated two or more times. Error bars are shown in the reported graphs. Where not specified, the error for the main products and the by-products are usually around  $\pm 2\%$ .

#### 4.7.4 Mass Spectrometry

MS analyses were performed on a Varian 1200L Quadrupole Ms/ms by direct ESI from organic solutions. Detected masses are given in  $m/z$  and correlated to calculated masses of the respective species.

#### 4.7.5 Gas chromatography

GC analyses of the liquid phases were performed on a *Trace GC Ultra* (ThermoScientific) using a packed *CP-WAX-52-CB* column (length = 60 m, diameter = 0.25 mm) isothermally at 50 °C for 5 min, then heated to 200 °C at 8 °C min<sup>-1</sup>. A constant flow of 1.5 mL min<sup>-1</sup> of He was applied. The gas chromatograph was equipped with a FID detector. GC analysis of butane and butene gases were performed on a *Sichromat* using a capillary *PLOT Al<sub>2</sub>O<sub>3</sub>* column (length = 50 m) isothermally at 60 °C for 5 min, then heated to 200 °C at 8 °C/min. A constant pressure of 0.8 bar of He was applied. The gas chromatograph was equipped with a FID detector. GC analysis of CO, CO<sub>2</sub> and H<sub>2</sub> gases were performed on a *HP6890* using a capillary *Chem Carbon ST* column (length = 2 m) isothermally at 35 °C for 5 min, then heated to 150 °C at 8 °C min<sup>-1</sup>. A constant flow of 25 mL min<sup>-1</sup> of He was applied. The gas chromatograph was equipped with a TCD detector. Examples of the different types of chromatograms are reported in Figure 4-23, Figure 4-24, Figure 4-25.

The liquid substances in the reaction solution were quantified using ( $\pm$ )-1-phenylethanol and/or *n*-dodecane as standard. Acetone was used as a solvent for the work up (for cyclohexanol, cyclohexanone and cyclohexane oxide reactions acetone was substituted by dichloromethane). The correction factor was calculated preparing solutions with known amount of substances and standard. The gaseous substances were quantified using ethane as standard. As for the liquid samples, the correction value ( $K_f$ ) was obtained from self-made gas solutions with known amount of gases. Given a molecule X, its mass was quantified using the following equation:

$$m_x = K_f \frac{A_x \times m_{standard}}{A_{standard}}$$

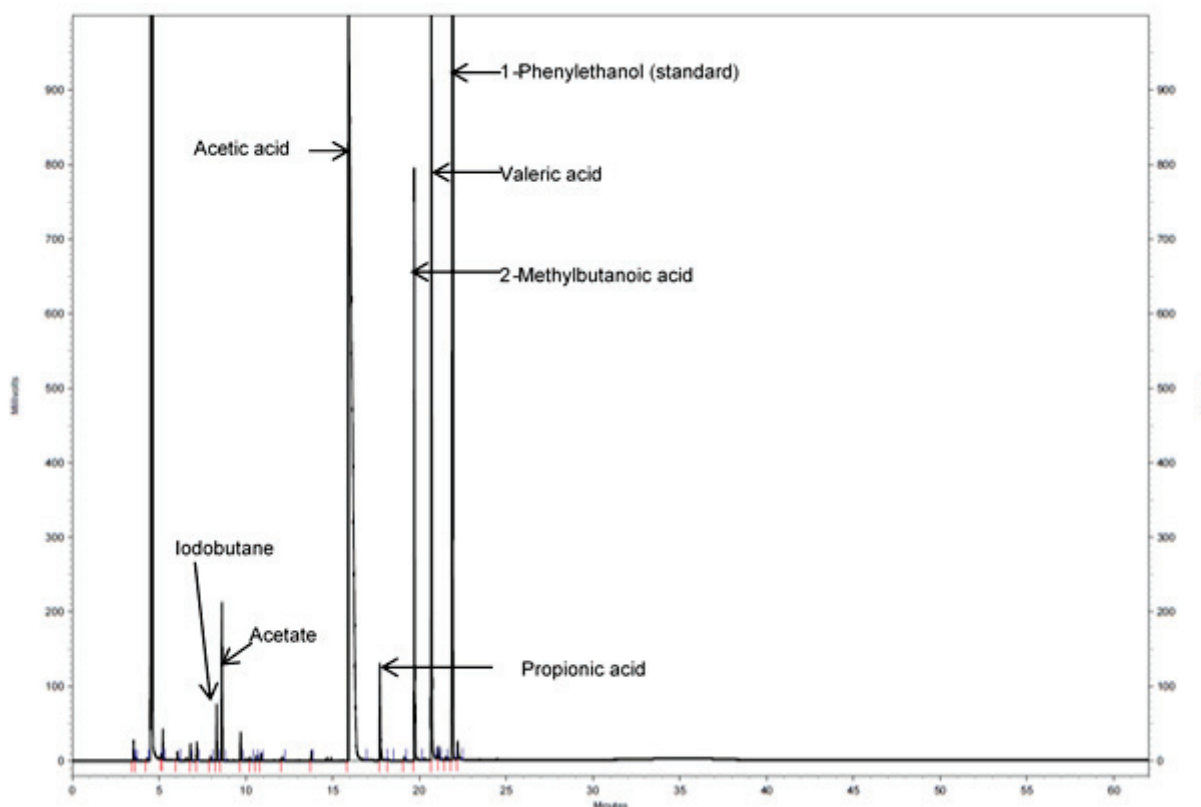


Figure 4-23: Example of chromatogram obtained from the analysis of the liquid reaction mixture of 1-BuOH. The same products are detected for 2-BuOH, Butanone, Butanal and 1,4-Butandiol. Propionic acid is probably present in the reaction mixture due to the reduction of acetic acid to ethanol which can be hydrocarboxylated to propionic acid.

#### 4.7.6 Design of Experiment (DoE)

The experimental equation and plots derived from the Design of Experiment approach were generated using the software *Design-Expert 8*. The reactions were prepared as explained in the previous section “Autoclaves” and the reaction mixtures were analyzed by gas chromatography.

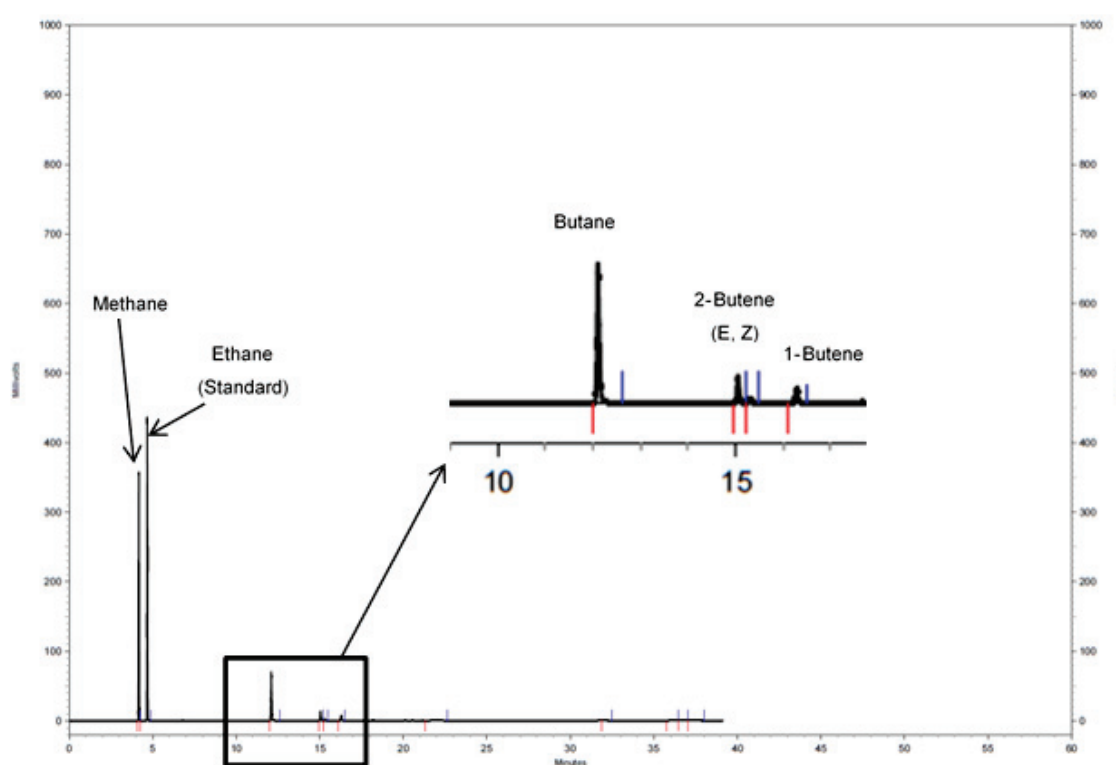


Figure 4-24: Example of gas phase chromatogram obtained from the reaction mixture of 1-BuOH. The same products are detected for 2-BuOH, Butanone, Butanal and 1,4-Butandiol. Methane is present in the mixture as product of the hydrogenation of  $\text{CHI}_3$ , as well as product of the decarbonylation of acetic acid.

#### 4.7.7 NMR analysis

Generally, NMR spectra were recorded with spectrometers Bruker AVIII-300 at ambient temperature. The  $^2\text{H}$ -NMR was registered with a Bruker AV-600 at ambient temperature at the frequency noted. For  $^1\text{H}$ ,  $^2\text{H}$  and  $^{13}\text{C}$  chemical shifts are given in ppm relative to tetramethylsilane. For  $^{31}\text{P}$ -NMR, the chemical shifts are given in ppm relative to  $\text{H}_3\text{PO}_4$ .

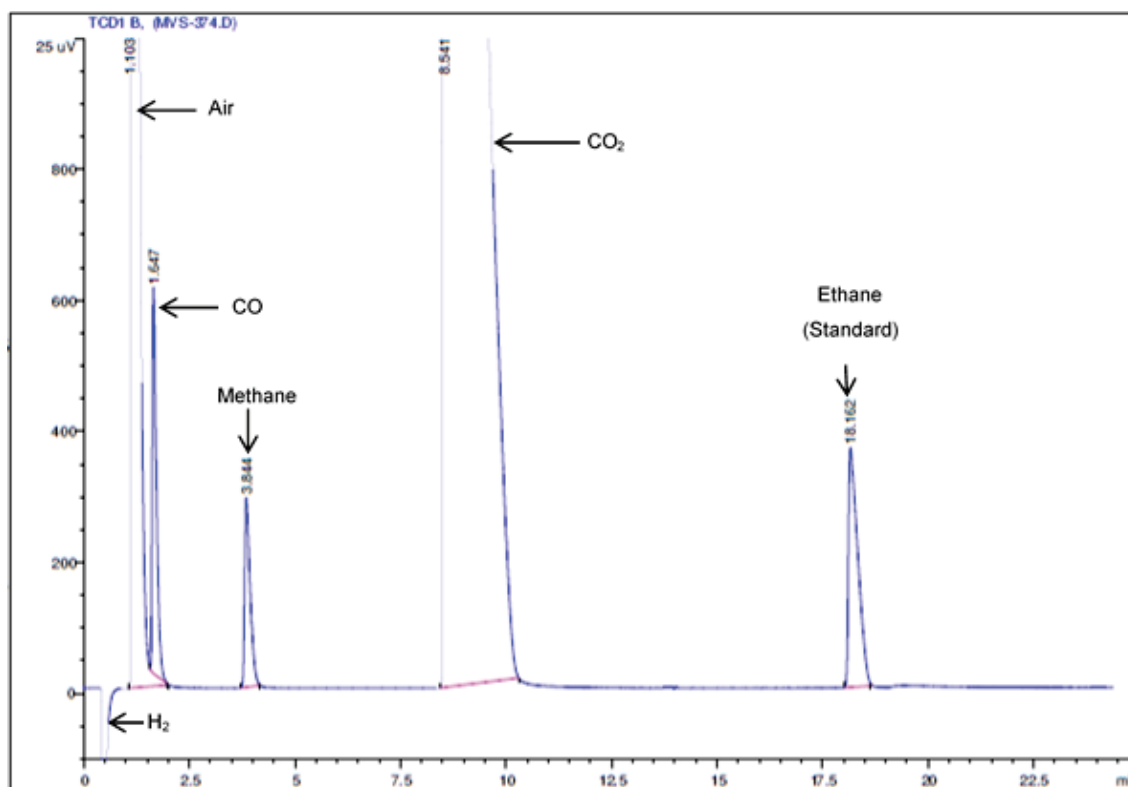


Figure 4-25: Example of gas phase chromatogram obtained from the  $r\text{WGSR}$ .



**5. Single atom catalysts (SACs)**





## 5.1 State of the art

The known catalysts for the production of carboxylic acids starting from CO<sub>2</sub> and organic substrates are homogeneous. Homogeneous catalysis has the general advantage of being highly active and selective, due to the well-defined catalytic sites. Unfortunately, the separation of the products and the recycling of the catalyst are usually challenging.<sup>18</sup> Moreover, the design of continuous processes is difficult. Heterogeneous catalysis can overcome these drawbacks, although usually heterogeneous catalysts are less active and less selective. Attempts to join the advantages of homogeneous and heterogeneous catalysis have been done in the past years. In particular, the immobilization of homogeneous species on insoluble supports has been extensively studied.<sup>18</sup> Remarkably, the immobilized Monsanto catalyst ([RhI<sub>2</sub>(CO)<sub>2</sub>]<sup>-</sup>) was successfully applied in the production of acetic acid from methanol, CO and H<sub>2</sub>O. The process (named “Acetica process”) is now industrially used thanks to a successful cooperation between chemical research, which allowed the synthesis of the catalyst, and engineering research, which developed a reactor setup able to use it on a large scale.<sup>78</sup> Zeolites based catalysts have been recently applied industrially by BP in the so-called SaaBre process.<sup>284</sup> In addition to these industrialized processes, SACs have been studied for the hydroformylation reactions. In particular, Rh on ZnO nanowires<sup>18</sup> and Rh on CoO nanosheets<sup>20</sup> were reported as very good catalyst for hydroformylation of alkenes. The selectivity and the TON are comparable and even higher than those obtained with the traditional Wilkinson catalyst. Moreover, Rh SACs on TiO<sub>2</sub> nanoparticles were reported as active for the *r*WGSR at temperature lower than 200 °C.<sup>19</sup>

Recently, the development of new and powerful analytical techniques allowed the characterization of heterogeneous catalysts based on Single Atom Catalysts (SACs). This leads to an increasing interest in this type of catalysts as clearly showed by the increasing number of publications in the recent years (Figure 5-1).<sup>285</sup>

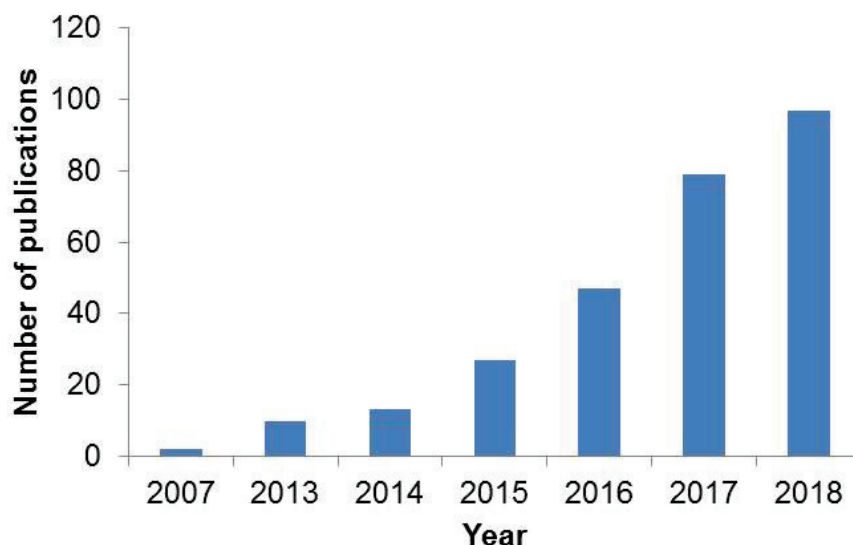


Figure 5-1: Results of a SciFinder research on Single Atom Catalysts.

Well defined metal sites supported on diverse supports have been studied in the past years. They are remarkable due to the high activity, selectivity and the low metal loading. A single metal atom is usually extremely unsaturated and therefore highly active (schematic representation of the activity of single atoms compared to supported nano-structure is reported in Figure 5-2).<sup>16-18</sup> Moreover, having only single atoms of metal on the support allows having very specific and well defined active sites<sup>15</sup>. These features remind of homogeneous catalysts, but at the same time they bring the advantages of heterogeneous catalysts such as easy separation and recyclability.<sup>18</sup>

Three classes of catalysts containing well defined single sites can be distinguished. Organometallic species supported on different materials,<sup>286, 287</sup> ion-exchanged metals supported on porous materials (MOF or zeolites) and mononuclear supported atoms were reported in the past years.<sup>16</sup>

One of the major issues regarding single-atom catalyst is the stability. The high activity is derived from the unsaturated environment, which could also lead to leaching, mobility or aggregation of the metal<sup>15</sup>. These phenomena would lead to lose or change the activity of the catalyst. To avoid it, strong interactions between the metal and the support must be provided.<sup>17</sup> This is usually the case for mononuclear supported atoms.

In the successful reported cases of mononuclear supported atoms, the support itself could be considered as the ligand for the metal atom and it stabilizes it. Usually, supports have large surface areas and provide specific anchoring sites to tightly grasp the metal atom. The metal is usually positioned on electronic defects (i.e. uncapped sites) or structural defects, where the metal bonds with more than one atom of the surface.<sup>17</sup> The stabilization is often due to electronic metal-support interaction (EMSI), which normally includes changes in the d-band centers relative to the Fermi level.<sup>288, 289</sup> The type of interaction depends highly on the supported metal atom and on the nature of the support.

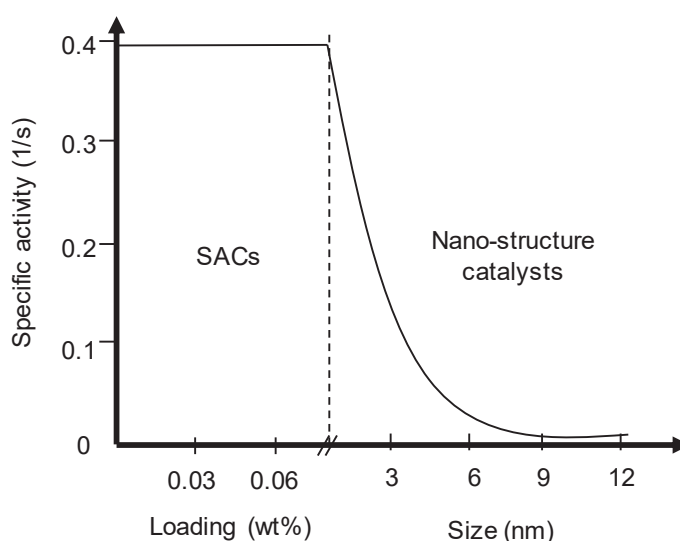


Figure 5-2: Schematic representation of the increasing of the activity switching from nano-structure catalysis to single-atom catalysis.

Metal oxides ( $\text{TiO}_2$ <sup>19, 290, 291</sup>,  $\text{CeO}_2$ <sup>292</sup>,  $\text{Al}_2\text{O}_3$ <sup>293, 294</sup>,  $\text{ZnO}$ <sup>18</sup>, zeolites<sup>295</sup>,  $\text{FeO}_x$ <sup>296, 297</sup>,  $\text{SiO}_2$ <sup>298</sup> etc.) are used to anchor single metal atoms on the surface (Figure 5-3a). A common type of stabilization comes from the interaction of the catalytically active metal (M) with the oxygens of the lattices.<sup>289, 299, 300</sup> For instance, Ag is stabilized by the interaction with the O atoms of a microporous hollandite manganese oxide (HMO). This leads to interferences with the d-electronic state of the Ag active site, which has a final oxidation state intermediate between 0 and +1.<sup>289</sup> Au on  $\text{FeO}_x$  results extremely stable catalysts for the CO oxidation, thanks to covalent bonds between the gold atom and the oxygens of the support. In this case, the Au is found in different oxidation state depending on the presence of O vacancies (oxidation state = +1) or not (oxidation state = +3). In other cases, the catalytically active metal can substitute the metal in the

support lattice. As an example, highly stable Au single atoms substitute the cerium atom in a  $\text{CeO}_2$  support and catalyze the preferential oxidation of CO reaction.<sup>296</sup> Besides, oxides catalytically active metal species can be bound to the surface in presence of hydroxyl groups.<sup>301</sup>  $\text{Pt-O(OH)}_x^-$  species were reported on different supports as active catalysts for the Water Gas Shift reaction. Depending on the support, an additional additive (NaOH) can be needed to generate the required sites on the metal oxides surface.<sup>301</sup> A charge transfer between the metal oxide support and the catalyst can happen. For example,  $\text{Rh}^0$  was found in vacancies and defects of ZnO after reduction. A possible explanation for this is the charge transfer from the partially reduced ZnO to the supported  $\text{Rh}^{+1}$ , which is reduced to  $\text{Rh}^0$  and stabilized on the surface. This catalyst is highly active for hydroformylation reaction.<sup>18</sup>

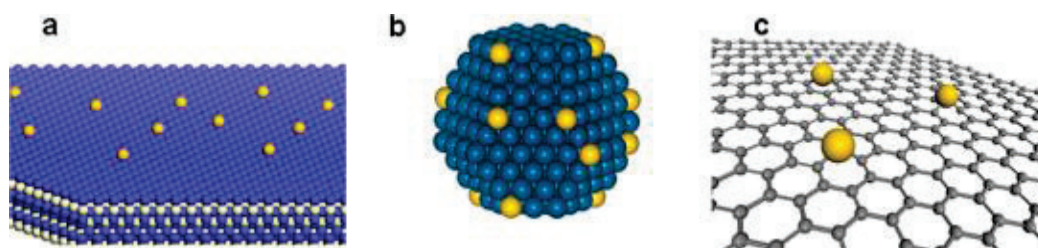


Figure 5-3: SACs supported on different materials: a) metal oxide; b) metal nanoparticles; c) graphene. Reprinted with permission from X.-F. Yang, A. Wang, B. Qiao, J. Li, J. Liu and T. Zhang, *Acc. Chem. Res.*, 2013, **46**, 1740-1748. Copyright (2013) American Chemical Society.

Supporting of single metal atom on nanoparticles is reported. In this case, the position and the distribution depend strongly on the different chemical potential of the supporting and supported metal (Figure 5-3b). Palladium atoms dispersed on copper nanoparticles supported on alumina ( $\text{Al}_2\text{O}_3$ ) were reported. In this example, the Pd is substituting some Cu atoms in the nanoparticles, forming well defined and highly active sites for hydrogenation reactions.<sup>302</sup>

Carbon materials are promising supports for single metal atoms (Figure 5-3c). In these supports, the metal is often found in the structure's defects and is stabilized by an electron donation from the support.<sup>16, 17, 30</sup> Clearly, depending on the material used the stabilization is different. Palladium single atoms dispersed on thermally treated graphene oxides have been reported as highly selective catalyst for the hydrogenation of 1,3-butadiene to butene. The metal ( $\text{Pd}^{+2}$ ) is linked to one carbon atom and one oxygen atom (from hydroxyl groups) of the structure and an oxygen molecule.<sup>22</sup>

Similarly, a Co atom was tightly anchored to a treated graphene oxide, always through the usage of the oxygen left on the surface, and it was active for the photocatalytic reduction of CO<sub>2</sub>.<sup>24</sup> Different transition metals were supported as single atoms on N-doped graphene. In these cases, the atom is normally stabilized by coordination of the N atoms, part of the carbon structure. Co on N-doped graphene is an active catalyst for the Hydrogen Evolution Reaction (HER).<sup>26</sup> The corresponding material supporting Ru is active for the Oxygen Evolution Reaction (OER),<sup>25</sup> while FeN<sub>4</sub> macrocycles incorporated in a graphene lattice are used for benzene oxidation to phenol.<sup>21</sup> Co atoms stabilized by P coordination were reported. g-C<sub>3</sub>N<sub>4</sub> support was doped with P and the resulting CoP<sub>4</sub>-N material is a good catalyst for the H<sub>2</sub>O splitting.<sup>29</sup> N-doped porous carbon can stabilize Fe atoms in the same way, providing a catalytic system for the OER reaction.<sup>28</sup> Graphene was investigated as a support for single atom transition metal catalyst, using a computational approach.<sup>23</sup>

The production of SACs on a large scale is another challenge linked to the use of these catalysts<sup>15</sup>. Two preparation methods are generally reported in literature: mass selected soft-landing methods<sup>22, 294</sup> and wet chemistry methods.<sup>18, 20, 25, 26</sup> The first class of methods includes the application of techniques normally used for the production of thin films such as Atomic Layer Deposition (ALD) and Chemical Vapour Deposition (CVD). A single cycle of ALD was proved an efficient method for the synthesis of Pd SACs on graphene oxide.<sup>22</sup> Wet chemistry methods are usually simple and they are feasible for the scale up.<sup>16, 17</sup> These techniques normally require the use of well-defined metal precursors (i.e. complexes), which are incorporated or deposited on the selected support. Following, treatment such reduction or annealing are giving the final material.<sup>18, 25, 26</sup>

Based on these reported examples, the development of Rh SACs for the hydrocarboxylation reaction was attempted. Carbon materials have the advantage of being easily modifiable by heteroatoms insertion, allowing the preparation of SACs with different chemical environment. This gives the chance of tuning the properties of the material and potentially the catalytic activity. Moreover, the high characteristic surface area (up to 2600 m<sup>2</sup>/g) is a helpful feature for the preparation of highly dispersed SACs. For this reason, in this study, this type of supports was used, planning different modifications inserting N and/or P atoms in the lattice (Figure 5-4). In addition, N-doped carbon materials are known to have basic sites on the surface which could be helpful to absorb CO<sub>2</sub>.<sup>303</sup> On the other side, P-doped graphene could generate an environment which remembers of the Rh-phosphine complexes which are known to be good

catalysts for the carbonylation reactions.<sup>254</sup> P-doped graphene can provide acidic sites which may be useful for mimicking the acidic environment present in the homogeneously catalyzed hydrocarboxylation. Rh on P-materials is indeed active for hydroformylation reaction.<sup>304</sup> Among the reported method to produce SACs, in this thesis the focus is on simple wet chemistry methods, due to their simplicity.

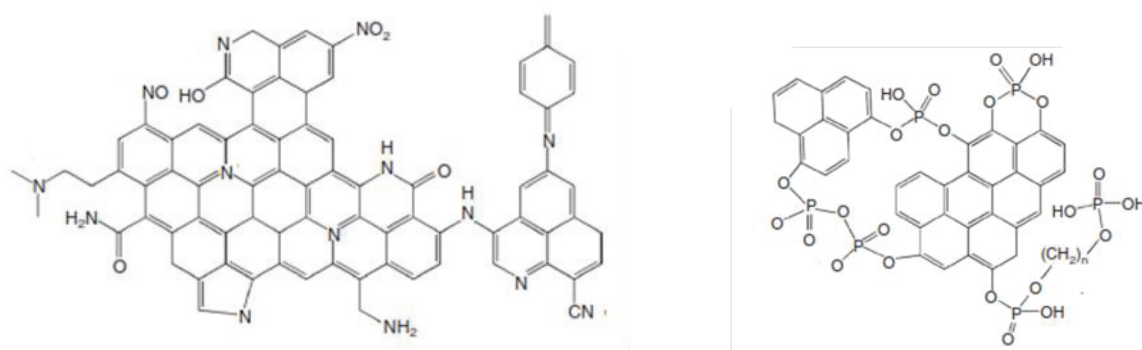


Figure 5-4: N-doped graphene (left) and P-doped graphene (right).

## 5.2 Synthesis of the catalysts

The catalysts were synthesized using a wet-chemistry approach. This means that a Rh complex was used as precursor, mixed with the support and treated to remove the ligand and stabilize the metal on the support surface.

Different catalysts have been synthesized with the method reported by Tour *et al.*<sup>26</sup> Initially, the GO is dissolved in water and sonicated. A metal solution is added to the water suspension and further sonicated. Lyophilization is used to remove the water (forming the sample xRh-GO). The lyophilization allows preserving the material more than other dehydration methods which require high temperatures. The obtained foam is annealed in different atmospheres up to 750 °C. This process leads to black flakes. A list of the obtained catalysts and details regarding the preparation parameters can be found in Table 5-1.

Table 5-1: List of heterogeneous catalysts synthesized.

Name	Metal and loading (wt%)	Additives	Annealing atmosphere
<b>Co-GN</b>	Co: 1.5%	-	NH <sub>3</sub> :Ar = 25:75
<b>2.8Rh-GN</b>	Rh: 2.8%	-	NH <sub>3</sub> :Ar = 25:75
<b>2.8Rh-tpGO</b>	Rh: 2.8%	-	Ar
<b>1Rh-GN</b>	Rh: 1%	-	NH <sub>3</sub> :Ar = 25:75
<b>1Rh-tpGO</b>	Rh: 1%	-	Ar
<b>1Rh-GP<sub>PPh<sub>3</sub></sub></b>	Rh: 1%	PPh <sub>3</sub>	Ar
<b>0.1Rh-GN</b>	Rh: 0.1%	-	NH <sub>3</sub> :Ar = 25:75
<b>0.01Rh-GN</b>	Rh: 0.01%	-	NH <sub>3</sub> :Ar = 25:75

The used metal precursors are: CoCl<sub>2</sub>·H<sub>2</sub>O for Co-GN and RhCl<sub>3</sub>·xH<sub>2</sub>O. Abbreviations: GO = graphene oxide, GN = N-doped thermally processed graphene oxide, tpGO = thermally processed graphene oxide, GP = P-doped thermally processed graphene oxide.

## 5.3 Characterization of the catalysts

The materials synthesized (summarized in Table 5-1) were characterized using different techniques which allow the investigation of the metal dispersion on the support and of the changes happening in the support.

TEM (Transmission Electron Microscopy) allows the characterization of the metal dispersion on the support. In particular, the use of HAADF-STEM (High-Angle Annular Dark-Field- Scanning Transmission Electron Microscope) and a high-resolution

instrument can identify single metal-atoms on the support.<sup>16, 25, 26</sup> This microscopy is also commonly used for the characterization of supported metal nanoparticles.<sup>19</sup>

During the microscopic characterization of the samples (TEM), EDX (Energy Dispersive X-ray Analysis) was also performed on the sample. This is a technique used to chemically characterize the materials. Elemental analysis was performed to quantify the Rh, the C and N present in the sample 0.1Rh-GN.

ATR-IR (Attenuated Total Reflection-IR) is a spectroscopic technique widely used to identify the functional groups present on the surface of carbon based materials.<sup>305-309</sup>

XRD (X-Ray Diffraction) allows the structural characterization of the material, enabling the identification of the type of support (GO, tpGO, reduced GO, graphite etc.).

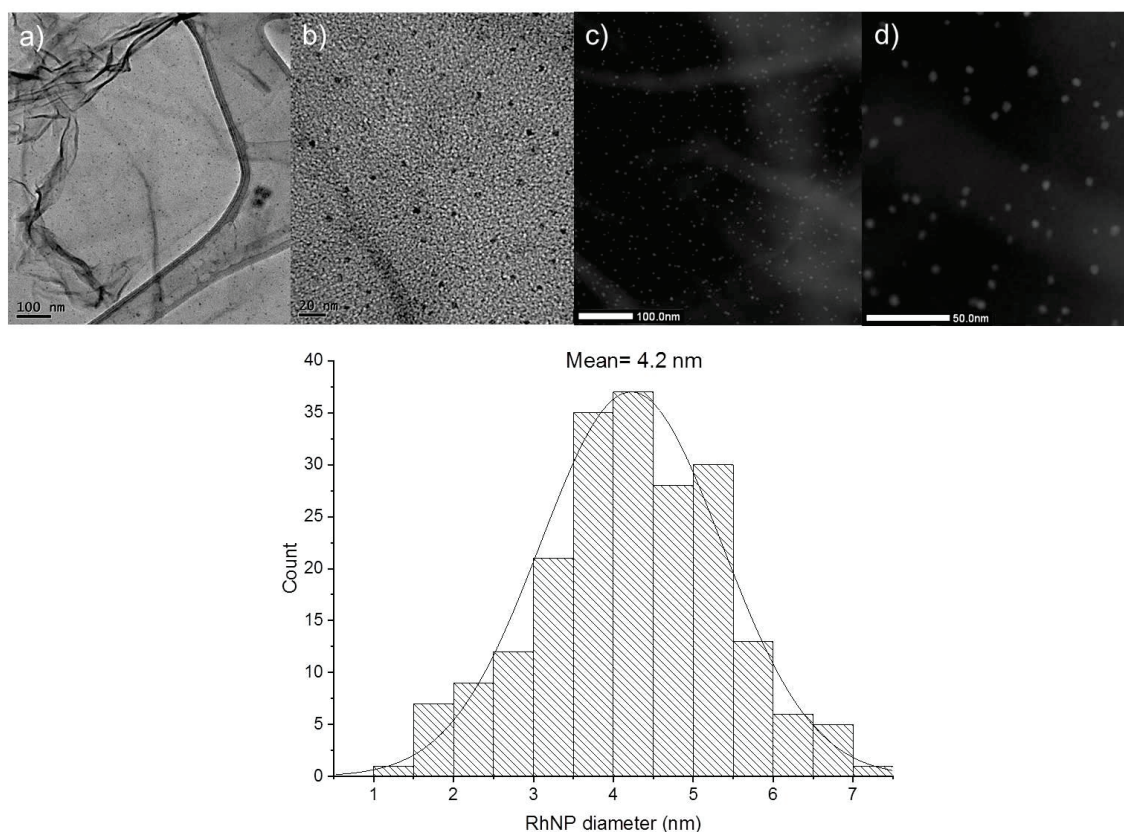


Figure 5-5: TEM images (a and b) and HAADF-STEM images (c and d) of the sample 1Rh-GN. The nanoparticles distribution is reported in the graph (bottom).



Raman spectroscopy is extremely useful in order to have information regarding the defects of carbon-based materials.

### **5.3.1 Characterization of the supported Rh**

The Rh is introduced as metal complex soluble in water. During the annealing, it can undergo through transformations which can lead to the production of large or small nanoparticles and/or agglomerates or dispersed single atoms.

TEM and HAADF-STEM were used to analyze 1Rh-GN, 1Rh-GP<sub>PPh<sub>3</sub></sub>, 0.1Rh-GN and 0.01Rh-GN.

The different amount of Rh appears to be crucial in determining the dispersion of the metal on the support. The samples with 1% of Rh shows the presence of nanoparticles, while the samples with 0.1% and 0.01% of Rh have Single Atoms dispersed on the surface.

The TEM and HAADF-STEM images of the sample 1Rh-GN are shown in Figure 5-5. The nanoparticles size was analyzed, and they resulted to have an average diameter of 4.2 nm. The distribution is fitted by a Gaussian curve with limits between 1 and 7 nm. The EDX analysis confirmed that the metal present in the sample is the Rh.

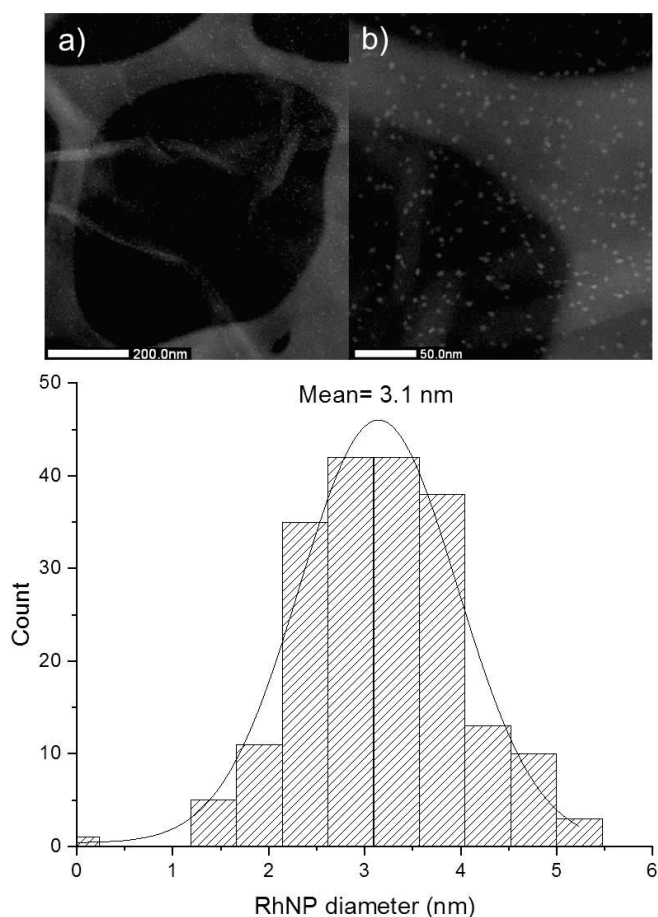


Figure 5-6: HAADF-STEM images (a and b) of the sample 1Rh-GP<sub>PPh<sub>3</sub></sub>. The nanoparticles distribution is reported in the graph (bottom).

The HAADF-STEM images of the sample 1Rh-GP<sub>PPh<sub>3</sub></sub> are shown in Figure 5-6. This procedure is leading to well distributed nanoparticles, clearly visible as bright spots on the support. The EDX analysis confirmed that the metal present in the sample is the Rh. The annealing in Ar and the use of PPh<sub>3</sub> during the synthesis lead to a different size of nanoparticles compared to those obtained using NH<sub>3</sub> during the annealing. In 1Rh-GP<sub>PPh<sub>3</sub></sub>, the nanoparticles have an average diameter of 3.1 nm and they appear to have a narrow distribution (from 1.5 to 5.5 nm) compared to those in 1Rh-GN.

Samples with a lower metal loading were prepared in order to achieve the synthesis of supported single atoms. In many reported examples, extremely low amount of Rh are used for the preparation of Single Atom Catalysts (SACs).<sup>18-20, 25, 29, 297</sup> This strategy is normally used for the preparation of SACs in wet-chemistry approaches, in order to reduce the tendency to aggregation during post-synthesis treatments (i.e. annealing).

During this phase, the ligands of the metal single-atom precursor are removed and the support should anchor the metal. Having a lower concentration of the metal reduces the risk of aggregation leading to the formation of nanoparticles.<sup>16</sup>

0.1Rh-GN analysis showed the presence of Rh single atom dispersed on the surface. The HAADF-STEM images collected are reported in Figure 5-7. The bright spots highlighted with red circles are identified as single atoms of Rh. The low resolution of the images is due to the mobility of the sample and of the Rh atoms in the conditions of the analysis, under the beam. The measurement of the bright spots revealed that the dimensions are between 0.14 and 0.26 nm, which correspond with the diameter of a single Rh atom forming a covalent bond. Due to the low resolution of the images the measurement does not result accurate, but it proves that Rh is present as isolated metal. These images proof the achievement of Rh SACs on N-doped thermally processed graphene oxide. The quantification of the metal amount resulted to be complex due to the small amount of metal present in the sample. The EDX analysis was performed during the analysis and showed the presence of 0.7% of Rh in the analyzed material. The quantification is not precise due to the very low amount of metal present in the sample. The elemental analysis should be affected by a smaller error compared to the EDX analysis. The elemental analysis reported that 0.19% of Rh is present in the sample, similarly to the theoretical amount of 0.1% of Rh.

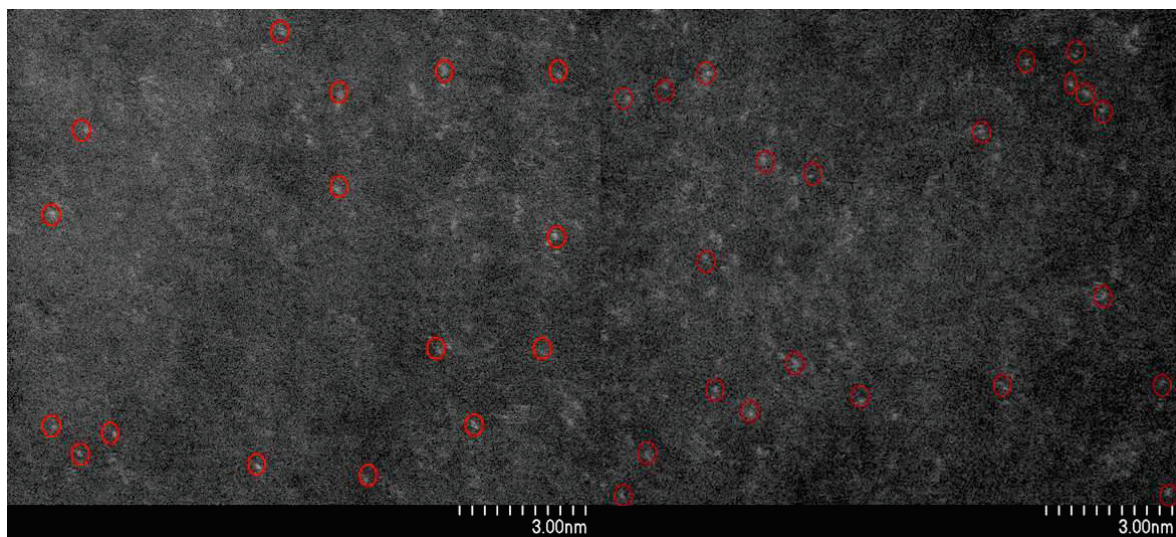


Figure 5-7: HAADF-STEM images of the sample 0.1Rh-GN.

Rh dispersed single atoms were found also in the sample 0.01Rh-GN. Also in this case, the sample was not stable during the analysis; therefore well resolved pictures could not be taken. The HAADF-STEM image of the sample 0.01Rh-GN is shown in Figure 5-8.

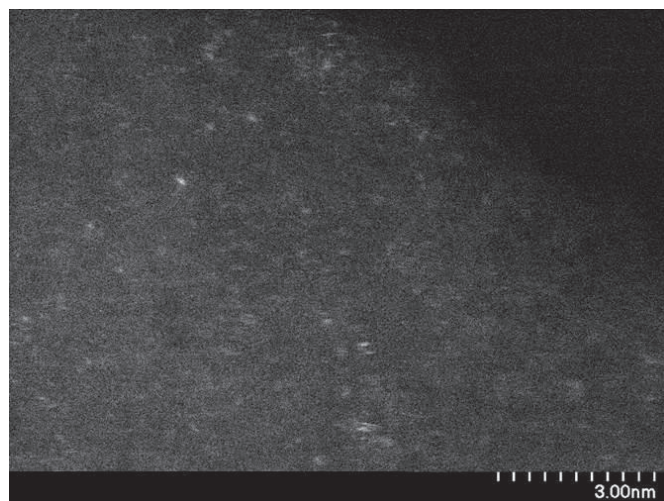


Figure 5-8: HAADF-STEM image of the sample 0.01Rh-GN.

The used techniques allowed the analysis of the Rh dispersion on the supports, highlighting the importance of the metal loading on the final distribution. Using small percentages of Rh (<0.1%) allows obtaining single atom catalysts (SACs).

### **5.3.2 Characterization of the carbon-based material**

The characterization of the carbon material is of high importance in order to fully understand the catalytic properties. It is known that carbon materials can be used as non-metal catalysts and that their activity is depending on structure, defects and functional groups present on them.<sup>310-312</sup>

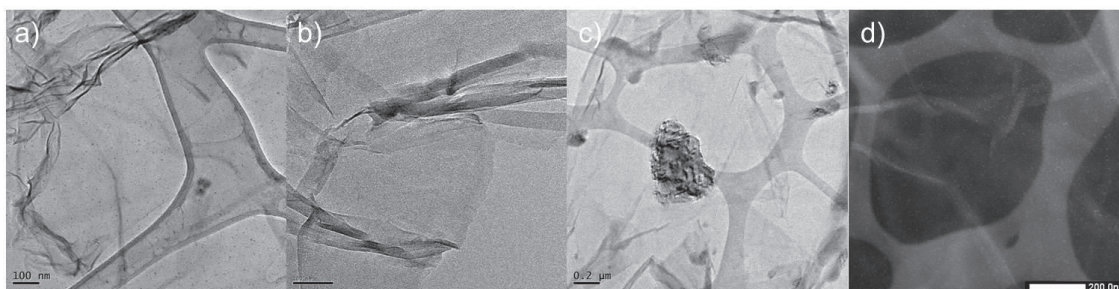


Figure 5-9: Low magnification TEM (a-c) and STEM (d) images of the samples 1Rh-GN (a), 0.1Rh-GN (b), 0.01Rh-GN (c) and 1Rh-GP<sub>PPh<sub>3</sub></sub> (d).

The TEM and STEM images at low magnification of the samples 1Rh-GN, 0.1Rh-GN, 0.01Rh-GN and 1Rh-GP<sub>PPh<sub>3</sub></sub> show that the materials are electron transparent (Figure 5-9). This means that the materials are formed of multi-layer structure with curling (for comparison see Xiong *et al.*<sup>313</sup> and Brycht *et al.*<sup>314</sup>). In the Figure 5-9c, a thicker particle can also be seen.

The position of the (002) diffraction peak gives information regarding the type of carbon material. In particular, it is possible to distinguish between GO, reduced GO, and N-doped GO. The XRD diffractograms of the samples GO, 1Rh-tpGO, 1Rh-GN, 0.1Rh-GN, 0.01Rh-GN, 1Rh-GP<sub>PPh<sub>3</sub></sub> are shown in Figure 5-10. The sample GO shows the characteristic diffraction peak at 10.2 °θ which testify the successful oxidation of the graphite.<sup>313</sup> This peak shifts to higher angles after the annealing treatment. In particular, in samples annealed in NH<sub>3</sub> atmosphere (1Rh-GN, 0.1Rh-GN and 0.01Rh-GN) a defined signal at 26.4 °θ is visible. This is typical of N-doped GO and testify the reduced number of oxygen-containing groups and the successful insertion of the N in the treated materials.<sup>313, 315</sup> The other samples do not show any well resolved peak. A signal around 25 °θ is characteristic of reduced GO, testifying the restoration of π conjugation.<sup>316</sup> In this case, the GO is not chemically reduced, but only thermally processed leading to more defective graphene, compared to a chemically reduced graphene oxide.<sup>317</sup> The high disorder can explain the weak (002) diffraction peak observed in the diffractograms of the thermally treated samples.

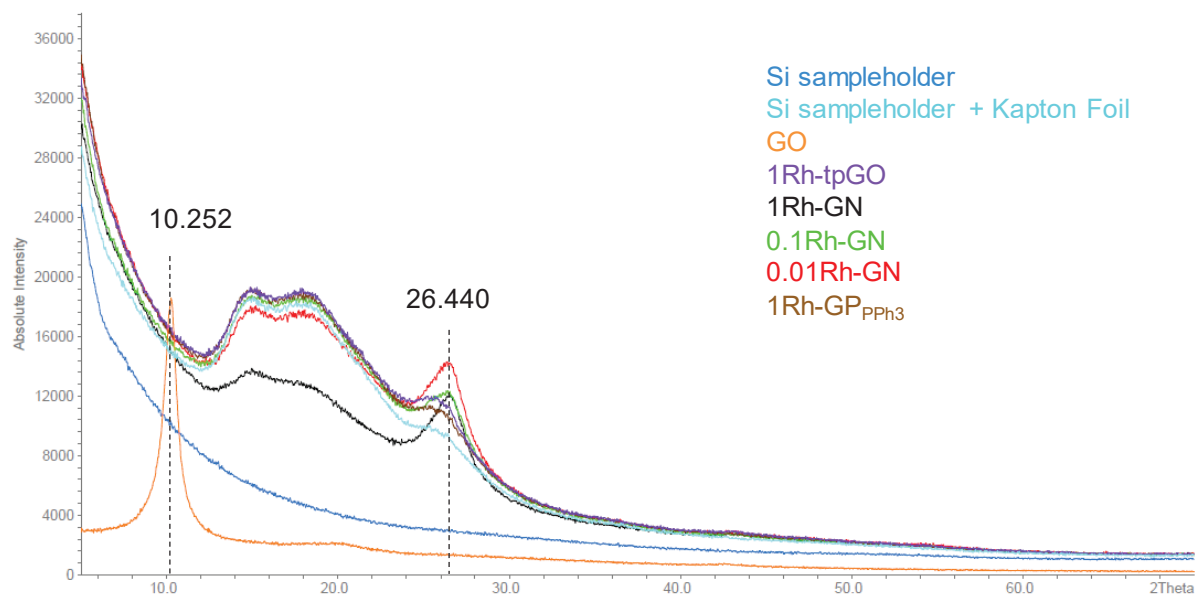


Figure 5-10: XRD diffractograms of the samples GO, 1Rh-tpGO, 1Rh-GN, 0.1Rh-GN, 0.01Rh-GN and 1Rh-GP. The samples were measure using a Si sampleholder with a Kapton Foil.

The Raman spectroscopy confirms the results obtained from the analysis of the XRD diffractograms. The measure of the amount of disorder in the sample can be determined from the distance between defects ( $L_D$ ). From the analysis of the full width at half-maximum of the D peak ( $\Gamma_D$ ) and of the intensity of D and G bands ( $I_D/I_G$ ) ratio, it is clear that the obtained materials are highly defective (Figure 5-11).<sup>318</sup> The  $\Gamma_D$  is over  $137\text{ cm}^{-1}$  for all the samples. This is very high and correspond to a  $L_D$  of about 1.5-2 nm (Figure 5-12, left).<sup>318</sup> An  $I_D/I_G$  ratio of 0.6-0.7 corresponds to the same  $L_D$  (Figure 5-12, right). In addition, this information demonstrates that the distance between defects in the synthesized materials is increasing at decreasing  $I_D/I_G$  ratio (Figure 5-12).<sup>318</sup> The samples annealed in  $\text{NH}_3$  have the same defect density as the starting GO materials, while the sample with  $\text{PPh}_3$  annealed in Ar has a higher defect density. The higher defectivity of the samples annealed in Ar can happen due to the full decomposition of the oxygen-containing functional group leading to defects in the structure. In case  $\text{NH}_3$  is present, new groups can be formed during the decomposition avoiding the formation of additional defects.

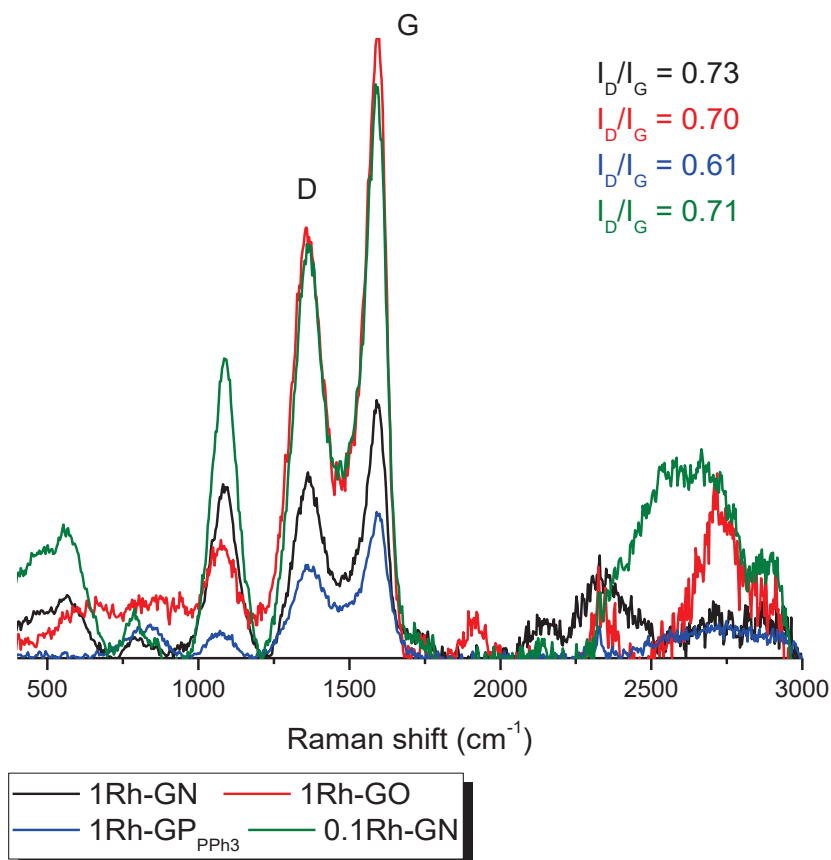


Figure 5-11: Raman spectra of the samples 1Rh-GN, 1Rh-GO, 1Rh-GP<sub>PPh<sub>3</sub></sub> and 0.1Rh-GN.

The synthesis of 1Rh-GN was followed via ATR spectroscopy (Figure 5-13). First, the synthesized GO was analyzed. It shows the peaks characteristic of graphene oxide:<sup>305-309</sup>

- 865  $\text{cm}^{-1}$ : C-O vibration of epoxides,
- 1000  $\text{cm}^{-1}$ : C-O stretch of C-OH (hydroxyl group),
- 1230  $\text{cm}^{-1}$ : C-O stretch of C-O (phenols, ethers and epoxy groups)
- 1370  $\text{cm}^{-1}$ : O-H bending and/or C-O vibration,
- 1615  $\text{cm}^{-1}$ : bending modes of adsorbed water molecules and C=C stretch of un-oxidized  $\text{sp}^2$  carbon domain,
- 1720  $\text{cm}^{-1}$ : C=O stretch attributed to carboxyl and carbonyl groups,
- 2985  $\text{cm}^{-1}$ : C-H stretching,
- 3200  $\text{cm}^{-1}$ : O-H stretching of adsorbed water molecules
- 3350  $\text{cm}^{-1}$ : O-H (hydroxyl) groups of GO,

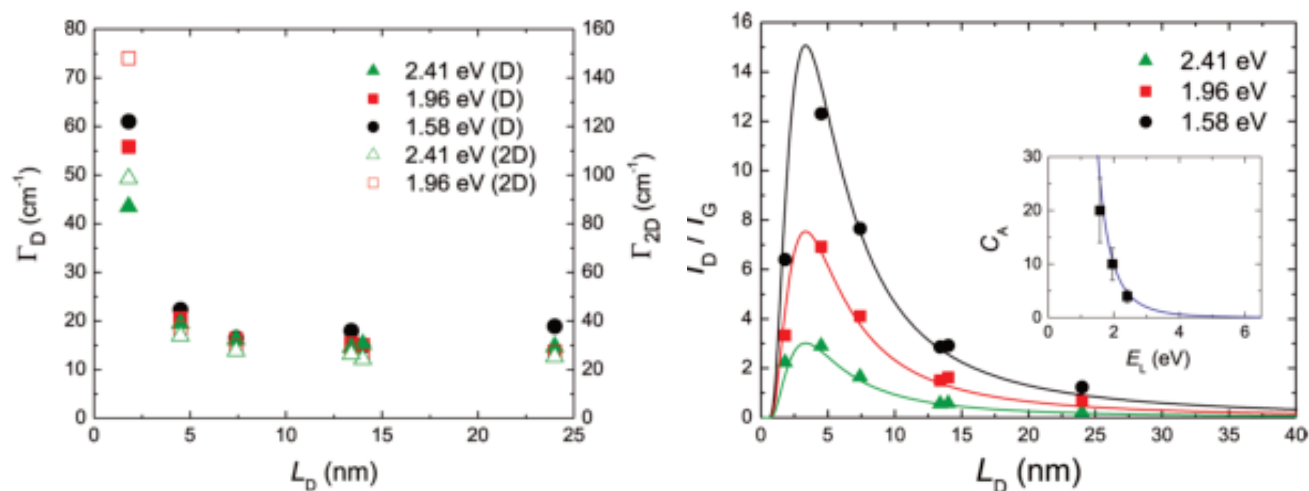


Figure 5-12: Full width at half-maximum ( $\Gamma_D$ ) and  $I_D/I_G$  relations to  $L_D$  as reported by Cancado *et al.*

- 3580  $\text{cm}^{-1}$ : O-H stretching of free water and/or of carboxylic acid groups.

The band due to –OH signal is very broad (normally between 3000 and 3700  $\text{cm}^{-1}$ ) due to the different types of OH bond present in the sample: free and intercalated  $\text{H}_2\text{O}$  (multilayer GO) interacting with different hydroxyl and carboxylic groups, as well as hydroxyl and carboxyl groups of the graphene oxide themselves.<sup>309</sup> In our case, the band is overlapping with other signals (C-H bonds) making it even broader (2300-3600  $\text{cm}^{-1}$ ).

In addition to the assigned peaks, the spectra may be the results of other less intense peaks, overlapping with the above-mentioned signals and not well defined. The area between 850 and 1500  $\text{cm}^{-1}$  is probably including additional signals from lactols, peroxides, dioxolanes, hydroxyls, 1,3-dioxan-2-ones, anhydrides, benzoquinones and ethers.<sup>309</sup>

The ATR analysis shows that no obvious change in the functional groups of the support happens during the sonication and lyophilization, meaning that the GO structure is retained (1Rh-GO). The functional groups are different after the annealing process in  $\text{NH}_3$  (1Rh-GN). This is expected as a consequence of a treatment at high temperature<sup>314, 317</sup> and in presence of a metal.<sup>307</sup> The treatment at high temperature is known to modify the GO structure. In particular, the functional groups are drastically reduced in number due to decomposition reactions such those reported in Scheme 5-1.<sup>317</sup> The  $\text{CO}_2$  produced in the decomposition process could be adsorbed on the



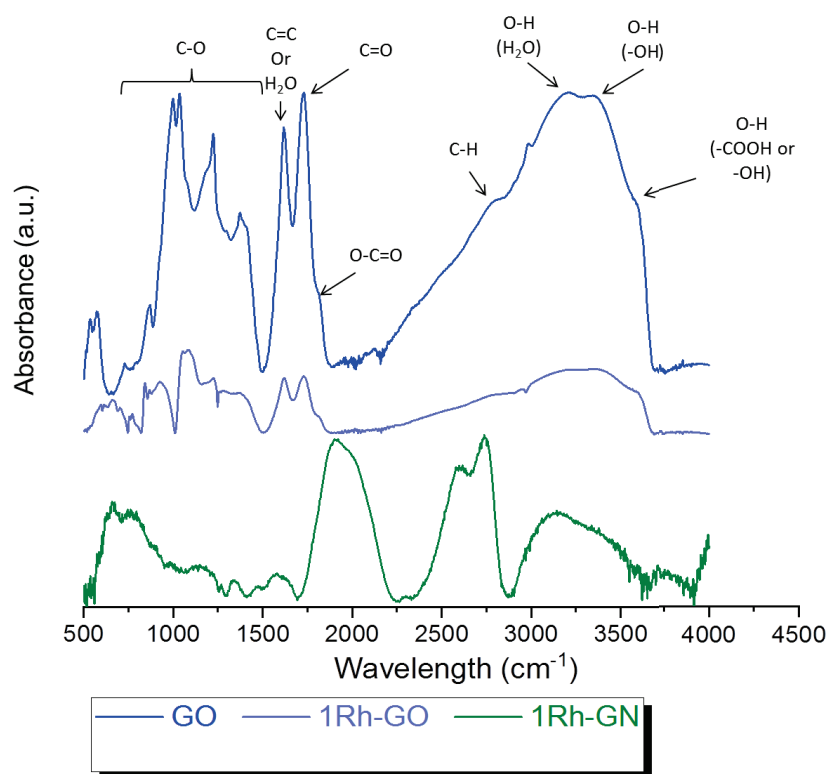


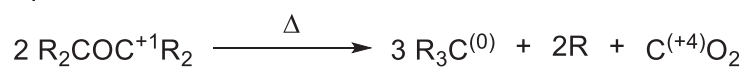
Figure 5-13: ATR spectra registered for GO (blue line), 1Rh-GO (light blue line) and 1Rh-GN (green line).

graphene giving a strong signal at  $2336\text{ cm}^{-1}$ .<sup>314</sup> This region is not showing any intense signal in the spectra of the 1Rh-GN (Figure 5-13), so  $\text{CO}_2$  is probably removed during the process. In addition, the metal can catalyze different reactions of the support and the functional groups present on it.<sup>307</sup>

The ATR spectroscopy gives more information regarding the materials obtained during the annealing process. The removing of most functional groups testified by the lower number of peaks in the spectra (Figure 5-14) demonstrates the success of the thermal process performed on the GO. It is worth noting that the presence of the Rh on the sample is leading to similar functional groups on the surface, regardless the treatment performed. The samples with Rh have a strong signal with a maximum at  $1890\text{--}1900\text{ cm}^{-1}$ . This signal can be likely assigned to  $\text{C}=\text{C}=\text{C}$  bonds (allenes)<sup>319, 320</sup>,  $\text{C}\equiv\text{C}$  bonds coordinated or not-coordinated to the Rh<sup>321, 322</sup>,  $\text{C}=\text{C}=\text{N}$  bonds (ketenimines)<sup>323</sup> and  $\text{C}\equiv\text{N}$  bonds<sup>324</sup>. The materials annealed in  $\text{NH}_3$  shows a stronger band from  $3000$  to  $3500\text{ cm}^{-1}$ . This can be assigned to N-H bonds in the carbon lattice<sup>285, 325, 326</sup> and to N-H bond of amine groups coordinated to the Rh.<sup>327</sup> The

presence of the stronger band in the samples treated with NH<sub>3</sub> can also depend on the adsorbed H<sub>2</sub>O. The insertion of N in the carbon lattice can increase the hydrophilicity of

*Epoxides*



*Ketones*



Scheme 5-1: Thermal decomposition reactions of epoxides (top) and ketones (bottom) group on GO surface: both the reactions are disproportion leading to C<sup>0</sup> and C<sup>+2</sup> or C<sup>+4</sup>.

the N-doped GO compared to the standard tpGO, where few polar bonds are present. In the samples xRh-GN, it seems that the presence of the Rh is favoring the insertion of the N in the carbon lattice. The large band observed in the spectra can as well be the result of different N group, some linked to the Rh particles or single atoms and some not coordinated. The effect of the Rh does not depend on the loading. Different loadings of Rh lead to same functional groups on the carbon surface (Figure 5-15).

The functional groups obtained during the annealing of GO in presence of NH<sub>3</sub> are different from those obtained in presence of the metal. In the NH<sub>3</sub> annealed GO the main functional groups could be assigned to ammine groups (mostly aromatic), which gives signals with a maximum at 1200 and 1550 cm<sup>-1</sup>.<sup>285, 325, 326</sup> It appears that the Rh is catalyzing different reactions on the support itself leading to a different thermal decomposition process.

The sample 0.1Rh-GN (where single Rh dispersed atoms are present) was characterized via elemental analysis. The analysis confirmed the insertion of the N in the carbon lattice. The percentages of the different elements (CHN analysis) detected are the following:

- C: 79.48% (wt %)
- N: 10.71 % (wt %),
- H: 1.87% (wt %).

To conclude, the synthesis used to prepare the samples leads to thermally processed graphene oxide with or without N in the carbon lattice. The synthesis with  $\text{PPh}_3$  as additive seems to generate a material similar to the one obtained without any heteroatom-doping agent. All the samples are highly defective and with lower variety of functional groups compared to the original GO material. The presence of the metal leads to the production of different bonds in the final materials. For instance, the presence of the Rh facilitates the insertion of the N dopant in the carbon lattice.

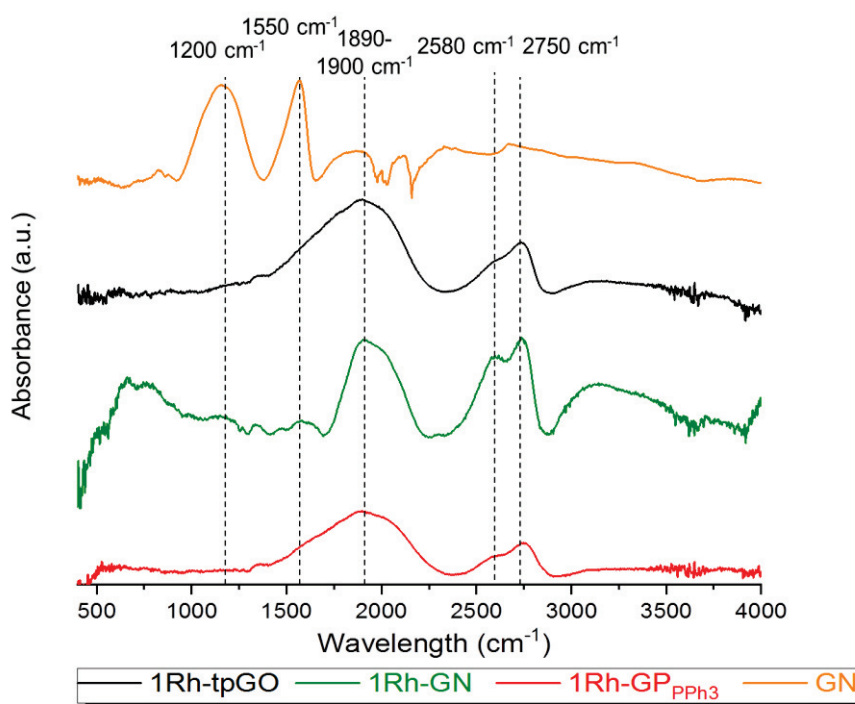


Figure 5-14: ATR spectra of the samples 1Rh-tpGO, 1Rh-GN, 1Rh-GP<sub>PPH3</sub> and GN.

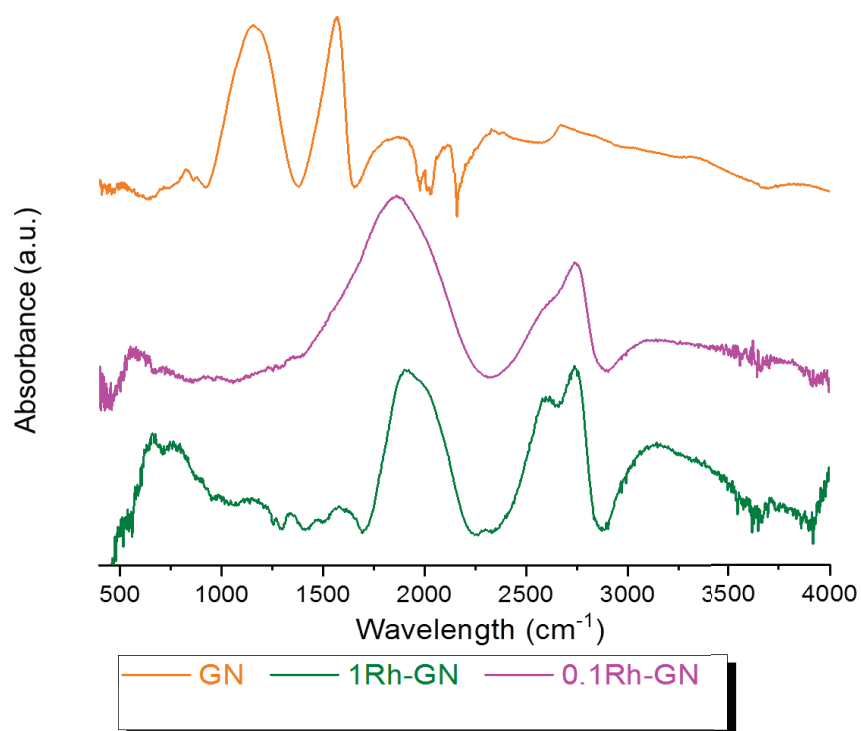
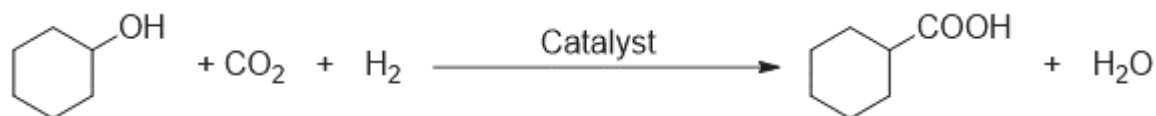


Figure 5-15: ATR spectra of the samples GN, 1Rh-GN and 0.1Rh-GN.

## 5.4 Catalytic tests

Table 5-2: Catalytic tests for the screening of different heterogeneous catalysts for the hydrocarboxylation reaction of the cyclohexanol.



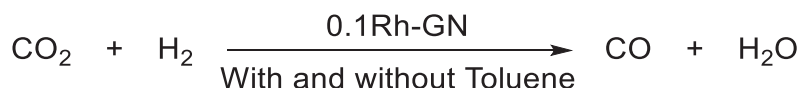
Entry	Catalyst <sup>[c]</sup>	[RhCl(CO) <sub>2</sub> ] (mmol <sub>Rh</sub> )	PPh <sub>3</sub> (mmol)	Solvent (2 ml)	Conv (%)	Mass Balance (%)	Cyclohexyl carboxylic acid (%)
1	-	1•10 <sup>-4</sup>	4•10 <sup>-2</sup>	Toluene	51	27	0
2	Co-GN	0	0	Toluene	90	56	0
3	1%Rh-GN	0	4•10 <sup>-2</sup>	Acetic acid	>99	96	0
4 <sup>[a]</sup>	1%Rh-GP	0	4•10 <sup>-2</sup>	Acetic acid	>99	35	0
5	1%Rh-GN	0	0	Toluene	42	64	0
6	1%Rh-GP	0	0	Toluene	63	68	0
7 <sup>[b]</sup>	1%Rh-GN	0	0	Toluene	32	68	0
8 <sup>[b]</sup>	1%Rh-GP	0	0	Toluene	23	77	0
9	1%Rh-GN	1•10 <sup>-4</sup>	0	Toluene	74	65	0
10	1%Rh-GN	1•10 <sup>-4</sup>	4•10 <sup>-2</sup>	Toluene	61	54	0
11	1%Rh-GP	1•10 <sup>-4</sup>	4•10 <sup>-2</sup>	Toluene	63	60	0
12	1%Rh-GP	1•10 <sup>-4</sup>	0	Toluene	80	53	0
13 <sup>[b]</sup>	0.1Rh-GN	-	0	Acetic acid	80	80	0
14 <sup>[b]</sup>	0.01Rh-GN	-	0	Acetic acid	83	83	0

Other parameters: 0.94 mmol of cyclohexanol, 2 ml of solvent, 160 °C, 20 bar of CO<sub>2</sub> and 10 bar of H<sub>2</sub>.

[a] 280 °C. [b] 0 eq. of CH<sub>3</sub>I and 0 eq. of p-TsOH•H<sub>2</sub>O. [c] 2.4•10<sup>-4</sup> mmol<sub>Rh</sub>.

Co-GN, 1Rh-GN and 1Rh-GP were tested for the hydrocarboxylation of cyclohexanol to cyclohexylcarboxylic acid (CA). 2.5 mg of catalyst was used leading to

a Rh:cyclohexanol of 0.00024:0.94 (0.03%). The catalyst loading results to be limited compared to the one used in the corresponding homogeneous system (5%). The catalytic tests were done in different reaction conditions. Initially, toluene was used as solvents. Using the same amount of homogeneous catalyst in toluene no activity was observed (Entry 1, Table 5-2). At the same time, using the heterogeneous systems did not lead to any improvement. Different conditions were applied: without any additional additives (PPh<sub>3</sub>, CHI<sub>3</sub> and *p*-TsOH•H<sub>2</sub>O), with all the additives and only with CHI<sub>3</sub> and *p*-TsOH•H<sub>2</sub>O, with acetic acid as solvent (details are reported in entries 2-8, Table 5-2). In all cases, the yield in carboxylic acid and CO was 0. The hydrogenation activity as well was reduced compared to the homogeneous system (almost no hydrogenation product was detected). To check if the heterogeneous catalysts were able to catalyze only one cycle but not both, we combined the homogeneous and the heterogeneous

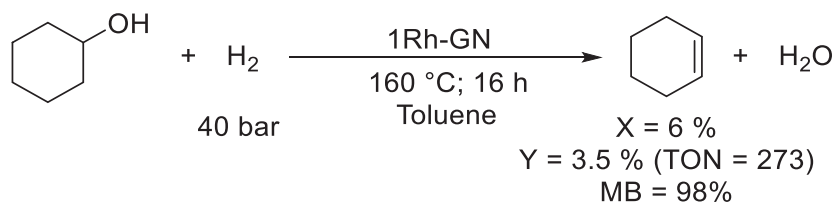


Scheme 5-2: Scheme of the *r*WGSR catalytic tests performed using SACs (0.1Rh-GN). Reaction conditions: 2.5 mg of 0.1Rh-GN, 20 bar of CO<sub>2</sub>, 20 bar of H<sub>2</sub>, 2 ml of toluene if used, 200 °C and 16 hours of reaction.

catalysts (Entries 9-12, Table 5-2). In this case, the hydrogenation is observed, but no CO or CA were produced. Similar results are obtained when 0.1Rh-GN and 0.01Rh-GN are used as catalysts (Entries 13-14, Table 5-2)

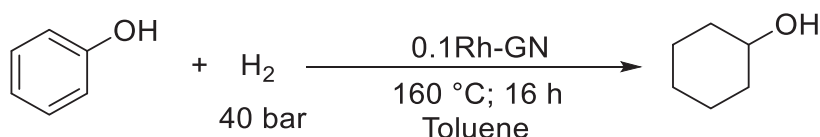
The catalysts were tested for the *r*WGSR in different conditions. The 0.1Rh-GN was used in the absence of solvent or in presence of 2 ml of toluene to transform CO<sub>2</sub> and H<sub>2</sub> into CO and H<sub>2</sub>O (Scheme 5-2). The catalysts are not active for the *r*WGSR, as no CO is detected.

Considering the hydrogenation activity of the homogeneous Rh catalyst, tests were carried out in order to test the hydrogenation activity of the heterogenous system. The tests were done using at first cyclohexanol, 40 bar of H<sub>2</sub>, toluene as solvent and the catalyst 1Rh-GN (as reported in Scheme 5-3). No hydrogenation activity was detected, but only the dehydration of 3.5 % of cyclohexanol to cyclohexene was achieved. Better results can be achieved by the use of the conditions reported in Entry 1, Table 5-2. For this reason, no more investigations were performed.



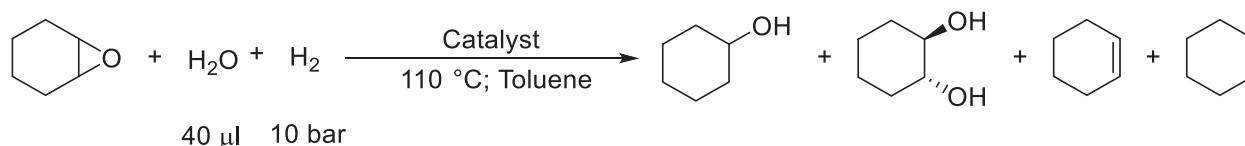
Scheme 5-3: Scheme of the hydrogenation reaction of cyclohexanol. Reaction conditions: 2.5 mg of 1Rh-GN, 1.88 mmol of cyclohexanol, 40 bar of H<sub>2</sub>, 2 ml of toluene, 160 °C and 16 hours of reaction.

The hydrogenation of the phenol to cyclohexanol would allow obtaining cyclohexyl carboxylic acid starting from the aromatic substrate. Therefore, 0.1Rh-GN was tested as catalyst for the hydrogenation of phenol using 40 bar of H<sub>2</sub> (Scheme 5-4). The material resulted not to be a catalyst for this reaction in the tested conditions, since no conversion was observed.



Scheme 5-4: Scheme of the hydrogenation of the phenol to cyclohexanol. Reaction conditions: 2 mg of 0.1Rh-GN, 2 mmol of phenol, 40 bar of H<sub>2</sub>, 2 ml of toluene, 160 °C and 16 hours of reaction.

As reported in Scheme 3-16, the homogenous Rh catalyst seems to be able to perform the transformation of the epoxide into the mono-alcohol or mono-iodide. The hydrogenolysis of the epoxide to mono-alcohols can happen in the absence of iodide sources and in the presence of H<sub>2</sub>O and H<sub>2</sub>. The hydrogenolysis of epoxide can be an interesting reaction in organic synthesis and the production of biologically active compounds.<sup>328</sup> This reaction is rarely reported in literature<sup>329-331</sup> and often requires a hydrogenation agent such as hydrazine<sup>332</sup>, NaBH<sub>4</sub><sup>328</sup> or formic acid<sup>333</sup>.



Scheme 5-5: Scheme of the hydrogenolysis reaction of cyclohexane oxide to cyclohexanol. Reaction conditions: 2 mg of catalyst, 1.88 mmol of cyclohexane oxide, 40  $\mu$ l of H<sub>2</sub>O, 10 bar of H<sub>2</sub>, 3 ml of toluene, 110 C and 16 hours of reaction.

The synthesized materials were tested as catalysts for this reaction using H<sub>2</sub>O (40  $\mu$ l) and H<sub>2</sub> (10 bar) as hydrogenolysis agents as reported in Scheme 5-5.

Table 5-3: Results of the catalytic hydrogenolysis of cyclohexane oxide to cyclohexanol using different synthesized materials. Entry 1 reports in bracket the results obtained when the reaction was reproduced with fresh catalyst (test # 2).

Entry	Cat	Conv (%)	Mass Balance (%)	Cyclohexane (%)	Cyclohexene (%)	Trans-cyclohexane diol (%)	Cyclohexanol (%)		
							Yield (%)	TON	Selectivity (%)
1	0.1Rh-GN (test # 2)	38 (8)	90 (98)	1 (0)	3 (4)	3 (1)	25 (1)	22758 (1091)	67 (15)
2	Recycled-0.1Rh-GN	16	96	0.5	4	1.5	6	5612	38
3 <sup>[a]</sup>	0.1Rh-GN	6	98	0	2	2	0	0	0
4 <sup>[b]</sup>	0.1Rh-GN	12	95	2	3	2	1	1397	8
5	-	26	91	1	3	5	9	-	35
6	0.01Rh-GN	19	93	0.3	3	3	5	48392	28
7	1Rh-GN	15	96	0.4	4	1	6	507	40
8	1Rh-G	13	97	0.6	4	2	3	299	26
9	1Rh-GP <sub>PPh<sub>3</sub></sub>	13	97	1	3	1	5	487	38
10	0.1Rh-GO	72	62	0	4	28	2	1813	3
11	[Rh] <sup>[c]</sup>	>99	63	1	3	58	0	0	0

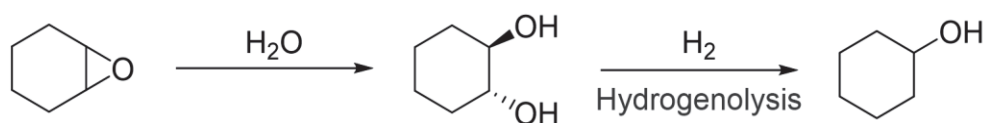
[a] No H<sub>2</sub> was used in this test. [b] No H<sub>2</sub>O was used in this test. [c] [RhCl(CO)<sub>2</sub>]<sub>2</sub>



The results of the catalytic tests are reported in Table 5-3. The best yield is achieved using the catalyst 0.1Rh-GN. 25 % of cyclohexane oxide is converted to cyclohexanol (Entry 1, Table 5-3). Considering the low amount of metal loading, this corresponds to a remarkable TON (Turnover Number) of 22758 ( $\text{mol}_{\text{product}}/\text{mol}_{\text{Rh}}$ ). This is the only catalyst giving higher yield of cyclohexanol compared to the blank test (Entry 5, Table 5-3). Higher TON were achieved using the catalyst 0.01Rh-GN (Entry 6, Table 5-3), but it is due only to the reduced amount of metal and not to higher yields. Higher metal loading did not bring to an improvement of the yield (Entries 7-9, Table 5-3), regardless the heteroatom inserted or not in the lattice. This behavior could be ascribed to the higher activity of isolated Rh atoms on the surface of the N-doped graphene. On the contrary, the presence of nanoparticles can lead to lower reactivity.

The use of the homogeneous catalyst does not produce cyclohexanol in the reaction conditions used for the test (Entry 11, Table 5-3). At the same time, the material 0.1Rh-GO ( $\text{RhCl}_3 \cdot x\text{H}_2\text{O}$  dispersed on GO) does not give good yields of cyclohexanol as the annealed 0.1Rh-GN, which contains Rh SACs.

The catalyst used in Entry 1, Table 5-3 was recycled via centrifugation and following removal of the supernatant solution. The same procedure was repeated using dichloromethane to wash the catalyst. After the catalyst was dried, it was used for a second test. Details regarding the recycling procedure are reported in the Experimental part of this chapter. The result of the test is reported in Entry 2, Table 5-3. This catalyst results to be still active, although the yield of cyclohexanol is lower (6 %) compared to the one obtained with the fresh catalyst.



Scheme 5-6: Suggested reaction pathway for the hydrogenolysis of cyclohexane oxide.

Tests in absence of  $\text{H}_2$  (Entry 3, Table 5-3) and in absence of  $\text{H}_2\text{O}$  (Entry 4, Table 5-3) were done. Both the reagents seem to be needed for the reaction. In absence of  $\text{H}_2$  only small amount of diol and alkene were formed, while in absence of  $\text{H}_2\text{O}$  the reaction proceeded to give the cyclohexane as well. The need of both the reagents indicates a mechanism like that reported in Scheme 5-6. The  $\text{H}_2\text{O}$  is probably needed to open the ring and form the diol, which is transformed in mono-alcohol through the

hydrogenolysis reaction. The hydrogenolysis of diols or other molecules with more hydroxyl groups was reported before. In particular, the hydrolysis of glycerol was widely studied.<sup>334</sup> It is reported that catalysts with acid/base properties and redox properties are needed to perform the transformation. Usually, the acidic or basic properties of the support (i.e. metal oxides) are essential for the removal of one –OH group. Following, the redox properties of the catalyst (i.e. metal nanoparticles) catalyze the addition of H<sub>2</sub>.<sup>334</sup> Accordingly to this theory, the N-doped graphene is known to have basic properties,<sup>335, 336</sup> and the presence of Rh single atom can provide the redox properties to the material.

The run with a second portion of the fresh catalyst (Entry 1, test # 2, Table 5-3) lead to only 1% yield of cyclohexanol.

The materials synthesized are highly interesting due to the presence of potentially highly active single Rh atoms dispersed on a tunable support such as doped graphene oxide. In particular, they seem promising catalysts for interesting hydrogenolysis reactions.

## 5.5 Conclusion and outlook

The development of Rh SACs for the hydrocarboxylation reaction was attempted. The characteristics of carbon materials make them good supports for SACs preparation. For this reason, in this study, this type of supports was used, inserting N and/or P atoms in the lattice. Using simple wet chemistry methods, many materials were synthesized. New materials can be produced starting from different GO, using different P-doping materials (more hydrophilic phosphines) and changing the Rh precursor.

The used techniques allowed the analysis of the Rh dispersion on the supports, revealing the presence single atom catalysts (SACs) on samples with Rh loading equal or lower than 0.1% (wt %). The use of other techniques (XPS, EXAFS and CO-adsorbed high resolution IR) would give further information regarding the oxidation state of the Rh atoms and the chemical environment of the metal.

The thermal treatments performed on the original GO lead to different materials: thermally processed GO or heteroatom-doped graphene-like materials. The presence of the metal leads to the production of different bonds in the final materials. For instance, the presence of the Rh facilitates the insertion of the N dopant in the carbon lattice. Further characterization of the materials can be performed in the future using techniques such as XPS, solid state NMR, Temperature Programmed Desorption/Mass Spectrometry (TPD/MS) in order to obtain a more detailed chemical characterization of the carbon materials. Surface area analysis would be highly interesting as well.

The materials synthesized contain potentially highly active single Rh atoms dispersed on a tunable support such as doped graphene oxide. In particular, they seem promising catalysts for interesting hydrogenolysis reactions. Nevertheless, further studies on the catalytic activity should be performed. At first, the reproducibility of the results should be assessed. Following, a variation of the reaction conditions should be studied in order to improve the results obtained. Further studies on the recycled catalysts and the leaching should be provided to evaluate the materials as catalysts.

## 5.6 Experimental

### 5.6.1 Preparation of SACs

Co-GN catalyst was prepared following the procedure reported elsewhere.<sup>26</sup> The used graphene oxide (GO) was prepared following a the improved Hummer method reported elsewhere.<sup>337</sup>

Rh-GN catalysts were prepared dissolving 100 mg of GO in 50 ml of deionized water. The suspension was sonicated for 2h. 1 ml of  $\text{RhCl}_3 \cdot x\text{H}_2\text{O}$  (40% Rh, Abcr supplier) water solution was added to the suspension and the obtained mixture was sonicated for 10 min. 0.1% Rh-GN was prepared with a solution  $0.25 \text{ mg}_{[\text{Rh}]} / \text{ml}_{\text{H}_2\text{O}}$ , 1%Rh-GN was prepared with a solution  $2.5 \text{ mg}_{[\text{Rh}]} / \text{ml}_{\text{H}_2\text{O}}$  and 2.8%Rh-GN with a solution  $6.5 \text{ mg}_{[\text{Rh}]} / \text{ml}_{\text{H}_2\text{O}}$ . The water was then removed by lyophilization overnight. The obtained foam was collected for the following thermal treatment. The sample was positioned in a quartz tube and flashed with Ar (100 ml/min) for 10 minutes. A 100 ml/min flow of  $\text{NH}_3/\text{Ar}$  (25/75 mol/mol bought from AirLiquid) was sent through the tube and the temperature was raised to 750 °C (ramp: 20 °C/min). The temperature was kept for 1 h. After, the sample was brought to room temperature under an Ar flow (100 ml/min). The black solid was recovered and stored under air. A scheme of the system used for the annealing procedure is reported in Figure 5-16.

Rh-GP catalysts were prepared dissolving 100 mg of GO and about 20 mol<sub>P</sub>/mol<sub>Rh</sub> of phosphine in 50 ml of deionized water. The suspension was sonicated for 2h. 1 ml of  $\text{RhCl}_3 \cdot x\text{H}_2\text{O}$  solution was added to the suspension and the obtained mixture was sonicated for 10 min. 0.1% Rh-GP<sub>PPh<sub>3</sub></sub> was prepared with a solution  $0.25 \text{ mg}_{[\text{Rh}]} / \text{ml}_{\text{H}_2\text{O}}$  adding 51 mg of PPh<sub>3</sub>. The water was then removed by lyophilization overnight. The obtained foam was collected for the following thermal treatment. The sample was positioned in a quartz tube and flashed with Ar (100 ml/min) for 10 minutes. The temperature was raised to 750 °C (ramp: 20 °C/min). The temperature was kept constant for 1 h. After, the sample was brought to room temperature under an Ar flow (100 ml/min). The black solid was recovered and stored under air.

Rh-tpGO catalysts were prepared dissolving 100 mg of GO in 50 ml of deionized water. The suspension was sonicated for 2h. 1 ml of  $\text{RhCl}_3$  solution was added to the suspension and the obtained mixture was sonicated for 10 min. 1%Rh-tpGO was prepared with a solution  $2.5 \text{ mg}_{[\text{Rh}]} / \text{ml}_{\text{H}_2\text{O}}$  and 2.8%Rh-tpGO with a solution  $6.5$

$\text{mg}_{[\text{Rh}]}/\text{ml}_{\text{H}_2\text{O}}$ . The water was then removed by lyophilization overnight. The obtained foam was collected for the following thermal treatment. The sample was positioned in a quartz tube and flashed with Ar (100 ml/min) for 10 minutes. The temperature was raised to 750 °C (ramp: 20 °C/min). The temperature was kept for 1 h. After, the sample was brought to room temperature under an Ar flow (100 ml/min). The black solid was recovered and stored under air.

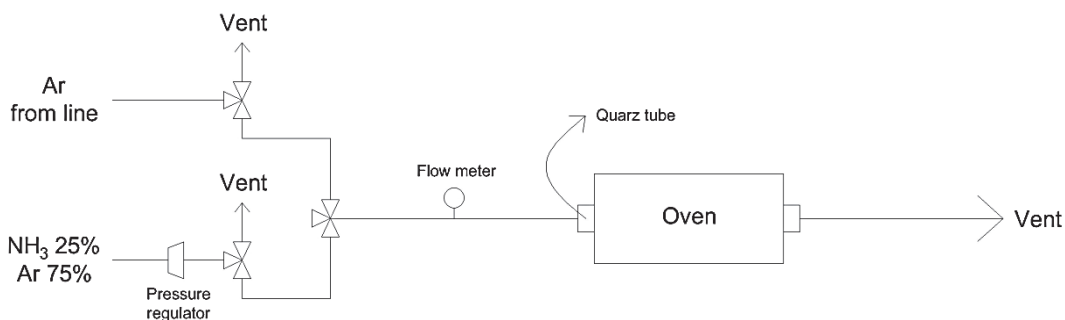


Figure 5-16: Flow sheet of the continuous flow system used to perform the annealing of the catalysts.

### 5.6.2 Autoclaves reactions

Acetic acid and toluene were pre-dried over molecular sieves (4 Å), then degassed by bubbling argon with a frit for at least 1 h, and stored over molecular sieves (4 Å) under argon. All substrates were degassed by three freeze-pump-thaw cycles and stored over molecular sieves (4 Å) under argon. Water contents were monitored by Karl-Fischer titration (*Metrohm 756 F Coulometer*) and typically kept under 100 ppm. All reagents were commercially supplied and used as received unless stated otherwise.

The catalytic runs were performed in 10 ml stainless steel autoclaves. To avoid blind activity, the autoclaves were equipped with glass inlets. The catalyst, iodide, acid and phosphine additives were weighed in the glass inlet and then put in the autoclaves. The autoclaves containing the catalyst, iodoform ( $\text{CHI}_3$ ), triphenylphosphine ( $\text{PPh}_3$ ) and *para*-toluenesulfonic acid monohydrate ( $p\text{-TsOH}\cdot\text{H}_2\text{O}$ ) were evacuated at high vacuum and then charged with an argon atmosphere. When no additive was used to perform the reaction the autoclave containing the catalyst was flashed with Ar carefully for 3 times. Following, the solvent and the substrates were added into the autoclave. The

autoclave was pressurized with CO<sub>2</sub> and/or H<sub>2</sub>. The obtained reaction mixture was analyzed via gaschromatography (GC).

The catalyst 0.1Rh-GN was recycled. The recycling procedure consisted of a first centrifugation (40 min, 2000 rpm) and following separation of the supernatant. The solid was washed with dichloromethane (DCM) and the same procedure was repeated. The catalyst was collected with clean DCM and transferred in an autoclave inlet. The remaining DCM was evaporated completely at 50 °C. In this way, 1.9 mg out of 2.0 mg of catalyst were recovered.

### 5.6.3 Gas chromatography

GC analyses of the liquid phases were performed on a *Trace GC Ultra* (ThermoScientific) using a packed *CP-WAX-52-CB* column (length = 60 m, diameter = 0.25 mm) isothermally at 50°C for 5 min, then heated to 200°C at 8°C min<sup>-1</sup>. A constant flow of 1.5 mL min<sup>-1</sup> He was applied. The gas chromatograph was equipped with a FID detector. GC analysis of CO, CO<sub>2</sub> and H<sub>2</sub> gases were performed on a *HP6890* using a capillary Chem Carbon ST column (length = 2 m) isothermally at 35 °C for 5 min, then heated to 150 °C at 8 °C/min. A constant flow of 25 ml/min of He was applied. The gas chromatograph was equipped with a TCD detector.

Liquid substances were analyzed using (±)-1-phenylethanol and/or dodecane as standard. Acetone was used as a solvent (for cyclohexanol reactions acetone was substituted by dichloromethane). The correction factor was calculated preparing solutions with known amount of substances and standard. The gas substances were analyzed using ethane as standard. As for the liquid samples, the correction value was obtained from self-made gas solutions with known amount of gases.

### 5.6.4 Infrared spectroscopy (FTIR) – Attenuated Total Reflection (ATR)

The ATR measurements were performed directly on the material (no dilution needed) after flashing the analytical region with N<sub>2</sub> for 30 minutes, to avoid the CO<sub>2</sub> signal in the spectra. The measurements were performed with the instrument NICOLET iS50 from 400 to 4000 cm<sup>-1</sup>.

### 5.6.5 Elemental Analysis

The analysis was performed by combustion analysis in an external laboratory: Mikroanalytisches Laboratorium Kolbe in Oberhausen.

### 5.6.6 Raman spectroscopy

The Raman analyses were performed with green laser (532 nm  $\approx$  2.4 eV, 10 mW). The instrument used was a Raman Horiba Jobin-Yvon ARAMIS.

### 5.6.7 X-Ray Diffraction (XRD)

The diffraction measurements were performed at the “Max-Planck-Institut für Kohlenforschung” in Mülheim an der Ruhr, Germany. A kapton foil was used to prevent the sample from falling out, because the sample holder tilt during the measurement (The kapton foil is visible in the measurement). A Si-Sampleholder was used to prevent reflections from the sample holder. The preparation method is illustrated in Figure 5-17. The diffractometer was a X’Pert from PANalytical, with Cu-radiation 40kV, 40mA.



Figure 5-17: Samples preparation for XRD analysis.

### 5.6.8 Transmission Electron Microscopy (TEM)

Micrographs of the samples 1Rh-GN and 1Rh-GP<sub>PPh<sub>3</sub></sub> were performed at the “centre technologique des microstructures (CT $\mu$ )”, Villeurbanne, France, on a Jeol 2010 transmission electron microscope. The acceleration voltage was 200 kV.

Micrographs of the samples 0.1Rh-GN and 0.01Rh-GN were performed at the “Max-Planck-Institut für Kohlenforschung” in Mülheim an der Ruhr, Germany, on a Hitachi HD-2700 C<sub>S</sub>-corrected dedicated STEM 200 kV, Cold FEG. The EDX analysis was performed with EDAX Octane T Ultra W 200mm<sup>2</sup> SDD TEAM-Software.





## 6. Conclusions

The exploitation of CO<sub>2</sub> as C<sub>1</sub> building block is a fascinating and important topic in “green chemistry”.<sup>106</sup> Moreover, carboxylic acids have several interesting industrial applications. The current production of carboxylic acids is based on CO, as they are mainly produced via aldehydes oxidation (obtained from hydroformylation processes) and hydroxycarbonylation of alkenes. Therefore, their synthesis starting from substrates, such as alcohols and other oxygenated substrates, and the renewable and non-toxic CO<sub>2</sub> is highly desirable.

During the PhD the optimization of a catalytic system for the synthesis of carboxylic acids from alcohols, CO<sub>2</sub> and H<sub>2</sub> was achieved. DoE approach and variation of the single parameters approach were used helping in finding the conditions to achieve yields up to 80 %. Primary, secondary and tertiary alcohols can all be used to obtain the carboxylic acids. Moreover, the same system was optimized for the first time for the conversion of ketones, aldehydes, epoxides, bifunctional substrates and mixture of substrates. Mechanistic studies confirmed that the reaction is going through two separate catalytic steps. First, the *r*WGS forms CO and H<sub>2</sub>O from CO<sub>2</sub> and H<sub>2</sub>; following, the hydroxycarbonylation convert the organic substrate, CO and H<sub>2</sub>O into the carboxylic acid. The catalytic system, in the correct condition, can perform both the cycles balancing the rates of them in order to give good yields in the desired carboxylic acids. Detailed studies of the hydroxycarbonylation step revealed that the in-situ produced alkene is coupling with CO and H<sub>2</sub>O. Therefore, the optimized reaction conditions vary according to the used substrates to obtain the organic intermediate (alkene) in the more efficient way, allowing a selective pathway towards carboxylic acids. The role of the additives was investigated, allowing a deeper knowledge of the catalytic active species. In particular, the role of the additional PPh<sub>3</sub> was found to be crucial in supplying the needed ligand for the system, due to the low amount of CO: Based on the findings herein reported and literature studies, a full reaction mechanism is suggested. The two catalytic cycles have already been reported in previous literature work on Rh homogeneous catalysis.<sup>13, 14</sup> Nevertheless, their unification, thanks to the additional PPh<sub>3</sub> ligand, allow the production of the carboxylic acid starting directly from CO<sub>2</sub>, avoiding the use of high amount of CO.

Based on the knowledge gained through the study of the homogeneous catalytic system, an attempt to perform the reaction with an heterogeneous catalyst was made.

Single Rh atoms dispersed on a N-doped graphene-like materials were successfully synthesized and characterized. The materials are not catalytically active for the hydrocarboxylation reaction. Nevertheless, supported single atoms can unify the benefits of both homogeneous and heterogeneous catalysis; therefore, they appear as attractive materials for further studies.

Overall, a new way to exploit CO<sub>2</sub> as C<sub>1</sub> building block to produce valuable compounds such as carboxylic acids has been designed. The system herein reported is the first one able to transform oxygenated substrates into carboxylic acids using CO<sub>2</sub> and H<sub>2</sub> as reducing agent, without the need of organometallic stoichiometric reagents. The goal of producing carboxylic acids with an innovative and theoretically more sustainable way is achieved using a large variety of oxygenated non-activated organic substrates, which are available both from the traditional petrochemical refinery and bio-refinery. Besides, the deeper knowledge gained regarding the catalytic cycle and the active species could lead to a more analytical and aware development for further applications. Increasing the TON, the selectivity, the scale and the substrate scope (i.e. including aromatic compounds and methanol) are envisioned follow up of the current state-of-the-art.

## 7. References

1. M. V. Solmi, M. Schmitz and W. Leitner, in *Horizons in Sustainable Industrial Chemistry and Catalysis*, eds. S. Albonetti, S. Perathoner and E. A. Quadrelli, Elsevier, In press.
2. W. Leitner and J. Klankermayer, *Science*, 2015, **350**, 629-630.
3. J. Klankermayer, S. Wesselbaum, K. Beydoun and W. Leitner, *Angew. Chem. Int. Ed.*, 2016.
4. J. Artz, T. E. Muller, K. Thenert, J. Kleinekorte, R. Meys, A. Sternberg, A. Bardow and W. Leitner, *Chem. Rev.*, 2018, **118**, 434–504.
5. G. Centi, E. A. Quadrelli and S. Perathoner, *Energy & Environmental Science*, 2013, **6**, 1711.
6. T. G. Ostapowicz, M. Schmitz, M. Krystof, J. Klankermayer and W. Leitner, *Angew. Chem. Int. Ed.*, 2013, **52**, 12119-12123.
7. K. Dong and X. F. Wu, *Angew. Chem. Int. Ed.*, 2017.
8. E. Kirillov, J. F. Carpentier and E. Bunel, *Dalton Trans.*, 2015, **44**, 16212-16223.
9. L. Wu, Q. Liu, R. Jackstell and M. Beller, *Angew. Chem. Int. Ed.*, 2014, **53**, 6310-6320.
10. L. Wu, Q. Liu, I. Fleischer, R. Jackstell and M. Beller, *Nat. Commun.*, 2014, **5**.
11. M. D. Porosoff, B. Yan and J. G. Chen, *Energy Environ. Sci.*, 2016, **9**, 62-73.
12. M. Schmitz, PhD, RWTH Aachen University, 2018.
13. D. Forster, A. Hershman and D. E. Morris, *Catalysis Reviews*, 1981, **23**, 89-105.
14. E. C. Baker, D. E. Hendriksen and R. Eisenberg, *J. Am. Chem. Soc.*, 1980, **102**, 1020-1027.
15. H. Yan, C. Su, J. He and W. Chen, *Journal of Materials Chemistry A*, 2018, **6**, 8793-8814.
16. X.-F. Yang, A. Wang, B. Qiao, J. Li, J. Liu and T. Zhang, *Acc. Chem. Res.*, 2013, **46**, 1740-1748.

## REFERENCES

17. S. Liang, C. Hao and Y. Shi, *ChemCatChem*, 2015, **7**, 2559-2567.
18. R. Lang, T. Li, D. Matsumura, S. Miao, Y. Ren, Y. T. Cui, Y. Tan, B. Qiao, L. Li, A. Wang, X. Wang and T. Zhang, *Angew. Chem. Int. Ed.*, 2016, **55**, 16054-16058.
19. J. C. Matsubu, V. N. Yang and P. Christopher, *J. Am. Chem. Soc.*, 2015, **137**, 3076-3084.
20. L. Wang, W. Zhang, S. Wang, Z. Gao, Z. Luo, X. Wang, R. Zeng, A. Li, H. Li, M. Wang, X. Zheng, J. Zhu, W. Zhang, C. Ma, R. Si and J. Zeng, *Nat. Commun.*, 2016, **7**, 14036.
21. D. Deng, X. Chen, L. Yu, X. Wu, Q. Liu, Y. Liu, H. Yang, H. Tian, Y. Hu, P. Du, R. Si, J. Wang, X. Cui, H. Li, J. Xiao, T. Xu, J. Deng, F. Yang, P. N. Duchesne, P. Zhang, J. Zhou, L. Sun, J. Li, X. Pan and X. Bao, *Sci. Adv.*, 2015, **1**, e1500462/1500461-e1500462/1500469.
22. H. Yan , H. Cheng , H. Yi , Y. Lin , T. Yao , C. Wang , J. Li , S. Wei and J. Lu, *J. Am. Chem. Soc.*, 2015, **137** 10484–10487.
23. L. Xu, L.-M. Yang and E. Ganz, *Theor. Chem. Acc.*, 2018, **137**.
24. C. Gao, S. Chen, Y. Wang, J. Wang, X. Zheng, J. Zhu, L. Song, W. Zhang and Y. Xiong, *Adv. Mater.*, 2018, **30**, e1704624.
25. C. Zhang, J. Sha, H. Fei, M. Liu, S. Yazdi, J. Zhang, Q. Zhong, X. Zou, N. Zhao, H. Yu, Z. Jiang, E. Ringe, B. I. Yakobson, J. Dong, D. Chen and J. M. Tour, *ACS Nano*, 2017.
26. H. Fei, J. Dong, M. J. Arellano-Jiménez, G. Ye, N. Dong Kim, E. L. G. Samuel, Z. Peng, Z. Zhu, F. Qin, J. Bao, M. J. Yacaman, P. M. Ajayan, D. Chen and J. M. Tour, *Nature Communication*, 2015, **6**, 1-8.
27. W. Liu, Y. Chen, H. Qi, L. Zhang, W. Yan, X. Liu, X. Yang, S. Miao, W. Wang, C. Liu, A. Wang, J. Li and T. Zhang, *Angew. Chem. Int. Ed.*, 2018, **57**, 7071-7075.
28. Y. Chen, S. Ji, Y. Wang, J. Dong, W. Chen, Z. Li, R. Shen, L. Zheng, Z. Zhuang, D. Wang and Y. Li, *Angew. Chem. Int. Ed.*, 2017, **56**, 6937-6941.
29. W. Liu, L. Cao, W. Cheng, Y. Cao, X. Liu, W. Zhang, X. Mou, L. Jin, X. Zheng, W. Che, Q. Liu, T. Yao and S. Wei, *Angew. Chem. Int. Ed.*, 2017.
30. S. Back, J. Lim, N.-Y. Kim, Y.-H. Kim and Y. Jung, *Chem Sci*, 2017, **8**, 1090-1096.
31. *WMO Greenhouse Gas Bulletin*, World Meteorological Organization and World Data Centre for Greenhouse Gases, 2017.

## REFERENCES

32. C. Le Quéré, R. M. Andrew, P. Friedlingstein, S. Sitch, J. Pongratz, A. C. Manning, J. I. Korsbakken, G. P. Peters, J. G. Canadell, R. B. Jackson, T. A. Boden, P. P. Tans, O. D. Andrews, V. K. Arora, D. C. E. Bakker, L. Barbero, M. Becker, R. A. Betts, L. Bopp, F. Chevallier, L. P. Chini, P. Ciais, C. E. Cosca, J. Cross, K. Currie, T. Gasser, I. Harris, J. Hauck, V. Haverd, R. A. Houghton, C. W. Hunt, G. Hurtt, T. Ilyina, A. K. Jain, E. Kato, M. Kautz, R. F. Keeling, K. Klein Goldewijk, A. Körtzinger, P. Landschützer, N. Lefèvre, A. Lenton, S. Lienert, I. Lima, D. Lombardozzi, N. Metzl, F. Millero, P. M. S. Monteiro, D. R. Munro, J. E. M. S. Nabel, S.-i. Nakaoka, Y. Nojiri, X. A. Padín, A. Peregon, B. Pfeil, D. Pierrot, B. Poulter, G. Rehder, J. Reimer, C. Rödenbeck, J. Schwinger, R. Séférian, I. Skjelvan, B. D. Stocker, H. Tian, B. Tilbrook, I. T. van der Laan-Luijkx, G. R. van der Werf, S. van Heuven, N. Viovy, N. Vuichard, A. P. Walker, A. J. Watson, A. J. Wiltshire, S. Zaehle and D. Zhu, *Earth Syst. Sci. Data Discuss.*, 2017, **2017**, 1-79.
33. E. Alper and O. Yuksel Orhan, *Petroleum*, 2017, **3**, 109-126.
34. M. Peters, B. Kohler, W. Kuckshinrichs, W. Leitner, P. Markewitz and T. E. Muller, *ChemSusChem*, 2011, **4**, 1216-1240.
35. A. Corma, S. Iborra and A. Velty, *Chem. Rev.*, 2007, **107**, 2411.
36. S. Shafiee and E. Topal, *Energy policy*, 2009, **37**, 181-189.
37. J. Klankermayer and W. Leitner, *Philos. Trans. R. Soc. London, Ser. A*, 2016, **374**.
38. M. Aresta, A. Dibenedetto and A. Angelini, *Chem. Rev.*, 2014, **114**, 1709-1742.
39. H. Arakawa, M. Aresta, J. N. Armor, M. A. Barteau, E. J. Beckman, A. T. Bell, J. E. Bercaw, C. Creutz, E. Dinjus and D. A. Dixon, *Chem. Rev.*, 2001, **101**, 953-996.
40. W. Leitner, *Angew. Chem. Int. Ed.*, 1995, **34**, 2207-2221.
41. F. Juliá-Hernández, T. Moragas, J. Cornella and R. Martin, *Nature*, 2017, **545**, 84-88.
42. C. F. Cordeiro and F. P. Petrocelli, in *Encyclopedia of Polymer Science and Technology*, 2004, DOI: 10.1002/0471440264.pst383.
43. A. W. Budiman, J. S. Nam, J. H. Park, R. I. Mukti, T. S. Chang, J. W. Bae and M. J. Choi, *Catalysis Surveys from Asia*, 2016, **20**, 173-193.
44. A. Anton and B. R. Baird, in *Encyclopedia of Polymer Science and Technology*, 2001, DOI: 10.1002/0471440264.pst250.
45. G. Swift, in *Encyclopedia of Polymer Science and Technology*, 2002, DOI: 10.1002/0471440264.pst009.

## REFERENCES

46. G. Reese, in *Encyclopedia of Polymer Science and Technology*, ed. I. John Wiley & Sons, 2001, DOI: 10.1002/0471440264.pst261, pp. 652-678.
47. K. J. Edgar, in *Encyclopedia of Polymer Science and Technology*, John Wiley & Sons, Inc., 2002, DOI: 10.1002/0471440264.pst045, pp. 129-158.
48. F. Röhrscheid, in *Ullmann's Encyclopedia of Industrial Chemistry*, 2000, DOI: 10.1002/14356007.a05\_249.
49. Z. W. Wicks, in *Encyclopedia of Polymer Science and Technology*, 2007, DOI: 10.1002/0471440264.pst016.pub2.
50. C. Le Berre, P. Serp, P. Kalck and G. P. Torrence, in *Ullmann's Encyclopedia of Industrial Chemistry*, 2014, DOI: 10.1002/14356007.a01\_045.pub3, pp. 1-34.
51. K. Weissermel and H. J. Arpe, *Industrial Organic Chemistry*, Wiley, 2008.
52. S. Moret, P. J. Dyson and G. Laurenczy, *Nat. Commun.*, 2014, **5**, 4017.
53. W. Riemenschneider and M. Tanifuji, in *Ullmann's Encyclopedia of Industrial Chemistry*, 2011, DOI: 10.1002/14356007.a18\_247.pub2.
54. J. Hietala, A. Vuori, P. Johnsson, I. Pollari, W. Reutemann and H. Kieczka, in *Ullmann's Encyclopedia of Industrial Chemistry*, 2016, DOI: 10.1002/14356007.a12\_013.pub3, pp. 1-22.
55. J. Kubitschke, H. Lange and H. Strutz, in *Ullmann's Encyclopedia of Industrial Chemistry*, 2014, DOI: 10.1002/14356007.a05\_235.pub2, pp. 1-18.
56. B. Olivier, L. Henri and B. Bernard, in *Ullmann's Encyclopedia of Industrial Chemistry*, eds. U. Fritz and B. Matthias, Wiley-VCH Verlag GmbH & Co. KGaA, Weinheim, 2005, pp. 1-8.
57. T. G. Kantor, *Pharmacotherapy: The Journal of Human Pharmacology and Drug Therapy*, 1986, **6**, 93-102.
58. M. Szilagyi, in *Patty's Toxicology*, 2012, DOI: 10.1002/0471435139.tox070.pub2, pp. 471-532.
59. J. P. Lange, R. Price, P. M. Ayoub, J. Louis, L. Petrus, L. Clarke and H. Gosselink, *Angew. Chem. Int. Ed.*, 2010, **49**, 4479-4483.
60. A. Álvarez, A. Bansode, A. Urakawa, A. V. Bavykina, T. A. Wezendonk, M. Makkee, J. Gascon and F. Kapteijn, *Chem. Rev.*, 2017, **117**, 9804-9838.
61. J. Klankermayer, S. Wesselbaum, K. Beydoun and W. Leitner, *Angew. Chem. Int. Ed.*, 2016, **55**, 7296-7343.

## REFERENCES

62. R. J. Sheehan, in *Ullmann's Encyclopedia of Industrial Chemistry*, 2011, DOI: 10.1002/14356007.a26\_193.pub2.
63. M. T. Musser, in *Ullmann's Encyclopedia of Industrial Chemistry*, 2000, DOI: 10.1002/14356007.a01\_269.
64. A. H. Reidies, in *Ullmann's Encyclopedia of Industrial Chemistry*, Wiley-VCH Verlag GmbH & Co. KGaA, 2000, DOI: 10.1002/14356007.a16\_123.
65. S. S. Nurttala, P. R. Linnebank, T. Krachko and J. N. H. Reek, *ACS Catalysis*, 2018, **8**, 3469-3488.
66. R. Franke, D. Selent and A. Borner, *Chem. Rev.*, 2012, **112**, 5675-5732.
67. H. Koch and W. Haaf, *Angew. Chem.*, 1958, **70**, 311-311.
68. W. Reppe and H. Kröper, *Justus Liebigs Annalen der Chemie*, 1953, **582**, 38-71.
69. U.-R. Samel, W. Kohler, A. O. Gamer, U. Keuser, S.-T. Yang, Y. Jin, M. Lin and Z. Wang, in *Ullmann's Encyclopedia of Industrial Chemistry.*, 2014, DOI: 10.1002/14356007.a22\_223.pub3, pp. 1-20.
70. A. Haynes, *Advances in catalysis*, 2010, **53**, 1-45.
71. P. B. Francoisse and F. C. Thyron, *Industrial & Engineering Chemistry Product Research and Development*, 1983, **22**, 542-548.
72. D. Forster, *Adv. Organomet. Chem.*, 1979, **17**, 255-267.
73. T. Singleton, L. Park, J. Price and D. Forster, *Am. Chem. Soc., Div. Pet. Chem., Prep.*, 1979, **24**.
74. E. C. Baker, D. E. Hendriksen and R. Eisenberg, *J. Am. Chem. Soc.*, 1980, 1020-1027.
75. D. Forster, A. Hershman and D. E. Morris, *Catalysis Reviews—Science and Engineering*, 1981, **23**, 89-105.
76. A. Haynes, P. M. Maitlis, G. E. Morris, G. J. Sunley, H. Adams, P. W. Badger, C. M. Bowers, D. B. Cook, P. I. P. Elliott, T. Ghaffar, H. Green, T. R. Griffin, M. Payne, J. M. Pearson, M. J. Taylor, P. W. Vickers and R. J. Watt, *J. Am. Chem. Soc.*, 2004, **126**, 2847-2861.
77. D. Forster, *J. Chem. Soc., Dalton Trans.*, 1979, DOI: 10.1039/DT9790001639, 1639-1645.

## REFERENCES

78. N. Yoneda, T. Minami, J. Weiszmann and B. Spehlmann, in *Stud. Surf. Sci. Catal.*, eds. H. Hideshi and O. Kiyoshi, Elsevier, 1999, vol. Volume 121, pp. 93-98.
79. T. W. Dekleva and D. Forster, *Mechanistic aspects of transition-metal-catalyzed alcohol carbonylations*, 1986.
80. J. Hjortkjaer and J. C. Aerbo Jørgensen, *J. Mol. Catal.*, 1978, **4**, 199-203.
81. J. Hjortkjaer and J. C. E. Jorgensen, *Journal of the Chemical Society, Perkin Transactions 2*, 1978, 763-766.
82. S. B. Dake, D. S. Kolhe and R. V. Chaudhari, *J. Mol. Catal.*, 1984, **24**, 99-113.
83. B. R. Sarkar and R. V. Chaudhari, *Catalysis Surveys from Asia*, 2005, **9**, 193-205.
84. R. S. Ubale, A. A. Kelkar and R. V. Chaudhari, *J. Mol. Catal. A: Chem.*, 1997, **118**, 9-19.
85. C. Carlini, M. Di Girolamo, M. Marchionna, A. M. R. Galletti and G. Sbrana, *Stud. Surf. Sci. Catal.*, 1998, **119**, 491-496.
86. *GB Pat.*, WO2009077726A1, 2009.
87. K. Matsushita, T. Komori, S. Oi and Y. Inoue, *Tetrahedron Lett.*, 1994, **35**, 5889-5890.
88. Q. Cao, N. L. Hughes and M. J. Muldoon, *Chemistry*, 2016, **22**, 11982-11985.
89. D. C. Roe, R. E. Sheridan and E. E. Bunel, *J. Am. Chem. Soc.*, 1994, **116**, 1163-1164.
90. E. Amadio, Z. Freixa, P. W. N. M. van Leeuwen and L. Toniolo, *Catalysis Science & Technology*, 2015, **5**, 2856-2864.
91. L. Wu, X. Fang, Q. Liu, R. Jackstell, M. Beller and X.-F. Wu, *ACS Catalysis*, 2014, **4**, 2977-2989.
92. S. M., S. I. and Y. A., *Bull. Chem. Soc. Jpn.*, 1996, **69**, 1065-1078.
93. K. Dong, R. Sang, J. Liu, R. Razzaq, R. Franke, R. Jackstell and M. Beller, *Angew. Chem. Int. Ed.*, 2017, **56**, 6203-6207.
94. N. Tsumori, Q. Xu, Y. Souma and H. Mori, *J. Mol. Catal. A: Chem.*, 2002, **179**, 271-277.



## REFERENCES

95. B. R. Sarkar and R. V. Chaudhari, *Catal. Today*, 2012, **198**, 154-173.
96. *USA Pat.*, US20080146833A1, 2008.
97. W. Riemenschneider, *Journal*, 2005, 1-15.
98. H. Kolbe, *Justus Liebigs Annalen der Chemie*, 1860, **113**, 125-127.
99. M. Wenzel, L. Rihko-Struckmann and K. Sundmacher, *Chem. Eng. J.*, 2018, **336**, 278-296.
100. A. M. Bazzanella and F. Ausfelder, *Low carbon energy and feedstock for the European chemical industry*, German Society for Chemical Engineering and Biotechnology (DECHEMA), 2017.
101. *Novel carbon capture and utilisation technologies*, European Commission - Directorate-General for Research and Innovation - Unit RTD.DDG1.02 - Scientific Advice Mechanism, Luxembourg, 2018.
102. P. Markewitz, W. Kuckshinrichs, W. Leitner, J. Linssen, P. Zapp, R. Bongartz, A. Schreiber and T. E. Müller, *Energy Environ. Sci.*, 2012, **5**, 7281-7305.
103. S. Peter and J. Daan, *Report: Carbon Capture and Utilisation in the green economy*, ECN and University of Sheffield, 2012.
104. G. Centi and S. Perathoner, *Catal. Today*, 2009, **148**, 191-205.
105. T. E. Muller and W. Leitner, *Beilstein Journal of Organic Chemistry*, 2015, **11**, 675-677.
106. M. Poliakoff, W. Leitner and E. S. Streng, *Faraday Discuss.*, 2015, **183**, 9-17.
107. M. Aresta, A. Dibenedetto and A. Angelini, *Chem. Rev.*, 2014, **114**, 1709-1742.
108. D. H. Gibson, *Chem. Rev.*, 1996, **96**.
109. M. Cokoja, C. Bruckmeier, B. Rieger, W. A. Herrmann and F. E. Kuhn, *Angew. Chem. Int. Ed.*, 2011, **50**, 8510-8537.
110. T. Iijima and T. Yamaguchi, *J. Mol. Catal. A: Chem.*, 2008, **295**, 52-56.
111. M. Aresta, C. F. Nobile, V. G. Albano, E. Forni and M. Manassero, *J. Chem. Soc., Chem. Commun.*, 1975, DOI: 10.1039/C39750000636, 636-637.
112. J. Klankermayer, S. Wesselbaum, K. Beydoun and W. Leitner, *Angew Chem Int Ed Engl*, 2016, **55**, 7296-7343.

## REFERENCES

113. Q. Liu, L. Wu, R. Jackstell and M. Beller, *Nat. Commun.*, 2015, **6**, 5933.
114. M. Aresta, A. Dibenedetto and A. Angelini, *Comprehensive Inorganic Chemistry II*, 2013, 563-586.
115. M. Borjesson, T. Moragas, D. Gallego and R. Martin, *ACS Catalysis*, 2016, **6**, 6739-6749.
116. L. Pastor-Pérez, F. Baibars, E. Le Sache, H. Arellano-García, S. Gu and T. R. Reina, *Journal of CO2 Utilization*, 2017, **21**, 423 - 428.
117. M. Ronda-Lloret, S. Rico-Francés, A. Sepúlveda-Escribano and E. V. Ramos-Fernandez, *Applied Catalysis A: General*, 2018, **562**, 28-36.
118. G. Yin, X. Yuan, X. Du, W. Zhao, Q. Bi and F. Huang, *Chemistry*, 2018, **24**, 2157-2163.
119. K. Tsuchiya, J.-D. Huang and K.-i. Tominaga, *ACS Catalysis*, 2013, **3**, 2865-2868.
120. J. Ettetdgui, Y. Diskin-Posner, L. Weiner and R. Neumann, *J. Am. Chem. Soc.*, 2011, **133**, 188-190.
121. D. Maiti, B. J. Hare, Y. A. Daza, A. E. Ramos, J. N. Kuhn and V. R. Bhethanabotla, *Energy Environ. Sci.*, 2018, **11**, 648-659.
122. A. Polyzos, M. O'Brien, T. P. Petersen, I. R. Baxendale and S. V. Ley, *Angew. Chem. Int. Ed.*, 2011, **50**, 1190--1193.
123. M. D. Greenhalgh and S. P. Thomas, *J. Am. Chem. Soc.*, 2012, **134**, 11900-11903.
124. G. Zweifel and C. C. Whitney, *J. Am. Chem. Soc.*, 1967, **89**, 1754-2755.
125. J. Eisch and M. Foxton, *J. Organomet. Chem.*, 1968, **11**, P7-P8.
126. Y. Hirai, T. Aida and S. Inoue, *J. Am. Chem. Soc.*, 1989, **111**, 3062-3063.
127. S. Tanaka, K. Watanabe, Y. Tanaka and T. Hattori, *Org. Lett.*, 2016, **18**, 2576-2579.
128. WO2000005187A1, 1998.
129. A. Nagaki, Y. Takahashi and J.-i. Yoshida, *Chem. Eur. J.*, 2014, **20**, 7931-7934.
130. V. Grignard, *C. R. Hebd. Seances Acad. Sci.*, 1900, **130**, 1322-1324.

## REFERENCES

131. G. R. M. Dowson, I. Dimitriou, R. E. Owen, D. G. Reed, R. W. K. Allen and P. Styring, *Faraday Discuss.*, 2015, **183**, 47-65.
132. J. Luo and I. Larrosa, *ChemSusChem*, 2017.
133. S. Tanaka, K. Watanabe, Y. Tanaka and T. Hattori, *Org. Lett.*, 2016, **18**, 2576-2579.
134. A. Correa and R. Martín, *Angew. Chem. Int. Ed.*, 2009, **48**, 6201-6204.
135. R. Johansson and O. F. Wendt, *Dalton Transactions*, 2007, 488-492.
136. C. S. Yeung and V. M. Dong, *J. Am. Chem. Soc.*, 2008, **130**, 7826-7827.
137. H. Ochiai, M. Jang, K. Hirano, H. Yorimitsu and K. Oshima, *Org. Lett.*, 2008, **10**, 2681-2683.
138. K. Kobayashi and Y. Kondo, *Org. Lett.*, 2009, **11**, 2035-2037.
139. S. Li, W. Yuan and S. Ma, *Angew. Chem. Int. Ed.*, 2011, **50**, 2578-2582.
140. S. Wang, P. Shao, C. Chen and C. Xi, *Org. Lett.*, 2015, **17**, 5112-5115.
141. M. Shi and K. M. Nicholas, *J. Am. Chem. Soc.*, 1997, **119**, 5057-5058.
142. K. Ukai, M. Aoki, J. Takaya and N. Iwasawa, *J. Am. Chem. Soc.*, 2006, **128**, 8706-8707.
143. T. Ohishi, M. Nishiura and Z. Hou, *Angew. Chem. Int. Ed.*, 2008, **47**, 5792-5795.
144. X. Zhang, W.-Z. Zhang, L.-L. Shi, C.-X. Guo, L.-L. Zhang and X.-B. Lu, *Chem. Commun.*, 2012, **48**, 6292-6294.
145. S. J. Thompson, T. R. Gohndrone and M. Lail, *Journal of CO2 Utilization*, 2018, **24**, 256-260.
146. M. Juhl, S. L. R. Laursen, Y. Huang, D. U. Nielsen, K. Daasbjerg and T. Skrydstrup, *ACS Catalysis*, 2017, **7**, 1392-1396.
147. M. E. Vol'pin, A. L. Sigan and E. V. Solomovich, *Russ. Chem. Bull.*, 1993, **42**, 1929-1930.
148. T. Mita, K. Michigami and Y. Sato, *Org. Lett.*, 2012, **14**, 3462-3465.
149. M. Yonemoto-Kobayashi, K. Inamoto, Y. Tanaka and Y. Kondo, *Org. Biomol. Chem.*, 2013, **11**, 3773-3775.

## REFERENCES

150. T. Mita, Y. Higuchi and Y. Sato, *Org. Lett.*, 2014, **16**, 14-17.
151. T. Mita, M. Sugawara, K. Saito and Y. Sato, *Org. Lett.*, 2014, **16**, 3028-3031.
152. X. Frogneux, W. N. von, P. Thuery, G. Lefevre and T. Cantat, *Chemistry*, 2016, **22**, 2930-2934.
153. P. Anastas and N. Eghbali, *Chem. Soc. Rev.*, 2010, **39**, 301-312.
154. P. M. Maitlis, A. Haynes, G. J. Sunley and M. J. Howard, *Journal of the Chemical Society, Dalton Transactions: Inorganic Chemistry*, 1996, 2187-2196.
155. A. Correa and R. Martin, *J. Am. Chem. Soc.*, 2009, **131**, 15974–15975.
156. T. Fujihara, K. Nogi, T. Xu, J. Terao and Y. Tsuji, *J. Am. Chem. Soc.*, 2012, **134**, 9106-9109.
157. H. Tran-Vu and O. Daugulis, *ACS Catalysis*, 2013, **3**, 2417-2420.
158. T. León, A. Correa and R. Martin, *J. Am. Chem. Soc.*, 2013, **135**, 1221-1224.
159. A. Fukuoka, N. Gotoh, N. Kobayashi, M. Hirano and S. Komiya, *Chem. Lett.*, 1995, **24**, 567-568.
160. Y. Liu, J. Cornella and R. Martin, *J. Am. Chem. Soc.*, 2014, **136**, 11212-11215.
161. F. Atsushi, G. Naotaka, K. Norikazu, H. Masafumi and K. Sanshiro, *Chem. Lett.*, 1995, **24**, 567-568.
162. M. van Gemmeren, M. Borjesson, A. Tortajada, S. Z. Sun, K. Okura and R. Martin, *Angew. Chem. Int. Ed.*, 2017, **56**, 6558-6562.
163. F. Rebih, M. Andreini, A. Moncomble, A. Harrison-Marchand, J. Maddaluno and M. Durandetti, *Chemistry*, 2016, **22**, 3758-3763.
164. K. Nogi, T. Fujihara, J. Terao and Y. Tsuji, *J. Org. Chem.*, 2015, **80**, 11618-11623.
165. A. Correa, T. León and R. Martin, *J. Am. Chem. Soc.*, 2014, **136**, 1062-1069.
166. T. Moragas, J. Cornella and R. Martin, *J. Am. Chem. Soc.*, 2014, **136**, 17702-17705.
167. T. Mita, Y. Higuchi and Y. Sato, *Chemistry*, 2015, **21**, 16391-16394.
168. Q. Qian, J. Zhang, M. Cui and B. Han, *Nat. Commun.*, 2016, **7**, 1-7.

## REFERENCES

169. M. Cui, Q. Qian, J. Zhang, C. Chen and B. Han, *Green Chem.*, 2017, **19**, 3558-3565.
170. M. van Gemmeren, M. Börjesson, A. Tortajada, S.-Z. Sun, K. Okura and R. Martin, *Angew. Chem. Int. Ed.*, 2017, **56**, 6558-6562.
171. Q. Qian, J. Zhang, M. Cui and B. Han, *Nat. Commun.*, 2016, **7**.
172. M. Cui, Q. Qian, J. Zhang, C. Chen and B. Han, *Green Chem.*, 2017, DOI: 10.1039/c7gc01391d.
173. L. J. Gooßen, N. Rodríguez, F. Manjolinho and P. P. Lange, *Advanced Synthesis & Catalysis*, 2010, **352**, 2913-2917.
174. D. Yu and Y. Zhang, *Proceedings of the National Academy of Sciences*, 2010, **107**, 20184-20189.
175. K. Inamoto, N. Asano, K. Kobayashi, M. Yonemoto and Y. Kondo, *Org. Biomol. Chem.*, 2012, **10**, 1514-1516.
176. Y. Fukue, S. Oi and Y. Inoue, *J. Chem. Soc., Chem. Commun.*, 1994, 2091-2091.
177. K. Nogi, T. Fujihara, J. Terao and Y. Tsuji, *Chem. Commun.*, 2014, **50**, 13052-13055.
178. P. Shao, S. Wang, G. Du and C. Xi, *RSC Adv.*, 2017, **7**, 3534-3539.
179. H. Hoberg, D. Schaefer, G. Burkhardt, C. Krüger and M. Romao, *J. Organomet. Chem.*, 1984, **266**, 203-224.
180. S. Derien, E. Dunach and J. Perichon, *J. Am. Chem. Soc.*, 1991, **113**, 8447-8454.
181. L. Zhang, J. Cheng, T. Ohishi and Z. Hou, *Angew. Chem. Int. Ed.*, 2010, **49**, 8670-8673.
182. X. Wang, M. Nakajima and R. Martin, *J. Am. Chem. Soc.*, 2015, **137**, 8924-8927.
183. M. Arndt, E. Risto, T. Krause and L. J. Goossen, *ChemCatChem*, 2012, **4**, 484-487.
184. R. Santhoshkumar, Y.-C. Hong, C.-Z. Luo, Y.-C. Wu, C.-H. Hung, K.-Y. Hwang, A.-P. Tu and C.-H. Cheng, *ChemCatChem*, 2016, DOI: 10.1002/cctc.201600279.

## REFERENCES

185. T. Fujihara, T. Xu, K. Semba, J. Terao and Y. Tsuji, *Angew. Chem. Int. Ed.*, 2011, **50**, 523-527.
186. N. Huguet, I. Jevtovikj, A. Gordillo, M. L. Lejkowski, R. Lindner, M. Bru, A. Y. Khalimon, F. Rominger, S. A. Schunk and P. Hofmann, *Chemistry-A European Journal*, 2014, **20**, 16858-16862.
187. M. L. Lejkowski, R. Lindner, T. Kageyama, G. É. Bódizs, P. N. Plessow, I. B. Müller, A. Schäfer, F. Rominger, P. Hofmann, C. Futter, S. A. Schunk and M. Limbach, *Chemistry – A European Journal*, 2012, **18**, 14017-14025.
188. S. Manzini, A. Cadu, A.-C. Schmidt, N. Huguet, O. Trapp, R. Paciello and T. Schaub, *ChemCatChem*, 2017, **9**, 2269-2274.
189. S. Manzini, N. Huguet, O. Trapp, R. A. Paciello and T. Schaub, *Catal. Today*, 2017, **281**, 379-386.
190. H. Hoberg, Y. Peres, C. Krüger and Y. H. Tsay, *Angew. Chem. Int. Ed.*, 1987, **26**, 771-773.
191. C. M. Williams, J. B. Johnson and T. Rovis, *J. Am. Chem. Soc.*, 2008, **130**, 14936–14937.
192. A. Lapidus, S. Pirozhkov and A. Koryakin, *Bull. Acad. Sci. USSR, Div. Chem. Sci.*, 1978, **27**, 2513-2515.
193. M. Aresta, C. Pastore, P. Giannoccaro, G. Kovács, A. Dibenedetto and I. Pápai, *Chemistry-A European Journal*, 2007, **13**, 9028-9034.
194. H. Hoberg and D. Schaefer, *Journal of Organometallic Chemistry*, 1983, **251**, c51-c53.
195. D. C. Graham, C. Mitchell, M. I. Bruce, G. F. Metha, J. H. Bowie and M. A. Buntine, *Organometallics*, 2007, **26**, 6784-6792.
196. T. G. Ostapowicz, M. Schmitz, M. Krystof, J. Klankermayer and W. Leitner, *Angew. Chem. Int. Ed.*, 2013, **52**, 12119-12123.
197. H. Kolbe and E. Lautemann, *Justus Liebigs Annalen der Chemie*, 1860, **115**, 157-206.
198. R. Schmitt, *Journal für Praktische Chemie*, 1885, **31**, 397-411.
199. G. A. Olah, B. Török, J. P. Joschek, I. Bucsi, P. M. Esteves, G. Rasul and G. K. Surya Prakash, *J. Am. Chem. Soc.*, 2002, **124**, 11379-11391.
200. A.-H. Liu, B. Yu and L.-N. He, *Greenhouse Gases Sci. and Technol.*, 2015, **5**, 17-33.

## REFERENCES

201. K. Nemoto, H. Yoshida, N. Egusa, N. Morohashi and T. Hattori, *J. Org. Chem.*, 2010, **75**, 7855-7862.
202. Y. Suzuki, T. Hattori, T. Okuzawa and S. Miyano, *Chem. Lett.*, 2002, **31**, 102-103.
203. P. Munshi, E. J. Beckman and S. Padmanabhan, *Industrial & Engineering Chemistry Research*, 2010, **49**, 6678-6682.
204. M. Gu and Z. Cheng, *Journal of Materials Science and Chemical Engineering*, 2015, **3**, 103.
205. A. N. Sarve, P. A. Ganeshpure and P. Munshi, *Industrial & Engineering Chemistry Research*, 2012, **51**, 5174-5180.
206. I. I. Boogaerts and S. P. Nolan, *J. Am. Chem. Soc.*, 2010, **132**, 8858-8859.
207. S. Fenner and L. Ackermann, *Green Chem.*, 2016, **18**, 3804-3807.
208. T. Suga, H. Mizuno, J. Takaya and N. Iwasawa, *Chem. Commun.*, 2014, **50**, 14360-14363.
209. G. R. Dick, A. D. Frankhouser, A. Banerjee and M. W. Kanan, *Green Chem.*, 2017, **19**, 2966-2972.
210. I. I. F. Boogaerts and S. P. Nolan, *J. Am. Chem. Soc.*, 2010, **132**, 8858-8859.
211. I. I. F. Boogaerts, G. C. Fortman, M. R. L. Furst, C. S. J. Cazin and S. P. Nolan, *Angew. Chem. Int. Ed.*, 2010, **49**, 8674-8677.
212. L. Ackermann, *Angew. Chem. Int. Ed.*, 2011, **50**, 3842-3844.
213. A. Banerjee, G. R. Dick, T. Yoshino and M. W. Kanan, *Nature*, 2016, **531**, 215.
214. A. Banerjee and M. W. Kanan, *ACS Central Science*, 2018, **4**, 606-613.
215. K. Plasch, G. Hofer, W. Keller, S. Hay, D. J. Heyes, A. Dennig, S. M. Glueck and K. Faber, *Green Chem.*, 2018, **20**, 1754-1759.
216. W. Huang, K.-C. Xie, J.-P. Wang, Z.-H. Gao, L.-H. Yin and Q.-M. Zhu, *J. Catal.*, 2001, **201**, 100-104.
217. N. Ikehara, K. Hara, A. Satsuma, T. Hattori and Y. Murakami, *Chem. Lett.*, 1994, **23**, 263-264.
218. V. Havran, M. P. Duduković and C. S. Lo, *Industrial & Engineering Chemistry Research*, 2011, **50**, 7089-7100.

## REFERENCES

219. K. Masanobu, N. Kazuyuki, J. Tetsuro, T. Yuki, T. Ken and F. Yuzo, *Chem. Lett.*, 1995, **24**, 244-244.
220. J.-F. Wu, S.-M. Yu, W. D. Wang, Y.-X. Fan, S. Bai, C.-W. Zhang, Q. Gao, J. Huang and W. Wang, *J. Am. Chem. Soc.*, 2013, **135**, 13567-13573.
221. K. Sekine, A. Takayanagi, S. Kikuchi and T. Yamada, *Chem. Commun.*, 2013, **49**, 11320-11322.
222. E. J. Corey and R. H. K. Chen, *J. Org. Chem.*, 1973, **38**, 4086.
223. E. Haruki, M. Arakawa, N. Matsumura, Y. Otsuji and E. Imoto, *Chem. Lett.*, 1974, 427-428.
224. H. Sakurai, A. Shirahata and A. Hosomi, *Tetrahedron Lett.*, 1980, **21**, 1967-1970.
225. B. J. Flowers, R. Gautreau-Service and P. G. Jessop, *Advanced Synthesis & Catalysis*, 2008, **350**, 2947-2958.
226. E. J. Beckman and P. Munshi, *Green Chem.*, 2011, **13**, 376.
227. K. Michigami, T. Mita and Y. Sato, *J. Am. Chem. Soc.*, 2017, **139**, 6094-6097.
228. Y. Y. Gui, W. J. Zhou, J. H. Ye and D. G. Yu, *ChemSusChem*, 2017, **10**, 1337-1340.
229. Y. Masuda, N. Ishida and M. Murakami, *J. Am. Chem. Soc.*, 2015, **137**, 14063-14066.
230. N. Ishida, Y. Masuda, S. Uemoto and M. Murakami, *Chemistry*, 2016, **22**, 6524-6527.
231. H. Seo, M. H. Katcher and T. F. Jamison, *Nat. Chem.*, 2017, **9**, 453-456.
232. J. P. Simonato, T. Walter and P. Métivier, *J. Mol. Catal. A: Chem.*, 2001, **171**, 91-94.
233. A. R. Katritzky, D. Toader and L. Xie, *Synthesis*, 1996, **1996**, 1425-1427.
234. D. V. Leusen and A. M. V. Leusen, in *Organic Reactions*, John Wiley & Sons, Inc., 2004, DOI: 10.1002/0471264180.or057.03.
235. A. S. C. Chan, W. E. Carroll and D. E. Willis, *J. Mol. Catal.*, 1983, **19**, 377-391.
236. S. Suzuki, J. B. Wilkes, R. G. Wall and S. J. Lapporte, *Ethylene glycol from methanol and synthesis gas via glycolic acid*, Plenum, 1984.



## REFERENCES

237. A. Jacobi von Wangelin, H. Neumann and M. Beller, in *Catalytic Carbonylation Reactions*, ed. M. Beller, Springer Berlin Heidelberg, Berlin, Heidelberg, 2006, DOI: 10.1007/3418\_022, pp. 207-221.
238. J. McNulty and P. Das, *Tetrahedron*, 2009, **65**, 7794-7800.
239. J. Zhang, Q. Qian, M. Cui, C. Chen, S. Liu and B. Han, *Green Chem.*, 2017.
240. J. Langanke, A. Wolf, J. Hofmann, K. Böhm, M. A. Subhani, T. E. Müller, W. Leitner and C. Gürtler, *Green Chem.*, 2014, **16**, 1865-1870.
241. S. J. Poland and D. J. Darensbourg, *Green Chem.*, 2017, **19**, 4990-5011.
242. M. Alves, B. Grignard, R. Mereau, C. Jerome, T. Tassaing and C. Detrembleur, *Catalysis Science & Technology*, 2017, **7**, 2651-2684.
243. D. E. De Vos, B. F. Sels and P. A. Jacobs, *Adv. Synth. Catal.*, 2003, **345**, 457-473.
244. D. Forster, *Ann. N.Y. Acad. Sci.*, 1977, **295**, 79-82.
245. T. W. Dekleva and D. Forster, *Advances in Catalysis*, 1986, **34**, 81-130.
246. J.-P. Simonato, *J. Mol. Catal. A: Chem.*, 2003, **197**, 61-64.
247. M. Schmitz, PhD, RWTH Aachen University, 2018.
248. A. I. M. Keulemans, A. Kwantes and T. van Bavel, *Recl. Trav. Chim. Pays-Bas Belg.*, 1948, **67**, 298-308.
249. *NIST/SEMATECH e-Handbook of Statistical Methods*, <http://www.itl.nist.gov/div898/handbook/>, 2012 (visited 08.11.2016).
250. C. E. Hickey and P. M. Maitlis, *J. Chem. Soc., Chem. Commun.*, 1984, 1609-1611.
251. B. G. Frederick, G. Apai and T. N. Rhodin, *J. Am. Chem. Soc.*, 1987, **109**, 4797-4803.
252. T. W. Dekleva and D. Forster, *J. Am. Chem. Soc.*, 1985, **107**, 3565-3567.
253. D. Forster and T. W. Dekleva, *J. Chem. Educ.*, 1986, **63**, 204.
254. C. Thomas and G. Suess-Fink, *Coord. Chem. Rev.*, 2003, **243**, 125-142.
255. C. K. Brown and G. Wilkinson, *Journal of the Chemical Society A: Inorganic, Physical, Theoretical*, 1970, 2753-2764.

## REFERENCES

256. M. Bassetti, G. J. Sunley and P. M. Maitlis, *J. Chem. Soc., Chem. Commun.*, 1988, 1012-1013.
257. P. Etayo and A. Vidal-Ferran, *Chem. Soc. Rev.*, 2013, **42**, 728-754.
258. R. Noyori and O. Takeshi, *Angew. Chem. Int. Ed.*, 2001, **40**, 40--73.
259. Y. Chi, W. Tang and X. Zhang, in *Modern Rhodium-Catalyzed Organic Reactions*, ed. P. A. Evans, WILEY-VCH Verlag GmbH & Co. KGaA, 2005, DOI: 10.1002/3527604693.ch1, pp. 1--31.
260. M. J. Burk, T. G. P. Harper, J. R. Lee and C. Kalberg, *Tetrahedron Lett.*, 1994, **35**, 4963-4966.
261. R. R. Schrock and J. A. Osborn, *Journal of the Chemical Society D: Chemical Communications*, 1970, 567-568.
262. V. Polo, R. R. Schrock and L. A. Oro, *Chem. Commun.*, 2016, **52**, 13881-13884.
263. H. Koch and W. Haaf, *Justus Liebigs Annalen der Chemie*, 1958, **618**, 251-266.
264. J. Clayden, *Organic Chemistry*, Oxford University Press, 2001.
265. W. E. Noack, *Theoretica chimica acta*, 1979, **53**, 101-119.
266. J. Hine and K. Arata, *Bull. Chem. Soc. Jpn.*, 1976, **49**, 3089-3092.
267. Y. Watanabe, K. Takatsuki and Y. Takegami, *Tetrahedron Letters* 1978, **36**, 3369 - 3370
268. J. H. Jones, *Platinum Met. Rev.*, 2000, **44**, 94-105.
269. A. Yahiaoui, M. Belbachir, J. C. Soutif and L. Fontaine, *Mater. Lett.*, 2005, **59**, 759-767.
270. J. Herzberger, K. Niederer, H. Pohlit, J. Seiwert, M. Worm, F. R. Wurm and H. Frey, *Chem. Rev.*, 2016, **116**, 2170-2243.
271. US4764626A, 1988.
272. L. F. Schmoyer and L. C. Case, *Nature*, 1960, **187**, 592-593.
273. M. A. Medeiros, M. H. Araujo, R. Augusti, L. C. A. de Oliveira and R. M. Lago, *J. Braz. Chem. Soc.*, 2009, **20**, 1667-1673.

## REFERENCES

274. S. Koso, I. Furikado, A. Shima, T. Miyazawa, K. Kunimori and K. Tomishige, *Chem. Commun.*, 2009, 2035-2037.
275. A. Tortajada, R. Ninokata and R. Martin, *J. Am. Chem. Soc.*, 2018, **140**, 2050-2053.
276. D. Garces, E. Diaz and S. Ordonez, *Industrial & Engineering Chemistry Research*, 2017, **56**, 5221-5230.
277. M. Chidambaram and A. T. Bell, *Green Chem.*, 2010, **12**, 1253-1262.
278. H. Koinuma, Y. Yoshida and H. Hirai, *Chem. Lett.*, 1975, **4**, 1223-1226.
279. T. W. Dekleva and D. Forster, *J. Am. Chem. Soc.*, 1985, **107**, 3568-3572.
280. T. Oku, M. Okada, M. Puripat, M. Hatanaka, K. Morokuma and J.-C. Choi, *Journal of CO2 Utilization*, 2018, **25**, 1-5.
281. I. J. Colquhoun and W. McFarlane, *Journal of Magnetic Resonance*, 1982, **46**, 525-528.
282. T. G. Ostapowicz, PhD, RWTH Aachen University, 2013.
283. T. G. Ostapowicz, M. Hölscher and W. Leitner, *Eur. J. Inorg. Chem.*, 2012, **2012**, 5632-5641.
284. WO2015193183A1, 2015.
285. *SciFinder (Online Database)*, <https://scifinder.cas.org/scifinder>, 2018, **25/07/2018**.
286. M. B. Chambers, X. Wang, N. Elgrishi, C. H. Hendon, A. Walsh, J. Bonnefoy, J. Canivet, E. A. Quadrelli, D. Farrusseng, C. Mellot-Draznieks and M. Fontecave, *ChemSusChem*, 2015, **8**, 603-608.
287. R. Srivastava, R. Moneuse, J. Petit, P. A. Pavard, V. Dardun, M. Rivat, P. Schiltz, M. Solari, E. Jeanneau, L. Veyre, C. Thieuleux, E. A. Quadrelli and C. Camp, *Chemistry*, 2018, **24**, 4361-4370.
288. C. T. Campbell, *Nat. Chem.*, 2012, **4**, 597-598.
289. P. Hu, H. Zhiwei, Z. Amghouz, M. Makkee, F. Xu, F. Kapteijn, A. Dikhtiarenko, Y. Chen, X. Gu and X. Tang, *Angew. Chem. Int. Ed.*, 2014, **53**, 3418-3421.
290. M. Yang, L. F. Allard and M. Flytzani-Stephanopoulos, *J. Am. Chem. Soc.*, 2013, **135**, 3768-3771.

## REFERENCES

291. J. Xing, J. F. Chen, Y. H. Li, W. T. Yuan, Y. Zhou, L. R. Zheng, H. F. Wang, P. Hu, Y. Wang, H. J. Zhao, Y. Wang and H. G. Yang, *Chemistry*, 2014, **20**, 2138-2144.
292. J. Jones, H. Xiong, A. T. DeLaRiva, E. J. Peterson, H. Pham, S. R. Challa, G. Qi, S. Oh, M. H. Wiebenga, X. I. Pereira Hernández, Y. Wang and A. K. Datye, *Science*, 2016, **353**, 150-154.
293. X. Cui, K. Junge, X. Dai, C. Kreyenschulte, M.-M. Pohl, S. Wohlrab, F. Shi, A. Brückner and M. Beller, *ACS Central Science*, 2017, **3**, 580-585.
294. S. Liu, J. M. Tan, A. Gulec, L. A. Crosby, T. L. Drake, N. M. Schweitzer, M. Delferro, L. D. Marks, T. J. Marks and P. C. Stair, *Organometallics*, 2017, **36**, 818-828.
295. M. Moliner, J. E. Gabay, C. E. Kliever, R. T. Carr, J. Guzman, G. L. Casty, P. Serna and A. Corma, *J. Am. Chem. Soc.*, 2016, **138**, 15743-15750.
296. B. Qiao, J. Liu, Y.-G. Wang, Q. Lin, X. Liu, A. Wang, J. Li, T. Zhang and J. Liu, *ACS Catalysis*, 2015, **5**, 6249-6254.
297. F. J. Caparrós, L. Soler, M. D. Rossell, I. Angurell, L. Piccolo, O. Rossell and J. Llorca, *ChemCatChem*, 2018, **10**, 2365-2369.
298. M. Yang, S. Li, Y. Wang, J. A. Herron, Y. Xu, L. F. Allard, S. Lee, J. Huang, M. Mavrikakis and M. Flytzani-Stephanopoulos, *Science*, 2014, **346**, 1498.
299. A. J. Therrien, A. J. R. Hensley, M. D. Marcinkowski, R. Zhang, F. R. Lucci, B. Coughlin, A. C. Schilling, J.-S. McEwen and E. C. H. Sykes, *Nature Catalysis*, 2018, **1**, 192-198.
300. B. Qiao, J.-X. Liang, A. Wang, C.-Q. Xu, J. Li, T. Zhang and J. J. Liu, *Nano Research*, 2015, **8**, 2913-2924.
301. M. Yang, J. Liu, S. Lee, B. Zugic, J. Huang, L. F. Allard and M. Flytzani-Stephanopoulos, *J. Am. Chem. Soc.*, 2015, **137**, 3470-3473.
302. M. B. Boucher, B. Zugic, G. Cladaras, J. Kammert, M. D. Marcinkowski, T. J. Lawton, E. C. Sykes and M. Flytzani-Stephanopoulos, *Phys. Chem. Chem. Phys.*, 2013, **15**, 12187-12196.
303. X. Li, Y. Jin, Q. Xue, L. Zhu, W. Xing, H. Zheng and Z. Liu, *Journal of CO2 Utilization*, 2017, **18**, 275-282.
304. EP3130399A1, 2017.
305. C. Hontoria-Lucas, A. J. Lopez-Peinado, J. D. D. Lopez-Gonzales, M. L. Rojas-Cervantes and R. M. Martin-Aranda, *Carbon*, 1995, **33**, 1585-1592.

## REFERENCES

306. H. P. Mungse and O. P. Khatri, *The Journal of Physical Chemistry C*, 2014, **118**, 14394-14402.
307. R.-C. Wang, Y.-C. Chen, S.-J. Chen and Y.-M. Chang, *Carbon*, 2014, **70**, 215-223.
308. S. Cervený, F. Barroso-Bujans, Á. Alegría and J. Colmenero, *The Journal of Physical Chemistry C*, 2010, **114**, 2604-2612.
309. M. Acik, C. Mattevi, C. Gong, G. Lee, K. Cho, M. Chhowalla and Y. J. Chabal, *ACS Nano*, 2010, **4**, 5861–5868.
310. S. Andreoli, P. Benito, M. V. Solmi, G. Fornasari, A. Villa, B. Wu and S. Albonetti, *ChemistrySelect*, 2017, **2**, 7590-7596.
311. C. Ampelli, S. Perathoner and G. Centi, *Chinese Journal of Catalysis*, 2014, **35**, 783-791.
312. G. Centi, S. Perathoner and D. S. Su, *Catalysis Surveys from Asia*, 2014, **18**, 149-163.
313. B. Xiong, Y. Zhou, Y. Zhao, J. Wang, X. Chen, R. O'Hayre and Z. Shao, *Carbon*, 2013, **52**, 181-192.
314. M. Brycht, A. Leniart, J. Zavašnik, A. Nosal–Wiercińska, K. Wasiński, P. Pórolniczak, S. Skrzypek and K. Kalcher, *Anal. Chim. Acta*, 2018.
315. S. Yang, G. Li, C. Qu, G. Wang and D. Wang, *RSC Adv.*, 2017, **7**, 35004-35011.
316. Y. Xu, K. Sheng, C. Li and G. Shi, *J. Mater. Chem.*, 2011, **21**, 7376.
317. S. Eigler and A. M. Dimiev, in *Graphene Oxide*, eds. S. Eigler and A. M. Dimiev, John Wiley & Sons, Ltd, 1 edn., 2017, DOI: doi:10.1002/9781119069447.ch6, ch. 6.
318. L. G. Cancado, A. Jorio, E. H. Ferreira, F. Stavale, C. A. Achete, R. B. Capaz, M. V. Moutinho, A. Lombardo, T. S. Kulmala and A. C. Ferrari, *Nano Lett.*, 2011, **11**, 3190-3196.
319. B. Hervé, W. M. Wah and W. Curt, *Chem. Eur. J.*, 1997, **3**, 237-248.
320. M. Krajewska, Z. Latajka, Z. Mielke, K. Mierzwicki, A. Olbert-Majkut and M. Sałdyka, *The Journal of Physical Chemistry B*, 2004, **108**, 15578-15586.
321. U. Rosenthal and W. Schulz, *J. Organomet. Chem.*, 1987, **321**, 103-117.

## REFERENCES

322. M. T. Flynn, V. L. Blair and P. C. Andrews, *Organometallics*, 2018, **37**, 1225-1228.
323. H. Inui, K. Sawada, S. Oishi, K. Ushida and R. J. McMahon, *J. Am. Chem. Soc.*, 2013, **135**, 10246-10249.
324. M. K. Georgieva and E. A. Velcheva, *Int. J. Quantum Chem*, 2006, **106**, 1316-1322.
325. X. Cao, S. K. Coulter, M. D. Ellison, H. Liu, J. Liu and R. J. Hamers, *The Journal of Physical Chemistry B*, 2001, **105**, 3759-3768.
326. P. E. Hande, A. B. Samui and P. S. Kulkarni, *RSC Adv.*, 2015, **5**, 73434-73443.
327. M. Valencia, A. Pereira, H. Muller-Bunz, T. R. Belderrain, P. J. Perez and M. Albrecht, *Chemistry*, 2017, **23**, 8901-8911.
328. N. Azizi, E. Batebi, S. Bagherpour and H. Ghafari, *RSC Adv.*, 2012, **2**, 2289.
329. K. M. Serk, P. I. Soo, J. J. Suk, L. J. Sung and P. Jaiwook, *Org. Lett.*, 2007, **9**, 3417-3419.
330. R. B. Richrath, T. Olyschlager, S. Hildebrandt, D. G. Enny, G. D. Fianu, R. A. Flowers, 2nd and A. Gansauer, *Chemistry*, 2018, **24**, 6371-6379.
331. G. Luo, L. Chen, C. M. Conway, W. Kostich, B. M. Johnson, A. Ng, J. E. Macor and G. M. Dubowchik, *J. Org. Chem.*, 2017, **82**, 3710-3720.
332. M. C. Kim, G. S. Hwang and R. S. Ruoff, *J. Chem. Phys.*, 2009, **131**, 064704.
333. S. V. Ley, C. Mitchell, D. Pears, C. Ramarao, J.-Q. Yu and W. Zhou, *Org. Lett.*, 2003, **5**, 4665-4668.
334. Y. Wang, J. Zhou and X. Guo, *RSC Adv.*, 2015, **5**, 74611-74628.
335. G. P. Hao, W. C. Li, D. Qian, G. H. Wang, W. P. Zhang, T. Zhang, A. Q. Wang, F. Schuth, H. J. Bongard and A. H. Lu, *J. Am. Chem. Soc.*, 2011, **133**, 11378-11388.
336. D. S. Su, S. Perathoner and G. Centi, *Chem. Rev.*, 2013, **113**, 5782-5816.
337. D. C. Marcano, D. V. Kosynkin, J. M. Berlin, A. Sinitskii, Z. Sun, A. Slesarev, L. B. Alemany, W. Lu and J. M. Tour, *ACS Nano*, 2010, **4**, 4806-4814.



## **Abstract**

This thesis reports the investigation and optimization of a Rh homogeneous catalytic system, used to produce aliphatic carboxylic acids starting from oxygenated substrates, CO<sub>2</sub> and H<sub>2</sub>. The reaction conditions were optimized for each class of investigated substrates (primary alcohols, secondary alcohols, ketones, aldehydes and epoxides) leading to yields up to 80%. The reaction mechanism and the catalytic active species were studied revealing the details of a reaction pathway consisting of a *reverse* Water Gas Shift Reaction (*r*WGSR) and a following hydrocarboxylation to give the final carboxylic acid product. Single Rhodium atoms dispersed on N-doped graphene for potential catalytic applications were synthesized and characterized.

## **Abstrakt**

Das Ziel dieser Arbeit ist die Untersuchung und Optimierung eines homogenen Rh-Katalysatorsystems zur Herstellung aliphatischer Carbonsäuren ausgehend von den sauerstoffhaltigen Substraten, CO<sub>2</sub> und H<sub>2</sub>. Die Reaktionsbedingungen wurden für jede Klasse von untersuchten Substraten optimiert (primäre Alkohole, sekundäre Alkohole, Ketone, Aldehyde und Epoxide) und mit Ausbeuten bis zu 80% zu Carbonsäuren umgesetzt. Der Reaktionsmechanismus und die katalytisch aktive Spezies wurden untersucht. Die Reaktion verläuft durch eine *reverse* Wassergas-Shift-Reaktion (*r*WGSR), und eine nachfolgende Hydrocarboxylierung unter Bildung der Carbonsäure. Verschiedene einzelne Rhodiumatome wurden auf N-dotiertem Graphen dispergiert, die wiederum für potentielle katalytische Anwendungen synthetisiert und charakterisiert wurden.

## **Résumé**

Cette thèse décrit l'étude et l'optimisation d'un système catalytique homogène de Rh, utilisé pour produire des acides carboxyliques aliphatiques à partir de substrats oxygénés, CO<sub>2</sub> et H<sub>2</sub>. Les conditions de réaction ont été optimisées pour chaque classe de substrats étudiés (alcools primaires, alcools secondaires, cétones, aldéhydes et époxydes), conduisant à des rendements jusqu'à 80%. Le mécanisme de réaction et les espèces catalytiques actives ont été étudiés, démontrant un route de réaction consistant de le *reverse* Water Gas Shift (*r*WGSR) et l'hydrocarboxylation suivante pour livrer l'acide carboxylique. Des atomes de rhodium simples dispersés sur du graphène dopé avec l'N, comme potentiels catalyseurs, ont été synthétisés et caractérisés.